8-2022

Isolation and Characterization of Extracellular Vesicles from Various Biological Matrices using Capillary-Channeled Polymer (C-CP) Fiber Solid-Phase Extraction Spin-Down Tips

Kaylan Jackson
kaylank@g.clemson.edu

ISOLATION AND CHARACTERIZATION OF EXTRACELLULAR VESICLES FROM VARIOUS BIOLOGICAL MATRICES USING CAPILLARY-CHANNELED POLYMER (C-CP) FIBER SOLID-PHASE EXTRACTION SPIN-DOWN TIPS

A Dissertation
Presented to
the Graduate School of
Clemson University

In Partial Fulfillment
of the Requirements for the Degree
Doctor of Philosophy
Chemistry

---

by
Kaylan K. Jackson
August 2022

Accepted by:
Dr. R. Kenneth Marcus, Committee Chair
Dr. Terri F. Bruce
Dr. Carlos Garcia
Dr. Byoungmoo Kim

ABSTRACT

A number of recent works have emphasized the need to isolate nanometer-scale analytes, like extracellular vesicles (EVs), from various biologically-relevant fluids. Exosomes are a subset of small EVs that range from 30-200 nm in diameter that serve as biomolecular snapshots of their cell of origin containing mother cell-specific DNA, miRNA, mRNA, and proteins. As critical components of intercellular communication, exosomes and other EVs play significant roles in many physiological and pathological processes. Diverse populations of these vesicles can be collected from biofluids, including blood, saliva, and urine, from cell culture conditioned media and primary cells, and even from plant fluid stocks. With their characteristic vector-like activities and accessible collection from renewable sources, the large-scale processing of EVs from patient biofluids for clinical diagnostics and from plant fluids or high-yield bioreactors for use as therapeutic vectors has been previously proposed. However, these applications are limited by extremely impure, low-yield exosome recoveries, despite the large availability of exosome sources. Hence, an isolation method that provides high concentrations of pure, bioactive EVs from diverse sources on reasonable scales of time and cost is of much interest.

Employed in this work is a rapid EV isolation method using a hydrophobic interaction chromatography (HIC) workflow on a capillary-channeled polymer (C-CP) fiber spin-down tip. Here, EVs are isolated from several biofluid sources, including mock biofluid matrices, clinical patient biofluid samples, cellular milieu from mammalian and

amoeba cell lines, and over 20 fruit and vegetable sample stocks. Representative populations of EVs are obtained using the C-CP tip method, where up to 12 samples are simultaneously processed in a standard tabletop centrifuge in less than 15 minutes. This batch solid-phase extraction technique allows up to 1 x 10^{12} EVs to be obtained from each µL-scale aliquot of the original biofluid. The tip-isolated EVs were characterized using transmission electron microscopy (TEM), multi-angle light scattering (MALS), nanoparticle tracking analysis (NTA), absorbance quantification, protein purity assay, and immunoassays to EV and source-specific proteins. The efficient HIC C-CP tip isolation method produces the required integrity and purity of recovered EVs to enable fundamental research to be performed and their therapeutic vector and clinical diagnostic potentials to be better explored.

DEDICATION

It was not by my strength, intelligence, or power that I was able to persevere throughout this degree. First, I give all honor to God who sustained me through every trial. Next, I give honor to my husband, Willie C. Jackson IV, who consistently challenged me to believe in myself, covered me when I was too weak to go on, and reminded me who I was when my vision was blurry. I love you honey. I'd also like to dedicate this work to our angels Wilson and little baby bean. I deeply wish I could have gotten to love you longer, but I know you two are having a blast together in heaven. I thank you for all the joy, hope, and comfort you brought into my life. I hold the time we had together so near and dear to my heart. I hope that the works presented in this dissertation can play some role in the development of a rapid, non-invasive insight into diseased states, so that the ailments that have stolen the ones I love can be caught early, and intervention and care will be possible in the future.

ACKNOWLEDGMENTS

First, I would like to thank my research advisor, Dr. R. Kenneth Marcus. Upon our meeting in 2018, you saw a potential for greatness in me that I did not yet see in myself. You have consistently guided me, challenged me, and opened the door for so many opportunities. I have grown tremendously throughout my time at Clemson, and that is due in part to your mentorship. For all of this, I am deeply grateful.

I would also like to thank my graduate committee Dr. Terri F. Bruce, Dr. Carlos Garcia, and Dr. Byoungmoo Kim. I genuinely appreciate all of the training, advice, knowledge, guidance, and support you all have sown into my graduate education. Your contribution to my success does not go unnoticed. I would like to thank the research groups of Dr. Terri Bruce and Dr. Sarah Harcum, as well as Dr. Brian Nelson and Dr. Diane Nelson (National Institutes of Standards and Technologies) for their training, advice, guidance, and collaboration.

I would like to also thank the past and present members of the Marcus group: Edward Hoegg, Hung Trang, Tyler Williams, Htoo Paing, Katja Hall, Lei Wang, Sisi Huang, Joseph Goodwin, Cameron Stouffer, Carolina Mata, and Khalid Bin Islam. But specifically, I would like to thank Lacey Billotto and Sarah Wysor. Though you've called me your "fearless leader", the truth is I would not have been able to do this without you two.

TABLE OF CONTENTS

Page

TITLE PAGE i

ABSTRACT ii

DEDICATION iv

ACKNOWLEDGMENTS v

LIST OF TABLES ix

LIST OF FIGURES x

CHAPTER

I. INTRODUCTION

1.1 Extracellular Vesicles 1
1.2 Extracellular Vesicle Sources and Applications 2
1.3 Approaches for Extracellular Vesicle Isolation 3
1.4 Capillary-Channeled Polymer Fiber-Based Extracellular Vesicle Isolations using Hydrophobic Interaction Chromatography 4
1.5 References 6
1.6 Summary of Chapters 16
1.7 List of Publications 24

II. SOLID-PHASE EXTRACTION OF EXOSOMES FROM DIVERSE MATRICES VIA A POLYESTER CAPILLARY-CHANNELED POLYMER (C-CP) FIBER STATIONARY PHASE IN A SPIN-DOWN TIP FORMAT 26

2.1 Introduction 26
2.2 Materials and Methods 30
2.3 Results and Discussion 35
2.4 Conclusions 49
2.5 Acknowledgements 51
2.6 References 52

III. RAPID ISOLATION OF EXTRACELLULAR VESICLES FROM DIVERSE BIOFLUID MATRICES VIA CAPILLARY-CHANNELED POLYMER FIBER SOLID-PHASE EXTRACTION MICROPIPETTE TIPS 62

3.1 Introduction 62
3.2 Experimental 67
3.3 Results and Discussion 73
3.4 Conclusions 85
3.5 Acknowledgements 87
3.6 References 87

IV. COMPARISON OF THE CAPILLARY-CHANNELED POLYMER (C-CP) FIBER SPIN-DOWN TIP APPROACH TO TRADITIONAL METHODS FOR THE ISOLATION OF EXTRACELLULAR VESICLES FROM HUMAN URINE 96

4.1 Introduction 96
4.2 Materials and Methods 100
4.3 Results and Discussion 107
4.4 Conclusions 121
4.5 Acknowledgements 123
4.6 References 123

V. FACILE, GENERIC CAPTURE AND ON-FIBER DIFFERENTIATION OF EXOSOMES VIA CONFOCAL IMMUNOFLUORESCENCE MICROSCOPY USING A CAPILLARY-CHANNELED POLYMER FIBER SOLID-PHASE EXTRACTION TIP 135

5.1 Introduction 135
5.2 Experimental 140
5.3 Results and Discussion 147
5.4 Conclusions 154
5.5 Acknowledgements 157
5.6 References 157

VI. ISOLATION OF PLANT-DERIVED EXTRACELLULAR VESICLES USING THE HYDROPHOBIC INTERACTION-BASED CAPILLARY-CHANNELED POLYMER FIBER SPIN-DOWN TIP 164

6.1 Introduction 164
6.2 Experimental 171
6.3 Results and Discussion 179

Table of Contents (Continued)

Page

6.4 Conclusions 189
6.5 Acknowledgements 191
6.6 References 191

VII. RAPID ISOLATION AND QUANTIFICATION OF EXTRACELLULAR VESICLES FROM SUSPENSION-ADAPTED HUMAN EMBRYONIC KIDNEY CELLS USING CAPILLARY-CHANNELED POLYMER FIBER SPIN-DOWN TIPS 205

7.1 Introduction 205
7.2 Materials and Methods 211
7.3 Results and Discussion 217
7.4 Conclusions 231
7.5 Acknowledgements 233
7.6 References 233

VIII. SUMMARY AND FUTURE WORK 242

APPENDICES 244

A: Supplementary Information for Chapter Two - *"Solid-phase extraction of exosomes from diverse matrices via a polyester capillary-channeled polymer (C-CP) fiber stationary phase in a spin-down tip format"* 245

B: Supplementary Information for Chapter Four - *"Facile, Generic Capture and On-Fiber Differentiation of Exosomes Via Confocal Immunofluorescence Microscopy using a Capillary-Channeled Polymer Fiber Solid-Phase Extraction Tip"* 251

LIST OF TABLES

Table Page

2.1 Absorbance response characteristics for exosome standards in aqueous solution at 203, 216, and 280 nm 41

6.1 Scientific name, reported size, and isolation method used for the extraction of plant-derived EVs. Sample categories: leafy greens (represented in green), vegetables (represented in red), and fruit (represented in blue) 173

LIST OF FIGURES

Figure Page

2.1 The practical steps of C-CP fiber tip fabrication and the spin-down approach to isolation and purification of EVs 33

2.2 Physical and biologic imaging of exosomes adsorbed to PET C-CP fiber surface via a) scanning electron microscopy and b) super-resolution confocal fluorescence microscopy 36

2.3 Physical and biological characterization of exosomes eluted from PET C-CP fiber spin-down tips via a) transmission electron microscopy and b) dot blot immunoassay 38

2.4 Breakthrough analysis of 50 µL aliquot additions of 4.65×10^{10} particles per dose. The 50% dynamic binding capacity is surpassed during trial 15 at 6.98×10^{11} particles 39

2.5 Post-isolation of exosome standards spiked into various matrices (50 µL) using the PETC-CP fiber tip spin-down method. The concentrations of exosomes recovered were determined based on absorbance response (1 µL) when compared to the standard curve of Table 2.1. a) Quantified recovery of exosomes from mock matrices of 1/100 concentration and b) quantified recovery of exosomes from mock matrices of 1/1000 concentration. The loaded 1/100 and 1/1000 solutions theoretically contain 2E10 and 2E9 exosomes, respectively 43

2.6 a) Quantification of exosomes in the eluates from aqueous solution (1/100), exosome-depleted FBS, and a spiked exosome-depleted FBS matrix (1/100). b–d) STEM images of eluted exosomes, all containing their characteristic spherical structure post isolation using the C-CP tip method 46

2.7 Post-isolation of exosome standards spiked into various matrices (50 µL) using the PET C-CP fiber tip spin-down method; the concentration of exosomes recovered were determined based on ELISA readout to an exosome standard curve of linear response was performed to quantitatively detect the expression of the exosomal tetraspanin protein-CD81 (n = 3) employing a capture antibody of 1:250 concentration. Quantified recovery of exosomes from mock matrices of 1/100 and 1/1000 concentration. The loaded 1/100 and 1/1000 solutions theoretically contain $2 \text{ X } 10^{10}$ and $2 \text{ X } 10^{9}$ exosomes, respectively 48

Figure Page

3.1 The capillary-channeled polymer (C-CP) fiber solid-phase extraction tip setup for the isolation of EVs from complex biofluids in a tabletop centrifuge 69

3.2 Standard addition curve using a commercial exosome standard stock of 1.1×10^{10} particles per mL concentration based on absorbance measurement at 203 nm (red). Quantification of EVs based on absorbance detection after employing aqueous EV solutions of known concentration to the C-CP tip (blue) 75

3.3 Determined EV particle concentrations (n = 3) for human urine, saliva, cervical mucus, blood serum and goat milk biofluid unknown samples spiked once, twice, and three times with a commercial exosome standard stock of 1.1×10^{10} particle per mL before EV isolation using the C-CP tip workflow. The biofluid-originating EV recoveries were quantified based on absorbance at 203 nm and compared to a response curve of linear response..... 77

3.4 Size distribution of vesicles in the EV recoveries resulting from the C-CP fiber tip isolation from human urine, saliva, cervical mucus, blood serum, and goat milk, measured using the Nanosight NS300 nanoparticle tracking analysis system. TEM micrographs of EVs isolated from biofluids using the C-CP fiber tip, taken using the Hitachi HT7830. 79

3.5 Comparison of the determined concentration of (a) EVs in each bulk biofluid sample and (b) EVs recovered from each biofluid using the C-CP tip method as determined using the method of standard addition by absorbance at 203 nm and by nanoparticle tracking analysis. 81

3.6 Bradford assay of raw biofluid matrices and concentrated EV recoveries after isolation with the C-CP tip. The total protein concentration was determined using the absorbance measurement of Bradford reagent at 595 nm, as compared to a BSA standard curve of linear response. n = 3..... 82

3.7 Indirect ELISA standard curve employing an antibody to the CD81 tetraspanin protein using serial dilutions of a commercial exosome standard (2.7×10^{12} particles per mL), and the CD81 responses of the C-CP tip isolated EVs from biofluid samples. 84

Figure Page

4.1 Transmission electron micrographs of commercial urine exosome standards (**a**), and extracellular vesicles (EVs) from the same urine sample, isolated using the capillary-channeled polymer (C-CP) fiber tip methods (acetonitrile (**b**) and glycerol (**c**)), exoEasy (**d**) and ExoQuick (**e**) kits, and the traditionally used ultracentrifugation method (**f**). The SEM images were taken using the Hitachi SU9000 108

4.2 Bar graph representing the concentration of EV yields obtained from the C-CP tip (acetonitrile and glycerol), exoEasy, ExoQuick, and ultracentrifugation methods based on absorbance detection and comparison to a calibration curve of linear response ($y = 2E - 13x + 0.0264$, $R^2 = 0.9935$, $n = 3$) ... 110

4.3 Size distribution and cumulative percentage of size distribution of commercial exosome standards and EVs isolated using the C-CP tip (acetonitrile and glycerol), exoEasy, ExoQuick, and ultracentrifugation methods as determined using the NanoSight NS300 NTA system. Average of $n = 5$ runs, 60 s each 114

4.4 Indirect ELISA for identification of the CD81 and CD63 tetraspanin EV marker in the commercial exosome standard and EVs recovered from urine by the C-CP tip (acetonitrile and glycerol), exoEasy, ExoQuick, and ultracentrifugation methods. All samples applied in triplicate and the average of the triplicate measurements minus the average response of the blank are presented 117

4.5 A microBCA assay was employed to determine the concentration of total protein in the exosome standards and EVs isolated from urine using the C-CP tip (acetonitrile and glycerol), exoEasy, ExoQuick, and ultracentrifugation methods. The concentration of EVs was compared to the total protein content as a measure of EV purity. All samples applied in triplicate and the average of the triplicate measurements minus the average response of the blank are presented. 120

5.1 Graphic depiction of the on-fiber exosome extraction and immunolabeling process 142

5.2 Confocal fluorescence images of C-CP fibers from process blank and test specimens following standard immunolabeling procedure. Red color depicts presence of the CD81 tetraspanin protein on exosome membranes, with green color representing the presence of CA125. 149

Figure Page

5.3 Confocal fluorescence images of C-CP fibers from process blank and test specimens following higher-throughput immunolabeling procedure. Red color depicts presence of the CD81 tetraspanin protein on exosome membranes, with green color representing the presence of CA125 153

6.1 Diagrammatic representation of the sample processing workflow for the isolation of plant-derived extracellular vesicles (PDEVs) using the capillary-channeled polymer (C-CP) fiber solid-phase extraction tip and a tabletop centrifuge 175

6.2 Transmission electron micrographs of commercial EVs from a) HEK293 exosome standards, and plant-derived extracellular vesicles (PDEVs) from b) green onion, c) blueberry, d) ginger, e) strawberry, f) red onion, g) baby spinach, and h) beefsteak tomato samples following isolation using the C-CP fiber spin-down tip method. The TEM images were taken using the Hitachi HT7830. Scalebar = 100 nm. 180

6.3 Size determinations of the C-CP tip isolated PDEVs using the Wyatt Dawn MALS instrument. Presented are the average sizes of the PDEVs resulting from 3 consecutive 60-second runs..... 181

6.4 a) Numbers of recovered PDEVs using the C-CP spin-down tip isolation method, determined using the method of standard addition, and b) recovered PDEV concentrations with respect to the mass of starting material 183

6.5 Total protein content (as determined by Bradford assays) of raw samples and the resulting PDEV isolates using the C-CP spin-down tip isolation method. All samples were analyzed in triplicate, corrected for the average response of triplicate blanks..... 185

6.6 Determined PDEV purities based on the EV recoveries presented in Fig. 6.4, and the residual protein content presented in Fig. 6.5 187

6.7 Indirect ELISA confirmation of the presence of the PEN1 marker protein for PDEVs recovered from plant samples using the C-CP spin-down tip method. Samples were analyzed in triplicate, corrected for the average response of triplicate blanks..... 188

Figure Page

7.1 Concentration of HEK293 cells in native CCM supernatant with the percentage viability on each day of cell culture as determined using the Vi-Cell XR instrument via trypan blue cell exclusion assay 218

7.2 Transmission electron micrographs of eluates from each step in the HIC C-CP tip EV process. Representative micrographs from the a) native HEK293 CCM supernatant, b and c) exposure to first and second protein elution buffers and d) the EV elution buffer. The TEM images were taken using the Hitachi HR7830, scalebar = 200 nm 220

7.3 a) Concentration of EVs collected from each CCM aliquot using the C-CP tip isolation method and b) concentration of EVs released per viable cell. Quantification performed using the method of standard addition via absorbance detection at 203 nm 222

7.4 CD9 and CD81 tetraspanin protein responses of C-CP tip isolated EV recoveries from each time point, determined using an indirect ELISA. All samples were applied in triplicate with the average of the triplicate measurements minus the average response of the blank is presented. 225

7.5 Size determination of the EVs recovered using the C-CP tip isolation method on each day of cell culture, performed using the Wyatt Dawn MALS instrument. Presented is the average size of the EVs resulting from 3 consecutive 60-second runs 227

7.6 a) Concentration of protein in HEK293 sample stocks and EV eluates from the C-CP tip at each step in the isolation, determined using a Bradford assay. b) EV purity ratio comparing number of EVs to the mass of protein. All samples applied in triplicate and the average of the triplicate measurements minus the average response of the blank is presented. Purity standard = 3×10^{10} EVs μg^{-1} 229

CHAPTER ONE

INTRODUCTION

1.1 Extracellular Vesicles

A diverse population of nanometer-scale extracellular vesicles (EVs) are secreted by all living cells as a part of their normal physiology and serve critical biological roles during cellular communication.[1] Though the area of EV research is a currently developing field, EVs are now known to be involved in a variety of functions, including immune modulation,[2] viral pathogenicity,[3] and disease progression.[4, 5] In each case, the physiological activities initiated by the release and uptake of EVs are allowed by the biomolecules incorporated into the internal and transmembrane EV spaces during their biogenesis.[6] In general, EVs are 30 – 1000 nm phospholipid bilayer membrane-bound vesicles that contain DNA, RNA, lipids, metabolites, and cytosolic and/or surface proteins from their cell of origin.[5, 6] As originally referred to as "cellular trash bags",[7-9] the purpose of EV secretion is to remove unneeded or excess cell by-products and maintain cellular homeostasis, though the entirety of their functional roles has yet to be fully understood.[1, 6] Still, EVs have been generically classified by size and creation mechanism as microvesicles– 30 to 1000 nm vesicles formed by the blebbing of the plasma membrane,[6, 10-12] apoptotic bodies– 100 to 1000 nm EVs stochastically formed during cell death,[10, 13] and exosomes– 30 to 200 nm sized-vesicles strategically created through the multivesicular body-mediated endosomal pathway.[5-7, 10, 14] Of most interest is the exosome EV sub-type, which has been suggested in many clinical and therapeutic applications because of the strategic biogenesis process, which allows them to contain

specific components that aid in the regulation of cellular signaling and communication.[1, 15, 16] Still, because of the overlap of size and the inability to differentiate between EV sub-types, vesicles in the 30 – 200 nm exosome size range have been generically referred to as EVs or small EVs (sEVs).[17]

1.2 EV Sources and Applications

Because EVs are secreted from all cells, they may be collected from many biofluids, including from cell culture milieu,[18] urine,[19, 20] saliva,[21] cervical mucus,[22] blood (serum and plasma),[19, 23] and breast milk.[24] With the ability to collect EVs non-invasively from patient biofluids (i.e., from urine or saliva), liquid biopsy approaches are currently under development, where there are numerous opportunities for the detection, monitoring, and characterization of diseases without direct contact with the primary area of infection.[25-27] EV-based liquid biopsies have shown particular promise for early cancer detection, as EVs are able to be collected from patient blood/urine effluents and allow for the assessment of the diseased state without direct contact with the cancerous tissues.[25, 26]

In the realm of therapeutics, EVs have been proposed as candidates for use as delivery vehicles to transport novel gene and/or drug therapies.[28-30] Therapeutically, EVs have been used in a variety of ways. Since EVs are innately bioactive nanovesicles that are reflective of their source, they have been isolated from environments that have been shown to promote cellular regeneration and healing (i.e., mesenchymal stem cells or ginger roots), where they are directly applied as therapeutic agents.[2, 31, 32] Alternatively, EVs have been isolated from generic cell culture environments (i.e., HEK293 cells), then

bioengineered to contain specific gene, drug, or protein cargos before being applied as therapeutic vectors for the targeted delivery of bioactive materials.[33, 34] A variety of studies have reported the use of EVs in the treatment of diseases, including Alzheimer's,[35] cancers,[36] liver disease,[37] opioid addiction,[38] and immune disorders.[39] But despite the promising performance of EVs as therapeutic vectors, the comprehensive assessment of EV fundamentals has been prevented by the lack of methods to isolate, quantify, and characterize EVs efficiently.

1.3 Approaches for Extracellular Vesicle Isolation

To date, several methods for EV isolation have been introduced. However, none of the available isolation methods can provide highly concentrated, pure collections of EVs in a manner that is fit for clinical or therapeutic use. Most commonly, ultracentrifugation, polymer precipitation, or ultrafiltration methods are used for EV isolation. However, all of these create low-yield un-representative vesicle recoveries that are consistently contaminated with protein and lipoprotein aggregates, limiting the downstream characterization/application of EVs. There is currently no consensus regarding the most efficient procedure to harvest pure, concentrated collections of EVs, causing an inevitable compromise between yield and purity of EVs obtained using the chosen isolation method.

Because of the limitations introduced by EV isolation, the characterization and quantification of EV populations has been prevented. Most commonly, to verify the presence of EVs, a combination of electron microscopy, immunoassay, and size

determination-based protocols are used. But with the challenge of EV isolation, many of the results obtained from these methods reveal that recovered EV populations are contaminated with proteins/lipoproteins and other matrix contaminants and are often structurally damaged and un-representative of the entire population of EVs. For the future progression of EV research, an isolation method able to efficiently provide high concentrations of pure, structurally-preserved EVs is essential.

1.4 Capillary-Channeled Polymer (C-CP) Fiber-based EV Isolations using Hydrophobic Interaction Chromatography

To address the shortcomings of currently-available EV isolation methods, Marcus and colleagues have developed a highly efficient EV isolation method using patented capillary-channeled polymer (C-CP) fiber stationary phases via a hydrophobic interaction chromatography solvent system.[40-48] In recent decades, Marcus and coworkers have demonstrated the use of C-CP stationary phases using a variety of separation modalities, including reversed phase (RP),[49-52] ion exchange (IEX),[50, 53, 54] affinity,[55] protein A (proA),[56, 57] and hydrophobic interaction (HIC)[40-44, 47, 48, 58-60] chromatography modes. In these applications, the C-CP phase has repeatedly demonstrated the ability to provide a platform for a variety of highly efficient separations to be performed, operating at lower back pressures (< 1000 psi) and higher linear velocities (> 50 mm sec^{-1}) than traditionally utilized packed bed stationary phases during traditional HPLC. The C-CP fibers employed in these separations are able to be created from commodity polymers such as polypropylene (PP), polyester (PET), and nylon-6, and have been created in eight-prong

or y-shaped configurations about their periphery. When collinearly aligned and packed into a column format, the finger-like protrusions along the fiber periphery interdigitate to create micron-wide channels with a low flow resistance, enabling excellent fluid transport characteristics and high throughput separations without the sacrifice of separation efficiency.

Recent works have demonstrated that a solvent-assisted HIC-based isolation mode employing the 8-prong shaped PET C-CP fiber stationary phase enables highly efficient EV isolations using solid-phase extraction (SPE) spin-down tip[41, 44-47] and traditional HPLC column[40-42, 48] formats. In the case of both applications, highly pure and concentrated EV yields (up to 7 x 10^{12} EVs) are able to be obtained from complex biofluid samples, including cell culture milieu, urine, saliva, cervical mucus, blood serum, and milk, with isolation performance uncompromised by matrix effects. Even further, the applied chromatographic solvents are able to be tailored for the downstream characterization of the recovered EVs by using acetonitrile, glycerol, or even detergent-based elution solvents. Overall, the HIC-based C-CP isolation of EVs is able to provide concentrated populations of EVs on relevant scales of time (< 10 min), cost (< $1), and practicality for fundamental research to be performed and application potential to be explored. The C-CP tip approach specifically, allows the simultaneous processing of up to 12 biofluid samples (which is only limited by the capacity of the tabletop centrifuge) and is able to rapidly provide concentrated EV aliquots ready for virtually any downstream characterization method, even with the ability to perform immunoaffinity-based biomarker probing and imaging directly on the isolation phase. The work presented

here outlines the foundational development of the C-CP spin-down tip method, where the rapid isolation of clean, pure EVs from cell culture, clinical biofluid, and plant fluid stocks has been allowed.

1.5 References

1. Tkach, M.; Thery, C., Communication by Extracellular Vesicles: Where We Are and Where We Need to Go. *Cell* 2016, 164 (6), 1226-1232.
2. Burrello, J.; Monticone, S.; Gai, C.; Gomez, Y.; Kholia, S.; Camussi, G., Stem Cell-Derived Extracellular Vesicles and Immune-Modulation. *Front. Cell Dev. Biol.* 2016, 4, 83.
3. Raab-Traub, N.; Dittmer, D. P., Viral effects on the content and function of extracellular vesicles. *Nat. Rev. Microbiol.* 2017, 15 (9), 559-572.
4. Buzas, E. I.; Gyorgy, B.; Nagy, G.; Falus, A.; Gay, S., Emerging role of extracellular vesicles in inflammatory diseases. *Nat. Rev. Rheumatol*. 2014, 10 (6), 356-64.
5. Kalluri, R.; LeBleu, V. S., The biology, function, and biomedical applications of exosomes. *Science* 2020, 367 (6478), eaau6977.
6. Raposo, G.; Stoorvogel, W., Extracellular vesicles: exosomes, microvesicles, and friends. *J. Cell Biol.* 2013, 200 (4), 373-83.
7. Kalluri, R., The biology and function of exosomes in cancer. *J. Clin. Invest.* 2016, 126 (4), 1208-15.

8. Wolf, P., The nature and significance of platelet products in human plasma. Br. *J. Haematol.* 1967, 13 (3), 269-88.

9. Anderson, H. C., Vesicles associated with calcification in the matrix of epiphyseal cartilage. *J. Cell Biol.* 1969, 41 (1), 59-72.

10. Akers, J. C.; Gonda, D.; Kim, R.; Carter, B. S.; Chen, C. C., Biogenesis of extracellular vesicles (EV): exosomes, microvesicles, retrovirus-like vesicles, and apoptotic bodies. *J. Neurooncol.* 2013, 113 (1), 1-11.

11. Cocucci, E.; Racchetti, G.; Meldolesi, J., Shedding microvesicles: artefacts no more. *Trends Cell Biol.* 2009, 19 (2), 43-51.

12. Muralidharan-Chari, V.; Clancy, J. W.; Sedgwick, A.; D'Souza-Schorey, C., Microvesicles: mediators of extracellular communication during cancer progression. *J. Cell Sci.* 2010, 123 (Pt 10), 1603-11.

13. Bergsmedh, A.; Szeles, A.; Henriksson, M.; Bratt, A.; Folkman, M. J.; Spetz, A. L.; Holmgren, L., Horizontal transfer of oncogenes by uptake of apoptotic bodies. *Proc. Natl. Acad. Sci. U. S. A.* 2001, 98 (11), 6407-11.

14. Thery, C.; Zitvogel, L.; Amigorena, S., Exosomes: composition, biogenesis and function. *Nat. Rev. Immunol.* 2002, 2 (8), 569-79.

15. Camussi, G.; Deregibus, M. C.; Bruno, S.; Cantaluppi, V.; Biancone, L., Exosomes/microvesicles as a mechanism of cell-to-cell communication. *Kidney Int.* 2010, 78 (9), 838-48.

16. Mathieu, M.; Martin-Jaular, L.; Lavieu, G.; Thery, C., Specificities of secretion and uptake of exosomes and other extracellular vesicles for cell-to-cell communication. *Nat. Cell Biol.* 2019, 21 (1), 9-17.

17. Thery, C.; Witwer, K. W.; Aikawa, E.; et. al, Minimal information for studies of extracellular vesicles 2018 (MISEV2018): a position statement of the International Society for Extracellular Vesicles and update of the MISEV2014 guidelines. *J. Extracell. Vesicles* 2018, 7 (1), 1535750.

18. Thery, C.; Amigorena, S.; Raposo, G.; Clayton, A., Isolation and characterization of exosomes from cell culture supernatants and biological fluids. *Curr. Protoc. Cell Biol.* 2006, Chapter 3 (1), Unit 3 22.

19. Li, M.; Zeringer, E.; Barta, T.; Schageman, J.; Cheng, A.; Vlassov, A. V., Analysis of the RNA content of the exosomes derived from blood serum and urine and its potential as biomarkers. *Philos. Trans. R. Soc., B* 2014, 369 (1652), 20130502.

20. Pisitkun, T.; Shen, R. F.; Knepper, M. A., Identification and proteomic profiling of exosomes in human urine. *Proc. Natl. Acad. Sci. U. S. A.* 2004, 101 (36), 13368-73.

21. Michael, A.; Bajracharya, S. D.; Yuen, P. S.; Zhou, H.; Star, R. A.; Illei, G. G.; Alevizos, I., Exosomes from human saliva as a source of microRNA biomarkers. *Oral Dis.* 2010, 16 (1), 34-38.

22. Flori, F.; Secciani, F.; Capone, A.; Paccagnini, E.; Caruso, S.; Ricci, M. G.; Focarelli, R., Menstrual cycle–related sialidase activity of the female cervical

mucus is associated with exosome-like vesicles. *Fertil. Steril.* 2007, 88 (4), 1212-1219.

23. Caby, M. P.; Lankar, D.; Vincendeau-Scherrer, C.; Raposo, G.; Bonnerot, C., Exosomal-like vesicles are present in human blood plasma. *Int. Immunol.* 2005, 17 (7), 879-87.

24. Admyre, C.; Johansson, S. M.; Qazi, K. R.; Filen, J. J.; Lahesmaa, R.; Norman, M.; Neve, E. P.; Scheynius, A.; Gabrielsson, S., Exosomes with immune modulatory features are present in human breast milk. *J. Immunol.* 2007, 179 (3), 1969-78.

25. Halvaei, S.; Daryani, S.; Eslami, S. Z.; Samadi, T.; Jafarbeik-Iravani, N.; Bakhshayesh, T. O.; Majidzadeh, A. K.; Esmaeili, R., Exosomes in Cancer Liquid Biopsy: A Focus on Breast Cancer. *Mol. Ther. Nucleic Acids* 2018, 10, 131-141.

26. Zhang, W.; Xia, W.; Lv, Z.; Ni, C.; Xin, Y.; Yang, L., Liquid Biopsy for Cancer: Circulating Tumor Cells, Circulating Free DNA or Exosomes? *Cell Physiol. Biochem.* 2017, 41 (2), 755-768.

27. Zhou, B.; Xu, K.; Zheng, X.; Chen, T.; Wang, J.; Song, Y.; Shao, Y.; Zheng, S., Application of exosomes as liquid biopsy in clinical diagnosis. *Signal Transduction Targeted Ther.* 2020, 5 (1), 1-14.

28. Das, C. K.; Jena, B. C.; Banerjee, I.; Das, S.; Parekh, A.; Bhutia, S. K.; Mandal, M., Exosome as a novel shuttle for delivery of therapeutics across biological barriers. *Mol. Pharmaceutics* 2018, 16 (1), 24-40.

29. Ferguson, S. W.; Nguyen, J., Exosomes as therapeutics: The implications of molecular composition and exosomal heterogeneity. *J. Control. Release* 2016, 228, 179-190.

30. Yamashita, T.; Takahashi, Y.; Takakura, Y., Possibility of Exosome-Based Therapeutics and Challenges in Production of Exosomes Eligible for Therapeutic Application. *Biol. Pharm. Bull.* 2018, 41 (6), 835-842.

31. Li, Z.; Wang, H.; Yin, H.; Bennett, C.; Zhang, H. G.; Guo, P., Arrowtail RNA for Ligand Display on Ginger Exosome-like Nanovesicles to Systemic Deliver siRNA for Cancer Suppression. *Sci. Rep.* 2018, 8 (1), 14644.

32. Ha, D. H.; Kim, H. K.; Lee, J.; Kwon, H. H.; Park, G. H.; Yang, S. H.; Jung, J. Y.; Choi, H.; Lee, J. H.; Sung, S.; Yi, Y. W.; Cho, B. S., Mesenchymal Stem/Stromal Cell-Derived Exosomes for Immunomodulatory Therapeutics and Skin Regeneration. *Cells* 2020, 9 (5), 1157.

33. Ahn, S. H.; Ryu, S. W.; Choi, H.; You, S.; Park, J.; Choi, C., Manufacturing Therapeutic Exosomes: from Bench to Industry. Mol. Cells 2022, 45 (5), 284-290.

34. Kim, J.; Song, Y.; Park, C. H.; Choi, C., Platform technologies and human cell lines for the production of therapeutic exosomes. *EVCNA* 2021, 2 (1), 3-17.

35. Iranifar, E.; Seresht, B. M.; Momeni, F.; Fadaei, E.; Mehr, M. H.; Ebrahimi, Z.; Rahmati, M.; Kharazinejad, E.; Mirzaei, H., Exosomes and microRNAs: New potential therapeutic candidates in Alzheimer disease therapy. *J. Cell Physiol.* 2019, 234 (3), 2296-2305.

36. Inamdar, S.; Nitiyanandan, R.; Rege, K., Emerging applications of exosomes in cancer therapeutics and diagnostics. Bioeng. *Transl. Med.* 2017, 2 (1), 70-80.

37. Masyuk, A. I.; Masyuk, T. V.; Larusso, N. F., Exosomes in the pathogenesis, diagnostics and therapeutics of liver diseases. *J. Hepatol.* 2013, 59 (3), 621-5.

38. Liu, Y.; Li, D.; Liu, Z.; Zhou, Y.; Chu, D.; Li, X.; Jiang, X.; Hou, D.; Chen, X.; Chen, Y.; Yang, Z.; Jin, L.; Jiang, W.; Tian, C.; Zhou, G.; Zen, K.; Zhang, J.; Zhang, Y.; Li, J.; Zhang, C. Y., Targeted exosome-mediated delivery of opioid receptor Mu siRNA for the treatment of morphine relapse. *Sci. Rep.* 2015, 5 (1), 17543.

39. Xu, H.; Jia, S.; Xu, H., Potential therapeutic applications of exosomes in different autoimmune diseases. *Clin. Immunol.* 2019, 205, 116-124.

40. Bruce, T. F.; Slonecki, T. J.; Wang, L.; Huang, S.; Powell, R. R.; Marcus, R. K., Exosome isolation and purification via hydrophobic interaction chromatography using a polyester, capillary-channeled polymer fiber phase. *Electrophoresis* 2019, 40 (4), 571-581.

41. Huang, S.; Ji, X.; Jackson, K. K.; Lubman, D. M.; Ard, M. B.; Bruce, T. F.; Marcus, R. K., Rapid separation of blood plasma exosomes from low-density lipoproteins via a hydrophobic interaction chromatography method on a polyester capillary-channeled polymer fiber phase. *Anal. Chim. Acta* 2021, 1167, 338578.

42. Huang, S.; Wang, L.; Bruce, T. F.; Marcus, R. K., Isolation and quantification of human urinary exosomes by hydrophobic interaction chromatography on a

polyester capillary-channeled polymer fiber stationary phase. *Anal. Bioanal. Chem.* 2019, 411 (25), 6591-6601.

43. Huang, S.; Wang, L.; Bruce, T. F.; Marcus, R. K., Evaluation of exosome loading characteristics in their purification via a glycerol-assisted hydrophobic interaction chromatography method on a polyester, capillary-channeled polymer fiber phase. *Biotechnol. Prog.* 2020, 36 (5), e2998.

44. Jackson, K. K.; Powell, R. R.; Bruce, T. F.; Marcus, R. K., Solid-phase extraction of exosomes from diverse matrices via a polyester capillary-channeled polymer (C-CP) fiber stationary phase in a spin-down tip format. *Anal. Bioanal. Chem.* 2020, 412 (19), 4713-4724.

45. Jackson, K. K.; Powell, R. R.; Bruce, T. F.; Marcus, R. K., Rapid isolation of extracellular vesicles from diverse biofluid matrices via capillary-channeled polymer fiber solid-phase extraction micropipette tips. *Analyst* 2021, 146 (13), 4314-4325.

46. Jackson, K. K.; Powell, R. R.; Bruce, T. F.; Marcus, R. K., Facile, generic capture and on-fiber differentiation of exosomes via confocal immunofluorescence microscopy using a capillary-channeled polymer fiber solid-phase extraction tip. *Sens. Diagn.* 2022, 1 (3), 525-533.

47. Jackson, K. K.; Powell, R. R.; Marcus, R. K.; Bruce, T. F., Comparison of the capillary-channeled polymer (C-CP) fiber spin-down tip approach to traditional methods for the isolation of extracellular vesicles from human urine. *Anal. Bioanal. Chem.* 2022, 414 (13), 3813-3825.

48. Wang, L.; Bruce, T. F.; Huang, S.; Marcus, R. K., Isolation and quantitation of exosomes isolated from human plasma via hydrophobic interaction chromatography using a polyester, capillary-channeled polymer fiber phase. *Anal. Chim. Acta* 2019, 1082, 186-193.

49. Randunu, K. M.; Marcus, R. K., Microbore polypropylene capillary channeled polymer (C-CP) fiber columns for rapid reversed-phase HPLC of proteins. *Anal. Bioanal. Chem.* 2012, 404 (3), 721-9.

50. Stanelle, R. D.; Straut, C. M.; Marcus, R. K., Nylon-6 capillary-channeled polymer fibers as a stationary phase for the mixed-mode ion exchange/reversed-phase chromatography separation of proteins. *J. Chromatogr. Sci.* 2007, 45 (7), 415-421.

51. Wang, L.; Stevens, K. A.; Haupt-Renaud, P.; Marcus, R. K., Dynamic evaluation of a trilobal capillary-channeled polymer fiber shape for reversed phase protein separations and comparison to the eight-channeled form. *J. Sep. Sci.* 2018, 41 (5), 1063-1073.

52. Youmans, K. B.; Wang, L.; Marcus, R. K., Application of trilobal capillary-channeled polymer (C-CP) fibers for reversed phase liquid chromatography and ESI-MS for the determination of proteins in different biological matrices. *Anal. Methods* 2019, 11 (30), 3800-3809.

53. Jiang, L.; Marcus, R. K., Microwave-assisted, grafting polymerization preparation of strong cation exchange nylon 6 capillary-channeled polymer fibers and their chromatographic properties. *Anal. Chim. Acta* 2017, 977, 52-64.

54. Jiang, L.; Marcus, R. K., Microwave-assisted grafting polymerization modification of nylon 6 capillary-channeled polymer fibers for enhanced weak cation exchange protein separations. *Anal. Chim. Acta* 2017, 954, 129-139.

55. Jiang, L.; Marcus, R. K., Biotin-functionalized poly (ethylene terephthalate) capillary-channeled polymer fibers as HPLC stationary phase for affinity chromatography. *Anal. Bioanal. Chem.* 2015, 407 (3), 939-951.

56. Trang, H. K.; Schadock-Hewitt, A. J.; Jiang, L.; Marcus, R. K., Evaluation of loading characteristics and IgG binding performance of Staphylococcal protein A on polypropylene capillary-channeled polymer fibers. *J. Chromatogr. B Analyt. Technol. Biomed.* Life Sci. 2016, 1015-1016, 92-104.

57. Trang, H. K.; Marcus, R. K., Application of protein A-modified capillary-channeled polymer polypropylene fibers to the quantitation of IgG in complex matrices. *J. Pharm. Biomed. Anal.* 2017, 142, 49-58.

58. Chosed, R. J.; Polley, E.; Pike, J. F. W.; Huang, S.; Zimmerman, S.; Bruce, T. F.; Marcus, R. K.; Roudebush, W. E., Isolation, purification and initial RNA sequence analysis of seminal fluid exosomes between pregnant and non-pregnant intrauterine insemination pregnancies. *Reprod. BioMed. Online* 2020, 41, e1.

59. Stanelle, R. D.; Marcus, R. K., Nylon-6 capillary-channeled polymer (C-CP) fibers as a hydrophobic interaction chromatography stationary phase for the separation of proteins. *Anal. Bioanal. Chem.* 2009, 393 (1), 273-281.

60. Wang, L.; Marcus, R. K., Evaluation of protein separations based on hydrophobic interaction chromatography using polyethylene terephthalate capillary-channeled polymer (C-CP) fiber phases. *J. Chromatogr. A* 2019, 1585, 161-171.

SUMMARY OF CHAPTERS

CHAPTER TWO

SOLID PHASE EXTRACTION OF EXOSOMES FROM DIVERSE MATRICES VIA A POLYESTER CAPILLARY-CHANNELED POLYMER (C-CP) FIBER STATIONARY PHASE IN A SPIN-DOWN TIP FORMAT

Exosomes, a subset of the extracellular vesicle (EV) group of organelles, hold great potential for biomarker detection, therapeutics, disease diagnosis, and personalized medicine applications. The promise and potential of these applications are hindered by the lack of an efficient means of isolation, characterization, and quantitation. Current methods for exosome and EV isolation (including ultracentrifugation, microfiltration, and affinity-based techniques) result in impure recoveries with regard to remnant matrix species (e.g., proteins, genetic material) and are performed on clinically irrelevant time and volume scales. To address these issues, a polyethylene terephthalate (PET) capillary-channeled polymer (C-CP) fiber stationary phase is employed for the solid-phase extraction (SPE) of EVs from various matrices using a micropipette tip-based format. The hydrophobic interaction chromatography (HIC) processing and a spin-down workflow are carried out using a table-top centrifuge. Capture and subsequent elution of intact, biologically active exosomes are verified via electron microscopy and bioassays. The performance of this method was evaluated by capture and elution of exosome standards from buffer solution and three biologically relevant matrices: mock urine, reconstituted non-fat milk, and exosome-depleted fetal bovine serum (FBS). Recoveries

were evaluated using UV-Vis absorbance spectrophotometry and ELISA assay. The dynamic binding capacity (50%) for the 1-cm-long (~ 5 μL bed volume) tips was determined using a commercial exosome product, yielding a value of ~ 7×10^{11} particles. The novel C-CP fiber spin-down tip approach holds promise for the isolation of exosomes and other EVs from various matrices with high throughput, low cost, and high efficiency.

CHAPTER THREE

RAPID ISOLATION OF EXTRACELLULAR VESICLES FROM DIVERSE BIOFLUID MATRICES VIA CAPILLARY-CHANNELED POLYMER FIBER SOLID-PHASE EXTRACTION MICROPIPETTE TIPS

Extracellular vesicles (EVs) play essential roles in biological systems based on their ability to carry genetic and protein cargos, intercede in cellular communication and serve as vectors in intercellular transport. As such, EVs are species of increasing focus from the points of view of fundamental biochemistry, clinical diagnostics, and therapeutics delivery. Of particular interest are 30–200 nm EVs called exosomes, which have demonstrated high potential for use in diagnostic and targeted delivery applications. The ability to collect exosomes from patient biofluid samples would allow for comprehensive yet remote diagnoses to be performed. While several exosome isolation methods are in common use, they generally produce low recoveries, whose purities are compromised by concomitant inclusion of lipoproteins, host cell proteins, and protein

aggregates. Those methods often work on lengthy timescales (multiple hours) and result in very low throughput. In this study, capillary-channeled polymer (C-CP) fiber micropipette tips were employed in a hydrophobic interaction chromatography (HIC) solid-phase extraction (SPE) workflow. Demonstrated is the isolation of exosomes from human urine, saliva, cervical mucus, serum, and goat milk matrices. This method allows for quick (<15 min) and low-cost (<$1 per tip) isolations at sample volume and time scales relevant for clinical applications. The tip isolation was evaluated using absorbance (scattering) detection, nanoparticle tracking analysis (NTA), and transmission electron microscopy (TEM). Exosome purity was assessed by Bradford assay, based on the removal of free proteins. An enzyme-linked immunosorbent assay (ELISA) to the CD81 tetraspanin protein was used to confirm the presence of the known exosomal-biomarker on the vesicles.

CHAPTER FOUR

COMPARISON OF THE CAPILLARY-CHANNELED POLYMER (C-CP) FIBER SPIN-DOWN TIP APPROACH TO TRADITIONAL METHODS FOR THE ISOLATION OF EXTRACELLULAR VESICLES FROM HUMAN URINE

Capillary-channeled polymer fiber (C-CP) solid-phase extraction tips have demonstrated the ability to produce clean and concentrated extracellular vesicle (EV) recoveries from human urine samples in the small EV size range (< 200 nm). An organic modifier-assisted hydrophobic interaction chromatography (HIC) approach is applied in

the spin-tip method under non-denaturing conditions-preserving the structure and bioactivity of the recovered vesicles. The C-CP tip method can employ either acetonitrile or glycerol as an elution modifier. The EV recoveries from the C-CP tip method (using both of these solvents) were compared to those obtained using the ultracentrifugation (UC) and polymer precipitation (exoEasy and ExoQuick) EV isolation methods for the same human urine specimen. The biophysical and quantitative characteristics of the recovered EVs using the five isolation methods were assessed based on concentration, size distribution, shape, tetraspanin surface marker protein content, and purity. In comparison to the traditionally used UC method and commercially available polymeric precipitation-based isolation kits, the C-CP tip introduces significant benefits with efficient (< 15 min processing of 12 samples here) and low-cost (< $1 per tip) EV isolations, employing sample volumes (10 μL^{-1} mL) and concentration (up to 4×10^{12} EVs mL^{-1}) scales relevant for fundamental and clinical analyses. Recoveries of the target vesicles versus matrix proteins were far superior for the tip method versus the other approaches.

CHAPTER FIVE

FACILE, GENERIC CAPTURE AND ON-FIBER DIFFERENTIATION OF EXOSOMES VIA CONFOCAL IMMUNOFLUORESCENCE MICROSCOPY USING A CAPILLARY-CHANNELED POLYMER FIBER SOLID-PHASE EXTRACTION TIP

There is great interest in advancing methodologies for the isolation and characterization of exosomes (30–150 nm, extracellular vesicles (EVs)) for fundamental biochemical research and liquid biopsy applications. This is due to the accessibility of exosomal surface biomarkers, providing relevant biochemical information from their cells of origin. Exosome-based techniques hold potential for diagnostic applications through less invasive sampling (versus the physical extraction methods of pathology). This study demonstrates a simple spin-down tip methodology for generic exosome capture, followed by immunoaffinity-based fluorescent labeling to classify EVs captured on a polyester capillary-channeled polymer (C-CP) fiber stationary phase. An antibody to the generic EV tetraspanin protein (CD81) is employed to confirm the presence of biologically active EVs on the fiber surface. An antibody to the CA125 protein, upregulated in the case of ovarian cell stress, is included as a cancer marker protein. Scanning electron microscopy and confocal fluorescence microscopy were performed directly on the capture fibers to visualize the morphology and assess the bioactivity/identity of captured vesicles. This report provides a proof-of-concept for an efficient means of isolating, purifying, immunolabeling, and fluorescent imaging for the biomarker assessment of extracellular vesicles on a single platform. Herein lies the novelty of the overall approach. The ability to affect the entire isolation, immunolabeling, and imaging process in <5 hours is demonstrated. The C-CP fiber spin-down tip is an efficient exosome isolation methodology for microliter samples from diverse media (human urine and cell culture media here) towards diverse means of characterization and identification.

CHAPTER SIX

A RAPID CAPILLARY-CHANNELED POLYMER (C-CP) FIBER SPIN-DOWN TIP APPROACH FOR THE ISOLATION OF PLANT-DERIVED EXTRACELLULAR VESICLES (PDEVS) FROM 20 COMMON FRUIT AND VEGETABLE SOURCES

In the emerging field of phyto-nanotechnology, 30-200 nm plant-derived extracellular vesicles (PDEVs) are now known to contain active biomolecules that mediate cell-to-cell communication processes in a manner very similar to exosomes in mammalian cells. The ability to deliver cargo across cellular membranes suggests that botanical systems could be used in the mass production of therapeutic vectors to transport exogenous molecules into human cells. The fundamental biochemical characteristics of PDEVs remain poorly understood due to the lack of efficient methods to isolate and characterize these nanovesicles. Described here is a rapid PDEV isolation method using a hydrophobic interaction chromatography (HIC)-based extraction performed on a capillary-channeled polymer (C-CP) fiber spin-down tip. The C-CP solid-phase extraction method is performed using a standard table-top centrifuge, enabling the isolation and concentration of PDEVs (>1 x 10^{10} particles from 100 µL of sample). PDEVs of 189 nm average diameter were obtained from 20 common fruit and vegetable stocks. The size, integrity, and purity of the recovered PDEVs were assessed using transmission electron microscopy (TEM), multi-angle light scattering (MALS), absorbance quantification, a protein purity assay, and an enzyme-linked immunosorbent assay (ELISA) to the PEN1 PDEV surface marker protein. The HIC C-CP tip isolation

method allows for concentrated PDEV recoveries (up to 2 x 10^{11} EVs) on reasonable time scales (<15 min) and low cost (<$1), with the purity and integrity fit for fundamental research and downstream applications.

CHAPTER SEVEN

RAPID ISOLATION AND QUANTIFICATION OF EXTRACELLULAR VESICLES FROM SUSPENSION-ADAPTED HUMAN EMBRYONIC KIDNEY CELLS USING CAPILLARY-CHANNELED POLYMER FIBER SPIN-DOWN TIPS

Exosomes, a subset of extracellular vesicles (EVs, 30-200 nm diameter), serve as biomolecular snapshots of their cell of origin and vehicles for intercellular communication, playing roles in biological processes including homeostasis maintenance and immune modulation. The large-scale processing of exosomes for use as therapeutic vectors has been proposed, but these applications are limited by impure, low-yield recoveries from cell culture milieu (CCM) across all volumes. Current isolation methods are also limited by tedious and laborious workflows, especially during the isolation of EVs from CCM for therapeutic applications. Employed is a rapid (<10 minute) EV isolation method on a capillary-channeled polymer (C-CP) fiber spin-down tip format. EVs are isolated from the CCM of suspension-adapted human embryonic kidney cells (HEK293), one of the candidate cell lines for commercial EV production. This batch solid-phase extraction technique allows 10^{12} EVs to be obtained from only 100 µL aliquots of milieu, processed using a benchtop centrifuge. The tip-isolated EVs were

characterized using transmission electron microscopy (TEM), multi-angle light scattering (MALS), absorbance quantification, an enzyme-linked immunosorbent assay (ELISA) to tetraspanin marker proteins, and a protein purity assay. It is believed that the demonstrated approach has immediate relevance in research and analytical laboratories, with opportunities for production-level scale-up projected.

LIST OF PUBLICATIONS

The following chapters in this dissertation are based on these papers:

Chapter Two: Jackson, K. K., Powell, R. R., Bruce, T. F., & Marcus, R. K. (2020). Solid-phase extraction of exosomes from diverse matrices via a polyester capillary-channeled polymer (C-CP) fiber stationary phase in a spin-down tip format. *Analytical and bioanalytical chemistry*, 412(19), 4713-4724.

Chapter Three: Jackson, K. K., Powell, R. R., Bruce, T. F., & Marcus, R. K. (2021). Rapid isolation of extracellular vesicles from diverse biofluid matrices via capillary-channeled polymer fiber solid-phase extraction micropipette tips. *Analyst*, 146(13), 4314-4325.

Chapter Four: Jackson, K. K., Powell, R. R., Marcus, R. K., & Bruce, T. F. (2022). Comparison of the capillary-channeled polymer (C-CP) fiber spin-down tip approach to traditional methods for the isolation of extracellular vesicles from human urine. *Analytical and Bioanalytical Chemistry*, 414(13), 3813-3825.

Chapter Five: Jackson, K. K., Powell, R. R., Bruce, T. F., & Marcus, R. K. (2022). Facile, generic capture and on-fiber differentiation of exosomes via confocal immunofluorescence microscopy using a capillary-channeled polymer fiber solid-phase extraction tip. *Sensors & Diagnostics*, 1(3), 525-533.

Chapter Six: Jackson, K. K. & Marcus, R. K. (2022). A Rapid Capillary-Channeled Polymer (C-CP) Fiber Spin-Down Tip Approach for the Isolation of Plant-Derived Extracellular Vesicles (PDEVs) from 20 Common Fruit and Vegetable Sources. *Talanta, submitted*.

Chapter Seven: Jackson, K. K. & Marcus, R. K. (2022). Rapid Isolation and Quantification of Extracellular Vesicles from Suspension-Adapted Human Embryonic Kidney Cells using Capillary-Channeled Polymer Fiber Spin-Down Tips. *Electrophoresis, submitted*.

CHAPTER TWO

SOLID PHASE EXTRACTION OF EXOSOMES FROM DIVERSE MATRICES VIA A POLYESTER CAPILLARY-CHANNELED POLYMER (C-CP) FIBER STATIONARY PHASE IN A SPIN-DOWN TIP FORMAT

2.1 Introduction

Exosomes are 30–130 nm-sized extracellular vesicles (EVs) containing genetic, proteomic, and intracellular content that reflect the biophysical characteristics of the cells of origin, and engage in diverse pathological and physiological roles [1, 2]. Exosomes are released from most cell types through multivesicular bodies (MVBs), which are distinctly created through the endosomal pathway [1, 3, 4], different from the biogenesis of many other extracellular vesicles [5, 6]. Exosomes carry intravesicular cargo, including DNA, RNA, miRNA, as well as surface biomarker proteins—all promising tools for unraveling the inner-workings of disease progression [7]. Exosomes mediate a plethora of inter- and intracellular processes, including cellular communication and signaling phenomena, and contain essential cargo for local and distal cargo transport processes [8]. Because the dysregulation of intercellular communication processes leads to cancers and immune-physical malfunctions, exosomes/EVs have become relevant to understanding many complex biochemical interactions [9,10,11]. Additionally, as the rate of exosome biogenesis differs based on the cell of origin, the simple ability to readily determine the concentration of exosomes is of high interest. An upregulation of exosome biogenesis is indicative of active disease progression [12, 13]. Increased exosome-mediated signaling

is characteristic of invasive tumor phenotypes [12], so it is essential to be able to efficiently quantify exosomes in various types of samples. A pool of cells is well represented by a collection of exosomes, making them a promising analytical target for liquid biopsy applications.

Exosomes/EVs are expressed by most cells and, as such, can be collected from bodily fluids, including urine [14], saliva [15], blood (plasma [15] and serum [16]), breast milk [17, 18], and cerebrospinal fluids [19, 20], and are also released in vitro by cultured cells [21]. Furthermore, exosomes and other extracellular vesicles have been identified in all three physiological domains of life (*archaea* [22], bacteria [23, 24], and *eukarya* [22]) and are active agents of nutrient delivery by interspecies communication through intake of foods like raw vegetables [25]. A challenge in the progression of exosome/EV-based applications lies in the recovery of clean, stable, and biologically relevant vesicles for genetic profiling, bioengineering, and biomarker classification.

A large number of approaches have been used for exosome/EV isolation, including ultracentrifugation, differential centrifugation, density-gradient centrifugation, size exclusion chromatography, affinity chromatography, and several polymer-based precipitation techniques [8, 26, 27]. These separation techniques rely on either the size and density of the EVs, or the affinity of the exosomes for antibodies to specific surface marker proteins such as Alix, CD9, CD81, TSG101, and HSP70 [27]. Current exosome/EV isolation methods are tedious and are often used following multiple high-speed ultracentrifugation (> 100,000×*g*) steps to remove debris and pelletize the exosomes [26]. While the high-speed ultracentrifugation method is the most widely used

technique for generic exosome isolation, it does not always efficiently isolate exosomes from large protein aggregates or other vesicular structures efficiently. In all, these techniques are time-consuming and sample-size burdensome to the point of limiting the use of exosomes on the clinical scale [27, 28]. Because biological sample matrices are extremely complex and varied, robust separation techniques are crucial for future clinical applications and fundamental research [29].

Marcus and co-workers have described the use of capillary-channeled polymer (C-CP) fibers as stationary phases for liquid chromatography (LC) separations of proteins via reversed-phase (RP), ion exchange (IEC), hydrophobic interaction (HIC), and affinity modalities [30,31,32,33,34,35,36]. The combination of high column permeability and low surface porosity provides high throughput and yield macromolecule separations [37,38,39]. Bruce, Marcus, and colleagues have also recently reported a method for exosome/EV isolation using an HIC mode on a poly (ethylene terephthalate) (PET) C-CP fiber phase [40,41,42,43]. The use of the HIC elution strategy allows for exosome isolations based on the vesicles' inherent hydrophobicity (partially a function of their size), allowing non-destructive bulk recoveries of exosomes/EVs for further interrogation and applications. Capture/elution under HIC solvent conditions preserves the morphology of the vesicles isolated from various matrices, including cell culture milieu [40], urine [40, 42], and human plasma [41]. In terms of potential implementation scenarios, isolations are performed on < 100 μL sample volumes on time scales of < 10 min. The simple chromatographic method also shows promise for bulk recovery of EVs for fundamental biochemistry and preparative applications.

While a standard liquid chromatograph is not overly burdensome in the analytical chemistry laboratory, it is not practical in many biochemical and clinical situations. Solid-phase extraction (SPE) techniques are widely applied for sample preparation of biological specimens, as they allow for efficient separation of analytes from the originating complex matrices [44,45,46]. SPE is a form of step-wise chromatography that is designed to extract and adsorb components of interest from a liquid phase onto a stationary phase (similar to LC separations), thus serving as a means of pre-concentration and affecting a matrix modification. Many modalities influence the passage of sample solutions through an SPE bed, but the use of a table-top or microcentrifuge is particularly attractive in terms of very low operational complexity and overhead [47, 48]. In this regard, C-CP fibers can be employed either as the stationary phase column for HPLC or employed in 1-cm segments fit to a micropipette tip to affect SPE in a spin-down mode using a table-top centrifuge [49,50,51]. In these applications, fiber phases have also been used as a means of desalting proteins before MS characterization [52] and also to affect immunoaffinity capture [51].

Here, PET C-CP fiber micropipette tips are employed in a novel spin-down HIC protocol for the timely, efficient, and structurally preserving isolation and quantification of exosomes from various matrices (aqueous solution, mock urine, reconstituted non-fat milk, and an exosome-depleted fetal bovine serum). Mock matrices were used to normalize and control the exosome quantity input, while also presenting basic sample constituents. The goal is to quantify and characterize exosome recoveries of known spike concentrations from the various matrices without interference or introduced bias from

native exosome-containing biofluids. The sequential aspects of immobilization and recovery are affected for multiple tips in parallel, in a total processing time of < 5 min. The capture of intact exosomes is verified via scanning electron microscopy (SEM) and confocal microscopy, with the efficacy of the elution confirmed via transmission electron microscopy (TEM) and dot blot analysis. The binding capacity of the 1 cm fiber tips is evaluated via sequential applications of sample aliquots until an observed breakthrough, with the recoveries determined spectrophotometrically. Finally, the ability to quantify EV recoveries via absorbance measurements is demonstrated and employed in the evaluation of recoveries of exosomes spiked into various mock-biofluid matrices. This simple and straightforward method for exosome isolation and quantification opens the door for future fiber platform optimization for selective EV-type isolations for clinical diagnostics and fundamental biochemistry research.

2.2 Materials and Methods

2.2.1 Materials

HPLC-grade acetonitrile (ACN) was obtained from ThermoFisher Scientific (Pittsburgh, PA, USA). Deionized water (DI-H_2O, 18.2 MΩ-cm) was obtained from a Milli-Q water purification system (Millipore Sigma, Merck, Germany, USA). Ultra-pure ammonium sulfate was obtained from VWR (Radnor, PA, USA). Biotechnology-grade glycerol was purchased from VWR (Sokon, OH, USA). Non-fat dry milk was purchased from Bio-Rad (Hercules, CA, USA). Phosphate-buffered saline (PBS, 0.067 M (PO_4), pH 7.4) and exosome-depleted fetal bovine serum (FBS) were obtained from ThermoFisher

Scientific (Waltham, MA, USA). Tris-buffered saline (TBS, 0.1 M, pH 8.0) was obtained from Sigma Aldrich (St. Louis, MO, USA). Uranyl acetate, 16% paraformaldehyde (formaldehyde) aqueous solution, and formvar/carbon film 10 nm/1 nm thick on square 200 mesh copper grids were obtained from Electron Microscopy Sciences (Hatfield, PA, USA). The 1-Step Ultra TMB-ELISA substrate was purchased from ThermoFisher Scientific (Pittsburgh, PA, USA). The Anti-rabbit IgG (H+L) 10nm Silver Conjugate (OD 7.5) and Silver Enhancer Kit for membranes were obtained from Cytodiagnostics (Burlington, ON, Canada).

The mock urine was prepared based on the recipe as reported by Khan et al. [52], consisting of an aqueous solution of potassium chloride (0.2 g L^{-1}), sodium chloride (8 g L^{-1}), disodium hydrogen phosphate (1.14 g L^{-1}), potassium dihydrogen phosphate (0.2 g L^{-1}), 200 μL L^{-1} McCormick yellow food coloring (water, propylene glycol, FD&C yellow 5, and propylparaben), urea (114.1 g L^{-1}) and DI-H_2O up to 1 liter. Hydrochloric acid and sodium hydroxide were used to adjust the pH to 7.5. The solution of 2% non-fat dry milk was dissolved in DI-H_2O to create the milk matrix.

2.2.2 Instrumentation

Three absorbance spectrophotometers were employed in these studies, based on the required sample volume for measurement, the instrument's sensitivity to changes in absorbance, and the sample introduction method. A NanoVue Plus UV-Vis spectrophotometer (GE Healthcare, Chicago, IL, USA) was used to measure the direct absorbance of the concentrated exosome eluates (1 μL) from the C-CP fiber tip (as shown in Fig. 2.4). A GENESYS 10S UV-Vis spectrophotometer (ThermoFisher Scientific,

Waltham, MA, USA) was used to measure the absorbance of diluted exosome eluate. (as shown in Fig. 2.5). The Synergy H1 Hybrid Multi-Mode Reader (BioTek, Winooski, VT) was used to determine the UV-Vis absorbance (450 nm) of samples in the 96-well format as employed in an ELISA assay employing the 1-Step Ultra TMB Substrate.

Electron microscopy was employed as a confirmatory tool for the structural integrity of both immobilized and eluted EVs. Scanning electron microscopy (SEM) was performed using a Hitachi S-4800 (Chiyoda, Tokyo, Japan) to confirm the capture of intact EVs on the C-CP fiber surface. Transmission electron microscopy (TEM) was performed using a Hitachi HT7830 (Chiyoda, Tokyo, Japan) to confirm the release of intact EVs from the C-CP fiber surface. STEM imaging was performed using the Hitachi SU9000 CFE SEM/STEM to observe the integrity of eluted exosomes. The methods for fixing and imaging of these populations, which are not innovative in their own right, are described in Appendix A.

Confocal microscopy was used to image the C-CP fiber tip-captured exosomes after undergoing immune-recognition procedures for the confirmation of the capture of exosomes exhibiting the CD81 tetraspanin marker protein. In preparation for this technique, the fiber-captured vesicles were stained using a mouse primary antibody to CD81 (Santa Cruz Biotechnology, Dallas, TX) followed by a goat anti-mouse secondary antibody labeled with AlexaFluor 647 before super-resolution confocal imaging with a Leica SP8 confocal microscope with Hyvolution super-resolution software (Leica Microsystems, Buffalo Grove, Illinois). A sandwich enzyme-linked immunosorbent assay (ELISA) was used to detect and quantify the expression of the tetraspanin exosomal

marker protein, CD81, in exosome recoveries following elution from the C-CP fiber tip from various matrices. CD81 expression in the recoveries of exosomes isolated by the C-CP spin-down tip was further confirmed using an immuno-dot blot assay. Briefly, recovered exosomes were captured by the immobilized CD81 mouse antibody on a PVDF membrane, and subsequently detected using rabbit primary antibodies to generic tetraspanin antibodies (CD9, CD81, CD63), and visualized using a goat anti-rabbit silver nanoparticle conjugate, followed by the use of a silver enhancement kit to amplify the resultant response (see Appendix A).

2.2.2 Methods

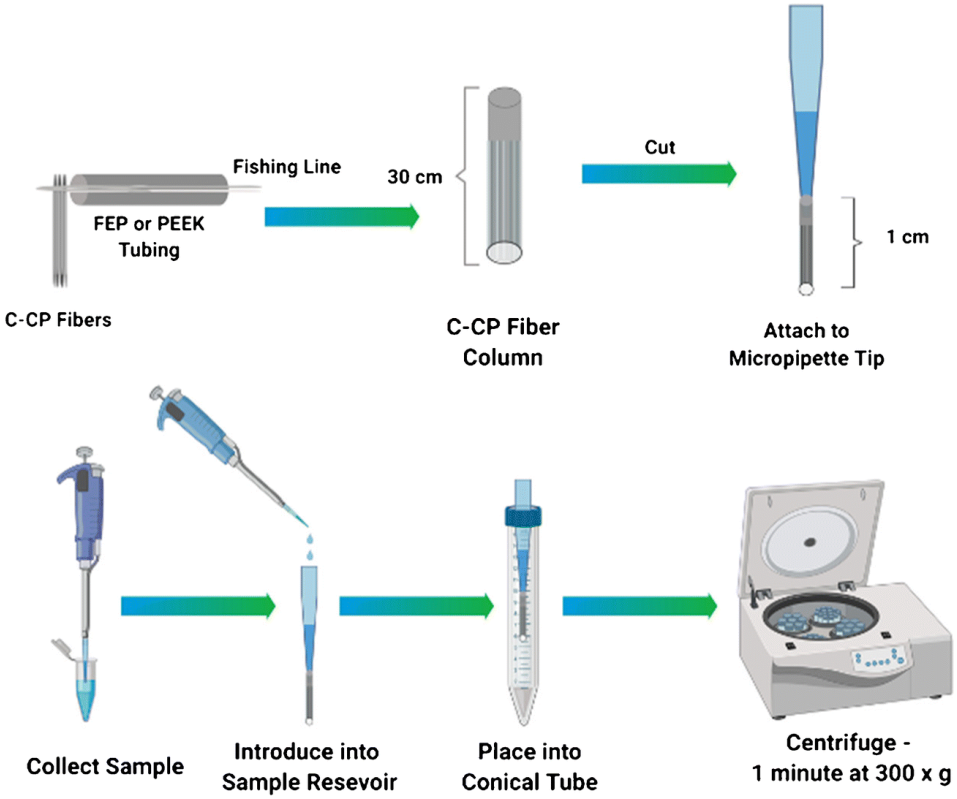

Figure 2.1: The practical steps of C-CP fiber tip fabrication and the spin-down approach to isolation and purification of EVs.

The C-CP fiber SPE tip assembly process is depicted in Fig. 2.1. Poly (ethylene terephthalate) (PET) capillary-channeled polymer fibers were extruded by the Clemson University School of Materials Science. The C-CP fiber tips were constructed as previously reported [48] (see Appendix A). Ultimately, tips of 1 cm-length, having an inner diameter of 0.8 mm, and an interstitial fraction of ~0.6, yielded bed volumes of ~3 μL. The method for mounting the spin-down tips for processing and collection of EV fractions has also been described previously [48] (see Appendix A). The efficient reuse (n>15) of the C-CP fiber stationary phase has been demonstrated in a column format used in HPLC isolation of exosomes from a mock urine matrix [1]. However, given the low consumable cost (<$0.5 USD per tip) and for the sake of convenience, new C-CP micropipette tips were employed for each exosome isolation here.

Lyophilized and purified exosomes from the urine of reportedly healthy donors were obtained from Galen Laboratory Supplies (North Haven, CT, USA) with a prepared suspension concentration of 2.27×10^{12} particles mL^{-1} (provider-determined by nanoparticle tracking analysis (NTA)). For HIC-based processing, EVs in the mock sample matrices were mixed 1:1 with 2 M ammonium sulfate at pH = 7.5. Aliquots of 100 μL per trial were passed through the C-CP fiber tips under 300 x g centrifugal force for 1 minute each. Under the high salt conditions, the target vesicles and latent proteins (from the original sample) were retained on-fiber. After the capture of the vesicles, the fiber surfaces were washed with 100 μL of DI-H_2O. Protein elution was induced by

passage of 50 µL of 25% glycerol in PBS under the same centrifugation conditions, with the final elution of the captured EVs induced using 50 µL of 50% glycerol in PBS. The elution of proteins by 25% glycerol and exosomes by 50% glycerol has been confirmed by SEM imaging of the fiber surfaces after the various steps in this workflow as well as in the use of acetonitrile as the mobile phase modifier [1, 2], as it is here. The eluted EVs were quantified by diluting a 3 µL aliquot to 1.5 mL with DI-H_2O. Absorbance measurements were performed using a GENESYS 10S UV-Vis spectrophotometer. Additionally, an enzyme-linked immunosorbent assay (ELISA) was used to confirm the presence of CD81-expressing EVs in the spin-down tip recoveries.

To determine dynamic binding capacity, breakthrough experiments were performed using 21 successive 50 µL aliquots of the diluted exosome standard (4.65 x 10^7 particles per 50 µL aliquot in 1M ammonium sulfate with 25% glycerol), spun through the tips (300 x g, 1 minute each). Use of the glycerol modifier inhibits the adsorption of adventitious proteins. The fiber surfaces were then washed five times with 50 µL aliquots of diH_2O.

2.3 Results and Discussion

2.3.1 Capture and elution fidelity

As with all forms of biomolecule/particle isolation, a successful SPE spin-down methodology for exosome/EV isolation and recovery must provide not only for separation, but must do so without compromising the physical and biological attributes of the EVs. In this case, EVs must be isolated with respect to the components of the sample

matrix, including salts, small molecules, such as amino acids, sugars, proteins, and genetic material. Previous reports have illustrated this capability via HIC separation of exosomes from diverse media [1, 3, 4]. In the case of the spin-down tip processing, the integrity of the physical and biological attributes of the exosomes was evaluated via SEM and immunofluorescence, respectively, following the elution steps to remove salts and adventitious proteins.

In Fig. 2.2a (for the case of the commercial exosomes dispersed in water), the surface of the C-CP fibers at this stage is pristine, as indicated by the presence of globular vesicles without any remnants of salt crystals or the like.

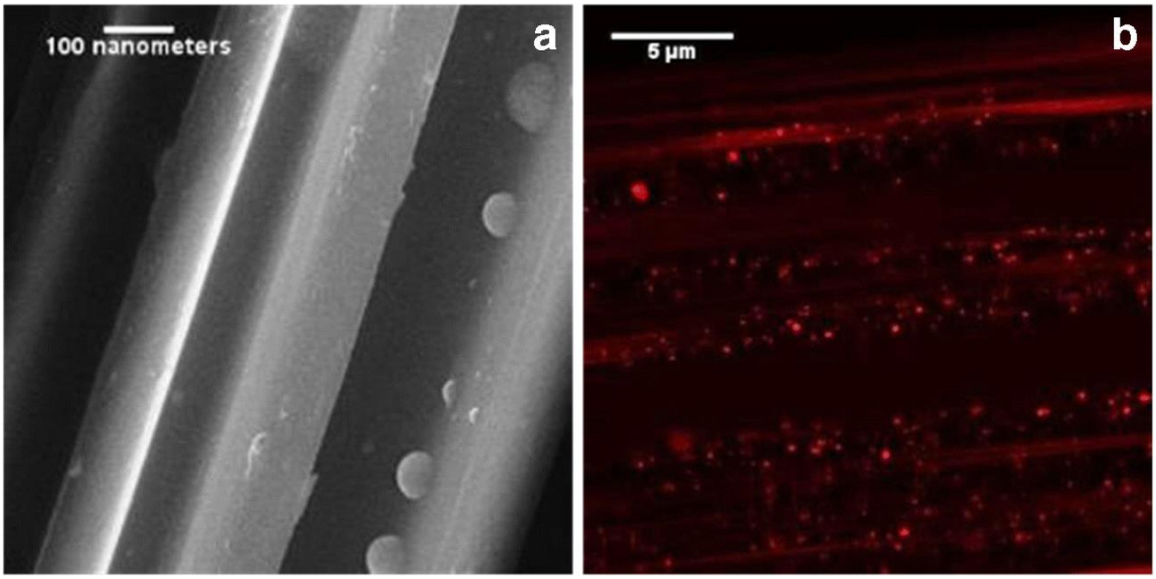

Figure 2.2: Physical and biologic imaging of exosomes adsorbed to PET C-CP fiber surface via a scanning electron microscopy and b super-resolution confocal fluorescence microscopy.

To further illustrate the integrity of the captured exosomes, super-resolution confocal microscopy imaging was performed. Exosomes captured on C-CP fiber surfaces were immuno-labeled using a primary antibody to the tetraspanin surface marker protein,

CD81, and a fluorescent secondary antibody (AlexaFluor 647 goat anti-mouse). As seen in Fig. 2.2b, there are dispersed nanobodies (of the size range expected for the target exosomes) within the ~25 x 25 μm^2 viewing region. Due to the resolution limits of the confocal microscope system used (~140 nm), it is important to note that the fluorescent particles observed here are not necessarily individual exosomes, but perhaps small aggregates producing a more intense fluorescent response. Nevertheless, with regards to capture, the target exosomes are well dispersed on the fiber surface (without substantial debris), while maintaining their basic physical morphology and surface protein makeup. Indeed, the characteristics depicted in Fig. 2.2 are the first steps towards affecting a practical exosome diagnostic platform.

In those cases where further exosome characterization is required, such as in the search for surface biomarkers or genetic analysis (e.g., RNA-Seq) of the vesicular cargo, the organelles must be recovered (eluted) while maintaining their physical integrity and biological function. The most common method for assessment of the morphology of individual exomes is transmission electron microscopy, where both the size and vesicular structure are revealed.

a

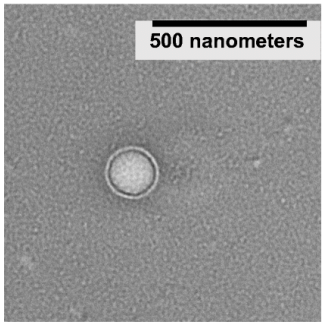

b

Antibody	Positive Control	Sample	Negative Control
CD9			
CD63			
CD81			

Figure 2.3: Physical and biological characterization of exosomes eluted from PET C-CP fiber spin-down tips via a) transmission electron microscopy and b) dot blot immunoassay.

The TEM micrograph of an HIC-eluted EV (Fig. 2.3a) illustrates the successful maintenance of the physical structure through the isolation process. The biological fidelity of exosome populations is readily assessed through the use of dot blot assays (Fig. 2.3b), wherein a positive immune-response is obtained for the CD9, CD81, and CD63 antibodies in the post-tip isolation eluates. As seen in the various exposures, the recovered exosomes do indeed retain the surface markers of the three tetraspanin proteins confirming the presence and viability of the exosomes. While the dot blots do not reflect the retention of the encapsulated genetic materials, they suggest that the expected membrane-bound proteins remain intact.

2.3.2 Dynamic binding capacity (DBC)

The ability to effectively isolate and purify EVs is only relevant to the extent that it yields the required density of EVs necessary to provide meaningful sample data. As a general rule, most RNA-sequencing analyses require $10^{9\text{-}10}$ exosomes for accurate profiling, while LC/MS proteomics studies require on the order of $10^{10\text{-}11}$ exosomes. [5-11] To this end, the dynamic binding capacity of the 1 cm C-CP fiber spin-down tips was determined (Fig. 2.4).

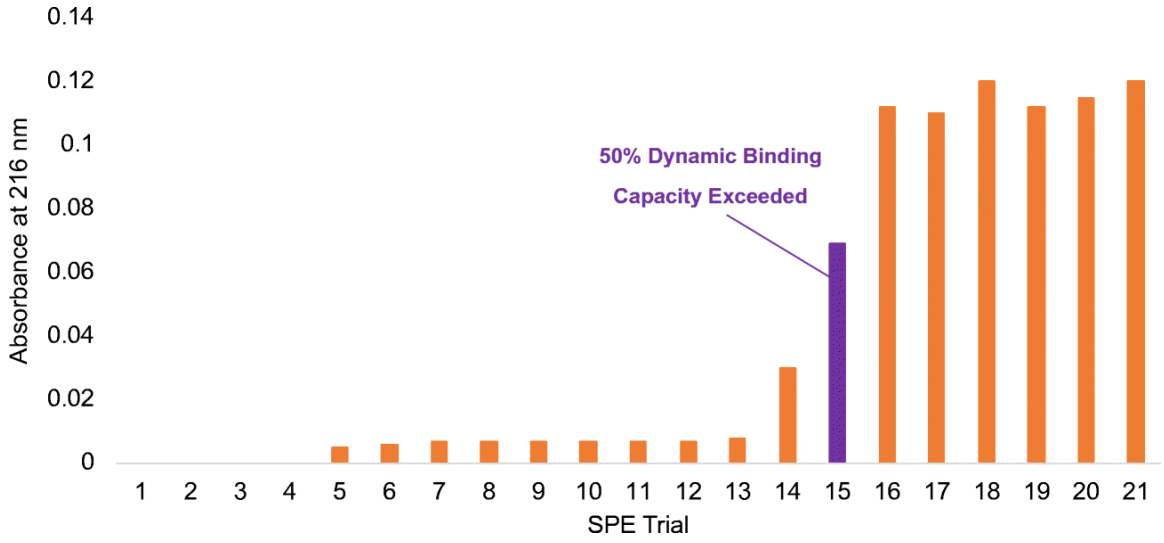

Figure 2.4: Breakthrough analysis of 50 µL aliquot additions of 4.65 × 10^{10} particles per dose. The 50% dynamic binding capacity is surpassed during trial 15 at 6.98 × 10^{11} particles.

Unlike in the case of continuous processes [12], a frontal analysis was required. This was performed using discrete 50 µL aliquots of test solutions (exosomes in 25% glycerol:1 M $(NH_4)_2 SO_4$), with the pass-through exosome content used to assess breakthrough/overload. Fig. 2.4 shows the determined absorbance values, obtained by diluting 3 µL of the eluate in DI-H_2O in a 1.5 mL cuvette. The absorbance response is not significant until aliquot #14, wherein the pass-through content increases rapidly, and a plateau is reached beyond aliquot #16, suggestive of surface saturation. Based on the general response, the eluate absorbance reaches one-half of the steady maximum value (a measure of reaching DBC) with aliquot #15. At this point, based on per-aliquot particle densities of 4.65 x 10^{10}, a DBC value on the order of ~7 x 10^{11} is achieved for a total volume of 750 µL. Though there is no consensus regarding a "healthy range" for exosome concentration, this value is in line with that expected in many native biofluids,

including urine, milk, serum, and plasma. The capacity demonstrated at this early stage is on-par for what would be desired in the clinical and biochemical laboratory arenas.

2.3.3 Quantification

In previous EV separations employing PET C-CP fiber columns in a Dionex Ultimate 3000 HPLC system (ThermoFisher Scientific, Waltham, MA, USA), UV-vis absorbance at 203, 216, and 280 nm was used as a method for EV detection [3]. Even with the well-known optical absorbance of some buffer/matrix components at these wavelengths, a successful method of exosome isolation should alleviate their contributions and allow ready quantification. The absorbance response observed in this instance is not due to the molecular absorption of an innate biomolecule, but rather corresponds to the light scattering due to the presence of the particles. Ultimately, the absorbance response was found to be directly proportional to the exosome content, for particles of different sources. As most methods of EV isolation carry along remnant proteins, there is a potential that the absorbance (scattering)-based measurement could be affected by their presence.

Based on the fact that the extent of scattering would be (nominally) inversely related to the incident wavelength, and that proteins (being composed of aromatic amino acids) absorb at 280 nm, response functions were prepared at 203, 216, and 280 nm. Lyophilized exosome standards from the urine of reportedly healthy donors (previously shown to have latent proteins present) were used to create standard curves. Here, 1-35 μL of the exosome standards (2.3×10^{12} particles mL^{-1}) were diluted to 1.0 mL in DI-H_2O, presenting a concentration range of ~2.3×10^{9} – 8.0×10^{10} particles mL^{-1} (Table 1).

Table 2.1: Absorbance response characteristics for exosome standards in aqueous solution at 203, 216, and 280 nm.

λ (nm)	Response function	R^2	LOD (particles mL^{-1})	LOQ (particles mL^{-1})
203	$y = 5E{-}16x + 0.0076$	0.9958	6.05×10^9	2.02×10^{10}
216	$y = 5E{-}16x + 0.0077$	0.9938	7.58×10^9	2.53×10^{10}
280	$y = 7E{-}16x + 0.0069$	0.9808	1.22×10^{10}	4.08×10^{10}

The slope of the 280 nm function is approximately 40% higher than the lower wavelengths. The stronger absorbance at 280 nm reflects the inevitable presence of proteins (which contain aromatic amino acids) in the commercial exosome material. Indeed, the characteristics for the lower wavelengths are virtually identical, with much better regression statistics than at the higher wavelength. Based on these figures of merit, and fewer contributions from background proteins, the shorter wavelengths are preferred. While the limits of detection and quantification are not as low as with other methods (e.g., immunoassays) [13-18], the values are relevant for most biological and clinical systems of interest, particularly in consideration of the total sample volume required (< 50 µL) and ease of determination.

2.3.4 Isolation and quantification of EVs/exosomes in diverse media

As proof of concept towards the efficacy of the HIC spin-down tip approach to exosome isolation and quantification, the commercial exosome standards (2.73 $x10^{12}$ particles mL^{-1}) were spiked into DI-H_2O, mock urine, reconstituted non-fat milk, and exosome-depleted fetal bovine serum (FBS) matrices. Two dilution factors were employed (1/100;1/1000), as a quantitative test of the response, as well as tolerance towards the challenges of the matrices themselves. The matrices were mixed (50:50 v/v) with the HIC loading solvent (2M $(NH_4)_2SO_4$) in PBS. While diH_2O presents a pristine

environment, the mock urine matrix presents high salinity and is small molecule-heavy, the milk has high protein content, and the FBS contains fat and high protein content. These model biofluids are obvious target matrices from which exosome/EVs may be extracted for diagnostic purposes. In terms of loading and elution, the procedure involved a spin-down under high salt conditions, followed by elution of proteins with 50 μL of 25% glycerol and 1M $(NH_4)_2SO_4$ in PBS. This fraction was collected for absorbance measurements of protein/exosome content. Finally, the EV fraction was eluted in 50 μL of 50% glycerol in PBS and collected for the determination of vesicle content. Though glycerol has been used as a biological preservative [19], it is not ideal for all downstream analyses (i.e., proteomic analysis) where necessary vesicle lysing may be hindered. In these cases, acetonitrile may be used as a substitute elution phase, as previously reported [1, 2].

Essential to the quantification process of EVs in different matrices is the assumption that EVs may be quantitatively immobilized and recovered from the fiber surfaces. The latter point has been evaluated in recent studies using the chromatographic (column) platform, wherein recoveries of adsorbed EVs were greater than 80% [2]. Parallel evaluation of the recoveries was performed here via UV absorbance (using the previously generated aqueous matrix calibration functions) and an ELISA assay.

The determined numbers of EV particles for the two dilution factors, as determined via optical absorbance (203 nm), are presented in Fig. 2.5.

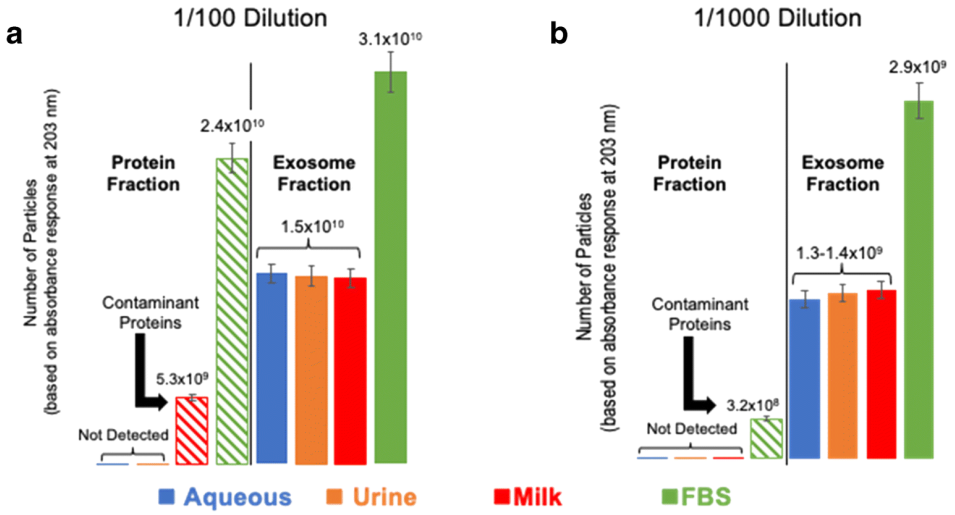

Figure 2.5: Post-isolation of exosome standards spiked into various matrices (50 µL) using the PET C-CP fiber tip spin-down method. The concentrations of exosomes recovered were determined based on absorbance response (1 µL) when compared to the standard curve of Table 1. a) Quantified recovery of exosomes from mock matrices of 1/100 concentration and b) quantified recovery of exosomes from mock matrices of 1/1000 concentration. The loaded 1/100 and 1/1000 solutions theoretically contain 2E10 and 2E9 exosomes, respectively.

Aliquots (50 µL) for both the protein and exosome elution fractions were diluted to 1 mL for the absorbance measurements. Starting with the lowest (1/100) dilution factor, no absorbance response is seen in the protein fractions for aqueous and mock-urine phases, but there is a measurable absorbance, equivalent to 5.3 x 10^9 and 2.4 x 10^{10} EVs, for the milk and exosome-depleted FBS matrices, respectively. These respective responses are not surprising, as the latter matrices have appreciable protein content, and corresponding appreciable absorbance, while the aqueous and urine matrices do not. On the other hand, absorbance measurements taken of the presumed EV fraction yield statistically identical values for the aqueous, mock urine, and non-fat milk matrices, as they would be expected. Interestingly, a much higher (~2x) recovery of EVs was observed in the

exosome-depleted FBS exosome elution fraction. The precision of triplicate measurements for each of the matrices was better than 8.4 %RSD.

For the case of the higher dilution factor (1/1000), it would be expected that the recoveries would be proportionally (~10x) less, but potential matrix effects would be lessened as well. Here, the responses for the protein elution fractions for the aqueous, mock urine, and non-fat milk matrices fall below the level for accurate determination. The FBS protein elution still shows a measurable absorbance response, equivalent to 3.2 x 10^8 EVs. This is to be expected with the high concentration of total protein in the original matrix. The greater than expected decrease in apparent concentration is due to lessened amounts of protein aggregation in the more dilute solution. That noted, the determined concentrations in the respective EV fractions are indeed ~10X less than the more concentrated case for all matrices. Here again, a high level of precision in the EV recovery is obtained (< 6.9 %RSD), with the determined particle numbers across the first three matrices being virtually the same, and a significantly higher exosome recovery again for the exosome-depleted FBS matrix. Thus, based on the absorbance-based quantification method, there is no significant difference in EV recoveries across the diverse aqueous, mock urine, and non-fat dry milk matrices. More importantly, the fractional recoveries for the two dilutions are approximately 75% versus the initial number of EVs applied to each tip for these matrices. This value reflects a significantly more efficient recovery of exosomes when compared to the fractional recoveries of other methods, such as ultracentrifugation, which results in equal or lesser concentrated recoveries of exosomes, though requiring nearly 90 times the starting sample volume. As

previously mentioned, a significant increase in recovery was observed from the FBS matrix. Marketed as an "exosome-depleted" FBS source, the manufacturer claims the depletion of 90% or more of native endogenous exosomes. The increase in EV recovery for the FBS matrix may be due to remnant exosomes from the native FBS matrix (known to contain high concentrations of EVs).

To verify and quantify the presence of remnant (native) extracellular vesicles in the exosome-depleted FBS matrix, the tip isolation of exosomes was performed on an exosome-spiked aqueous solution, the exosome-depleted FBS, and the FBS spiked with the exosome standard. In the spiked-solution cases, the primary stock solution was added at a 1:100 μL ratio to the matrix. The optical absorbance of the eluate was detected at the 203 nm wavelength and used to quantify the exosomes based on the previous aqueous-solution calibration function.

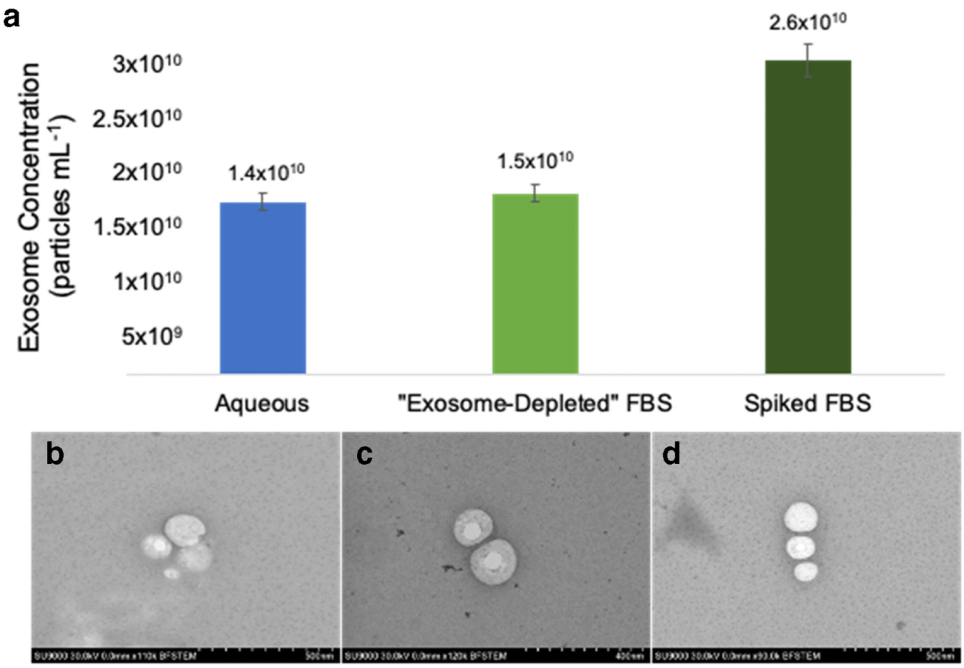

Figure 2.6: a) Quantification of exosomes in the eluates from aqueous solution (1/100), exosome-depleted FBS, and a spiked exosome-depleted FBS matrix (1/100). b–d) STEM images of eluted exosomes, all containing their characteristic spherical structure post isolation using the C-CP tip method.

Fig. 2.6a shows the resulting exosome concentrations, where approximately the same number of exosomes were quantified in the eluates from the aqueous and native exosome-depleted FBS solutions. Addition of the spike to the FBS yields an ~73% increase in the determined density, a value in-line with a combination of the responses for the aqueous solution and the FBS sample, as would be expected as the spike values are the same for the first and third cases. Importantly, the levels of precision are very uniform ranging from 5.4 – 8.2 %RSD for triplicate isolation and measurement sets. Based on the determinations performed here, the exosome concentration in the "depleted" FBS is approximately 1.5 x 10^{10} particles per mL. This value is less than recently published values of 2.27-2.93 10^{11} particles per mL [20]. Based on those values, the material

employed here meets the stated 90% clearance target stated by the manufacturer, with ~6.6% remaining based on the published values.

The presence of exosomes in the depleted FBS was further confirmed physically using STEM and nanoparticle tracking analysis. Figures 2.6b-d are micrographs of the exosome eluted fractions for the same three cases, exosomes spiked (1:100) in aqueous solution, the native FBS, and exosomes spiked into FBS. In all three cases, the typical halo-structure objects associated with exosomes are clearly revealed, having diameters on the order of 80-120 nm. NTA analysis was performed to analyze the size distribution of the eluted exosome populations. The graphical size distributions of the eluted exosomes are presented in Appendix A. Statistically, larger numbers of exosomes are observed in the case of the spiked-FBS (as suggested in the data of Fig. 2.5), though the means (~96 nm) and modes (74.3 and 77.7 nm) of the distributions are very similar. What are quite different are the broader distribution aspects, where the spiked-FBS displays a D90 (upper limit inclusive of 90% of the population) of 155.4 nm, while the spiked-aqueous population exhibits a D90 of 130.1 nm. This relationship is not surprising as the FBS is a far more diverse matrix than the human-urine originating spike matrix.

As a complement to the use of absorbance spectrophotometry to perform quantification, spin-down tip recoveries were also assessed via a standard ELISA assay for the antibody response to the CD81 tetraspanin surface protein.

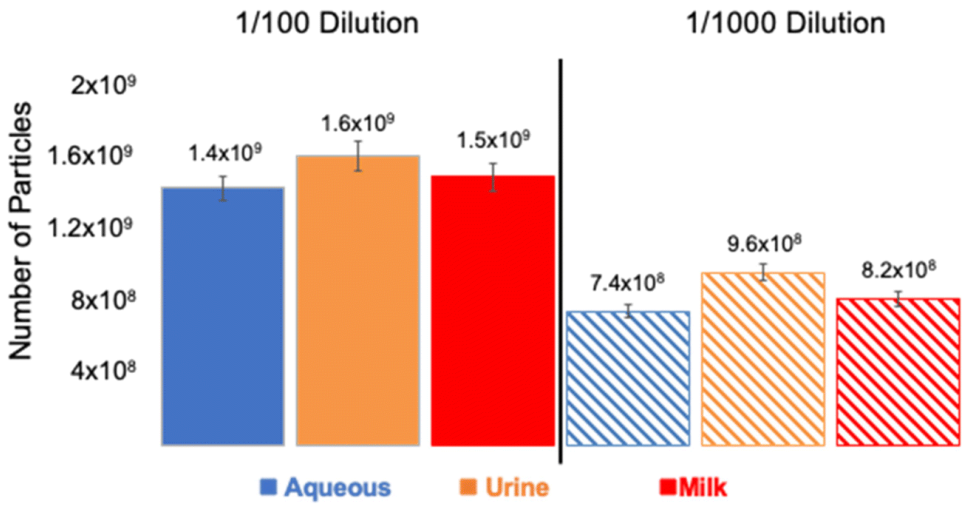

Figure 2.7: Post-isolation of exosome standards spiked into various matrices (50 µL) using the PET C-CP fiber tip spin-down method; the concentration of exosomes recovered were determined based on ELISA readout to an exosome standard curve of linear response was performed to quantitatively detect the expression of the exosomal tetraspanin protein-CD81 (n = 3) employing a capture antibody of 1:250 concentration. Quantified recovery of exosomes from mock matrices of 1/100 and 1/1000 concentration. The loaded 1/100 and 1/1000 solutions theoretically contain 2 × 10^{10} and 2 × 10^{9} exosomes, respectively.

Presented in Fig. 2.7 are the determined number of particles is reported for the same two dilution values (1/100 and 1/1000) as depicted in Fig. 2.5 aqueous, mock urine, and non-fat milk test matrices. (The FBS material was received after the University ELISA facilities were closed due to COVID-19 protocols, and so were not part of this assay.) The determinations were made on the same collected EV elution fractions as used in the absorbance measurements. As reported for the 1/100 dilution samples, the numbers of collected EVs are statistically identical for the three different matrices. As expected, the

level of precision of the bioassay is somewhat degraded from the absorbance measurements, but with a variability of < 9.1 %RSD, the results are in-line with what would be expected. With increased dilution, the number of particles is statistically lower, with similar repeatability, but not in the direct proportion seen in the absorbance case. Again, the recoveries across the matrices are similar, maintaining the same relative responses among each. The measured CD81 expression reflects the fact that the exosome biogenesis process, and therefore, surface protein expression is due to many stochastic processes. Though exosomes from identical cells may be produced via the same mechanisms, exosome populations are heterogeneous, and differences in protein expression are expected. Also, while glycerol in the elution buffer was used to increase exosome stability and prevent aggregation, the presence of glycerol may also have an effect on the conformation of exosome surface proteins in the eluate. Changes in protein conformation due to the presence of glycerol has been previously reported [21, 22], where proteins are altered to more compact states. This has been found to affect antigen-antibody binding interactions, specifically in ELISA applications [23]. The observation of non-linear quantification of exosomes seen in Fig. 2.7 when compared to absorbance-based results in Fig. 2.5, is most likely due to these effects.

2.4 Conclusions

Presented here is an efficient, timely, and vesicle-preserving method for exosome/EV isolation using a simple PET C-CP fiber tip workflow followed by quantitation via absorbance and ELISA assay quantification. There is a high demand for clean and

reproducible EV recoveries from complex matrices for potential uses as targets of clinical, diagnostic, and therapeutic relevance. The isolation of exosomes using hydrophobicity-based chemical separation allows for the gentle and effective capture and subsequent release of exosomes despite the complexity of the matrix of origin. It should be pointed out that the process is not directly related to, nor is it impacted by, traditional size-exclusion effects as the fibers are non-porous and the inter-fiber channels have widths of 1-4 μm. That said, there may be some size-based effects in terms of elution characteristics as size will affect the extent of hydrophobic interactions with the fiber surface. The combination of low-volume, high throughput processing, high recoveries, and practical simplicity of the method bodes well in comparison to other approaches, particularly for clinical situations.

The HIC mode C-CP fiber tip workflow introduces a plethora of potential capabilities as modes of fiber capture selectivity are explored and optimized. The present method would be classified as a generic exosome/EV capture approach, but previously demonstrated methods of fiber surface modification could be implemented for selective capture based on the presence of target surface proteins [50,36]. Likewise, as shown here, protein-specific immunofluorescent labeling could be affected for on-fiber detection. Continued optimization of this technique and characterization of the purity (freedom from matrix species) and the proteomic and genetic cargo are essential to the future implementation of this technique to complex biofluid samples. To this end, there indeed may be instances, such as mass spectrometry-based proteomics, where the use of acetonitrile will be the preferred elution phase modifier, allowing more efficient

processing to recover surface and sequestered proteins. Ultimately, the use of other C-CP fiber platforms could be implemented to affect point-of-care (POC) assays. Importantly, each of these aspects could be scaled-up to volumes necessary for the isolation and purification of exosomes/EVs for various biotherapeutic applications.

2.5 Acknowledgments

Financial support for the chromatography development efforts from the National Science Foundation, Division of Chemistry under grant CHE-1608663 is gratefully acknowledged. Financial support for the EV and exosome isolation efforts from the Eppley Foundation for Scientific Research is gratefully acknowledged. The Gibson Foundation, the Prisma Health ITOR Biorepository, and the Greenville Hospital System are gratefully acknowledged. Special thanks to George Wetzel, Clemson University Electron Microscopy Facility, for assistance with EM. The content of this material and any opinions, findings, conclusions, or recommendations expressed in this material are solely the responsibility of the author(s) and do not necessarily represent the official views of the National Science Foundation. The research in this publication was conducted using a Leica SP8X Confocal multiphoton/HyVolution microscope system, housed in the Clemson Light Imaging Facility (CLIF). CLIF gratefully acknowledges the support of the Clemson University Division of Research, NIH EPIC COBRE Award #P20GM109094, NIH SCBiocraft COBRE Award #5P20RR021949-03, and NSF MRI Award #1126407.

Compliance with Ethical Standards

The authors declare no conflicts of interest.

2.6 References

1. Thery C, Zitvogel L, Amigorena S (2002) Exosomes: composition, biogenesis and function. *Nat. Rev. Immunol.* 2 (8):569-579.
2. H. RM, Bayraktar E, Helal GK, Abd-Ellah MF, Amero P, Chavez-Reyes A, Rodriguez-Aguayo C (2017) Exosomes: From Garbage Bins to Promising Therapeutic Targets. *Int. J. Mol. Sci.* 18 (3):538.
3. Keller S, Sanderson MP, Stoeck A, Altevogt P (2006) Exosomes: from biogenesis and secretion to biological function. *Immunol. Lett.* 107 (2):102-108.
4. Tkach M, Thery C (2016) Communication by Extracellular Vesicles: Where We Are and Where We Need to Go. *Cell* 164 (6):1226-1232.
5. Melo SA, Sugimoto H, O'Connell JT, Kato N, Villanueva A, Vidal A, Qiu L, Vitkin E, Perelman LT, Melo CA, Lucci A, Ivan C, Calin GA, Kalluri R (2014) Cancer exosomes perform cell-independent microRNA biogenesis and promote tumorigenesis. *Cancer Cell* 26 (5):707-721.
6. Raposo G, Stoorvogel W (2013) Extracellular vesicles: exosomes, microvesicles, and friends. *J. Cell Biol.* 200 (4):373-383.
7. Li M, Rai AJ, DeCastro GJ, Zeringer E, Barta T, Magdaleno S, Setterquist R, Vlassov AV (2015) An optimized procedure for exosome isolation and analysis using serum samples: Application to cancer biomarker discovery. *Methods* 87:26-30.

8. Schageman J, Zeringer E, Li M, Barta T, Lea K, Gu J, Magdaleno S, Setterquist R, Vlassov AV (2013) The complete exosome workflow solution: from isolation to characterization of RNA cargo. *Biomed. Res. Int.* 2013:253957.
9. Harischandra DS, Ghaisas S, Rokad D, Kanthasamy AG (2017) Exosomes in Toxicology: Relevance to Chemical Exposure and Pathogenesis of Environmentally Linked Diseases. *Toxicol. Sci.* 158 (1):3-13.
10. Wendler F, Bota-Rabassedas N, Franch-Marro X (2013) Cancer becomes wasteful: emerging roles of exosomes(dagger) in cell-fate determination. *J. Extracell. Vesicles* 2:22390.
11. Kucharzewska P, Belting M (2013) Emerging roles of extracellular vesicles in the adaptive response of tumour cells to microenvironmental stress. *J. Extracell. Vesicles* 2.
12. King HW, Michael MZ, Gleadle JM (2012) Hypoxic enhancement of exosome release by breast cancer cells. *BMC Cancer* 12:421.
13. Koritzinsky EH, Street JM, Star RA, Yuen PS (2017) Quantification of Exosomes. *J. Cell Physiol.* 232 (7):1587-1590.
14. Pisitkun T, Shen RF, Knepper MA (2004) Identification and proteomic profiling of exosomes in human urine. *Proc. Natl. Acad. Sci. U. S. A.* 101 (36):13368-13373.
15. Lasser C, Alikhani VS, Ekstrom K, Eldh M, Paredes PT, Bossios A, Sjostrand M, Gabrielsson S, Lotvall J, Valadi H (2011) Human saliva, plasma and breast milk exosomes contain RNA: uptake by macrophages. *J. Transl. Med.* 9:9.
16. Gallo A, Tandon M, Alevizos I, Illei GG (2012) The majority of microRNAs detectable in serum and saliva is concentrated in exosomes. *PLoS One* 7 (3):e30679.

17. Halvaei S, Daryani S, Eslami SZ, Samadi T, Jafarbeik-Iravani N, Bakhshayesh TO, Majidzadeh AK, Esmaeili R (2018) Exosomes in Cancer Liquid Biopsy: A Focus on Breast Cancer. *Mol. Ther. Nucleic Acids* 10:131-141.
18. Admyre C, Johansson SM, Qazi KR, Filen JJ, Lahesmaa R, Norman M, Neve EP, Scheynius A, Gabrielsson S (2007) Exosomes with immune modulatory features are present in human breast milk. *J. Immunol.* 179 (3):1969-1978.
19. Yoo YK, Lee J, Kim H, Hwang KS, Yoon DS, Lee JH (2018) Toward Exosome-Based Neuronal Diagnostic Devices. *Micromachines (Basel)* 9 (12).
20. Saman S, Kim W, Raya M, Visnick Y, Miro S, Saman S, Jackson B, McKee AC, Alvarez VE, Lee NC, Hall GF (2012) Exosome-associated tau is secreted in tauopathy models and is selectively phosphorylated in cerebrospinal fluid in early Alzheimer disease. *J. Biol. Chem.* 287 (6):3842-3849.
21. Thery C, Amigorena S, Raposo G, Clayton A (2006) Isolation and characterization of exosomes from cell culture supernatants and biological fluids. *Curr. Protoc. Cell Biol.* Chapter 3:Unit 3 22.
22. Koonin EV, Wolf YI, Aravind L (2001) Prediction of the archaeal exosome and its connections with the proteasome and the translation and transcription machineries by a comparative-genomic approach. *Genome Res*. 11 (2):240-252.
23. Heusermann W, Hean J, Trojer D, Steib E, von Bueren S, Graff-Meyer A, Genoud C, Martin K, Pizzato N, Voshol J, Morrissey DV, Andaloussi SE, Wood MJ, Meisner-Kober NC (2016) Exosomes surf on filopodia to enter cells at endocytic hot spots, traffic within endosomes, and are targeted to the ER. *J. Cell Biol.* 213 (2):173-184.

24. Bhatnagar S, Schorey JS (2007) Exosomes released from infected macrophages contain Mycobacterium avium glycopeptidolipids and are proinflammatory. *J. Biol. Chem.* 282 (35):25779-25789.

25. Mu J, Zhuang X, Wang Q, Jiang H, Deng ZB, Wang B, Zhang L, Kakar S, Jun Y, Miller D, Zhang HG (2014) Interspecies communication between plant and mouse gut host cells through edible plant derived exosome-like nanoparticles. *Mol. Nutr. Food Res.* 58 (7):1561-1573.

26. Momen-Heravi F, Balaj L, Alian S, Mantel PY, Halleck AE, Trachtenberg AJ, Soria CE, Oquin S, Bonebreak CM, Saracoglu E, Skog J, Kuo WP (2013) Current methods for the isolation of extracellular vesicles. *Biolog. Chem.* 394:1253-1262.

27. Tauro BJ, Greening DW, Mathias RA, Ji H, Mathivanan S, Scott AM, Simpson RJ (2012) Comparison of ultracentrifugation, density gradient separation, and immunoaffinity capture methods for isolating human colon cancer cell line LIM1863-derived exosomes. *Methods* 56 (2):293-304.

28. Jeppesen DK, Hvam ML, Primdahl-Bengtson B, Boysen AT, Whitehead B, Dyrskjot L, Orntoft TF, Howard KA, Ostenfeld MS (2014) Comparative analysis of discrete exosome fractions obtained by differential centrifugation. *J. Extracell. Vesicles* 3:25011.

29. Rekker K, Saare M, Roost AM, Kubo AL, Zarovni N, Chiesi A, Salumets A, Peters M (2014) Comparison of serum exosome isolation methods for microRNA profiling. *Clin. Biochem.* 47 (1-2):135-138.

30. Nelson DM, Marcus RK (2006) Characterization of capillary-channeled polymer fiber stationary phases for high-performance liquid chromatography protein separations: Comparative analysis with a packed-bed column. *Anal. Chem.* 78 (24):8462-8471.
31. Stanelle RD, Straut CM, Marcus RK (2007) Nylon-6 capillary-channeled polymer fibers as a stationary phase for the mixed-mode ion exchange/reversed-phase chromatography separation of proteins. *J. Chromatogr. Sci*. 45 (7):415-421.
32. Jiang L, Jin Y, Marcus RK (2015) Polyethylenimine Modified Poly(ethylene terephthalate) Capillary Channeled-Polymer (C-CP) Fibers for Anion Exchange Chromatography of Proteins. *J. Chromatogr. A* 1410:200-209.
33. Stanelle RD, Marcus RK (2009) Nylon-6 capillary-channeled polymer (C-CP) fibers as a hydrophobic interaction chromatography stationary phase for the separation of proteins. *Anal. Bioanal. Chem.* 393 (1):273-281.
34. Wang L, Marcus RK (2019) Evaluation of protein separations based on hydrophobic interaction chromatography using polyethylene terephthalate capillary-channeled polymer (C-CP) fiber phases. *J. Chromatogr. A* 1585:161-171.
35. Trang HK, Marcus RK (2017) Application of protein A-modified capillary-channeled polymer polypropylene fibers to the quantitation of IgG in complex matrices. *J. Pharm. Biomed. Anal.* 142:49-58.
36. Jiang L, Marcus RK (2015) Biotin-functionalized poly(ethylene terephthalate) capillary-channeled polymer fibers as HPLC stationary phase for affinity chromatography. *Anal. Bioanal. Chem.* 407 (3):939-951.

37. Randunu KM, Marcus RK (2012) Microbore polypropylene capillary channeled polymer (C-CP) fiber columns for rapid reversed-phase HPLC of proteins. *Anal. Bioanal. Chem.* 404 (3):721-729.

38. Randunu KM, Dimartino S, Marcus RK (2012) Dynamic evaluation of polypropylene capillary-channeled fibers as a stationary phase in high-performance liquid chromatography. *J. Sep. Sci.* 35 (23):3270-3280.

39. Randunu KM, Marcus RK (2013) Initial evaluation of protein throughput and yield characteristics on nylon 6 capillary-channeled polymer (C-CP) fiber stationary phases by frontal analysis. *Biotechnol. Prog.* 29 (5):1222-1229.

40. Bruce TF, Slonecki TJ, Wang L, Huang S, Powell RR, Marcus RK (2019) Exosome isolation and purification via hydrophobic interaction chromatography using a polyester, capillary-channeled polymer fiber phase. *Electrophoresis* 40 (4):571-581.

41. Wang L, Bruce TF, Huang S, Marcus RK (2019) Isolation and quantitation of exosomes isolated from human plasma via hydrophobic interaction chromatography using a polyester, capillary-channeled polymer fiber phase. *Anal. Chim. Acta.* 1082:186-193.

42. Huang S, Wang L, Bruce TF, Marcus RK (2019) Isolation and quantification of human urinary exosomes by hydrophobic interaction chromatography on a polyester capillary-channeled polymer fiber stationary phase. *Anal. Bioanal. Chem.* 411 (25):6591-6601.

43. Huang S, Wang L, Bruce TF, Marcus RK (2020) Evaluation of Exosome Loading Characteristics in their Purification via a Glycerol-Assisted Hydrophobic Interaction Chromatography Method on a Polyester, Capillary-Channeled Polymer Fiber Phase. *Biotechnol. Prog.* in press.

44. Snow NH (2000) Solid-phase micro-extraction of drugs from biological matrices. *J. Chromatogr. A* 885 (1-2):445-455.

45. Hennion MC (1999) Solid-phase extraction: method development, sorbents, and coupling with liquid chromatography. *J. Chromatogr. A* 856 (1-2):3-54.

46. Xu H, Wang S, Zhang G, Huang S, Song D, Zhou Y, Long G (2011) A novel solid-phase microextraction method based on polymer monolith frit combining with high-performance liquid chromatography for determination of aldehydes in biological samples. *Anal. Chim. Acta.* 690 (1):86-93.

47. Zarei M, Sprenger A, Gretzmeier C, Dengjel J (2013) Rapid combinatorial ERLIC-SCX solid-phase extraction for in-depth phosphoproteome analysis. *J. Proteome Res.* 12 (12):5989-5995.

48. Brambilla G, Fiori M, Rizzo B, Crescenzi V, Masci G (2001) Use of molecularly imprinted polymers in the solid-phase extraction of clenbuterol from animal feeds and biological matrices. *J. Chromatogr. B* 759 (1):27-32.

49. Burdette CQ, Marcus RK (2013) Solid phase extraction of proteins from buffer solutions employing capillary-channeled polymer (C-CP) fibers as the stationary phase. *Analyst* 138 (4):1098-1106.

50. Manard BT, Jones SM, Marcus RK (2015) Capillary-channeled polymer (C-CP) fibers for the rapid extraction of proteins from urine matrices prior to detection with MALDI-MS. *Proteomics Clin. Appl.* 9 (5-6):522-530.

51. Schadock-Hewitt AJ, Marcus RK (2014) Initial evaluation of protein A modified capillary-channeled polymer fibers for the capture and recovery of immunoglobulin G. *J. Sep. Sci.* 37 (5):495-504.

52. Fornea DS, Wu Y, Marcus RK (2006) Capillary-channeled polymer fibers as a stationary phase for desalting of protein solutions for electrospray ionization mass spectrometry analysis. *Anal. Chem.* 78 (15):5617-5621.

53. Li M, Zeringer E, Barta T, Schageman J, Cheng A, Vlassov AV (2014) Analysis of the RNA content of the exosomes derived from blood serum and urine and its potential as biomarkers. *Philos. Trans. R. Soc. Lond. B Biol. Sci.* 369 (1652).

54. Guidi L, Felice C, Procoli A, Bonanno G, Martinelli E, Marzo M, Mocci G, Pugliese D, Andrisani G, Danese S, De Vitis I, Papa A, Armuzzi A, Rutella S (2013) FOXP3(+) T regulatory cell modifications in inflammatory bowel disease patients treated with anti-TNFalpha agents. *Biomed. Res. Int.* 2013:286368.

55. Bellingham SA, Coleman BM, Hill AF (2012) Small RNA deep sequencing reveals a distinct miRNA signature released in exosomes from prion-infected neuronal cells. *Nucleic Acids Res.* 40 (21):10937-10949.

56. Zhao X, Wu Y, Duan J, Ma Y, Shen Z, Wei L, Cui X, Zhang J, Xie Y, Liu J (2014) Quantitative proteomic analysis of exosome protein content changes induced by hepatitis B virus in Huh-7 cells using SILAC labeling and LC-MS/MS. *J. Proteome Res.* 13 (12):5391-5402.

57. Kruger S, Abd Elmageed ZY, Hawke DH, Worner PM, Jansen DA, Abdel-Mageed AB, Alt EU, Izadpanah R (2014) Molecular characterization of exosome-like vesicles from breast cancer cells. *BMC Cancer* 14:44.

58. Griffiths SG, Cormier MT, Clayton A, Doucette AA (2017) Differential Proteome Analysis of Extracellular Vesicles from Breast Cancer Cell Lines by Chaperone Affinity Enrichment. *Proteomes* 5 (4):16.

59. An M, Wu J, Zhu J, Lubman DM (2018) Comparison of an optimized ultracentrifugation method versus size-exclusion chromatography for isolation of exosomes from human serum. *J. Proteome Res.* 17:3599-3605.

60. He M, Zeng Y (2016) Microfluidic Exosome Analysis toward Liquid Biopsy for Cancer. *J. Lab Autom.* 21 (4):599-608.

61. Ko J, Hemphill MA, Gabrieli D, Wu L, Yelleswarapu V, Lawrence G, Pennycooke W, Singh A, Meaney DF, Issadore D (2016) Smartphone-enabled optofluidic exosome diagnostic for concussion recovery. *Sci. Rep.* 6:31215.

62. He M, Crow J, Roth M, Zeng Y, Godwin AK (2014) Integrated immunoisolation and protein analysis of circulating exosomes using microfluidic technology. *Lab Chip* 14 (19):3773-3780.

63. Contreras-Naranjo JC, Wu HJ, Ugaz VM (2017) Microfluidics for exosome isolation and analysis: enabling liquid biopsy for personalized medicine. *Lab Chip* 17 (21):3558-3577.

64. He F, Liu H, Guo X, Yin BC, Ye BC (2017) Direct Exosome Quantification via Bivalent-Cholesterol-Labeled DNA Anchor for Signal Amplification. *Anal. Chem.* 89 (23):12968-12975.

65. van der Pol E, Coumans FA, Grootemaat AE, Gardiner C, Sargent IL, Harrison P, Sturk A, van Leeuwen TG, Nieuwland R (2014) Particle size distribution of exosomes and microvesicles determined by transmission electron microscopy, flow cytometry, nanoparticle tracking analysis, and resistive pulse sensing. *J. Thromb. Haemost.* 12 (7):1182-1192.

66. Sumida S (2006) Transfusion and transplantation of cryopreserved cells and tissues. *Cell and Tissue Banking* 7 (4):265-305.

67. Lehrich BM, Liang YX, Khosravi P, Federoff HJ, Fiandaca MS (2018) Fetal Bovine Serum-Derived Extracellular Vesicles Persist within Vesicle-Depleted Culture Media. *Int. J. Mol. Sci.* 19 (11):11.

68. Vagenende V, Yap MGS, Trout BL (2009) Mechanisms of Protein Stabilization and Prevention of Protein Aggregation by Glycerol. *Biochemistry* 48 (46):11084-11096.

69. Vagenende V, Han AX, Pek HB, Loo BLW (2013) Quantifying the Molecular Origins of Opposite Solvent Effects on Protein-Protein Interactions. *PLoS Comput. Biol.* 9 (5):9.

70. Kjaer S, Stausbol-Gron B, Wind T, Ravn P, Jensen KP, Kahns L, Clark BFC (1998) Glycerol diversifies phage repertoire selections and lowers non-specific phage absorption. *FEBS Lett*. 431 (3):448-452.

CHAPTER THREE

RAPID ISOLATION OF EXTRACELLULAR VESICLES FROM DIVERSE BIOFLUID MATRICES VIA CAPILLARY-CHANNELED POLYMER FIBER SOLID-PHASE EXTRACTION MICROPIPETTE TIPS

3.1 Introduction

Extracellular vesicles (EVs) are a diverse group of cell-derived membrane vesicles, typically ranging in size from 30 nm to 1 μm in diameter.[1,2] EVs are released by all cell types and contain the biomolecular characteristics of the mother cell (i.e., DNA, RNA, miRNA, mRNA, biomarker proteins).[3–7] While no official EV classification system exists, three main EV subtypes have been identified based on size and mechanism of biogenesis.[8,9] Microvesicles are 100 nm to 1 μm vesicles created by the outward budding of a cell membrane. Apoptotic bodies (reflective of cell death[10]) are 1 to 5 μm vesicles created during the programmed cell death process. Exosomes are 30 to 200 nm vesicles created through the multivesicular body (MVB) endosomal pathway. Due to their similarities in composition, overlapping size range, and characteristic cup/dimpled shape when observed by electron microscopy, the exosome and microvesicle subtypes are difficult to differentiate. For this reason, the vesicles are generically referred to as EVs.[11] Not surprisingly, within the heterogeneity in EV sources, size, and content, the specific mechanisms of action and distribution of potential biomarkers varies immensely.[12]

EVs are primary vehicles in intercellular communication, signal transduction, and local and distal transport processes.[13,14] The exosome subset of EVs has become

increasingly targeted both as mediums for diagnostic information and cargo transmission.[15,16] The lack of understanding of EV physiochemical and biological characteristics, along with a lack of field-wide consensus, has hindered the progress of the fundamental and clinical use of exosomes. A thorough understanding of exosome biophysical attributes would allow for details of several vital cell interaction mechanisms to be revealed (i.e., immune regulation, communication, and disease progression).[17,18] The analysis of EV-associated biomarker components during liquid biopsies has become a valued tool for cancer detection, allowing for the surveillance of progression and treatment with a reduced physical burden on the patient.[16,19] Alternatively, the large-scale processing of exosomes has become a key goal for researchers in many areas, including in the biopharmaceutical industry. EVs from mesenchymal stem cell (MSC) origin are of particular interest, having demonstrated the ability to enhance therapeutic transport of targeted drugs,[20] initiate tissue regeneration,[21] and support immune response modulation.14 Nevertheless, for the full extent of EV analyses to be realized, the inefficient tools for EV retrieval must be addressed.

Due to their ubiquitous nature in terms of the cells of origin, exosomes and other EVs are found in diverse biofluids, including urine,[22–24] saliva,[25–27] blood (serum and plasma),[28–30] cervical mucus,[25,31,32] breast milk,[20–22] and cerebrospinal,[33,34] lymph,[35,36] synovial,[37] and amniotic[38] fluids. As such, these media are reservoirs to derive clinical and research scale populations. EVs may also be harvested from cell culture media during the cell growth process for fundamental studies or subsequent use as biotherapeutic

vectors.[39] Despite the high bioavailability of EVs, the extraction of EVs from biofluids has proven to be a challenge due to sample and vesicle heterogeneity and intense matrix effects. In terms of characterizing the effectiveness of generic EV isolation processes, several metrics exist relative to the final product's quality (versus the cost/time aspects of the procedures). The first, most obvious feature is the yield; how many microvesicles can be extracted per unit volume of the primary matrix. Practical working volumes can range from tens of microliters of cerebrospinal fluid (CSF) to milliliters of urine and liters of cell culture media. The second is the purity of the isolate. In the case of EVs, the primary contaminants/co-eluates are matrix and host cell proteins. In the case of serum/plasma samples, these would typically include albumins and, most problematically, lipoproteins.[40,41] Finally, the most critical aspect is the retention of biological functionality. Whether the end-use is clinical analysis, fundamental research, or production of biotherapeutic vectors, the recovered EVs' physical and chemical integrity must remain intact. Additional metrics come into play during high-specificity isolations of targeted EV populations. In all instances, aspects regarding processing time, capital and supply costs, and operational complexity must be considered.

It has been documented the needs for the development and optimization of methods specifically for the isolation and quantification of EVs from complex biofluid samples.[42] The available methods for these purposes limit the downstream characterization and application of EV recoveries due to concentration and purity concerns. The lack of efficient EV isolation methods has become the rate-limiting step towards realizing the full potential of EVs in clinical and fundamental research and

prevents large-scale processing of EVs. Many EV isolation methods are available based on a wide variety of chemical/physical properties. Riekkola and co-workers have recently presented an excellent review of the topic,[43] with many papers describing comparisons of the methods. At this point, it is clear that no single method can be universally applied.[44,45] The employed isolation method is usually chosen based on the subsequent means of characterization and utilization of the EVs. At present, ultracentrifugation (UC) methods are most commonly used to isolate EVs.[46] The UC isolation method consists of several differential centrifugation steps, potentially reaching 200 000g.[13] UC introduces high-costs regarding time (2 hours to overnight), sample volume (10–45 mL), and capital (up to $100 000 for equipment, and $3000 in running costs per year), producing low recovery/yields (5–25%) which are typically contaminated with protein/lipoprotein aggregates.[46,47] Variations of this technique employing density gradients and other reagents have also been implemented but continue to present the previously-mentioned challenges.[46,48] Other size/density-based methods include ultrafiltration, size-exclusion spin downs, and field flow fractional.[49–51] Here again, low purity recoveries are problematic. As a final class of methods, immune-affinity and polymer precipitation "kits" are finding increased use.[52,53] Still, concerns lie in the low yield and impure recoveries, skewing the downstream characterization of the vesicles. Ultimately, an isolation method with the ability to efficiently produce high-yield, high-purity EVs on practical time/cost scales is of critical importance.

To address the aforementioned issues, researchers from the Bruce and Marcus groups have demonstrated the use of a polyester (PET) capillary-channeled polymer (C-

CP) fiber stationary phase in hydrophobic interaction chromatography (HIC) workflows for EV isolation.[54–60] The C-CP fibers consist of an 8-legged periphery that creates 1 to 4 μm-wide channels upon colinear packing in a column format. The relative hydrophobicity of the stationary phase and the high-salt retention of the EVs allows for the capture and elution of the vesicles based on hydrophobicity. HIC has been traditionally applied to protein separations[61] due to the non-denaturing, on–off partitioning of the solute, allowing the preservation of structure/function.[62–64] Taking advantage of this, the efficient and vesicle-preserving isolation of EVs from urine,[54,56] blood plasma,[55] and cell culture milieu[54,58] have been demonstrated in a 10 min HPLC workflow enabling simultaneous EV isolation and quantification. Importantly, recent proteomics analysis of the eluates has revealed a very efficient removal of serum proteins and lipoproteins, yielding extremely high purity fractions in comparison to other methods.[59] The method has been extended to a more clinically-favorable EV isolation workflow using 1 cm C-CP fiber phases attached to micropipette tips, allowing for the solid-phase extraction (SPE) of EVs to occur in a table-top centrifuge.[57] Both methods have proven to be beneficial in terms of efficiency, purity, and yield, producing recoveries of EVs on clinically relevant scales of time (<15 minutes) and cost (<$1 per column per tip). Here, the versatility of the C-CP fiber spin-down tip to produce concentrated and contaminant-free EV recoveries is demonstrated for the complex matrices of urine, saliva, cervical mucus, serum, and milk. The tip recovery of exosomes was evaluated using absorbance (scattering) detection, nanoparticle tracking analysis (NTA), and transmission electron microscopy (TEM). The exosome purity was assessed

by Bradford assay of free proteins. The bioactivity and identity of the recovered vesicles was confirmed with an enzyme-linked immunosorbent assay (ELISA) to the CD81 tetraspanin protein. It is believed that the methodology presented here will have relevance to both clinical and fundamental biology research settings.

3.2 Experimental

3.2.1 Chemicals and reagents

Deionized water (DI-H_2O, 18.2 MΩ cm) was obtained from a Milli-Q water purification system (Millipore Sigma, Merck, Darmstadt, Germany). Biotechnology-grade glycerol and ammonium sulfate were purchased from VWR (Sokon, OH, USA). Phosphate buffered saline (PBS, pH = 7.4), bovine serum albumin (BSA), and Pierce™ Coomassie Plus (Bradford) Assay Reagent were purchased from ThermoFisher Scientific (Waltham, MA, USA).

3.2.2 Instrumentation

A NanoVue Plus UV-Vis spectrophotometer (GE Healthcare,Chicago, IL, USA) was used to measure the absorbance/scattering (203 nm) of the EV fractions. A Synergy H1 Hybrid Multi- Mode Plate Reader (BioTek, Winooski, VT, USA) was used to measure the UV-Vis absorbance (595 nm) of samples in the 96 cell-well format during the Bradford assay of protein content, employing the colorimetric Pierce™ Coomassie Plus (Bradford) Assay Reagent. The plate reader was also used in the chemiluminescent

detection of the Pierce™ ECL Substrate during the enzyme-linked immunosorbent (ELISA) assay. A Hitachi HT7830 transmission electron microscope (Chiyoda City, Tokyo, Japan) was used for TEM imaging to determine the structural integrity, size, and purity of the EVs in the C-CP tip recoveries from various biofluids. A Malvern Panalytical NanoSight NS300 nanoparticle tracking analysis (NTA) system (Malvern, Worcestershire, United Kingdom) was used to determine the concentration and size distribution of isolated vesicles.

3.2.3 Extracellular vesicles

Commercial lyophilized "exosome standards" from the urine of healthy donors were obtained from Galen Laboratories Supplies (Craigavon, Northern Ireland). To be clear, the material has not been certified as a reference standard. No information regarding purity or classification was supplied from the manufacturer. However, the product is a means of preparing EV solutions of known concentration (2.7×10^{12} particles per mL), though vesicles exceeding typical exosome diameter, lipoproteins, and other protein contaminants have been previously identified in the material.[65] Despite the potential of systematic error (impurities) introduced by these standards, they have proven useful for order-of-magnitude estimation of recovered EV concentrations. Fresh-morning urine, saliva, and cervical mucus (collected using a cotton swab and dissolved in PBS) were obtained from consenting, anonymous donors. After sample collection, the cervical mucus samples were stored at −80 °C until thawed for EV processing. Corning™ Human AB Blood Serum was obtained from ThermoFisher Scientific (Waltham, MA, USA). The frozen human serum was thawed and aliquoted before use. Unpasteurized raw goat milk

(serving as a surrogate for human breast milk) was obtained from Split Creek Farm (Anderson, SC, USA). All biofluid samples were filtered using a sterile syringe filter of 0.22 µm pore size (Frogga Bio, Toronto, Canada) prior to processing.

3.2.4 C-CP fiber tip creation and methodology

The C-CP fiber micropipette tips were assembled as previously reported,[57] with the same HIC isolation workflow employed. Briefly, the 1 cm long C-CP fiber tips were cut from 30 cm long, 0.8 mm inner diameter fluorinated ethylene–propylene (FEP) C-CP packed columns consisting of ~450 PET C-CP fibers. The C-CP tips had an interstitial fraction of ~0.6, with ~3 µL of bed volume, which was press-fit to 200 µL low-retention micropipette tips and secured with a small amount of superglue, as depicted in Fig. 3.1.

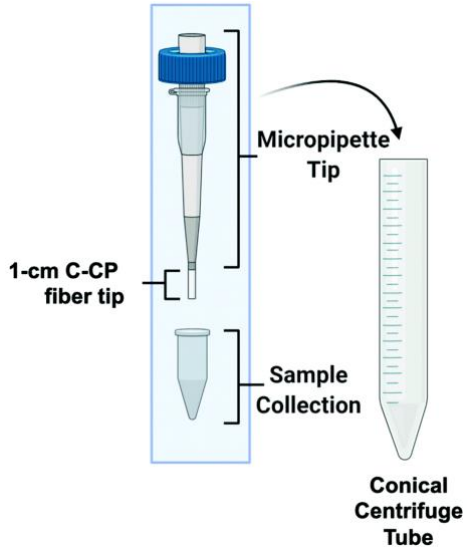

Figure 3.1: The capillary-channeled polymer (C-CP) fiber solid-phase extraction up setup for the isolation of EVs from complex biofluids in a tabletop centrifuge.

The EV isolation methodology for the various biofluids was initiated by mixing 100 µL of the raw biofluid with 100 µL of ammonium sulfate (2M final concentration) to

induce the hydrophobic interaction between the biofluid components and the fibers. The total volume was vortexed, then deposited inside the sample reservoir of the C-CP tip assembly. The apparatus was then placed inside a 15 mL conical, table-top centrifuge tube and spun-down at 300g for 1 minute. (Due to the high viscosity of the saliva matrix, the tip containing the saliva sample was centrifuged at 500g for 10 minutes.) Next, the fiber-bound vesicles were washed with 200 µL of DI-water (300g, 1 min) before inducing the elution of free proteins (including lipoproteins[59,60]) using 200 µL of 25% glycerol with 1 M ammonium sulfate in PBS (300g, 1 min). For the protein-rich serum and milk matrices, two protein elution steps were employed to minimize protein carryover in the EV elution. Finally, the elution of the EVs was induced using 50 µL of 50% glycerol in PBS (300g, 1 min) and the final fraction collected. Based on the respective sample/elution volumes, a 2X concentration factor is realized.

3.2.5 Quantification and characterization of EV recoveries

Previous reports have demonstrated the validity of using standard absorbance (scattering) measurements as a means of quantifying isolated exosomes.[54–56] In those efforts, quantification was achieved by generating linear response curves based on serial dilutions of the commercial exosome standards in the elution solvent. Given the high complexity and presence of matrix-associated components in the diverse biofluid matrices, the method of standard addition was also used to more accurately quantify the EVs. For the method, 10 µL of the unknown sample (S_0) was spiked once (S_1), twice (S_2), and three times (S_3) with 10 µL of EV standards of known concentration (2.7×10^{10} particles per mL), with the total sample volumes adjusted to 50 µL using DI-water. The

absorbance of each sample was measured at 203 nm (n = 5). The optical absorbance of the raw and spiked samples ($S_{0–4}$) and the known added concentrations of exosome standards were used to create a standard addition response curve for EV quantification. The resulting linear regression was extrapolated to determine the concentration of EVs in the unknown sample.

The structure, size, and concentration of the recovered EVs were evaluated using TEM and NTA. The sample preparation for TEM imaging was performed as previously reported.[57] The size distribution of the eluted EVs was determined using the NanoSight NS300 NTA system, equipped with a 532 nm laser. Throughout NTA experimentation, five replicates were collected for each sample in 60-second intervals, with a minimum of 200 valid tracks recorded per video and a minimum of 1000 valid tracks recorded per sample. The focal plane for each sample was manually adjusted using the focus knob to achieve the best optical field of view. The syringe pump for sample introduction was set to a constant flow rate of 50 μL per minute. The camera level was set to 14, and the detection threshold was set to 3, as optimized by Vestad et al. [66] To clarify, the concentration values based on the NTA data are not the direct concentration values of the EV recoveries. Instead, the recovered EVs were diluted to be compatible with the NTA system's working concentration range (10^7–10^9 particles per mL).

Protein components of the biofluids and EV recoveries were evaluated using a Bradford assay and an indirect enzyme-linked immunosorbent assay (ELISA). The Bradford assay was used to determine the total protein concentration of both the whole samples and EV elution fractions. For the total protein determinations, 250 μL of

Bradford reagent was added to 25 μL of each sample and allowed to incubate at room temperature for 20 minutes before detecting the absorbance response at 595 nm using the Synergy H1 Plate Reader. The absorbance responses were compared to a standard curve using BSA standards. All samples and standards were applied to the cell well plate in triplicate.

The presence of EVs in biofluids is commonly confirmed using antibodies to the CD81, CD63, and CD9 tetraspanin proteins, which are incorporated in the transmembrane space of EVs during biogenesis.[67] Despite their wide use as marker proteins, tetraspanins are in fact not universally expressed in EVs, and the overall expression is also heterogeneous among singular EV populations.[68] Therefore, the presence of EVs may be confirmed by the detection of these proteins, but their absence does not preclude the presence of EVs. Prior to chemical processing for the CD81 ELISA assay, the tip-isolated EVs were applied to a 100 kDa filter unit to remove latent glycerol, as high concentrations of glycerol are known to interfere with antibody binding.[69,70] The EVs isolated from the target biofluids were first diluted in 1:1 ELISA coating buffer (0.05 M carbonate–bicarbonate in PBS) and then incubated on a shaker overnight at 4 °C to coat the cell well plate with the analytes. An exosome standard positive control and negative controls of PBS, protein elution buffer, and EV elution buffer were also applied to the cell well plate. All samples and controls were applied to the cell well plate in triplicate. After incubation, the cell well plates were washed with sterile PBS (200 μL per well, 30 min, 6 buffer changes) and then blocked with 5% BSA in PBS at room temperature for 30 min. The wells were incubated overnight with 50 μL of a mouse

monoclonal antibody to the CD81 protein (1 μg mL^{-1}) on an orbital shaker (4 °C). The washing and blocking steps were repeated before applying 200 μL of the goat anti-mouse HRP conjugated secondary antibody (1 μg mL^{-1}, 200 μL, RT, 2 hours). The cell well plate was washed using 200 μL of PBS per well and 6 buffer changes. Finally, the Pierce ECL Substrate was applied and incubated at room temperature for 30 minutes before detection. The Synergy H1 microplate reader was used to measure the chemiluminescent response resulting from the HRP catalyzed oxidation of the substrate, correlating to the concentration of species containing the CD81 antigen.

3.3 Results and Discussion

3.3.1 EV quantification via standard addition

Concentrated EV recoveries with high purity, preserved morphology, viability, and stability are essential for the most efficient use of EVs derived via any isolation method. Given the complexity and diversity of the biofluids (and culture media), removing matrix contaminants is of utmost importance. Carryover of matrix species with the target EV isolates, including proteins and genetic material, hinders the implementation of downstream characterization techniques (i.e., MS proteomics or RNA-Seq), their use in clinical analysis schemes, and use as vectors in gene therapy applications. In this regard, the use of optical absorbance as an EV quantification tool is particularly susceptible to interferences due to the presence of low concentrations of matrix species. However, the quantification of isolated EVs by absorbance has been

previously demonstrated using simple optical absorbance measurements at 203 nm.[54–59,61] To be clear, the absorbance response observed at this wavelength is not credited to the common electronic transitions typical of biomolecules in solution. Instead, the "absorbance" response is caused by light scattering due to the presence of the nanobodies, which is conveniently proportional to the EV concentration. A cause for concern with this method for quantifying EVs is that matrix proteins and nucleic acids will skew the absorbance detection, especially at the 216 and 280 nm wavelengths traditionally used for determinations of proteins. These effects are lessened at 203 nm, where a higher absorbance (light scattering) response is observed at shorter wavelengths.[48] In fact, absorbance spectra obtained for EV solutions follow the anticipated responses (exponentially decreasing with wavelength) for particles of ~150 nm, based on Mie scattering theory.

The method of standard addition is widely used for the quantification of analytes whose responses (regardless of the methodology) are subjected to significant matrix interferences. [71] The method has not been previously employed for the quantification of EVs in biofluids, but could prove useful in this application as diverse matrices are being evaluated. A proof of concept for this method is illustrated in Fig. 3.2, where the method of standard addition was used to quantify EVs in aqueous solution using the commercial exosome stock.

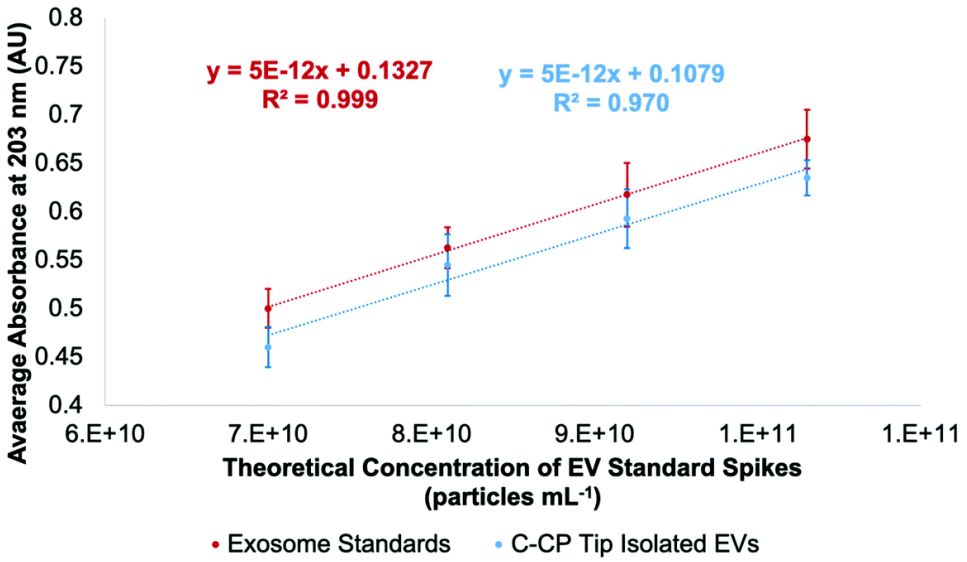

Figure 3.2: Standard addition curve using a commercial exosome standard stock of 1.1 × 10^{10} particles per mL concentration based on absorbance measurement at 203 nm (red). Quantification of EVs based on absorbance detection after employing aqueous EV solutions of known concentration to the C-CP tip (blue).

The method was first applied to test the "unknown", which was the initial exosome stock solution of 7.0 × 10^{10} particles per mL. The test unknown (S_0) was spiked once (S_1), twice (S_2), and three times (S_3) with aqueous aliquots of the EV standard, increasing the theoretical concentrations by 1.1 × 10^{10}, 2.2 × 10^{10}, and 3.2 × 10^{10} particles per mL, respectively. As shown in Fig. 2 (red line), the absorbance responses for the un-spiked (S_0) and spiked (S_1, S_2, S_3) EV stock aliquots in DI-water are well behaved, yielding a correlation coefficient (R2) of >0.999. Based on the linear regression, the "unknown" concentration was determined to be 7.4 × 10^{10} particles per mL, a 5% error. As a point of reference, the concentration of the same solution determined by a standard calibration curve (R^2 value = 0.998) yielded a concentration of 6.3 × 10^{10} particles per mL, a 10% error (accuracy that would be considered outstanding by virtually any other EV assay method).

As mentioned previously, the stock exosome material is known to contain undetermined amounts of proteinaceous material and other vesicular bodies. As a further test of the use of the standard addition quantification method, the "unknown" sample and the equivalent spike samples were put through the spin-down protocol. As seen in the response curve (blue line), proportional recoveries are indeed maintained, reflecting a lack of any sort of overloading of the fiber phase. Indeed, the recoveries are quite high versus the EVs in the stock aqueous solution, ranging from 96–102% (concentration of recovered EVs /raw stock), with the lower y-intercept being attributed to the removal of the latent proteins in the original stock material. Also of relevance, the average variation for the bulk measurements was 4%RSD, while for the full extraction process the variability averaged 5%RSD. There is some level of degraded quantitative performance (scatter) in the tip recoveries, as seen in the lessened goodness-of-fit ($R^2 = 0.970$).

3.3.2 EV recoveries from diverse matrices

After confirming the ability of the standard addition method to determine the concentration of EVs and the C-CP tip's ability to produce quantitative EV recoveries, the experimental protocol was applied to the raw biofluid matrices. The urine, saliva, cervical mucus, serum, and milk biofluids samples were spiked as described above, followed by tip isolation. The raw biofluids were spiked once, twice, and three times with EV stock solutions of increasing concentration (1.1×10^{10} particles per mL per spike), then diluted to 200 μL with ammonium sulfate (2M final concentration) before applying to the C-CP spin-down tips for the isolation process (load, protein wash, EV elution). The absorbance response of the EV eluates was measured at 203 nm. The relative absorbance

responses presented in Fig. 3.3 reflect the fact that the C-CP tip does produce EV recoveries of proportionally increasing concentrations, despite the biofluid sample complexity.

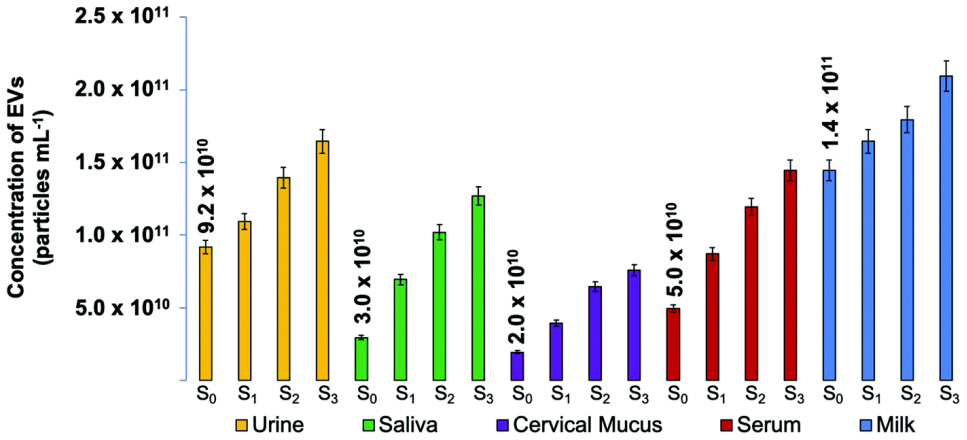

*Figure 3.3: Determined EV particle concentrations (*n = *3) for human urine, saliva, cervical mucus, blood serum and goat milk biofluid unknown samples spiked once, twice, and three times with a commercial exosome standard stock of 1.1 × 10^{10} particle per mL before EV isolation using the C-CP tip workflow. The biofluid-originating EV recoveries were quantified based on absorbance at 203 nm and compared to a response curve of linear response.*

The respective regressions of each have an R^2 correlation coefficient of > 0.98. The determined values for each of the biofluids are provided in each case, with respective values each falling in line with expectations based on literature values.[72–76] The relative precision of the determined values (n = 3) is excellent, with an average value of ~7% RSD across the matrices.

The relative responses for the spikes across the different matrices are fundamentally instructive. In theory, consecutive increases of 1.1 × 10^{10} particles per mL EV concentration were applied. Therefore, given a homogenous and ideal biofluid

sample, the difference between the determined concentrations of the S_x and S_{x+n} samples should be 1.1×10^{10} particles per mL. While the responses here are proportional within each matrix type, there is a definitive difference in the slopes; i.e. the method of standard addition reveals the existence of matrix effects. That said, given the vast physico-chemical differences among these biofluids, the extent of the effects, based on the slopes of the response curves, are less than a factor of 2X. As such, the use of a single absorbance calibration function would deliver that level of accuracy, with higher levels achieved with the use of matrix-matched standards. Analysis across multiple matrices would benefit most using the standard addition method.

3.3.3 Physical characterization of EV isolates

To confirm that the C-CP tip elution fractions do indeed contain EVs in the correct size range and consist of the expected characteristic shape, NTA and TEM imaging were performed. Fig. 3.4 presents both the size distributions observed via NTA and electron micrographs of the intact vesicles following isolation.

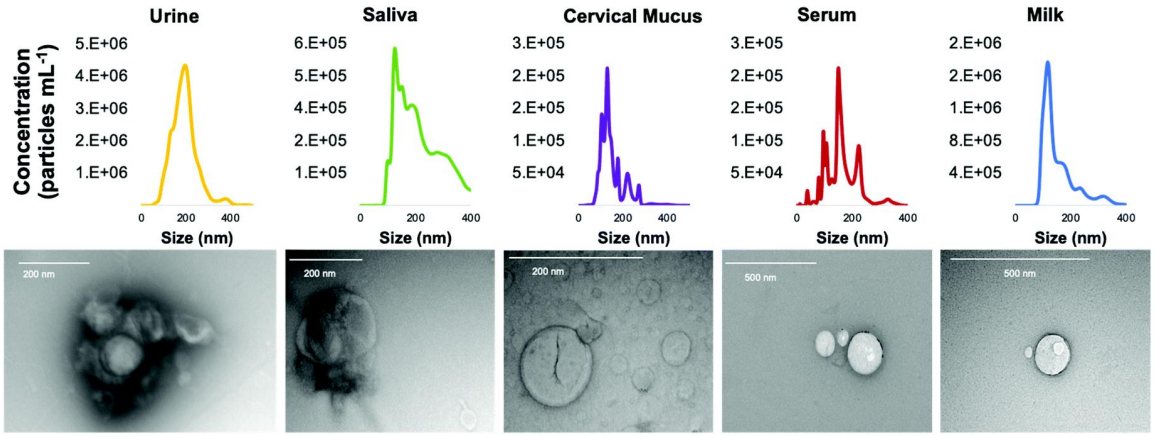

Figure 3.4: Size distribution of vesicles in the EV recoveries resulting from the C-CP fiber tip isolation from human urine, saliva, cervical mucus, blood serum, and goat milk, measured using the Nanosight NS300 nanoparticle tracking analysis system. TEM micrographs of EVs isolated from biofluids using the C-CP fiber tip, taken using the Hitachi HT7830.

The eluted EVs presented average diameters from 121.7–160.3 nm across the matrices. Based on the NTA data, the populations of EVs recovered from the urine, saliva, and milk samples presented the most "gaussian-like" size distributions, though with minor subsets of vesicles detected at larger sizes (as is typical). On the other hand, the EVs isolated from the cervical mucus and blood serum samples were far less homogeneous, with several distinct subpopulations.

Visualization via transmission electron microscopy (TEM) is another benchmark method to identify extracellular vesicles. The TEM micrographs presented in Fig. 3.4 confirm that EVs were isolated from the biofluids using the C-CP spin-down tips. In each of the images, either cup-shaped, donut-shaped, or spherical-shaped vesicles with a dark halo can be observed. The EVs observed in the TEM micrographs fall within the exosome size range. One key aspect to emphasize is that, even in the potentially

lipoprotein-heavy biofluids (cervical mucus, serum, milk), no vesicles are observed that would correspond to the anticipated lipoprotein size range (~20 nm) characteristic of LDLs. The isolation of EVs from lipoproteins is a fundamental challenge due to the similarities of the vesicles' size, structure, composition, and biological interactions.[40,41] High purity recovery of EVs (i.e., the lack of matrix proteins/lipoproteins) using the fiber isolation methodology has been demonstrated in recent mass spectrometric proteomics analyses,[59,60] and is a significant advantage of the C-CP tip isolation technique. This point is further demonstrated in the following section. The TEM images show that the HIC-based C-CP tip isolation preserves the characteristic vesicular shape with no visual contamination.

Beyond the size distribution, NTA can also be used as a semi-quantitative means of determining nanoparticle densities. As presented in Fig. 3.5a, the particle densities determined for the raw biofluids via NTA can be appreciably higher than the corresponding values generated by absorbance measurements.

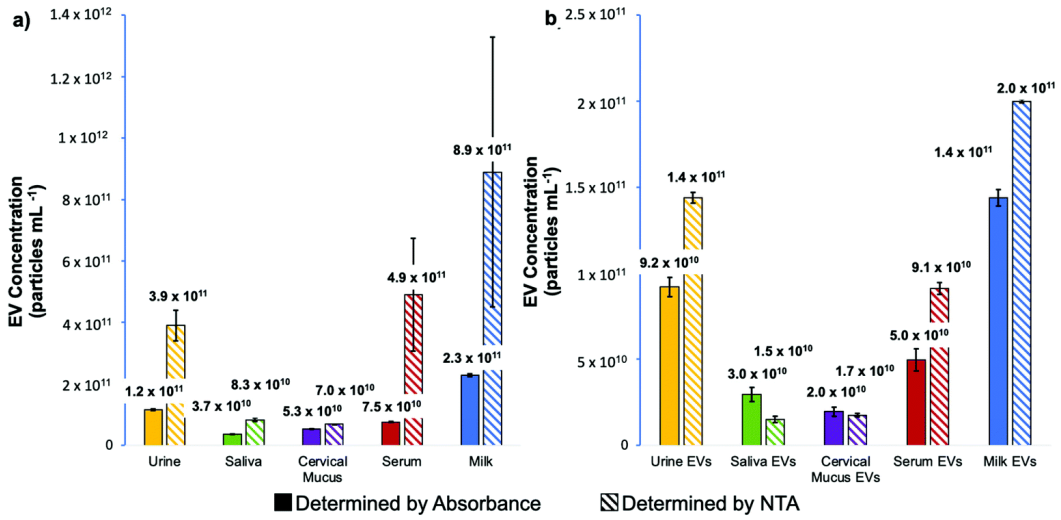

Figure 3.5: Comparison of the determined concentration of (a) EVs in each bulk biofluid sample and (b) EVs recovered from each biofluid using the C-CP tip method as determined using the method of standard addition by absorbance at 203 nm and by nanoparticle tracking analysis.

Not surprisingly, this is particularly true for the most proteinaceous matrices (where agglomeration would likely occur). In these cases, the densities determined by NTA can exceed those of absorbance by as much as an order of magnitude, with the measurement variability also highest for those samples. Importantly, the same analyses performed on the spin-down isolates (Fig. 3.5b) yield values in far better agreement between the two quantification methods, with much-improved measurement precision realized for the NTA. It is noteworthy that the relative concentrations across the matrices parallel each other between the two independent measurement methods, with the values not differing by more than 2X. This level of agreement is seen as validation of the efficacy of the C-CP fiber spin-down tip methodology.

3.3.4 Characterization of EV purity

To investigate the purity of EVs (based on the removal of matrix proteins) isolated using the C-CP tip method, a Bradford assay was performed. The total protein concentrations of the whole biofluid samples and the EVs eluted from those biofluids using the C-CP tip isolation method were determined. To be clear, a Bradford assay reflects the total proteinaceous material present in a sample. As such, in the ideal case of perfect isolation of EVs, a positive response will still result due to the interaction between the Bradford reagent and surface proteins and externally exposed basic and aromatic amino acid residues.

The Bradford assay results for the raw matrix materials and the EV isolates are presented in Fig. 3.6.

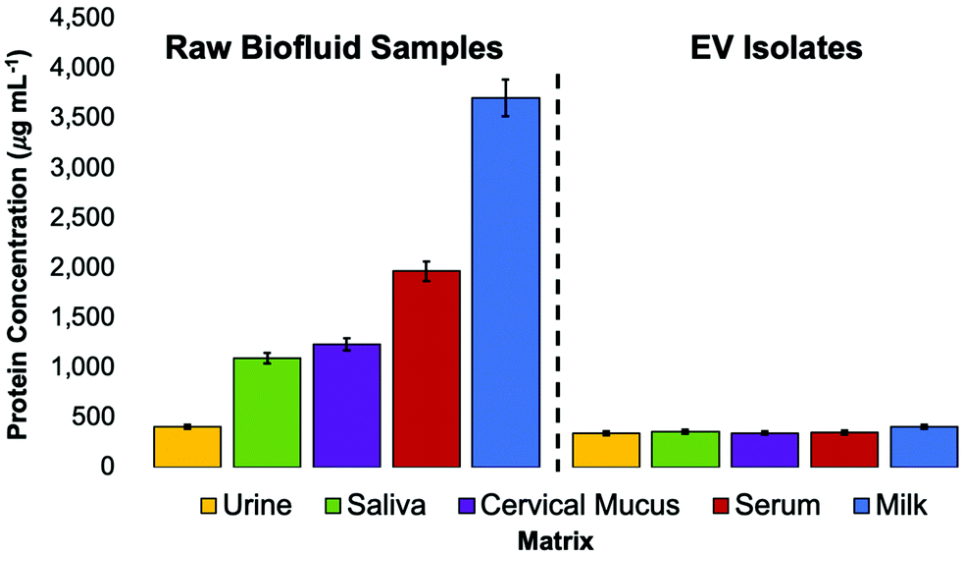

Figure 3.6: Bradford assay of raw biofluid matrices and concentrated EV recoveries after isolation with the C-CP tip. The total protein concentration was determined using the absorbance measurement of Bradford reagent at 595 nm, as compared to a BSA standard curve of linear response. n = 3.

As would be anticipated, the goat milk and human blood serum matrices were the most protein-dense, with the human urine matrix having the lowest amount of protein present. After conducting the C-CP fiber spin-down tip EV isolation workflow, most of the contaminating proteins were removed while leaving behind the EVs, which contribute to only a small fraction of the total protein response for the protein-rich matrices.

Here, the 67–89% removal of "total protein" was demonstrated for the saliva, cervical mucus, serum, and milk biofluid samples. A much lower (17%) removal of proteins was observed from the human urine sample, as expected given the much lower relative concentration of free protein in healthy urine samples. The EV recoveries present a low (346–412 μg mL^{-1}) total protein concentration based on the Bradford assay. While not perceivable on this scale, the relative amounts of determined protein for the isolates are a very close reflection of their relative EV densities determined via the standard addition and NTA methods (Fig. 3.3 and 3.5), suggesting the efficacy of the method to yield high-purity EVs. The C-CP tip method demonstrates here the ability to remove up to 89% of protein contaminant species. The efficiency of the method is demonstrated by the absence of proteinaceous aggregates in the TEM micrographs of EVs after the tip isolation process. Perhaps most definitive, recent MS proteomic analysis work has confirmed the removal of common contaminant lipoprotein species from serum samples using this method, based on the virtual absence (<0.3% of total proteins) of the Apo-B100 content in the EV isolates.[60] The depletion of the lipid marker protein was confirmed by ELISA analysis, as well.[60]

3.3.5 Verification of EV identity

While no universally expressed EV/exosome marker exists, the CD81 tetraspanin protein has been identified in high concentrations in many exosome populations.[55] (The CD63 and CD9 tetraspanins have been used as identifiers in previous works from this laboratory,[57] but CD81 generally exists in higher concentrations.) As such, the marker has been accepted as a general marker for the presence of EVs, with the acknowledgment that it is expressed to different extents even within the same EV population, and in some cases not at all. To confirm the presence of EVs in the C-CP tip eluates and assess the recovered vesicles' bioactivity, a semi-quantitative ELISA using an antibody to the CD81 tetraspanin protein was employed.

As shown in Fig. 3.7, serial dilutions of the commercial exosome standard stock were used to create a standard curve for the ELISA response quantification.

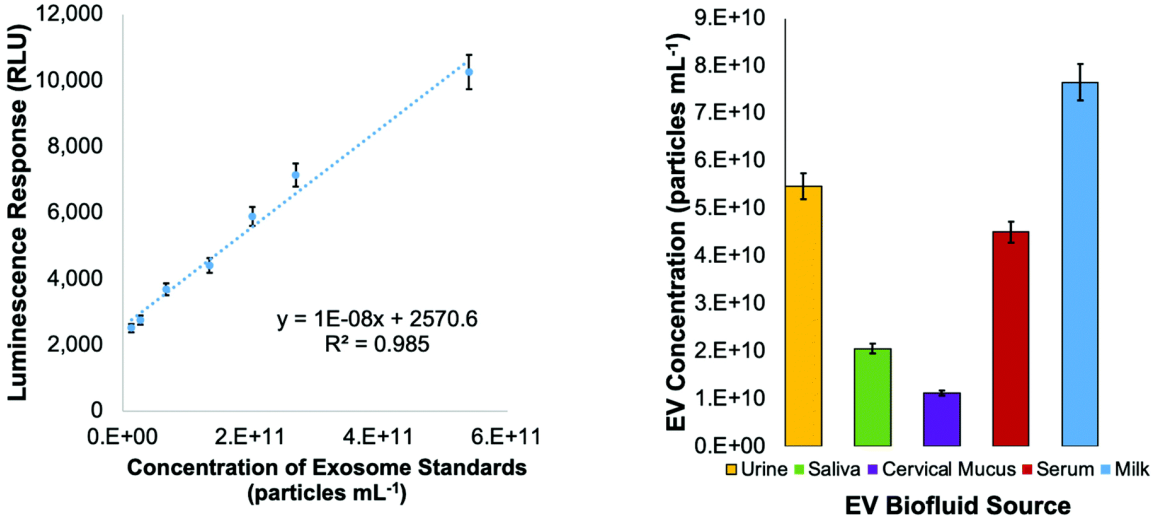

Figure 3.7: Indirect ELISA standard curve employing an antibody to the CD81 tetraspanin protein using serial dilutions of a commercial exosome standard (2.7×10^{12} particles per mL), and the CD81 responses of the C-CP tip isolated EVs from biofluid samples.

With this standard curve of linear response ($R^2 = 0.985$), the concentration of recovered EVs containing the CD81 tetraspanin protein was estimated. When the concentration of EV standards presenting a CD81 response was compared to the EV concentration as determined by absorbance detection (Fig. 3.3), the relative concentrations show the same general trends among the matrices. Even so, the quantitative numbers for the exosome concentrations reflect recoveries of 53–91% across the matrix types versus the absorbance-determined concentrations (Fig. 3.3). This level of agreement between the highly generic (absorbance) and highly specific (ELISA) means of quantification is quite remarkable. Based solely on the CD81 ELISA, the highest percentage of recovery for EVs containing CD81 was found for the blood serum sample (91%), followed by the saliva (70%), urine (59%), cervical mucus (58%), and the goat milk (53%). This level of variation is not at all surprising because CD81 is not universally expressed and is upregulated/downregulated in EVs of different origins.

3.4 Conclusions

The C-CP fiber tip isolation method has proven to be an efficient means of EV isolation, with the ability to withstand potentially complex matrix effects from human urine, saliva, cervical mucus, blood serum, and goat milk. The HIC-based EV isolation technique presents significant benefits regarding time, cost, and ease of use. The C-CP spin-down tip workflow enables the processing of multiple samples simultaneously in 15 min, limited only by the table-top centrifuge capacity. The method of standard addition

employing a commercial exosome standard stock was demonstrated as an accurate means to determine the concentration of EVs, regardless of the matrix type. That said, the respective responses showed very little difference in sensitivity (i.e., minimal matrix effects). NTA analysis provided the determination of particle size distributions and overall particle densities for the different matrices. TEM analysis confirms that the EVs isolated from all biofluids retained the characteristic cup or donut-shaped morphology after the isolation process. The purity of the EV isolates was confirmed through Bradford assays, revealing total protein content before and after isolation, with up to 89% of biofluid-originating proteins being removed. The efficacy of the method to isolate bioactive EVs was demonstrated through an ELISA assay for the CD81 tetraspanin marker protein. Overall, there was a self-consistency in the relative (and absolute) amounts of EVs isolated from the different matrices based on the multiple, independent measurement approaches. This agreement serves to validate the quantitative aspects of the isolation process.

The bench-top C-CP spin-down tip protocol introduces a relatively facile means of EV isolation. The C-CP tip HIC isolation method's capabilities make it an ideal candidate for use in laboratory settings. The ability to work with microliter volumes while achieving high EV yields and purity lends itself to both clinical and fundamental EV research applications. For example, the ability to alleviate the complicating aspects of serum/lipoproteins is an essential element in performing high-fidelity proteomics analysis. Likewise, the same factors are key in developing bioassays based on the presence of targeted surface marker proteins. Finally, while likely requiring the use of

preparative scale columns, the characteristics demonstrated here are essential in the development of EVs as gene therapy vectors.

Conflicts of interest

The authors declare no conflicts of interest.

3.5 Acknowledgements

Financial support for the chromatography development efforts came from the National Science Foundation, Division of Chemistry under grant CHE-1608663. Financial support for the EV and exosome isolation efforts came from the Eppley Foundation for Scientific Research and The Gibson Foundation. Dr Larry Puls (Prisma Health), the Prisma Health ITOR Biorepository, and Prisma Health are gratefully acknowledged for patient identification and sample collection. Special thanks to George Wetzel, Clemson University Electron Microscopy Facility for assistance with EM. The content of this material and any opinions, findings, conclusions, or recommendations expressed in this material are solely the responsibility of the author(s) and do not necessarily represent the official views of the National Science Foundation. The graphical abstract presented here was created with BioRender.com.

3.6 References

1. F. Momen-Heravi, L. Balaj, S. Alian, P.-Y. Mantel A. E. Halleck, A. J. Trachtenberg, C. E. Soria, S. Oquin C. M. Bonebreak and E. Saracoglu, *Biol. Chem.,* 2013, 394, 1253–1262.
2. F. M. Heravi, S. Bala, K. Kodys and G. Szabo, Sci. Rep., 2015, 5, 9991.

3. Y. Ouyang, A. Bayer, T. Chu, V. A. Tyurin, V. E. Kagan, A. E. Morelli, C. B. Coyne and Y. Sadovsky, *Placenta*, 2016, 47, 86–95.

4. S. Keerthikumar, D. Chisanga, D. Ariyaratne, H. Al Saffar, S. Anand, K. Zhao, M. Samuel, M. Pathan, M. Jois, N. Chilamkurti, L. Gangoda and S. Mathivanan, *J. Mol. Biol.,* 2016, 428, 688–692.

5. S. Pant, H. Hilton and M. E. Burczynski, *Biochem. Pharmacol.,* 2012, 83, 1484–1494.

6. Z. J. Smith, C. Lee, T. Rojalin, R. P. Carney, S. Hazari, A. Knudson, K. Lam, H. Saari, E. L. Ibanez, T. Viitala, T. Laaksonen, M. Yliperttula and S. Wachsmann-Hogiu, *J. Extracell. Vesicles*, 2015, 4, 28533.

7. K. L. Schey, J. M. Luther and K. L. Rose, Methods, 2015, 87, 75–82.

8. M. Colombo, C. Moita, G. van Niel, J. Kowal, J. Vigneron, P. Benaroch, N. Manel, L. F. Moita, C. Thery and G. Raposo, *J. Cell Sci.,* 2013, 126, 5553–5565.

9. J. Kowal, M. Tkach and C. Théry, Curr. Opin. *Cell Biol.,* 2014, 29, 116–125.

10. M. Kanada, M. H. Bachmann and C. H. Contag, *Trends Cancer*, 2016, 2, 84–94.

11. V. Sokolova, A. K. Ludwig, S. Hornung, O. Rotan, P. A. Horn, M. Epple and B. Giebel, *Colloids Surf., B,* 2011, 87, 146–150.

12. E. Willms, H. J. Johansson, I. Mager, Y. Lee, K. E. M. Blomberg, M. Sadik, A. Alaarg, C. I. E. Smith, J. Lehtio, S. E. L. Andaloussi, M. J. A. Wood and P. Vader, *Sci. Rep.,* 2016, 6, 12.

13. A. Bobrie, M. Colombo, S. Krumeich, G. Raposo and C. Thery, *J. Extracell. Vesicles,* 2012, 1, 18397.

14. A. Bobrie, M. Colombo, G. Raposo and C. Thery, Traffic, 2011, 12, 1659–1668.

15. A. V. Vlassov, S. Magdaleno, R. Setterquist and R. Conrad, *Biochim. Biophys. Acta,* 2012, 1820, 940–948.

16. S. Roy, F. H. Hochberg and P. S. Jones, *J. Extracell. Vesicles*, 2018, 7, 1438720.

17. D. M. Pegtel and S. J. Gould, *Annu. Rev. Biochem.,* 2019, 88, 487–514.

18. L. L. Yu, J. Zhu, J. X. Liu, F. Jiang, W. K. Ni, L. S. Qu, R. Z. Ni, C. H. Lu and M. B. Xiao, *BioMed. Res. Int.,* 2018, 2018, 3634563.

19. S. Halvaei, S. Daryani, Z. Eslami-S, T. Samadi, N. Jafarbeik- Iravani, T. O. Bakhshayesh, K. Majidzadeh-A and R. Esmaeili, *Mol. Ther. – Nucleic Acids,* 2018, 10, 131–141.

20. K. B. Johnsen, J. M. Gudbergsson, M. N. Skov, L. Pilgaard, T. Moos and M. Duroux, *Biochim. Biophys. Acta,* 2014, 1846, 75–87.

21. R. C. Lai, F. Arslan, M. M. Lee, N. S. K. Sze, A. Choo, T. S. Chen, M. Salto-Tellez, L. Timmers, C. N. Lee, R. M. El Oakley, G. Pasterkamp, D. P. V. de Kleijn and S. K. Lim, *Stem Cell Res.,* 2010, 4, 214–222.

22. X. Yang, Z. Weng, D. L. Mendrick and Q. Shi, *Toxicol. Lett*., 2014, 225, 401–406.

23. M. L. Merchant, I. M. Rood, J. K. J. Deegens and J. B. Klein, *Nat. Rev. Nephrol.,* 2017, 13, 731–749.

24. J. Q. Gerlach, A. Kruger, S. Gallogly, S. A. Hanley, M. C. Hogan, C. J. Ward, L. Joshi and M. D. Griffin, *PLoS One*, 2013, 8, e74801.

25. C. Lasser, V. S. Alikhani, K. Ekstrom, M. Eldh, P. T. Paredes, A. Bossios, M. Sjostrand, S. Gabrielsson, J. Lotvall and H. Valadi, *J. Transl. Med.,* 2011, 9, 9.

26. L. A. Aqrawi, H. K. Galtung, B. Vestad, R. Øvstebø, B. Thiede, S. Rusthen, A. Young, E. M. Guerreiro, T. P. Utheim and X. Chen, *Arthritis Res. Ther.,* 2017, 19, 14.

27. F. V. Winck, A. C. Prado Ribeiro, R. R. Domingues, L. Y. Ling, D. M. Riano-Pachon, C. Rivera, T. B. Brandao, A. F. Gouvea, A. R. Santos-Silva, R. D. Coletta and A. F. Paes Leme, *Sci. Rep*., 2015, 5, 16305.

28. B. Pang, Y. Zhu, J. Ni, J. Ruan, J. Thompson, D. Malouf, J. Bucci, P. Graham and Y. Li, Int. *J. Nanomed.,* 2020, 15, 10241–10256.

29. T. Shtam, S. Naryzhny, A. Kopylov, E. Petrenko, R. Samsonov, R. Kamyshinsky, Y. Zabrodskaya, D. Nikitin, M. Sorokin, A. Buzdin and A. Malek, *J. Hematol.,* 2018, 7, 149–153.

30. X. Zhao, Y. Wu, J. Duan, Y. Ma, Z. Shen, L. Wei, X. Cui, J. Zhang, Y. Xie and J. Liu, *J. Proteome Res.,* 2014, 13, 5391– 5402.

31. K. Blans, M. S. Hansen, L. V. Sorensen, M. L. Hvam, K. A. Howard, A. Moller, L. Wiking, L. B. Larsen and J. T. Rasmussen*, J. Extracell. Vesicles,* 2017, 6, 1294340.

32. M. I. Zonneveld, A. R. Brisson, M. J. van Herwijnen, S. Tan, C. H. van de Lest, F. A. Redegeld, J. Garssen, M. H. Wauben and E. N. Nolte-'t Hoen, *J. Extracell. Vesicles,* 2014, 3, 24215.

33. Y. K. Yoo, J. Lee, H. Kim, K. S. Hwang, D. S. Yoon and J. H. Lee, *Micromachines*, 2018, 9, 634.

34. D. Chiasserini, J. R. van Weering, S. R. Piersma, T. V. Pham, A. Malekzadeh, C. E. Teunissen, H. de Wit and C. R. Jimenez, J. Proteomics, 2014, 106, 191–204.

35. A. Milasan, N. Tessandier, S. Tan, A. Brisson, E. Boilard and C. Martel, *J. Extracell. Vesicles,* 2016, 5, 31427.

36. N. Tessandier, I. Melki, N. Cloutier, I. Allaeys, A. Miszta, S. Tan, A. Milasan, S. Michel, A. Benmoussa, T. Levesque, F. Cote, S. E. McKenzie, C. Gilbert, P. Provost, A. R. Brisson, A. S. Wolberg, P. R. Fortin, C. Martel and E. Boilard, *Arterioscler. Thromb. Vasc. Biol.,* 2020, 40, 929–942.

37. E. I. Buzas, B. Gyorgy, G. Nagy, A. Falus and S. Gay, *Nat. Rev. Rheumatol.,* 2014, 10, 356–364.

38. C. Balbi, M. Piccoli, L. Barile, A. Papait, A. Armirotti, E. Principi, D. Reverberi, L. Pascucci, P. Becherini, L. Varesio, M. Mogni, D. Coviello, T. Bandiera, M. Pozzobon, R. Cancedda and S. Bollini, *Stem Cells Transl. Med.,* 2017, 6, 1340–1355.

39. C. Gardiner, D. Di Vizio, S. Sahoo, C. Thery, K. W. Witwer, M. Wauben and A. F. Hill, *J. Extracell. Vesicles,* 2016, 5, 32945.

40. J. B. Simonsen, *Circ. Res.,* 2017, 121, 920–922.

41. B. W. Sódar, Á. Kittel, K. Pálóczi, K. V. Vukman, X. Osteikoetxea, K. Szabó-Taylor, A. Németh, B. Sperlágh, T. Baranyai and Z. Giricz, *Sci. Rep.,* 2016, 6, 24316–24327.

42. C. Thery, K. W. Witwer, E. Aikawa, et. al, *J. Extracell. Vesicles,* 2018, 7, 43.

43. T. Liangsupree, E. Multia and M.-L. Riekkola, *J. Chromatogr. A,* 2021, 1636, 461773.

44. K. W. Witwer, C. Soekmadji, A. F. Hill, M. H. Wauben, E. I. Buzás, D. Di Vizio, J. M. Falcon-Perez, C. Gardiner, F. Hochberg, I. V. Kurochkin, J. Lötvall, S. Mathivanan, R. Nieuwland, S. Sahoo, H. Tahara, A. C. Torrecilhas, A. M. Weaver, H. Yin, L. Zheng, Y. S. Gho, P. Quesenberry and C. Théry, *J. Extracell. Vesicles,* 2017, 6, 1396823.

45. M. Macias, V. Rebmann, B. Mateos, N. Varo, J. L. Perez- Gracia, E. Alegre and A. Gonzalez, *Clin. Chem. Lab. Med.,* 2019, 57, 1539–1545.

46. Y. Yuana, J. Levels, A. Grootemaat, A. Sturk and R. Nieuwland, *J. Extracell. Vesicles*, 2014, 3, 23262.

47. B. J. Tauro, D. W. Greening, R. A. Mathias, H. Ji, S. Mathivanan, A. M. Scott and R. J. Simpson, *Methods*, 2012, 56, 293–304.

48. D. Freitas, M. Balmaña, J. Poças, D. Campos, H. Osório, A. Konstantinidi, S. Y. Vakhrushev, A. Magalhães and C. A. Reis, *J. Extracell. Vesicles*, 2019, 8, 1621131.

49. G. Vergauwen, B. Dhondt, J. Van Deun, E. De Smedt, G. Berx, E. Timmerman, K. Gevaert, I. Miinalainen, V. Cocquyt, G. Braems, R. Van den Broecke, H. Denys, O. De Wever and A. Hendrix, *Sci. Rep.,* 2017, 7, 2704.

50. A. Gámez-Valero, M. Monguió-Tortajada, L. Carreras- Planella, M. L. Franquesa, K. Beyer and F. E. Borràs, *Sci. Rep.,* 2016, 6, 33641.

51. H. Zhang, D. Freitas, H. S. Kim, K. Fabijanic, Z. Li, H. Chen, M. T. Mark, H. Molina, A. B. Martin, L. Bojmar, J. Fang, S. Rampersaud, A. Hoshino, I. Matei, C. M. Kenific, M. Nakajima, A. P. Mutvei, P. Sansone, W. Buehring, H. Wang, J. P. Jimenez, L. Cohen-Gould, N. Paknejad, M. Brendel, K. Manova-Todorova, A. Magalhães, J. A. Ferreira, H. Osório, A. M. Silva, A. Massey, J. R. Cubillos-Ruiz, G. Galletti, P. Giannakakou, A. M. Cuervo, J. Blenis, R. Schwartz, M. S. Brady, H. Peinado, J. Bromberg, H. Matsui, C. A. Reis and D. Lyden, *Nat. Cell Biol.,* 2018, 20, 332–343.

52. R. Stranska, L. Gysbrechts, J. Wouters, P. Vermeersch, K. Bloch, D. Dierickx, G. Andrei and R. Snoeck, *J. Transl. Med.,* 2018, 16, 1.

53. M. Macías, V. Rebmann, B. Mateos, N. Varo, J. L. Perez- Gracia, E. Alegre and Á. González, *Clin. Chem. Lab. Med.,* 2019, 57, 1539–1545.

54. T. F. Bruce, T. J. Slonecki, L. Wang, S. Huang, R. R. Powell and R. K. Marcus, *Electrophoresis*, 2019, 40, 571–581.

55. L. Wang, T. F. Bruce, S. Huang and R. K. Marcus, *Anal. Chim. Acta*, 2019, 1082, 186–193.

56. S. Huang, L. Wang, T. F. Bruce and R. K. Marcus, *Anal. Bioanal. Chem.,* 2019, 411, 6591–6601.

57. K. K. Jackson, R. R. Powell, T. F. Bruce and R. K. Marcus, *Anal. Bioanal. Chem.*, 2020, 412, 4713–4724.

58. S. Huang, L. Wang, T. F. Bruce and R. K. Marcus, *Biotechnol. Prog*., 2020, e2998.

59. X. Ji, S. Huang, J. Zhang, T. F. Bruce, Z. Tan, D. Wang, J. Zhu, R. K. Marcus and D. M. Lubman, *Electrophoresis*, 2021, 42, 245–256.

60. S. Huang, X. Ji, K. K. Jackson, T. F. Bruce, D. M. Lubman and R. K. Marcus, *Anal. Chim. Acta,* 2021, 1167, 338578.

61. L. Wang and R. K. Marcus, *J. Chromatogr. A,* 2019, 1585, 161–171.

62. J. Fausnaugh and F. Regnier*, J. Chromatogr. A,* 1986, 359, 131–146.

63. A. Jungbauer, C. Machold and R. Hahn, *J. Chromatogr. A,* 2005, 1079, 221–228.

64. J. A. Queiroz, C. T. Tomaz and J. M. Cabral, *J. Biotechnol.,* 2001, 87, 143–159.

65. S. Sitar, A. Kejžar, D. Pahovnik, K. Kogej, M. TušekŽnidarič, M. Lenassi and E. Žagar, *Anal. Chem.,* 2015, 87, 9225–9233.

66. B. Vestad, A. Llorente, A. Neurauter, S. Phuyal, B. Kierulf, P. Kierulf, T. Skotland, K. Sandvig, K. B. F. Haug and R. Øvstebø, *J. Extracell. Vesicles*, 2017, 6, 1344087.

67. Z. Andreu and M. Yanez-Mo, *Front. Immunol.,* 2014, 5, 442.

68. E. Willms, C. Cabanas, I. Mager, M. J. A. Wood and P. Vader, *Front. Immunol.,* 2018, 9, 738.

69. V. Vagenende, A. X. Han, M. Mueller and B. L. Trout, *Chem. Biol.,* 2013, 8, 416–422.

70. V. Vagenende, M. G. Yap and B. L. Trout, *Biochemistry*, 2009, 48, 11084–11096.

71. B. E. Saxberg and B. R. Kowalski, *Anal. Chem.,* 1979, 51, 1031–1038.

72. K. Vaswani, M. D. Mitchell, O. J. Holland, Y. Q. Koh, R. J. Hill, T. Harb, P. S. W. Davies and H. Peiris, *J. Nutr. Metab.,* 2019, 2019, 5764740.

73. L. Musante, S. V. Bontha, S. La Salvia, A. Fernandez-Piñeros, J. Lannigan, T. H. Le, V. Mas and U. Erdbrügger, *Sci. Rep.,* 2020, 10, 3701.

74. S. R. Kumar, E. T. Kimchi, Y. Manjunath, S. Gajagowni, A. J. Stuckel and J. T. Kaifi, *Sci. Rep.,* 2020, 10, 2800.

75. P. J. Wermuth, S. Piera-Velazquez and S. A. Jimenez, *Clin. Exp. Rheumatol.,* 2017, 35(Suppl. 106), 21–30.

76. C. Conzelmann, R. Groß, M. Zou, F. Krüger, A. Görgens, M. O. Gustafsson, S. El Andaloussi, J. Münch and J. A. Müller, *J. Extracell. Vesicles*, 2020, 9, 1808281.

CHAPTER FOUR

COMPARISON OF THE CAPILLARY-CHANNELED POLYMER (C-CP) FIBER SPIN-DOWN TIP APPROACH TO TRADITIONAL METHODS FOR THE ISOLATION OF EXTRACELLULAR VESICLES FROM HUMAN URINE

4.1 Introduction

Extracellular vesicles (EVs) are phospholipid bilayer–bound vesicles released by cells to mediate various intercellular communication processes through the delivery of essential biomolecular cargos, including proteins, nucleic acids, and lipids [1,2,3]. Though no official nomenclature classification system exists, EVs are roughly categorized based on size and theoretical modes of biogenesis [4, 5]. Among EV subtypes, exosomes, microvesicles, and apoptotic bodies are the most commonly studied. Exosomes (or small EVs, sEVs) have become targets for EV–based diagnostic and therapeutic applications [6,7,8] by virtue of inherent characteristics derived from their creation through a multivesicular body (MVB) endosomal pathway [9]. Because of this, exosomes serve as “genetic snapshots” of their cell of origin, encompassing DNA, varied RNA types, and surface biomarker proteins from the mother cell [10]. Microvesicles and apoptotic bodies, while generally < 1000 nm in diameter, are similar, but highly variable in size [11]. However, they have distinctive proposed biogenesis modes: apoptotic bodies are formed as a by-product of cell death, while microvesicles result from generic cell membrane budding. With the size overlap between exosomes and microvesicles (30–200 nm), classifying EVs based on size alone is not necessarily indicative of their origin.

Thus, an EV nomenclature system based on size alone may lead to incorrect conclusions about EV biogenesis. Despite these classification difficulties, due to their similar contents and sizes, exosomes and microvesicles are targeted in fundamental biochemical studies and clinical analyses, where they are generically referred to as EVs.

Mother cell–originating species like DNA, RNA, and biomarker proteins are incorporated during EV biogenesis and facilitate transfer of essential biomolecules to recipient cells [12]. Their small size, biocompatibility, and stability through the varying microenvironmental conditions of biological systems make EVs ideal for communication between cells in close and distant proximity, even across the blood–brain barrier [13]. EVs have been identified in over 30 biofluid types in all biological domains, including urine [14], saliva [15], blood serum [16], and plasma [17], and analysis of their contents has provided insights into the progression and transmission of several diseases [4, 18]. Yet, the efficient collection, isolation, and characterization of EVs remain challenging. A lack of clear standardization and the complexity of their biofluid matrices of origin have become limiting factors in advancing the EV studies [19].

One obstacle to EV research is efficient isolation. Current methods often produce recoveries unfit for analysis and contaminated with unwanted matrix species. For example, the presence of background proteins, particularly lipoproteins, can affect high-quality exosome-specific proteomics. Thus, development of a method that consistently provides high-concentration, pure, structurally preserved EVs is still needed. The most widely employed EV isolation methods rely upon vesicle harvesting by size, density, or the presence of surface biomarkers [20,21,22,23,24,25]. These methods include

ultracentrifugation (UC) [26], ultrafiltration [27], size exclusion [28], and immunoaffinity [29] approaches, but there is no optimal technique for all situations [30]. The method should be chosen based on the post-isolation intent and/or application of the isolated EVs. The scale of the process is also relevant, ranging in size from clinical diagnostics to fundamental studies and preparative scales for vector production.

Inevitably, the choice of EV isolation method presents a compromise between specificity (referring to both vesicle type and contaminant content) and efficiency [31]. Of the available techniques, the UC method, consisting of several sequential low- to high-speed centrifugation steps, has become the most utilized [31]. However, despite its wide use, this labor-intensive, time-consuming method results in low EV recoveries contaminated by protein and lipoprotein aggregates [32]. Several commercial EV isolation kits are available, including the exoEasy (Qiagen, Hilden, Germany) and ExoQuick (System Biosciences, Palo Alto, CA) kits [33, 34]. Though many commercial kits are marketed to produce "pure" EV recoveries, concerns about concentration and purity (defined here as the freedom from matrix proteins and other materials) remain, as proprietary polymeric precipitation reagents can present an additional source for eluate complexity and challenges downstream. Many groups have conducted studies to compare various isolation techniques, including evaluation of the isolated exosomes for stability and biochemical efficacy [35,36,37,38,39,40]. Unfortunately, when examined together, these studies have shown contradictory or inconclusive results.

A hydrophobicity-based isolation method on a capillary-channeled polymer (C-CP) fiber stationary phase has been previously applied to EV isolations on both high-

performance liquid chromatography (HPLC) [41,42,43,44,45] and spin-down micropipette tip [46, 47] formats. The method is driven by an organic modifier-assisted hydrophobic interaction chromatography (HIC) solvent system, which efficiently harvests EVs from biofluids, while excluding free proteins and lipoprotein aggregates [42]. The purity of isolates from human serum has been confirmed by mass spectrometric proteomic analysis [42]. Subsequently, a synthetic mixture of LDLs and EVs was separated using the method, with the relative abundance of Apo B-100 within the sample accounting for only 0.3% of the protein content (279 identified) in the EV fraction [48]. In the development of the HIC–based technique, both acetonitrile and glycerol solvent modifiers were used to quicken the EV isolation while preserving vesicle integrity [45]. The acetonitrile solvent modifier has proven best for EVs undergoing post-isolation immunoaffinity characterization. While high acetonitrile concentrations are not ideal for long-term EV preservation, the majority of latent acetonitrile can be off-gassed under minimal vacuum. The glycerol solvent modifier is ideal when long-term preservation of EV structure is required, as glycerol is a common cryoprotectant for cell preservation [49]. However, high glycerol concentrations can interfere with some immunoassays [50, 51], potentially hindering some downstream characterization. However, latent glycerol can be readily removed using a post-isolation filtration step [42]. Still, the C-CP tip methods have repeatedly demonstrated the ability to provide highly concentrated, pure EVs from a number of complex biofluid matrices (including urine, saliva, blood plasma/serum, and cervical mucus) with up to 99% removal of contaminant proteins/lipoproteins.

Here, the HIC C-CP tip method performance (using both aforementioned organic modifiers) is compared to UC and two commercial kits for isolation of EVs from the same human urine sample. The EVs recovered via each method are assessed using UV–VIS absorbance (scattering) quantification, Nanosight nanoparticle tracking analysis (NTA) for quantification and sizing, transmission electron microscopy (TEM) for vesicle structure validation, an enzyme-linked immunosorbent assay (ELISA) utilizing antibodies to accepted EV marker proteins as a means of quantification and validation of surface chemical integrity, and a purity assessment by protein assay. It is believed that the C-CP fiber spin-down tip methodology offers pronounced benefits over the commonly employed methods across the metrics of practicality and target EV collection efficiency and purity. Furthermore, once isolated, EVs extracted by this method are ready for downstream characterization and utilization.

4.2 Materials and Methods

4.2.1 EV Sources

Commercial lyophilized exosome standards of 9.3 x 10^{12} particles mL^{-1} concentration from the urine of healthy patients were obtained from Hansa BioMed (Tallinn, Estonia). The exosome standards were reconstituted in 100 µL of Milli-Q water as instructed by the manufacturer and used to prepare the absorbance-based response curves. To be clear, these EV "standards" are not EV reference standards but are EVs of known concentration (methods not disclosed) for quantitative measures. Therefore, no quantitative/qualitative variables (e.g., purity) apart from concentration are supplied,

which is acknowledged here. For the inter-method comparison, first-morning urine was collected from a healthy, consenting, anonymous donor in accordance with a standing Clemson University IRB protocol. The sample was filtered with a 0.22 µm sterile polyethersulfone (PES) syringe filter (FroggaBio, Toronto, Canada) then immediately employed in the various isolation workflows.

4.2.2 Chemicals, Solvents, and Antibodies

The deionized water (DI-H2O, 18.2 MΩ-cm) used here was obtained from a Milli-Q water purification system (Millipore Sigma, Merck, Darmstadt, Germany). Biotechnology-grade glycerol and ammonium sulfate were purchased from VWR (Sokon, OH, USA). Phosphate buffered saline (PBS, pH = 7.4), bovine serum albumin (BSA), a Pierce™ BCA Protein Assay Kit, and a Pierce™ ECL Substrate were purchased from ThermoFisher Scientific (Waltham, MA, USA). Paraformaldehyde and formvar/carbon 200 mesh copper grids were obtained from Electron Microscopy Sciences (Hatfield, PA). The mouse monoclonal antibody to CD81 (200 µg mL^{-1}) was obtained from Santa Cruz Biotechnology (Dallas, TX). Mouse monoclonal antibody to CD63 (0.5 mg mL^{-1}) was obtained from ThermoFisher Scientific. Goat anti-mouse horseradish peroxidase (HRP)-conjugated secondary antibody (0.7 mg mL^{-1}) was obtained from MP Bio (Santa Ana, CA).

4.2.3 Isolation Methods

In order to assure the efficacy and validity of the inter-method comparison, each of the isolation methods was carried out explicitly as described in either the commercial manufactures' instructions or by following well-described methods in the literature, as in

the case of the C-CP fiber tips and the UC. All extractions/ determinations were performed in parallel, triplicate. Every effort was exercised to ensure that the singular, pooled human urine sample was in a state of homeostasis throughout the samplings. That is, all isolation procedures were commenced at the same time, and/or the sub-samplings were performed at the same time and held at 4 ºC until use, with the solutions agitated to ensure homogeneity.

4.2.3.1 C-CP Tip Construction and Workflow

The capillary-channeled polymer (C-CP) fiber micropipette tips were created through the previously described process. [46,52] Polyester (polyethylene terephthalate, PET) C-CP fibers were melt-extruded from commodity bulk polymer into an 8-pronged periphery by the Clemson University School of Materials Science. Eight rotations of the PET fiber phase, approximately 450 polymer fibers per tip, were packed collinearly into fluorinated ethylene propylene (FEP) tubing of 0.8 mm inner diameter. Next, the column was repeatedly pulled and cut to create 1 cm of fiber-packed tubing with 0.5 mm of empty tubing to allow for attachment to a 200 µL micropipette tip. The micropipette tip with the C-CP fiber phase attached was placed inside a 1 mL micropipette tip, then set into a 15 mL conical receiver with an adapter-modified cap to hold the C-CP phase connected tip in place.

Two hydrophobic interaction chromatography solvent systems were employed, including acetonitrile and glycerol organic modifiers. In both cases, 200 µL of filtered urine was mixed with an equal part of ammonium sulfate (2M final concentration), then applied to the C-CP tip's sample reservoir, placed into the tabletop centrifuge, and spun

down at 300 x g for 1 minute. Here, the method diverts to employ the two different organic modifier solvents. For the acetonitrile method, the elution of proteins was induced using 100 µL of 25% acetonitrile in 1M ammonium sulfate, with the elution of EVs induced using 100 µL of 50% acetonitrile in PBS. Similarly, for the glycerol solvent modifier, the elution of proteins was induced using the same volumes of 25% glycerol in 1M ammonium sulfate, and EV elution was induced using 50% glycerol in PBS.

4.2.3.2 Commercial EV Isolation Kits

EVs were extracted from the filtered urine samples by the Qiagen exoEasy and System Biosciences ExoQuick isolation kits by following the manufacturer's instructions explicitly. For the ExoQuick-TC isolation, 10 mL of filtered urine was centrifuged at 3,000 x g for 15 minutes, then mixed with 2 mL of ExoQuick-TC by inverting the conical tube several times. The sample mixed with the ExoQuick reagent was incubated upright at 4°C overnight. Next, the ExoQuick-biofluid mixture was centrifuged at 1,500 x g for 30 minutes. The supernatant was removed, and the EV pellet was resuspended in 100 µL of PBS. For the Qiagen exoEasy isolation, 8 mL of filtered urine was mixed with equal parts of buffer "XBP" and mixed by inverting the conical tubes several times before applying the 16 mL of the mixture to the exoEasy spin column and centrifuging at 500 x g for one minute. This step was repeated 8 times to allow the entire volume to pass through the membrane. The flow-through solution was discarded, and 10 mL of buffer "XWP" was added before centrifuging at 5,000 x g for 5 minutes. Again, the flow-through solution was discarded. Then 400 µL of buffer "XE" was added to the membrane and incubated for 1 minute before centrifuging at 500 x g for five minutes to collect the

eluate. The eluate was reapplied to the column and incubated for one minute before centrifuging twice at 5,000 x g for 5 minutes to collect the EVs.

4.2.3.3 Ultracentrifugation

EVs were isolated from the filtered urine using an ultracentrifugation protocol for urine similar to that as published by Gheinani et al.,[53] using several differential centrifugation steps. First, 45 mL of the filtered urine sample was centrifuged at 200 × g for 20 minutes. The resulting pellet was discarded, and the supernatant was centrifuged at 2,000 × g for 20 minutes to remove remnant cellular debris and protein contaminants. Next, the supernatant was centrifuged at 16,000 × g for 20 minutes to remove larger particles, and the resulting supernatant was ultracentrifuged at 120,000 × g for 70 minutes. Finally, the supernatant was removed, and the resulting EV pellet was resuspended in 500 µL of PBS.

4.2.4 EV Characterization

4.2.4.1 Transmission Electron Microscopy (TEM)

TEM is the gold standard in the physical identification of EVs, where the vesicular structure and cup-like forms are characteristic features. The sample preparation for electron microscopy imaging was adapted from the negative staining protocol described by Jung et al. [54] The isolated EVs were fixed for five minutes using 2% paraformaldehyde, and 7 µL of the EV suspension was loaded onto the copper grid and incubated for 10 minutes. The grids were blotted dry before washing with water for 5 minutes, and a 50 µL drop of 2% paraformaldehyde was placed on the grid for 5 minutes. The grid was immediately stained using 20 drops of filtered 1% uranyl acetate solution.

Excess uranyl acetate solution was removed, and the grip was rinsed with a drop of water before allowing it to dry in a cell culture dish for 10 minutes at room temperature.

4.2.4.2 UV-Vis Absorbance Quantification

Previous reports from this laboratory have proven the efficacy of using HPLC post-column absorbance detectors to quantify EVs very simply based on their scattering of light.[43-45] Likewise, standalone UV-Vis spectrometers can be employed to determine concentrations following spin-down tip processing.[46,48] EVs were quantified using absorbance (scattering) detection at 203 nm using a NanoVue Plus UV-Vis spectrophotometer (GE Healthcare, Chicago, IL, USA).[46,48] The absorbance response of each EV isolate at 203 nm was compared to a response curve generated using serial dilutions of the commercial exosome standards (9.3×10^{12} particles mL^{-1} stock). Again, because this commercial exosome standard stock is not a well-characterized or standardized reference material, only general approximations of the EV concentration method can be made here. No purity or antigen expression metrics were provided by the exosome standard manufacturer; therefore, no conclusions of this sort are able to be drawn based on comparison to the exosome "standard" stock.

4.2.4.3 Nanoparticle Tracking Analysis (NTA)

Nanoparticle tracking analysis is the benchmark method for the sizing, and to a lesser extent, EV concentration measurement, though its limitations and peculiarities are well documented.[55] The NanoSight NS300 (Malvern Panalytical, Westborough, MA) NTA system was used to analyze the size distribution of the eluted EVs. For all NTA experiments, replicates of 5 runs were used for each sample in 60-second intervals, with

the syringe pump set to a constant flow of 50 µL min^{-1}. A minimum of 200 valid tracks per video and 1000 valid tracks per sample were recorded. The camera level was set to 14, and the detection threshold was set to 3 as optimized by Vestad et al. [56] Each sample was diluted 500X to be in the operating range (1 x 10^7- 10^9 particles mL^{-1}) of the NS300 instrument.

4.2.4.4. Enzyme-Linked Immunosorbent Assay (ELISA)

An indirect ELISA was used to detect the presence of the EVs in the isolates based on antibodies to the CD63 and CD81 tetraspanin proteins present on the vesicle surfaces. Before this assay, the latent solvents from the tip-isolated EVs were removed by off-gassing overnight at 4°C (for acetonitrile isolates) and using a 100-kDa filter unit (for glycerol isolates), as high concentrations of these solvents have been previously shown to affect antibody binding interactions specifically in ELISA assays [50,51,57]. The isolated EVs (25 µL) were loaded onto the ELISA 96-well plate in triplicate, using equal volumes (25 µL of ELISA coating buffer - 0.05 M carbonate-bicarbonate in PBS) and incubated overnight at 4°C. An exosome standard positive control, along with negative controls of the PBS, protein elution buffers, and EV elution buffers, were also employed here in triplicate. After sample incubation, each well was washed with 200 µL of sterile PBS over 30 minutes, with six buffer changes. The wells were then blocked using 200 µL of 5% BSA in PBS at room temperature for 30 minutes before incubation with 50 µL of the CD63 and CD81 mouse monoclonal antibodies, both of 1 µg mL^{-1} concentration. The primary antibody was allowed to incubate on a shaker overnight at 4°C. The washing and blocking steps using PBS and 5% BSA, respectively, were repeated here before applying

50 µL of the goat anti-mouse HRP conjugated secondary antibody. Finally, 100 µL of the chemiluminescent substrate was applied, and the chemiluminescent response was detected using a Synergy H1 Hybrid (BioTek, Winooski, VT) plate reader.

4.2.4.5 microBCA Protein Assay

A standard BCA assay determined the concentration of proteins present in the EV isolates. For the microBCA assay, a 25 µL aliquot of the isolated EVs was added to 125 µL of PBS and 150 µL of the assay working reagent. The 96 well plates were covered and allowed to incubate at 37°C for 2 hours, then cooled to room temperature. The absorbance response at 562 nm was measured using the Synergy H1 Hybrid plate reader. A standard curve using BSA standard solutions was used to determine the concentration of protein in each unknown sample. The average absorbance reading of the blank (PBS) was subtracted from all standards and the UC isolated EVs. The average absorbance reading of the elution buffers for the commercial kit and C-CP tip isolates from a blank sample (PBS) were used for the blank subtraction of the urine isolates. The standards and samples were applied in triplicate to the 96 well plate, and the absorbance response for each well was measured in triplicate.

4.3 Results and Discussion

4.3.1 Structural Verification via TEM

Despite the variety of available EV characterization methods, electron microscopy techniques, like TEM, are definitive methods to confirm the presence of EVs based on their physical structure. TEM analysis visually confirms the presence of EVs by revealing

the characteristic size and cup shape. There is a universality in the approach, as there is little concern relative to purity or complications that arise from too much chemical selectivity, which also brings a high susceptibility to errors/contamination. TEM analysis was used in this study to compare the size, shape, and integrity of the EV populations obtained using the various isolation methods. Representative micrographs of human urine-derived EVs isolated using each method are presented in Fig. 4.1, along with the as-delivered commercial EVs.

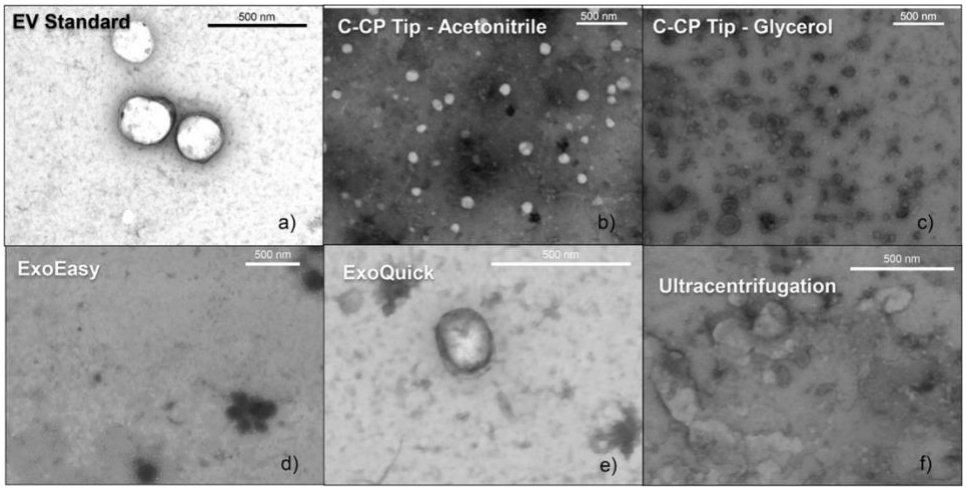

Figure 4.1: Transmission electron micrographs of commercial urine exosome standards (a), and extracellular vesicles (EVs) from the same urine sample, isolated using the capillary-channeled polymer (C-CP) fiber tip methods (acetonitrile (b) and glycerol (c)), exoEasy (d) and ExoQuick (e) kits, and the traditionally used ultracentrifugation method (f). The SEM images were taken using the Hitachi SU9000.

As expected, the TEM micrograph of the exosome standard stock (Fig. 4.1a) reveals the cup or donut-shaped EVs from the reconstituted EV standard stock. Smaller, more cup-shaped vesicles are observed in the human subject urine EVs recovered by the C-CP fiber tips, employing both the acetonitrile and glycerol organic solvent modifiers (Figs. 4.1b and 4.1c). A somewhat more pronounced cup shape is observed in the vesicles

recovered using the C-CP tip with the glycerol solvent system (Fig. 4.1c), confirming the EV preservation qualities of the glycerol solvent. The TEM images visually confirm the ability of the C-CP tip method to isolate EVs from urine samples and reveal the production of concentrated, structurally preserved vesicle recoveries.

Significant differences in vesicle populations are observed in Figs. 4.1d-f, where many large and agglomerated collections of EVs are shown for the commercial and UC methods. This is not surprising for the EVs obtained by the polymeric precipitation techniques (Fig. 4.1d and e) as they isolate the vesicles based on an overall entrapment mechanism, capturing the vesicles from the biofluid samples using a polymer network. Large aggregates are also observed in the EVs obtained by the ultracentrifugation-based method, which is a basic characteristic of the process. In the UC EVs (Fig. 4.1f), many agglomerate particles are observed in protein/contaminant aggregates, but still, the characteristic cup-shaped EV morphologies are observed here. As visualized in Fig. 4.1, one of the main issues in EV isolation techniques is the co-precipitation of biofluid-originating contaminants and the creation of large agglomerated and contaminated EV recoveries. Comparing the visual integrity of EV isolates from the C-CP tips to those recovered by the commercial kits and traditional EV isolation method, significant differences are revealed in the overall shape and degree of aggregation. As shown in Figs. 4.1b and 4.1c, the observed average diameters of vesicles isolated via the C-CP tip acetonitrile and glycerol solvent systems are approximately 100 nm. The C-CP tip methods allowed for more dispersed EV isolations to be obtained with fewer visual contaminants. Most importantly moving forward, the tip method allows for the structural

preservation of the EVs with the characteristic cup shape, suggesting retention of structural integrity.

4.3.2 Recovery Quantification via UV-Vis Absorbance

EV quantification using commercial stocks of EVs based on the absorbance at 203 nm has been previously reported. [46] With serial dilutions of a commercial exosome stock of known concentration, a calibration curve enables the quantification of EVs based on a simple absorbance measurement at 203 nm. This detected absorbance response is not credited to the electronic transitions that typically cause spectrophotometric absorbance responses, but more accurately, the scattering response due to the presence of the EVs. To be sure, scattering characteristics are a function of particle size/composition, but in this single-source case, the relative responses should be solely related to numbers. As such, the resulting measured absorbance at the 203 nm wavelength is proportional to the concentration of EVs in solution. Figure 4.2 shows the concentration of EVs obtained from human urine by the employed isolation methods.

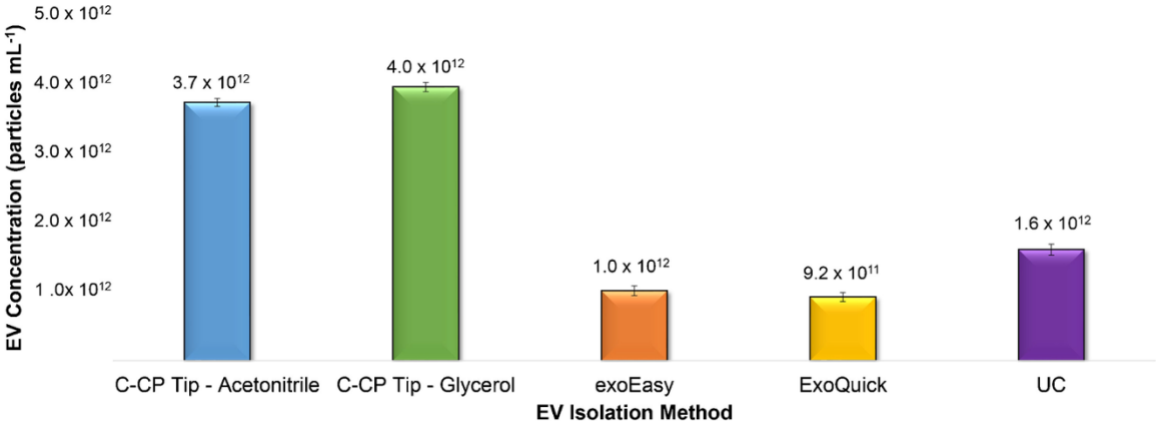

Figure 4.2: Bar graph representing the concentration of EV yields obtained from the C-CP tip (acetonitrile and glycerol), exoEasy, ExoQuick, and ultracentrifugation methods based on absorbance detection and comparison to a calibration curve of linear response ($y = 2E - 13x + 0.0264$, $R^2 = 0.9935$, $n = 3$).

Based on absorbance quantification, concentrations of approximately 4 x 10^{12} EV mL^{-1} in the 200 µL test aliquots were obtained using the two C-CP tip methods, recoveries of 2 to 4X lower concentration are obtained using the other EV isolation methods. Both polymeric precipitation techniques resulted in recoveries of approximately 1 x 10^{12} EV particles mL^{-1}, with the ultracentrifugation method resulting in an EV recovery of ~2 x 10^{12} EV particles mL^{-1}. With the significant contaminants observed in the TEM images of EVs from the polymeric precipitation and UC isolation methods, this absorbance-based quantification of EVs is potentially skewed by the protein/contaminant aggregates, actually overrepresenting the EV concentrations in those isolates.

It is important to draw a distinction between the respective starting volumes of the applied EV isolation methods, wherein the tip isolations began with 200 µL volumes of the human urine, the commercial kits began with 8 to 10 mL (ExoQuick-TC and exoEasy, respectively) of the urine sample, and the UC was performed with a 45 mL starting volume. In all, the C-CP tip method using both the acetonitrile and the glycerol solvent systems were able to produce higher concentrations of EVs than commonly employed EV isolation methods, despite using less than 3% of the initial urine sample volume. As such, there may be significant advantages to using the tip isolation methods in critical sample volume-limited applications.

Currently, there are no standardized methods for EV isolation, quantification, or characterization. Limiting EV research is the lack of reference standards to serve as a comparison point for the classification, purity, concentration, and composition of EVs. Commercial stocks of "exosome standards" have been used in many proof-of-concept EV demonstrations (as included here), but the characterization of these products has introduced concerns regarding vesicle size, purity, and concentration of those materials themselves.[58] Field-wide standardization has become a focal point for many scientists, including the International Society for Extracellular Vesicles (ISEV), whose efforts have established minimal guidelines for the studies of EVs (MISEV).[30] Important factors emphasized in the MISEV guidelines[30] are the revelation of physical (size and structure) surface species and cargo-related characteristics. In these defined guidelines, no standard experimental approaches for EV research were established. Since the upregulated release of EVs has been shown to be an indicator of stress or disease, EV quantification in itself could serve as a method to monitor disease or treatment effectiveness. [59,60] However, the MISEV guidelines emphasize a lack of EV quantification techniques, and the consortium was unable to suggest efficient approaches for EV quantification [30]. Again, an EV reference standard would be an essential catalyst towards the optimization and development of EV quantification techniques. Despite these shortcomings of employing commercial EV stocks during quantitative approaches, the commercially obtained exosome standard stock was included and enabled a sufficient approximation of EV concentration to be performed despite this potential area for systematic error.

4.3.3 Vesicle Sizing and Densities via NTA

To assess the size distribution, and to a lesser extent concentration, of the recovered EVs, nanoparticle tracking analysis was employed. In doing so, it is important to understand that such interpretations are extremely subjective as the species which contribute to "signals" in the NTA experiment are highly varied. This is because a number of species exist across the relevant size range of ~ 30–300 nm, including the different EV classes, other vesicles, lipoproteins, protein agglomerates, protein-vesicle aggregates, and vesicle clusters. Apparent sizing can also be affected by the solvent system, including its chemistry and viscosity, which can influence mobility and intraparticle associations. Finally, NTA signals can be affected by "generic particles" existing in the test solution and indeed the laboratory environment. Interpretations also rely on the starting hypotheses; for example, isolated exosomes should fit in the 70–120-nm size range, which again is not definitive, and everything else is a perversion. Shown in Fig. 4.3 are the NTA–determined size distributions of EVs from the commercial standard stock and the populations recovered from human-subject urine using the various EV isolation methods.

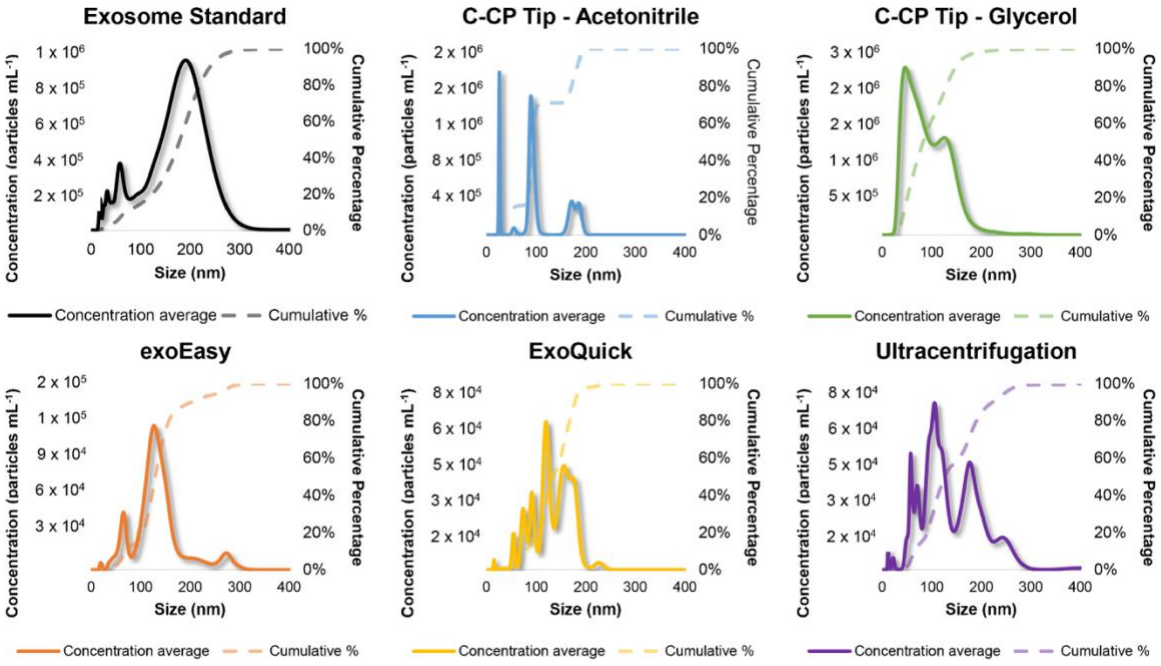

Figure 4.3: Size distribution and cumulative percentage of size distribution of commercial exosome standards and EVs isolated using the C-CP tip (acetonitrile and glycerol), exoEasy, ExoQuick, and ultracentrifugation methods as determined using the NanoSight NS300 NTA system. Average of n = 5 runs, 60 s each.

It is important to note that the EV concentration results presented in Fig. 4.3 are not directly reflective of the total EV concentration. The isolated EVs were diluted for compatibility with the working range of the NTA system (1×10^7 to 1×10^9 particles mL^{-1} concentration). The NTA size distribution data indeed confirm the size variability of the components included in the "exosome standard" source, as seen in Fig. 4.3. It is important to note here that though marketed as an exosome standard product, variation in size and large amounts of contaminating protein content are revealed. The exosome standard presents a pseudo-Gaussian distribution of the vesicles centered at approximately 200 nm (much larger than ascribed to EVs) and with some smaller

populations of vesicles with diameters of 75 nm or less. The inclusion of smaller populations of particulate species suggests protein and/or lipoprotein aggregates contaminating the "standard" product. This confirms the inclusion of non-exosomal materials in the commercial exosome standard stock as suggested in the TEM micrograph, which is not surprising given that the material is isolated by UC. This observation is not unique to this study, as issues with MV and non-sEV materials being included in commercialized exosome standard products have been previously observed [58]. This reiterates the need for standardization and regulation of exosome products, the delivery of high-purity materials, and requirements for accurate nomenclature marketing to be employed. The NTA–determined size distributions present a wide diversity of recoveries or at minimum measurement environments. For example, the comparison of the distributions of the two C-CP tip isolates is very telling. Two very distinct populations are seen in the case of the acetonitrile-modified elution system, the "expected" one at ~ 100 nm and the much smaller one at ~ 2 × the diameter. On the other hand, the glycerol-based isolate shows a very broad distribution of sizes, with sub-populations at ~ 60 and 120 nm. As the same immobilization chemistry is employed, the differences here may reflect the two organic environments. It would not be hard to postulate that the smaller size could be glycerol globules, with perhaps the larger being EVs that are solvated in glycerol to yield larger sizes. The melding of the two populations perhaps reflects the high viscosity of the solvent.

Just as the two tip isolates exhibit differences in the size of the recovered EVs, the two polymer kit approaches also reveal differences in this regard. In the case of the

exoEasy kit, one can readily interpret a population of protein aggregates of ~ 75 nm and a broad EV population ~ 100–180 nm. In addition, ~ 15% of the particles exist in a size fraction from 275 to 300 nm. In the case of the ExoQuick process, a number of distinct size populations are seen, which can likely be attributed to different EV classes, protein aggregates, and perhaps vesicle-protein complexes. To be clear, these distinct groups may be shifted/merged in different measurement cycles. Ultimately, while very different in profile, the two polymer precipitation methods yield similar "average" particle sizes of ~ 130 nm. Finally, the NTA size distribution of the EVs isolated via UC again shows a variety of size groupings, but with much broader population breadths than the one seen for the ExoQuick data. That said, it is clear that there are families of protein aggregates, likely isolated EVs, and species that are either vesicle or vesicle-protein aggregates. As cautioned above, while the results of these NTA analyses suggest that all of the methods yield particles of the anticipated size range of exosomes, with contributions from proteinaceous material present in most, the profiles are still subject to interpretation and presuppositions. That said, the NTA profile of the C-CP tip isolates using acetonitrile as the organic modifier most clearly represents eluates composed predominately of EVs, with little to no contributions from protein impurities as suggested in MS proteomics analyses [42, 48].

4.3.4 Recovery Assessment via Indirect Enzyme-Linked Immunosorbent Assay

While physical methods of TEM and NTA are valuable components of the EVs characterization toolbox, they must be complemented by bioassays to confirm that vesicles/particles are indeed EVs. To confirm the presence of EVs and assess biomarker

activity of EVs recovered by the employed isolation method, indirect ELISAs to the CD81 and CD63 tetraspanin proteins were used. The CD81 and CD63 transmembrane proteins are cell membrane structural components commonly associated with the trafficking and compartmental organization of EVs during their biogenesis through the proposed MVB-mediated endosomal pathway.[61] The antibodies to the CD63 and CD81 proteins were used in this study to confirm the presence of active EVs. The commercial exosome standard stock and the EVs recovered from the various isolation methods were evaluated (in triplicate) by ELISA.

As shown in Fig. 4.4, a significant antibody response is observed for both the CD81 and CD63 tetraspanin proteins from EVs originating from the commercial exosome standard stock and in the EV recoveries from urine after processing with all five isolation methods.

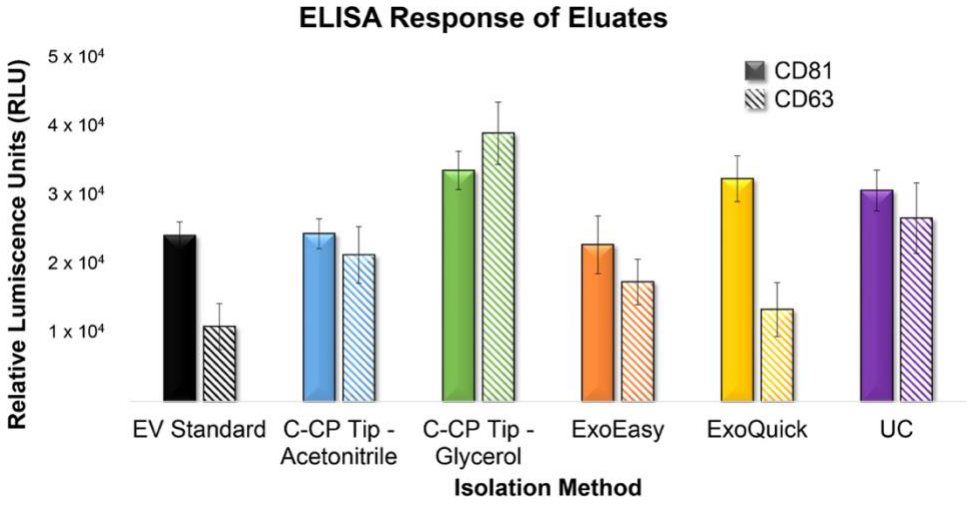

Figure 4.4: Indirect ELISA for identification of the CD81 and CD63 tetraspanin EV marker in the commercial exosome standard and EVs recovered from urine by the C-CP tip (acetonitrile and glycerol), exoEasy, ExoQuick, and ultracentrifugation methods. All samples applied in triplicate and the average of the triplicate measurements minus the average response of the blank are presented.

It is critical to point out that the isolate aliquots employed in the assay were of the same volume across the methods and were sampled from the same isolates as the concentration determinations. Thus the values determined by both assays should provide a level of comparability. The CD63 and CD81 proteins were readily detected in the commercial exosome stock, with an approximately 2X higher response for CD81 than CD63. The EVs recovered by the C-CP tip method using the glycerol solvent resulted in the highest ELISA responses for both the CD81 and CD63 proteins. This result is not surprising given that this is the sample having highest EV concentration, as depicted in Fig. 4.2. High concentrations of glycerol have previously been reported to decrease the overall performance of antibody-based immunoassays, specifically in cases of ELISAs, by interfering with the mechanisms of antibody binding.[50,51] But even with this potential cause for diminished antibody activity (and therefore ELISA response), the addition of the solvent removal step using the centrifugal filter to remove the latent glycerol allows for a sufficient ELISA response to be obtained and tetraspanin targets in the C-CP tip eluates to be detected. Based on the respective EV concentration determinations (Fig. 4.2), the slightly reduced response seen for the C-CP tip method employing the acetonitrile organic modifier falls nicely in line. What may be somewhat surprising is the fact that the ELISA responses for the polymer precipitation and UC methods are very much on par with the tip methods, though the determined EV number densities were higher in the tip isolates by a factor of 2-4. The disagreement here, while certainly not out of line based on the accuracy of the assays (the precision for the triplicates is quite good), may be due to carryover of “free” tetraspanin proteins (i.e., not

EV associated) in those approaches. This is not surprising as it has been shown that UC, for example, causes rupture of urine-derived vesicles during the isolation process.[62] Even so, based on the starting material volumes (200 µL vs. 8-45 mL of urine), the EV recoveries, based on ELISA determinations, is still a factor of 50-250 higher in comparison to the commercial kit and UC approaches.

4.3.5 Purity Assessment Based on Ratio of EV Concentration per µg Protein Determine via BCA

BCA determinations of total protein content are common across many biological matrices and media. The basic premise of the assay is based on the amino acid content as reflected in the absorbance measurement. In the present case of urine (and most matrices), a BCA analysis will reflect the free protein content but will also register positive results based on the amino acid/proteins present on the surface of EVs. As stated previously, the 'purity' of an exosome isolate relates to any free protein carryover (e.g. serum proteins or lipoproteins). Therefore, as a measure of the isolate purity, the total concentration of EVs as determined by absorbance was compared to the protein concentration of the EV eluate as measured using a microBCA assay, a commonly used measure of EV purity.[63] Thus, what is desired is a large number of EVs versus a low total protein value, presented in the units of numbers of EV per microgram of total protein (EV μg^{-1}). Presented in Fig. 4.5 are the determined "total" protein concentrations of the exosome standard and those for the urine isolates by the respective methods.

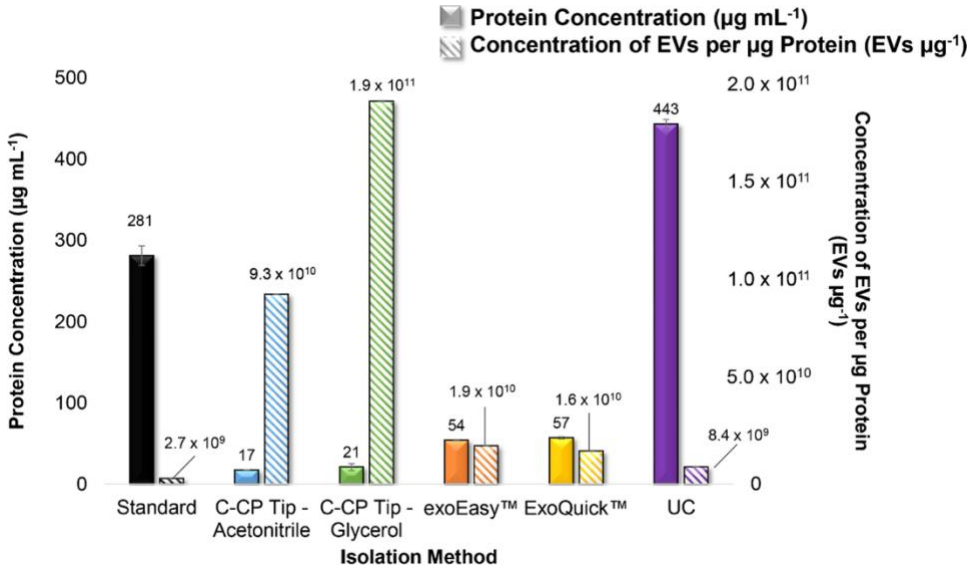

Figure 4.5: A microBCA assay was employed to determine the concentration of total protein in the exosome standards and EVs isolated from urine using the C-CP tip (acetonitrile and glycerol), exoEasy, ExoQuick, and ultracentrifugation methods. The concentration of EVs was compared to the total protein content as a measure of EV purity. All samples applied in triplicate and the average of the triplicate measurements minus the average response of the blank are presented.

What is desired here are low values of protein in isolates. As would be anticipated, the raw exosome standard and the UC method of isolation yield the highest protein values. The protein content of the recovery from the kit-based isolates are a factor of 4 – 8X lower, with those of the spin-down tip isolates being a factor of 3X lower, still. Thus, the C-CP tip urine EV isolates have a much lower protein content than the other methods.

As noted, the critical metric is the ratio of the number of EVs per unit volume versus the protein content for the same volume. As anticipated based on previous MS proteomic evaluations, [42,48] Fig. 4.5 confirms that the EV recoveries having the highest purity were those from the C-CP tip isolation methods, with 1 - 2 x 10^{11} EVs μg^{-1}

of total protein. On the other hand, a factor of 10X lower levels of purity are observed in the exoEasy and ExoQuick polymeric precipitation techniques (2 x 10^{10} EVs μg^{-1} of protein), and the lowest EV purity (8 x 10^{9} EVs μg^{-1}) observed in the EVs from the ultracentrifugation-based isolation method. As would be anticipated, the low purity of the exosome standard source was confirmed here with only 3 x 10^{9} EVs μg^{-1} of protein, on the same order of magnitude as the UC urine isolate. Based on this purity assay, the EVs isolated using the C-CP tip glycerol method were found to be most pure in comparison to all other isolation methods employed here. Further, this purity assay confirms the ability of the C-CP tip method to provide highly pure vesicle preparations, providing values very much higher than the literature recommendation of EV-to-protein ratios of >3 x 10^{10} particles $\mu g^{-1}$of protein. [63,64]

4.4 Conclusions

The novel capillary-channeled polymer fiber spin-down tip method has been demonstrated here as a more efficient means of EV isolation in comparison to the traditionally used ultracentrifugation and polymeric precipitation kits. As the first point of practical relevance, the C-CP fiber tip method requires human urine volumes of only 200 µL for the assays employed here versus volumes ranging from 4 – 45 mL. Second, the spin-down processing is readily performed on a tabletop centrifuge, with 12 samples completely processed in less than 15 mins. Third, the C-CP tip method can be adapted to either the acetonitrile or the glycerol elution solvent systems, enabling efficient isolations to be tailored to the downstream analyses of the recovered vesicles, e.g., acetonitrile for

further MS proteomics analysis. Fourth, though not yet commercially available as a "kit", the commercial purchase of the materials required for C-CP tip processing of EV-rich samples (fibers, tips, etc.) is < $5 per spin-down tip. Finally, as applied to urine-derived EVs, the method produces EV recoveries of > 40X higher concentration and > 10X higher purity than the other methods. The EVs collected by the C-CP tip isolation methods will allow for the isolation of EVs from a full range of relevant biofluid samples (urine, plasma/serum, milk, seminal fluid, culture, media, etc.). Indeed, while the initial concentration of EVs will vary with the matrix, each tip has a capacity of $>10^{12}$ EVs. This novel isolation method will enable more comprehensive EV assessments of clinical and fundamental significance to be performed with higher efficiency – towards the end goal of non-invasive diagnostics based on the analysis of EVs. Of course, larger numbers of EVs can be secured by the use of the C-CP fiber columns implemented on conventional liquid chromatography platforms. [43-45] Indeed, the methodology can be readily scaled up for applications where EVs are cultured for use as therapeutic agent vectors, following a comprehensive assessment of the long-term EV stability in the elution solvents employed here.

Declarations

Conflicts of Interest/Competing Interests

TF Bruce is a co-owner of Victory ExoFibres, LLC. All other authors have nothing to declare.

Ethics Approval

All human samples were obtained in accordance with the protocols approved by the Clemson University Institutional Review Board (Protocol No. Pro00070988).

Source of Biological Material

Lyophilized exosomes from human urine were obtained from Hansa BioMed (Tallinn, Estonia). Human urine samples were obtained from a consenting healthy anonymous donor.

Funding

Method and materials development work at Clemson University was supported by the National Science Foundation, Division of Chemistry under grant CHE-1608663. Financial support for the exosome isolation efforts from the Eppley Foundation for Scientific Research and the Gibson Foundation through the Prisma Health System (Greenville, SC) are gratefully acknowledged.

4.5 Acknowledgments

The authors gratefully acknowledge George Wetzel and the Clemson Electron Microscopy Facility for assistance with the EM micrographs.

4.6 References

1. Malkin EZ, Bratman SV (2020) Bioactive DNA from extracellular vesicles and particles. *Cell Death Dis.* 11 (7):584. doi:10.1038/s41419-020-02803-4
2. Gyorgy B, Szabo TG, Pasztoi M, Pal Z, Misjak P, Aradi B, Laszlo V, Pallinger E, Pap E, Kittel A, Nagy G, Falus A, Buzas EI (2011) Membrane vesicles, current

state-of-the-art: emerging role of extracellular vesicles. *Cell Mol. Life Sci.* 68 (16):2667-2688. doi:10.1007/s00018-011-0689-3

3. Thery C, Zitvogel L, Amigorena S (2002) Exosomes: composition, biogenesis and function. *Nat. Rev. Immunol.* 2 (8):569-579. doi:10.1038/nri855
4. S ELA, Mager I, Breakefield XO, Wood MJ (2013) Extracellular vesicles: biology and emerging therapeutic opportunities. *Nat. Rev. Drug Discov.* 12 (5):347-357. doi:10.1038/nrd3978
5. van der Pol E, Boing AN, Harrison P, Sturk A, Nieuwland R (2012) Classification, functions, and clinical relevance of extracellular vesicles. *Pharmacol. Rev.* 64 (3):676-705. doi:10.1124/pr.112.005983
6. Ferguson SW, Nguyen J (2016) Exosomes as therapeutics: The implications of molecular composition and exosomal heterogeneity. *J. Control. Release* 228:179-190. doi:10.1016/j.jconrel.2016.02.037
7. Willis GR, Kourembanas S, Mitsialis SA (2017) Toward Exosome-Based Therapeutics: Isolation, Heterogeneity, and Fit-for-Purpose Potency. *Front. Cardiovasc. Med.* 4:63. doi:10.3389/fcvm.2017.00063
8. Sheridan C (2016) Exosome cancer diagnostic reaches market. *Nat. Biotechnol.* 34 (4):359-360. doi:10.1038/nbt0416-359
9. Kalishwaralal K, Kwon WY, Park KS (2019) Exosomes for Non-Invasive Cancer Monitoring. *Biotechnol. J.* 14 (1):e1800430. doi:10.1002/biot.201800430
10. Pegtel DM, Gould SJ (2019) Exosomes. *Annu. Rev. Biochem.* 88 (1):487-514. doi:10.1146/annurev-biochem-013118-111902

11. Akers JC, Gonda D, Kim R, Carter BS, Chen CC (2013) Biogenesis of extracellular vesicles (EV): exosomes, microvesicles, retrovirus-like vesicles, and apoptotic bodies. *J. Neurooncol.* 113 (1):1-11. doi:10.1007/s11060-013-1084-8

12. M HR, Bayraktar E, G KH, Abd-Ellah MF, Amero P, Chavez-Reyes A, Rodriguez-Aguayo C (2017) Exosomes: From Garbage Bins to Promising Therapeutic Targets. *Int. J. Mol. Sci.* 18 (3):538. doi:10.3390/ijms18030538

13. Yang T, Martin P, Fogarty B, Brown A, Schurman K, Phipps R, Yin VP, Lockman P, Bai S (2015) Exosome delivered anticancer drugs across the blood-brain barrier for brain cancer therapy in Danio rerio. *Pharm. Res.* 32 (6):2003-2014. doi:10.1007/s11095-014-1593-y

14. Pisitkun T, Shen RF, Knepper MA (2004) Identification and proteomic profiling of exosomes in human urine. *Proc. Natl. Acad. Sci. U. S. A.* 101 (36):13368-13373. doi:10.1073/pnas.0403453101

15. Gallo A, Tandon M, Alevizos I, Illei GG (2012) The majority of microRNAs detectable in serum and saliva is concentrated in exosomes. *Plos One* 7 (3):e30679. doi:10.1371/journal.pone.0030679

16. Rekker K, Saare M, Roost AM, Kubo AL, Zarovni N, Chiesi A, Salumets A, Peters M (2014) Comparison of serum exosome isolation methods for microRNA profiling. *Clin. Biochem.* 47 (1-2):135-138. doi:10.1016/j.clinbiochem.2013.10.020

17. Caby MP, Lankar D, Vincendeau-Scherrer C, Raposo G, Bonnerot C (2005) Exosomal-like vesicles are present in human blood plasma. *Int. Immunol.* 17 (7):879-887. doi:10.1093/intimm/dxh267

18. Zhou B, Xu K, Zheng X, Chen T, Wang J, Song Y, Shao Y, Zheng S (2020) Application of exosomes as liquid biopsy in clinical diagnosis. *Signal Transduct. Tar.* 5 (1):144. doi:10.1038/s41392-020-00258-9

19. Witwer KW, Buzas EI, Bemis LT, Bora A, Lasser C, Lotvall J, Nolte-'t Hoen EN, Piper MG, Sivaraman S, Skog J, Thery C, Wauben MH, Hochberg F (2013) Standardization of sample collection, isolation and analysis methods in extracellular vesicle research. *J. Extracell. Vesicles* 2 (1):20360. doi:10.3402/jev.v2i0.20360

20. Tiwari S, Kumar V, Randhawa S, Verma SK (2021) Preparation and characterization of extracellular vesicles. *Am. J. Reprod. Immunol.* 85 (2):e13367. doi:10.1111/aji.13367

21. Zhao Z, Wijerathne H, Godwin AK, Soper SA (2021) Isolation and analysis methods of extracellular vesicles (EVs). *EVCNA* 2:80-103

22. Jiang Z, Liu G, Li J (2020) Recent Progress on the Isolation and Detection Methods of Exosomes. *Chem-Asian J.* 15 (23):3973-3982. doi:10.1002/asia.202000873

23. Liangsupree T, Multia E, Riekkola ML (2021) Modern isolation and separation techniques for extracellular vesicles. *J. Chromatogr. A* 1636:461773. doi:10.1016/j.chroma.2020.461773

24. Zhang Y, Qian H, Xu A, Yang G (2020) Increased expression of CD81 is associated with poor prognosis of prostate cancer and increases the progression of prostate cancer cells in vitro. *Exp. Ther. Med.* 19 (1):755-761. doi:10.3892/etm.2019.8244

25. Serrano-Pertierra E, Oliveira-Rodriguez M, Matos M, Gutierrez G, Moyano A, Salvador M, Rivas M, Blanco-Lopez MC (2020) Extracellular Vesicles: Current Analytical Techniques for Detection and Quantification. *Biomolecules* 10 (6):19. doi:10.3390/biom10060824

26. Momen-Heravi F (2017) Isolation of Extracellular Vesicles by Ultracentrifugation. *Methods Mol. Biol.* (Clifton, NJ) 1660:25-32. doi:10.1007/978-1-4939-7253-1_3

27. Vergauwen G, Dhondt B, Van Deun J, De Smedt E, Berx G, Timmerman E, Gevaert K, Miinalainen I, Cocquyt V, Braems G, Van den Broecke R, Denys H, De Wever O, Hendrix A (2017) Confounding factors of ultrafiltration and protein analysis in extracellular vesicle research. *Sci. Rep.* 7 (1):2704. doi:10.1038/s41598-017-02599-y

28. Boing AN, van der Pol E, Grootemaat AE, Coumans FA, Sturk A, Nieuwland R (2014) Single-step isolation of extracellular vesicles by size-exclusion chromatography. *J. Extracell. Vesicles* 3 (1):23430. doi:10.3402/jev.v3.23430

29. Brett SI, Lucien F, Guo C, Williams KC, Kim Y, Durfee PN, Brinker CJ, Chin JI, Yang J, Leong HS (2017) Immunoaffinity based methods are superior to kits for

purification of prostate derived extracellular vesicles from plasma samples. *Prostate* 77 (13):1335-1343. doi:10.1002/pros.23393

30. Witwer KW, Soekmadji C, Hill AF, Wauben MH, Buzas EI, Di Vizio D, Falcon-Perez JM, Gardiner C, Hochberg F, Kurochkin IV, Lotvall J, Mathivanan S, Nieuwland R, Sahoo S, Tahara H, Torrecilhas AC, Weaver AM, Yin H, Zheng L, Gho YS, Quesenberry P, Thery C (2017) Updating the MISEV minimal requirements for extracellular vesicle studies: building bridges to reproducibility. *J. Extracell. Vesicles* 6 (1):1396823. doi:10.1080/20013078.2017.1396823

31. Taylor DD, Shah S (2015) Methods of isolating extracellular vesicles impact down-stream analyses of their cargoes. *Methods* 87:3-10. doi:10.1016/j.ymeth.2015.02.019

32. Takov K, Yellon DM, Davidson SM (2019) Comparison of small extracellular vesicles isolated from plasma by ultracentrifugation or size-exclusion chromatography: yield, purity and functional potential. *J. Extracell. Vesicles* 8 (1):1560809. doi:10.1080/20013078.2018.1560809

33. Wiersum Stranska R, Wouters J, Bloch K, Snoeck R, Andrei G (2016) Comparison of exoEasy Maxi kit (Qiagen) with size-exclusion chromatography qEV columns (Izon Science) for isolation of extracellular vesicles from human plasma. *J. Extracell. Vesicles* 5:31552

34. Johnsen KB, Gudbergsson JM, Andresen TL, Simonsen JB (2019) What is the blood concentration of extracellular vesicles? Implications for the use of

extracellular vesicles as blood-borne biomarkers of cancer. *Biochim. Biophys. Acta* 1871 (1):109-116

35. Tang YT, Huang YY, Zheng L, Qin SH, Xu XP, An TX, Xu Y, Wu YS, Hu XM, Ping BH, Wang Q (2017) Comparison of isolation methods of exosomes and exosomal RNA from cell culture medium and serum. Int. J. Mol. Med. 40 (3):834-844. doi:10.3892/ijmm.2017.3080

36. Yakimchuk K (2015) Exosomes: Isolation and Characterization Methods and Specific Markers. *Mater. Methods* 5 (1450)

37. Soares Martins T, Catita J, Martins Rosa I, O ABdCES, Henriques AG (2018) Exosome isolation from distinct biofluids using precipitation and column-based approaches. *Plos One* 13 (6):e0198820. doi:10.1371/journal.pone.0198820

38. Helwa I, Cai J, Drewry MD, Zimmerman A, Dinkins MB, Khaled ML, Seremwe M, Dismuke WM, Bieberich E, Stamer WD, Hamrick MW, Liu Y (2017) A Comparative Study of Serum Exosome Isolation Using Differential Ultracentrifugation and Three Commercial Reagents. *Plos One* 12 (1):e0170628. doi:10.1371/journal.pone.0170628

39. Konoshenko MY, Lekchnov EA, Vlassov AV, Laktionov PP (2018) Isolation of Extracellular Vesicles: General Methodologies and Latest Trends. *Biomed. Res. Int.* 2018:8545347. doi:10.1155/2018/8545347

40. Van Deun J, Mestdagh P, Sormunen R, Cocquyt V, Vermaelen K, Vandesompele J, Bracke M, De Wever O, Hendrix A (2014) The impact of disparate isolation

methods for extracellular vesicles on downstream RNA profiling. *J. Extracell. Vesicles* 3. doi:10.3402/jev.v3.24858

41. Huang S, Bruce TF, Ding H, Wei Y, Marcus RK (2021) Rapid isolation of lentivirus particles from cell culture media via a hydrophobic interaction chromatography method on a polyester, capillary-channeled polymer fiber stationary phase. *Anal. Bioanal. Chem.* 413 (11):2985-2994. doi:10.1007/s00216-021-03232-8

42. Ji X, Huang S, Zhang J, Bruce TF, Tan Z, Wang D, Zhu J, Marcus RK, Lubman DM (2021) A novel method of high-purity extracellular vesicle enrichment from microliter-scale human serum for proteomic analysis. *Electrophoresis* 42 (3):245-256. doi:https://doi.org/10.1002/elps.202000223

43. Wang L, Bruce TF, Huang S, Marcus RK (2019) Isolation and quantitation of exosomes isolated from human plasma via hydrophobic interaction chromatography using a polyester, capillary-channeled polymer fiber phase. *Anal. Chim. Acta* 1082:186-193. doi:10.1016/j.aca.2019.07.035

44. Huang S, Wang L, Bruce TF, Marcus RK (2019) Isolation and quantification of human urinary exosomes by hydrophobic interaction chromatography on a polyester capillary-channeled polymer fiber stationary phase. *Anal. Bioanal. Chem.* 411 (25):6591-6601. doi:10.1007/s00216-019-02022-7

45. Huang S, Wang L, Bruce TF, Marcus RK (2020) Evaluation of exosome loading characteristics in their purification via a glycerol-assisted hydrophobic interaction

chromatography method on a polyester, capillary-channeled polymer fiber phase. *Biotechnol. Prog.* 36 (5):e2998

46. Jackson KK, Powell RR, Bruce TF, Marcus RK (2020) Solid-phase extraction of exosomes from diverse matrices via a polyester capillary-channeled polymer (C-CP) fiber stationary phase in a spin-down tip format. *Anal. Bioanal. Chem.* 412 (19):4713-4724. doi:10.1007/s00216-020-02728-z

47. Jackson KK, Powell RR, Bruce TF, Marcus RK (2021) Rapid isolation of extracellular vesicles from diverse biofluid matrices via capillary-channeled polymer fiber solid-phase extraction micropipette tips. *Analyst* 146 (DOI: 10.1039/D1AN00373A):4314-4325. doi:10.1039/d1an00373a

48. Huang S, Ji X, Jackson KK, Lubman DM, Ard MB, Bruce TF, Marcus RK (2021) Rapid separation of blood plasma exosomes from low-density lipoproteins via a hydrophobic interaction chromatography method on a polyester capillary-channeled polymer fiber phase. *Anal. Chim. Acta* 1167:338578. doi:10.1016/j.aca.2021.338578

49. Storey BT, Noiles EE, Thompson KA (1998) Comparison of glycerol, other polyols, trehalose, and raffinose to provide a defined cryoprotectant medium for mouse sperm cryopreservation. *Cryobiology* 37 (1):46-58. doi:10.1006/cryo.1998.2097

50. Vagenende V, Yap MG, Trout BL (2009) Mechanisms of protein stabilization and prevention of protein aggregation by glycerol. *Biochemistry* 48 (46):11084-11096. doi:10.1021/bi900649t

51. Vagenende V, Han AX, Mueller M, Trout BL (2013) Protein-associated cation clusters in aqueous arginine solutions and their effects on protein stability and size. *ACS Chem. Biol.* 8 (2):416-422. doi:10.1021/cb300440x

52. Burdette CQ, Marcus RK (2013) Solid phase extraction of proteins from buffer solutions employing capillary-channeled polymer (C-CP) fibers as the stationary phase. *Analyst* 138 (4):1098-1106. doi:10.1039/c2an36126d

53. Gheinani AH, Vogeli M, Baumgartner U, Vassella E, Draeger A, Burkhard FC, Monastyrskaya K (2018) Improved isolation strategies to increase the yield and purity of human urinary exosomes for biomarker discovery. *Sci. Rep.* 8 (1):3945. doi:10.1038/s41598-018-22142-x

54. Jung MK, Mun JY (2018) Sample Preparation and Imaging of Exosomes by Transmission Electron Microscopy. *J. Vis. Exp.* (131):56482. doi:10.3791/56482

55. Dragovic RA, Gardiner C, Brooks AS, Tannetta DS, Ferguson DJP, Hole P, Carr B, Redman CWG, Harris AL, Dobson PJ, Harrison P, Sargent IL (2011) Sizing and phenotyping of cellular vesicles using Nanoparticle Tracking Analysis. *Nanomed. Nanotechnol.* 7 (6):780-788. doi:10.1016/j.nano.2011.04.003

56. Vestad B, Llorente A, Neurauter A, Phuyal S, Kierulf B, Kierulf P, Skotland T, Sandvig K, Haug KBF, Ovstebo R (2017) Size and concentration analyses of extracellular vesicles by nanoparticle tracking analysis: a variation study. *J. Extracell. Vesicles* 6 (1):1344087. doi:10.1080/20013078.2017.1344087

57. Chen JJ, Jiang JQ (2013) Monoclonal antibody-based solvent tolerable indirect competitive ELISA for monitoring ciprofloxacin residue in poultry samples. *Food Agr. Immunol.* 24 (3):331-344. doi:10.1080/09540105.2012.689817

58. Sitar S, Kejzar A, Pahovnik D, Kogej K, Tusek-Znidaric M, Lenassi M, Zagar E (2015) Size characterization and quantification of exosomes by asymmetrical-flow field-flow fractionation. *Anal. Chem.* 87 (18):9225-9233. doi:10.1021/acs.analchem.5b01636

59. Liang K, Liu F, Fan J, Sun D, Liu C, Lyon CJ, Bernard DW, Li Y, Yokoi K, Katz MH, Koay EJ, Zhao Z, Hu Y (2017) Nanoplasmonic Quantification of Tumor-derived Extracellular Vesicles in Plasma Microsamples for Diagnosis and Treatment Monitoring. *Nat. Biomed. Eng.* 1 (4):1-11. doi:10.1038/s41551-016-0021

60. 60. Hartjes TA, Mytnyk S, Jenster GW, van Steijn V, van Royen ME (2019) Extracellular Vesicle Quantification and Characterization: Common Methods and Emerging Approaches. *Bioengineering (Basel)* 6 (1):7. doi:10.3390/bioengineering6010007

61. 61. Raposo G, Stoorvogel W (2013) Extracellular vesicles: exosomes, microvesicles, and friends. *J. Cell Biol.* 200 (4):373-383. doi:10.1083/jcb.201211138

62. 62. Guan S, Yu H, Yan G, Gao M, Sun W, Zhang X (2020) Characterization of Urinary Exosomes Purified with Size Exclusion Chromatography and

Ultracentrifugation. *J. Proteome Res.* 19 (6):2217-2225. doi:10.1021/acs.jproteome.9b00693

63. 63. Webber J, Clayton A (2013) How pure are your vesicles? *J. Extracell. Vesicles* 2 (1):19861. doi:10.3402/jev.v2i0.19861

64. 64. Lobb RJ, Becker M, Wen SW, Wong CS, Wiegmans AP, Leimgruber A, Moller A (2015) Optimized exosome isolation protocol for cell culture supernatant and human plasma. *J. Extracell. Vesicles* 4 (1):27031. doi:10.3402/jev.v4.27031

CHAPTER FIVE

FACILE, GENERIC CAPTURE AND ON-FIBER DIFFERENTIATION OF EXOSOMES VIA CONFOCAL IMMUNOFLUORESCENCE MICROSCOPY USING A CAPILLARY-CHANNELED POLYMER FIBER SOLID-PHASE EXTRACTION TIP

5.1 Introduction

The concept of the liquid biopsy, wherein a readily accessible biofluid is used to harvest relevant biomarkers versus the excision of tissue specimens, is moving towards realization.[1,2] Crucial treatment time is often lost in early instances of infection, tumor growth, and disease progression simply because of the lack of efficient, early detection, diagnostic tools. Particularly in the case of aggressive cancers like ovarian cancer (OC),[3,4] much time is lost due to the inability to identify malignant ailments non-invasively, as many cancers are asymptomatic during early stages of disease.[1,5] The introduction of accessible, non-invasive methods for disease detection would open the door for a head-on approach to clinical diagnostics. Taken a step further, this would allow routine screenings for diseases such as OC to become commonplace. This would drastically increase patient survival rates by identifying cancerous instances prior to the presentation of noticeable symptoms.

Exosomes are 30–150 nm-sized, cell-derived extracellular vesicles (EVs) released from most cell types by multivesicular bodies (MVBs) uniquely created through the endosomal pathway,[6,7] allowing them to consist of origin-representative genetic and

molecular cargoes. Exosomes are essential elements in cell-to-cell communication, disease progression, cancer metastasis, tumor growth, and other physiological processes.[6,7] Because exosomes contain molecular constituents of their host cells, including DNA, microRNA, and biomarker surface proteins, they are a treasure trove of biomarkers. Likewise, as they are present in many bodily fluids, including urine, blood serum and plasma, saliva, and in cell culture media, they can be harvested to assess the status of the biosystem. Importantly, mother cell-derived exosome surface proteins allow for the identification of the originating environment without direct contact to the primary area of concern (i.e., tumor or infection site).[8,9] Profiling of genetic material from the interior of disease-derived exosomes allows for monitoring of disease progression and perhaps treatment effectiveness. To that end, liquid biopsies based on the biomarker analysis of exosome cargoes from readily available biofluids have been investigated.[2,10,11]

An issue limiting exosome-based biochemical research and their implementation in diagnostics is the lack of efficient tools to isolate the vesicles. Exosome isolations have proven to be a challenge due to their relative size, protein affinity, and innate heterogeneity in size and surface protein makeup.[1] Though many techniques are widely used, i.e., ultracentrifugation (UC), density gradient centrifugation, size exclusion chromatography, microfiltration, affinity isolation, and polymer precipitation,[12,13] all available isolation methods present concerns regarding purity and recovery efficiency. Because these techniques rely on the density, size, or affinity for antibodies to specific proteins, purification of exosomes from free protein or lipoprotein aggregates is particularly challenging.[4,14] Many of these isolation techniques require expensive, time-

consuming, and tedious processes, and still produce impure, low yield recoveries, limiting the ultimate progress of the study and use of exosomes. Another limiting factor in the clinical arena is the required primary sample volume, often a few milliliters of the original biofluid. To reduce these sample volume requirements, several microfluidic approaches for EV isolation have been recently explored, using immunoaffinity capture,[15] nanoporous membrane sieving,[16] and physical EV trapping[17] (via nanowires/micropillars) approaches. Despite reductions in applied sample/reagent volume, concerns of purity and yield remain, especially since pre-concentration steps using the common EV isolation methods (e.g., UC) are still required.[18]

In the realm of EV biochemical assessment, few methods are available for simultaneous imaging and EV biomarker characterization; all fall short in providing both on the same platform. The ExoView R100 (NanoView Biosciences, Boston, MA, USA) is a recently-introduced EV analysis method, consisting of an immunoaffinity capture array chip and interferometry imaging module – designed to assess EV size and surface biomarker content. In theory, this technique would allow for simultaneous insight into the size and tetraspanin compositions of an EV population. However, with the relatively high limits of detection (3.94×10^9 particles per mL) and low specificity of the immunoaffinity capture chip,[19] EV pre-purification steps are required. Hence, the challenges faced by impure EV recoveries obtained using the above-mentioned isolation methods remain. Ultimately, while small volumes of material are subjected to these sorts of assays, the volume of the primary sample is not reduced. The introduction of an isolation method to provide highly concentrated, biologically-active, and pure EV

populations fit for immunological assessment methods, from minute (μL) initial sample volumes, is of much interest. The future of exosome-based clinical and diagnostic applications relies on the implementation of timely, yet efficient exosome isolation and screening methods, able to be tailored to a diversity of relevant biomarkers.

Demonstrated here is a method for rapid EV isolations using a hydrophobic interaction chromatography (HIC) immobilization/purification process and the subsequent immunofluorescence (IF) labeling of exosomes based on their surface marker proteins; on a singular platform. This is done using a capillary-channeled polymer (C-CP) fiber stationary phase and a solid phase extraction (SPE) spin-down tip process. The generic capture of EVs is driven by the HIC solvent system, wherein ionic species and proteins are sequentially removed from the host matrix, allowing exosome isolations from diverse biofluids and culture media.[20–22] The capture and sequential release of free proteins and EVs are induced by a solvent change from high (2M $(NH_4)_2SO_4$) – to – zero salt content in either continuous or step gradient workflows. The method's efficiency has been demonstrated in protein and exosome separations on C-CP fiber columns via HPLC[20–22] and by SPE on spin-down tips.[23,24] Overall, the process has proven to provide high EV yields (up to 1×10^{12} EVs per mL) and extremely low concomitant protein content (<0.5% lipoprotein carryover in serum),[25,26] on time scales of less than 10 min, without any other form of pre-isolation. While no direct comparisons have been made, the SPE tips have yielded total exosome binding capacities of $\sim 8 \times 10^{11}$ EVs from commercial standards,[23] while the 30 cm columns more fitting for downstream

processing have shown capacities ~5×10^{12} for the far more complex, direct cell milieu purification.[22]

In this demonstration, EVs from different sources are captured and retained on the fiber surfaces, contaminating host cell proteins (HCPs) are eluted, and the exosome isolates are subjected to immunolabeling and on-fiber identification via confocal fluorescence microscopy. Specifically, exosomes are visualized by fluorescent antibody tagging of the ubiquitous CD81 tetraspanin surface protein and the CA125 protein, a biomarker previously identified as being common to OC.[27,28] Other tetraspanins such as CD9 and CD63 have been identified in isolated EVs; however, their contents are highly variable. CD81 is of most prevalence and interest in the populations under study here, as CD81 is also reported to be overexpressed in cancerous EV populations.[29,30] EVs originating from known cancer cell lines and patients are readily distinguished from those where OC (or other gynecologic ailments presenting CA125) are not anticipated. In the first demonstration, fiber-immobilized exosomes are processed using standard IF incubation protocols prior to imaging analysis. In this instance, the primary benefits lie in the ability to remove potentially-interfering HCPs and performance of in situ imaging, albeit on much shorter time scales than other methods. Confocal microscopy provides for IF screening on the single-vesicle level. In the subsequent demonstration, a more rapid IF processing concept is broached, wherein EVs are efficiently captured, immunolabeled, and imaged in under 5 hours (a 3× reduction in processing time). The novelty of this work lies in the ability to isolate, purify, immunolabel, and image EVs on a single substrate. While confocal microscopy may not be practical for clinical screening, the

rapid, high purity isolation, followed by IF analysis on a single platform, points to significant advances in exosome processing, regardless of the subsequent mode of characterization, biomarker identification, and quantification.

5.2 Experimental

5.2.1 Chemicals and reagents

In order to demonstrate the concept of exosome capture and differentiation via immunofluorescence labeling and imaging techniques, EVs were isolated from distinct sources. One example of a generic, non-cancerous source was a cell culture of *Dictyostelium discoideum* (*D. discoideum*, a soil-dwelling amoeba), AX2 cells, which were obtained from The Dicty Stock Center (Northwestern University, Chicago, IL, USA). The *D. discoideum* cells were grown and maintained axenically in HL5 medium supplemented with 100 μg mL^{-1} ampicillin at room temperature in 25 mL culture flasks. Likewise, HEK293 (human embryonic kidney) cells obtained from the American Type Culture Collection (ATCC, Manassas, VA, USA) were cultured in Dulbecco's Modified Eagle Medium (DMEM) supplemented with 10% exosome-depleted fetal bovine serum (FBS), and 1% penicillin/streptomycin in a standard humidified incubator at 37°C with 5% CO_2. As an example of an exosome sample derived from a representative human biofluid source, a commercial exosome stock was obtained (HansaBioMed, Tallinn, Estonia), consisting of a urine-derived exosome isolate from supposedly healthy subjects was employed. The example sources that should definitively present biomarkers for OC were the IHOE (immortalized human ovarian epithelial), SKOV-3 (human ovarian

adenocarcinoma), and CaOv-3 (human ovarian adenocarcinoma) cell lines. The IHOE cell line was obtained from Applied Biological Materials (Richmond, BC, Canada) and the SKOV-3 and CaOv-3 cell lines were obtained from the ATCC (Manassas, VA, USA). The IHOE and CaOv-3 cells were grown in DMEM, and the SKOV3 cells were grown in McCoy's 5a media. All of the aforementioned ovarian cell lines were supplemented with 10% exosome-depleted FBS and 1% penicillin/streptomycin and cultured in a standard humidified incubator at 37°C with 5% CO_2. Finally, the practical (clinical) efficacy of the method was demonstrated in the extraction and immunofluorescent assay of exosomes derived from a urine sample obtained from an unidentified patient currently under treatment for OC.

Ultra-pure ammonium sulfate and biotechnology-grade glycerol were purchased from VWR (Radnor, PA, USA). Bovine serum albumin (BSA) was purchased from Sigma-Aldrich (St. Louis, MO USA). Phosphate-buffered saline (PBS, 0.067 M (PO_4), pH 7.4) was obtained from ThermoFisher Scientific (Waltham, MA, USA). The VWR® Symphony™ 4417/R table-top centrifuge (Radnor, PA, USA) was used for SPE spin-down tip processing. A mouse monoclonal antibody to CD81 (1 mg mL^{-1}) was obtained from Santa Cruz Biotechnology (Dallas, TX, USA). A rabbit monoclonal antibody to CA125/MUC16 (1 mg mL^{-1}) was obtained from ThermoFisher (Waltham, MA, USA). A goat anti-rabbit IgG (H+L) cross-adsorbed secondary antibody (Alexa Fluor 488, 2 mg mL^{-1}) and a goat anti-mouse IgG (H+L) cross-adsorbed secondary antibody (Alexa Fluor 647, 2 mg mL^{-1}) were obtained from ThermoFisher Scientific (Waltham, MA).

5.2.2 C-CP fiber spin-down tip SPE procedure

The exosome isolation and on-fiber immunofluorescence labeling steps are depicted diagrammatically in Fig. 5.1.

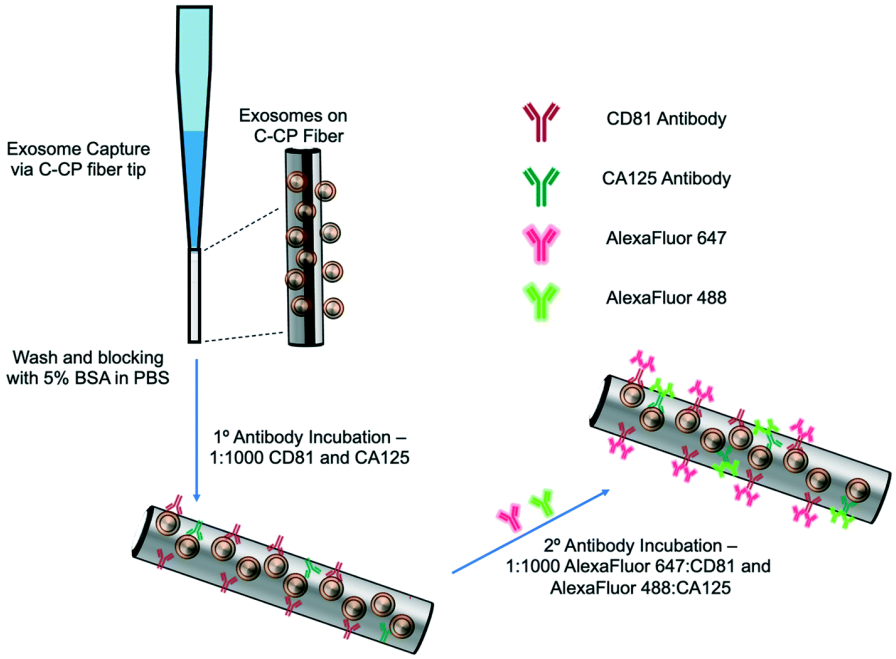

Figure 5.1: Graphic depiction of the on-fiber exosome extraction and immunolabeling process.

The isolation method, to the point of presenting purified EVs on the fiber surface, was executed as described previously,[24, 25] with the initial labeling and imaging procedures following what is normal in the fluorescence immunoimaging field.[26] Following the basic demonstration of the methodology, efforts towards more rapid on-fiber processing were initiated.

The polyester (PET) SPE tips were prepared as previously published[24] using an eight-rotation loop of PET fibers (a total of 448 fibers) collinearly pulled through 30 cm of 0.8 mm ID fluorinated ethylene polypropylene (FEP) polymer tubing (Cole Parmer, Vernon Hills, IL, USA). The fiber bundle hanging from the end of the 30 cm piece of

FEP tubing was pulled and repeatedly cut to create 1 cm fiber-packed tips with a 0.5 cm open space for attachment to a 200 μL micropipette tip (Fisherbrand, Waltham, MA). During spin-down processing, the fiber stationary phase was attached to a 200 μL micropipette tip using super glue and placed inside a 1000 μL micropipette tip (Fisherbrand, Waltham, MA) to provide structural support. The spin-down tip set-up was held in place within a 1.5 mL microfuge tube cut laterally, then placed inside of a hollowed center cap of a 15 mL centrifuge tube. The C-CP fiber tips were conditioned by washing with water, acetonitrile, and the starting mobile phase solution before application.

5.2.3 Exosome SPE immobilization

The isolation of EVs from the test matrices was accomplished by first mixing 100 μL of the sample supernatants with 100 μL of 4M ammonium sulfate to achieve a 2M final concentration before being applied to the tip. The total volume (200 μL) of the sample loading mixture was applied to the PET C-CP fiber SPE tip and centrifuged at 300 *x g* for 60 s. Under these conditions, salts and low molecular weight polar species pass through the tip, while proteinaceous materials and vesicles were retained on the fiber surface. The elution of free proteins and protein aggregates was induced using a mobile phase of 1M $(NH_4)_2SO_4$ in 25% glycerol (200 μL, 300 *x g*, 60 s). Before beginning the immunolabeling process, the fiber surface was further washed five times with 200 μL aliquots of PBS (300 *x g*, 60 s each, 15 min. incubation, 3 buffer changes). For the STEM imaging, the captured exosomes were fixed and imaged directly on the fiber

surface after the protein elution step and after release from the fiber surface using 50% glycerol (200 μL, 300 *x g*, 60 s) upon fixation to a silica wafer, as described in Appendix B.

5.2.4 Immunolabeling and Imaging

The initial demonstration of the exosome differentiation via immunofluorescence microscopy employed what would be termed a standard labeling protocol.[26] In brief, after the sample HIC capture step, the fiber-captured vesicles were washed with PBS and incubated with 5% BSA before and after primary antibody incubation overnight, and incubation of the secondary antibody for 2 hours. That procedure, based on a limited amount of optimization of the antibody concentration and incubation times, is detailed in ESI. An alternative, higher throughput method was investigated as a means of expediting the labeling process. After the tip capture process, the immobilized and washed exosomes were exposed to a 5% BSA blocking solution in PBS (5 times, 200 μL ea. 300 *x g*, 60 s ea.) and allowed to incubate in 1 mL of blocking solution for 15 min. to decrease potential non-specific binding between the antibodies to target the exosomal surface biomarkers as well as the PET C-CP fiber surface. Following the blocking step, the fiber surface was washed three times using 200 μl aliquots of PBS and allowed to wash in 1 mL of PBS on a shaker for 15 min (3 buffer changes). Next, antibodies (1:1000 in PBS) to the CD81 EV marker protein (mouse) and CA125 (rabbit) biomarker protein were applied to the fiber-captured vesicles (200 μL), allowed to wick down the fiber tip for 5 minutes, then placed in the centrifuge for a spin-down at 150 *x g* for 3 min before incubation in 1 mL of antibody (2 hours, RT). The blocking step was repeated (5 times,

200 μL, 300 *x g*, 1 min each, 15 min., RT), followed by another PBS wash (5 times, 50 μL, 300 *x g*, 1 min each, 15 min, RT) to reduce non-specific binding. After this blocking step, more centrifugal force was required to allow the solutions to pass through the fiber tip due to the stationary phase surface saturation. The primary antibody-labeled exosomes on the tip surface were then exposed to AlexaFluor 488 (anti-rabbit) and Alexa Fluor 647 (anti-mouse) secondary antibodies (1:1000, 200 μL, 500 *x g*, 3 min) and allowed to incubate in 1 mL of antibody for 1 hour at room temperature. With the addition of the secondary antibody, the solution was allowed to wick down the fiber surface, like previously done with the addition of the primary antibody (200 μL, 5 min), then spun down using the table-top centrifuge (500 x g, 5 min), and allowed to incubate in 1 mL of solution (1 hr, RT). Finally, a PBS wash (5 times, 200 μL, 1,500 *x g*, 1 min ea, 15 min.) was used to remove unbound secondary antibodies from the fiber tip before confocal microscopy imaging. This entire process is completed in less than 5 hours (with multiple samples processed in parallel) but is by no means rigorously optimized at this point. To be clear, the presented confocal fluorescence approach is not directed at direct antigen quantification. However, the presence of disease states are qualitatively assessed (screened) based on the comparison of the fluorescent images from "healthy" (HEK293, *Dictyostelium discoideum*) and CA125 protein-upregulating EV sources (SKOV3, CaOv-3). Among other limitations discussed subsequently, without the ability to apply specimen-specific reference material controls in parallel during this experimental workflow, a quantitative microscopic approach remains a challenge. That said, multiple previous efforts have demonstrated the ability to employ simple optical absorbance

detection to quantify the total EV content from very diverse biological and culture media.[3, 4, 24, 25, 27, 28] Those methods have been validated through use of diverse quantification modes (e.g. direct response functions and standard addition) as well as the common standard, nanoparticle tracking analysis (NTA).

To perform the confocal imaging, the PET C-CP fibers (with the immunolabeled exosomes on the surface) were removed from the FEP tubing and placed in one chamber of a 2-well Nunc Lab-Tek Chambered cover glass with a No. 1 borosilicate glass bottom (ThermoFisher Scientific, Waltham, MA). Optimized excitation wavelengths of 499 and 653 nm were chosen using the Leica Dye Assistant and used to visualize the CA125 and CD81 antigens, respectively, during the confocal imaging using the Leica SP8 confocal microscope. All microscope settings, including the white light laser intensity and power, gain, offset, pinhole, and frame count, remained consistent for the confocal imaging. With this, the localized fluorescence was used to identify specific biomarker protein antigens on the captured EVs. It is important to note that due to the optical resolution limitations of the confocal microscope, it is possible that the vesicles observed as the CD81 and CA125-positive species captured on the C-CP tip may not be individual EVs, but instead, a collection of vesicles in very close proximity, creating the collective fluorescent immune response.

Clean C-CP fiber tips (without the exposure to the EV solution) were run in parallel during the two isolation and immunolabeling protocols to serve as relevant negative controls and are presented with the relevant diagnostic images, herein. Additionally, negative control imaging experiments were carried out using the standard

antibody labeling protocol, inclusive of fluorescent imaging of blank fibers, purified CD81 protein exposed to the native fiber surfaces, and a CD81 protein-antibody complex exposed to exosome-immobilized fibers. The latter two situations illustrate the freedom from non-specific binding of the proteins (and subsequently their antibodies) to the native fiber surfaces as well those subjected to the exosome immobilization step. These essential results are included as Figs. B-1a-c.

5.3 Results and Discussion

5.3.1 Confirmation of Exosome Physical Integrity

To confirm the capture and release of intact vesicles on the C-CP tip surface during the course of the HIC workflow, SEM imaging was performed directly on the surface of the fiber tips as well as on eluted particles. The electron microscopy techniques were employed to investigate the morphological nature and structural integrity of the exosomes captured on the C-CP tip surface. EVs were imaged after fixation, dehydration, and negative staining (as described in Appendix B). The SEM images revealed the vesicles' intact morphology on the stationary phase and highlight the channeled structure of the C-CP fibers, affecting highly efficient EV binding. Fig. B-2a presents an SEM micrograph of the commercial-sourced, human urine-derived exosomes bound to the fiber surface after the HIC workflow to the point of the protein wash using 25% glycerol and PBS. As seen, the vast majority of the EVs captured on the fiber surface fall under the 150 nm size cut-off for exosomes and display their expected spherical shape. The visually smooth fiber surface is reflective of the efficient removal of media components

and host cell proteins, as needed for high fidelity imaging or chemical characterization. To observe the integrity of the EVs after they are fully processed, the complete spin-down tip method was performed, with the eluted vesicles deposited onto a silica wafer for STEM imaging. Just as an efficient capture of EVs is essential, the release of pure and biologically relevant populations of EVs is vital for further downstream processing, whether for further characterization or biological testing. The STEM micrograph presented in Fig. B-2b provides a magnified view of the exosomes, wherein it is clear that the vesicular structures (as evidenced by the "rings" on the periphery) are indeed retained following complete C-CP fiber tip processing. Because the aim was to capture, retain, and characterize the EVs directly on the fiber tip surface, the vesicles were not subsequently eluted from the stationary phase as demonstrated in previous works.[24, 25] However, the ability to capture *and* release of cell-derived EVs (in the exosome size range) using this C-CP tip method was confirmed using nanoparticle tracking analysis (NTA). As shown in Fig. B-3, the NTA size determinations revealed that >93% of the EVs recovered from 100 μL of HEK293 cell culture milieu, fell within the 30 – 150 nm size range (100.1 nm average diameter, 5.6 x 10^{10} particles mL^{-1}). This confirms the ability to capture and release highly concentrated, structurally-preserved exosomes using the C-CP tip method.

5.3.2 Differentiation of Exosome Types using a Standard Immunolabeling Protocol

The ability to differentiate exosome populations via on-fiber immunofluorescence imaging is demonstrated in Fig. 5.2.

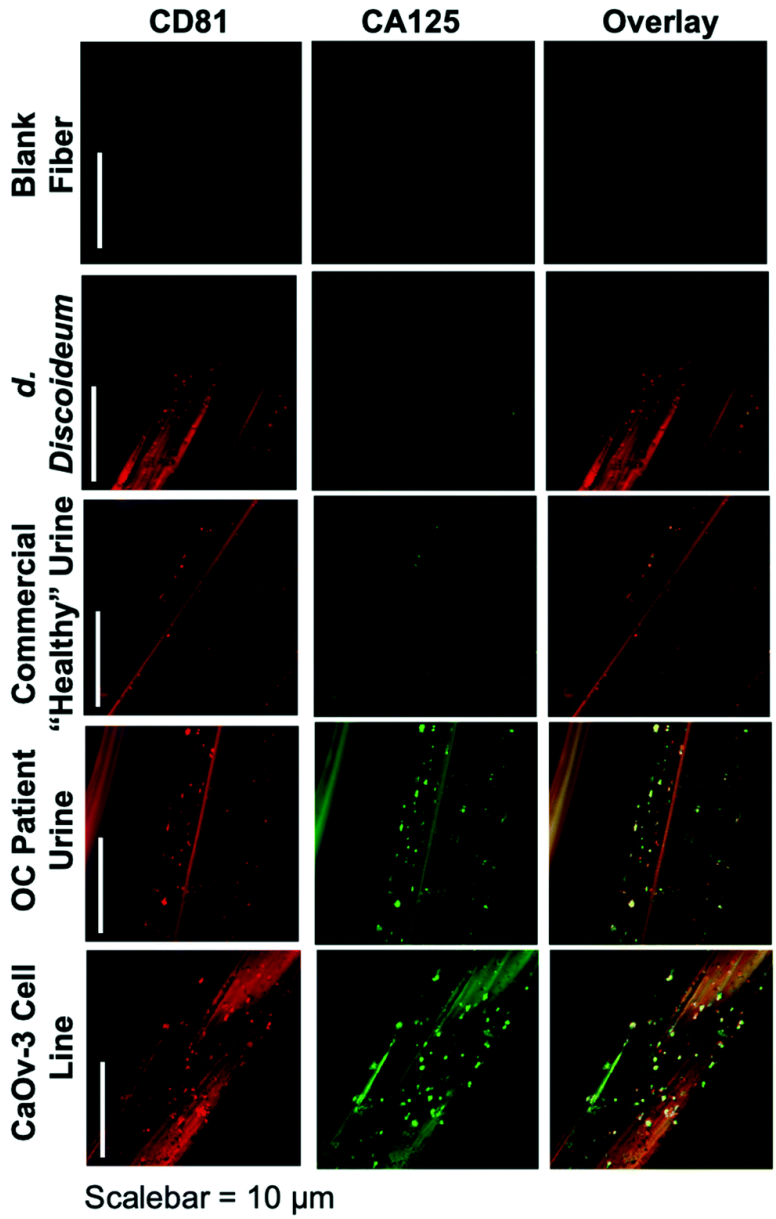

Figure 5.2: Confocal fluorescence images of C-CP fibers from process blank and test specimens following standard immunolabeling procedure. Red color depicts presence of the CD81 tetraspanin protein on exosome membranes, with green color representing the presence of CA125.

The fluorescence micrographs encompass the process negative control (blank) and the four EV sources, with the two distinct surface biomarkers probed in situ. It is important to point out that the scales of these images equate to only a couple of channels of a single

fiber, making up a very small fraction of the full SPE tip. In this example, the tetraspanin CD81, which is fairly ubiquitous among all EV populations, is used as the benchmark exosome identifier and thus is a positive indication of the vesicles. The target for this analysis is the presence of the CA125 protein, which is one of the primary cancer antigens associated with OC.[29, 30] To be clear, CA125 is not solely related to OC, as it is also known to be associated with other cancers.[31, 32] The images presented in Fig. 5.2 provide confirmation of the presence/location of EVs based on the CD81 (red) responses and those which have CA125 (green) present on the vesicle surfaces (taken simultaneously), following the overnight immunolabeling protocol. The third column is an overlay of the respective responses, providing a correlative verification of the presence of these antigens in close proximity, presumably associated with a given exosomal particle.

Going through the exosome sources, the immunofluorescence method yields the anticipated results in each case, along with some unanticipated ones. In the case of the non-mammalian *D. discoideum* amoeba, the imaging only yields positive results towards the CD81 tetraspanin moiety. *D. discoideum* have previously been reported to contain active homologs to the CD81 EV tetraspanin protein,[33] this is further confirmed here. The commercially-sourced sample derived from the urine of supposedly healthy individuals provides positive responses for CD81, but perhaps not anticipated is the fact that some positive responses for CA125 are seen as well. Indeed, the overlay reflects the coexistence of the two proteins on many particles. High levels of CA125 are often released in the body during states of ovarian-related ailments (i.e., endometriosis or

ovarian cancers), but healthy women also express low levels of CA125.[34] Thus, while CA125 is clearly present on the isolated exosomes, this is not a direct indication of OC because of the comparatively low fluorescent response. As would be expected, the isolates from the CaOv-3 cell line are replete with exosomes presenting both the CD81 and CA125 markers. Again the overlay of the fluorescent images verifies the presence of the same-source exosomes. Finally, the images of the exosomes isolated from the urine of the anonymous OC patient likewise show a high density of particles whose surfaces are populated with both CD81 and CA125. In this way, while CA125 is not solely attributed to OC, it is fairly convincing evidence that a CA125-upregulating source of malignancy (presumably cancer) is present. As a final comment, it is no coincidence that the isolated particle densities (as reflected in the CD81 responses) from the cancerous subject sources appear far higher than the corresponding non-cancerous sources; i.e., the CaOv-3 culture distributions appear far more dense than the *D. discoiduem* culture, and the patient urine yields far more than the "healthy-source" urine. Certainly, no direct quantitative conclusion can be made here, but it is well known that systems under the stress of disease exhibit far higher EV production and excretion rates.[35, 36] Ultimately, the method presented suggests a route to a facile, multi-biomarker EV screening and source differentiation.

It is important to note that, as an extension of the SEM images of Fig. B-2, the presence of discrete sources of fluorescence on the EV size scale, provides evidence that the EVs remain intact through the course of the isolation and immunolabeling processes. Should the vesicles have ruptured in the processing, the corresponding fluorescence

images would be very diffuse across the fiber surface. Additionally, one might also wish to extend the imaging methodology to the quantitative determination of CD81 and CA125, but that would come with many future challenges, including the detailed characterization of potential non-specific binding, autofluorescence of the fiber substrate, and indeed the ability to generate analytical EV blanks.

5.3.3 Differentiation of Exosome Type Using a Higher-Throughput Immunolabeling Protocol

As presented, the method demonstrated above holds particular promise in terms of the use of minute (100 μL) sample volumes, providing high purity isolates on an inert substrate and ready imaging capabilities, and the possibility to recover exosomes for further characterization or biochemical study. The advantage of sample processing time versus other isolation methods is somewhat negated by the typical overnight antibody/labeling incubation times. As an initial demonstration of the potential to affect higher throughput in the immunolabeling step, Fig. 5.3 depicts the blank and product images obtained for various-sourced samples following the 5-hour immunolabeling procedure detailed above. In this instance, the commercial, human urine-derived exosomes and a HEK293 culture supernatant are used as *presumably* CA125-free samples, with the IHOE and SKOV3 cell lines used as likely CA125-positive sources.

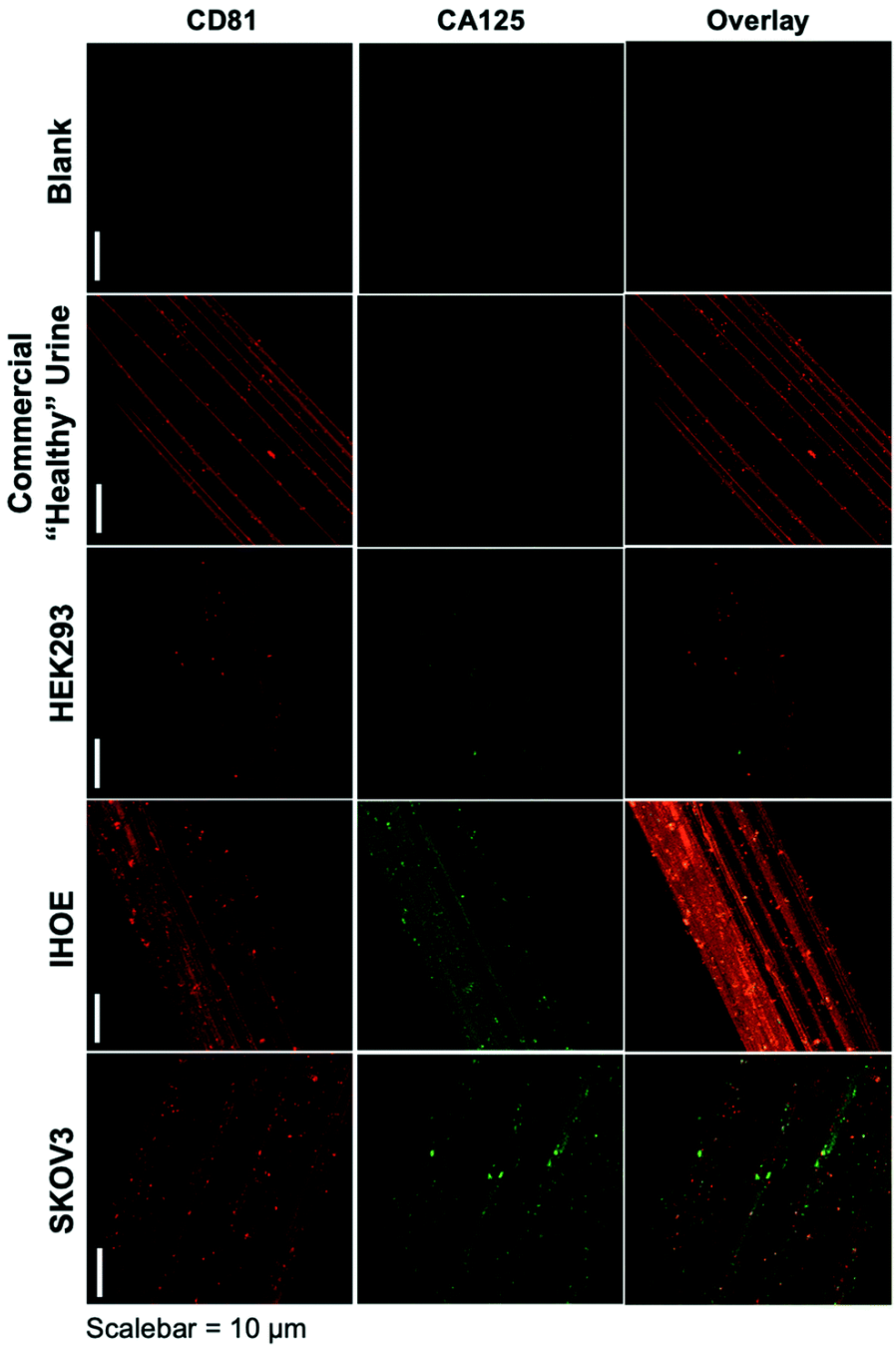

Figure 5.3 Confocal fluorescence images of C-CP fibers from process blank and test specimens following higher-throughput immunolabeling procedure. Red color depicts presence of the CD81 tetraspanin protein on exosome membranes, with green color representing the presence of CA125.

As seen in the case of the standard immunolabeling protocol, the higher-throughput approach does indeed yield the anticipated results regarding the presence of the expected biomarkers on the exosome surfaces. Here, the commercially sourced exosomes (derived from human urine) and the HEK293 cell line supernatant yield positive results towards the CD81 tetraspanin but little-to-no response towards CA125. The particles providing response to CA125 show little correlation with CD81 in the overlays. Admittedly, the CA125 response seen for the commercial specimen here is far less than the extended incubation time method, which may reflect some sacrifice in sensitivity towards low-abundance proteins (presumably due to the shorter incubation time). As depicted in Fig. 5.3, the responses towards both immunolabels (CD81 and CA125) are dramatically enhanced in density and correlation for the case of the SKOV3 and IHOE cell lines. While not quantified at this point, this result is surely reflective of the presence of a cancer, with results obtained in less than 5 hours on primary sample volumes of 100 μL. Both metrics lie well in line with what would be desired for a liquid biopsy. Certainly, an extension of the method to urine specimens and a liquid biopsy, as in the case of Fig. 5.3, is the target following optimization of the high-throughput labeling methodology.

5.4 Conclusions

This work has demonstrated a novel platform for the isolation and immunolabeling of extracellular vesicles, allowing imaging to be performed directly on

the capture fiber. The HIC capture and immunolabeling of EVs isolated on the C-CP fibers opens the door for many research, clinical, and diagnostic applications to be developed. The rapid concentration and classification of exosomal materials based on vesicle-associated biomarker proteins can be tailored to a variety of diagnostic challenges. Advantages in the method are first realized in terms of the sample sizes and the speed and purity of affecting the immobilization. Once isolated, the exosomes' quantity and identity can be determined by multiple on-fiber and post-elution methods. In the example presented here, confocal fluorescence immunoassays provide exquisite sensitivity and specificity, with as few as 10s of EVs being present in the illumination volume. While this method of determination is not suitable for portable point-of-care applications, based on instrument cost and complexity, it is certainly appropriate for many research and clinical laboratories. Further, the biochemical mechanisms of the work demonstrated here can surely be extended to other, more clinically practical, detection approaches (i.e., a C-CP lateral flow immunoassay) for the batch processing of large clinical cohorts on necessary scales of time and cost. Even in the research and clinical laboratory environments, the potential for further optimization of the high-throughput immunolabeling method would be advantageous. For example, Cappi et al. have described an automated 4-plex multistaining technique with 15 min. immunolabel incubation times using horseradish peroxidase (HRP)-labeled primary antibodies with tyramide signal amplification-Alexa Fluor secondary antibodies.[37] A similar abbreviated EV immunolabeling process is an obvious avenue for future exploration.

Beyond the on-fiber single particle detection, one can readily imagine less expensive fluorometric methods applied to the fiber bundles in-mass. Alternatively, on-fiber labeling could be followed by exosome release into microliter volumes for solution-phase immunofluorescence assay, again on very short time scales. Rapid isolation and purification could also be followed by use of conventional dot blot assays, targeting specific biomarkers. Eluted exosomes could also be subsequently lysed for genetic profiling of the vesicle contents. Finally, as has been demonstrated using the C-CP fibers in a column format, the spin-down approach could be readily applied as an isolation stage prior to mass spectrometric exosome proteomics analysis. Ultimately, this method's main benefit may lie in its ease of tailoring to capture nanovesicles from various origins, including viruses, bacteria-derived outer membrane vesicles, lipoproteins, liposomes, and synthetic nanoparticles.

Electronic supplementary information (ESI)/Appendix B: Experimental details for "standard" exosome immunolabeling procedure and methods employed, images resulting from negative control experiments, and images for SEM/STEM confirmation of captured exosomes.

CRediT Authorship contribution statement

Kaylan K. Jackson: Methodology, Data Curation, Visualization, Writing – Original Draft Preparation; **Rhonda R. Powell**: Methodology; **R Terri F. Bruce:** Conceptualization,

Supervision; R**. Kenneth Marcus:** Conceptualization, Supervision, Writing – Reviewing and Editing

Conflicts of interest

There are no conflicts to declare.

5.5 Acknowledgements

Financial support from the National Science Foundation under grant nos. CHE-1608663 and 2107882 is gratefully acknowledged.

5.6 References

1. Huang, S.; Wang, L.; Bruce, T. F.; Marcus, R. K., Isolation and quantification of human urinary exosomes by hydrophobic interaction chromatography on a polyester capillary-channeled polymer fiber stationary phase. *Anal. Bioanal. Chem.* **2019,** *411* (25), 6591-6601.
2. Huang, S.; Wang, L.; Bruce, T. F.; Marcus, R. K., Evaluation of Exosome Loading Characteristics in their Purification via a Glycerol-Assisted Hydrophobic Interaction Chromatography Method on a Polyester, Capillary-Channeled Polymer Fiber Phase. *Biotechnol. Prog.* **2020,** *in press*.
3. Bruce, T. F.; Slonecki, T. J.; Wang, L.; Huang, S.; Powell, R. R.; Marcus, R. K., Exosome isolation and purification via hydrophobic interaction

chromatography using a polyester, capillary-channeled polymer fiber phase. *Electrophoresis* **2019,** *40* (4), 571-581.

4. Wang, L.; Bruce, T. F.; Huang, S.; Marcus, R. K., Isolation and quantitation of exosomes isolated from human plasma via hydrophobic interaction chromatography using a polyester, capillary-channeled polymer fiber phase. *Anal. Chim. Acta* **2019,** *1082*, 186-193.
5. Li, M.; Zeringer, E.; Barta, T.; Schageman, J.; Cheng, A.; Vlassov, A. V., Analysis of the RNA content of the exosomes derived from blood serum and urine and its potential as biomarkers. *Philos. Trans. R. Soc. Lond. B Biol. Sci.* **2014,** *369* (1652).
6. Guidi, L.; Felice, C.; Procoli, A.; Bonanno, G.; Martinelli, E.; Marzo, M.; Mocci, G.; Pugliese, D.; Andrisani, G.; Danese, S.; De Vitis, I.; Papa, A.; Armuzzi, A.; Rutella, S., FOXP3(+) T regulatory cell modifications in inflammatory bowel disease patients treated with anti-TNFalpha agents. *Biomed. Res. Int.* **2013,** *2013*, 286368.
7. Bellingham, S. A.; Coleman, B. M.; Hill, A. F., Small RNA deep sequencing reveals a distinct miRNA signature released in exosomes from prion-infected neuronal cells. *Nucleic Acids Res.* **2012,** *40* (21), 10937-49.
8. Zhao, X.; Wu, Y.; Duan, J.; Ma, Y.; Shen, Z.; Wei, L.; Cui, X.; Zhang, J.; Xie, Y.; Liu, J., Quantitative proteomic analysis of exosome protein content changes induced by hepatitis B virus in Huh-7 cells using SILAC labeling and LC-MS/MS. *J. Proteome Res.* **2014,** *13* (12), 5391-402.

9. Kruger, S.; Abd Elmageed, Z. Y.; Hawke, D. H.; Worner, P. M.; Jansen, D. A.; Abdel-Mageed, A. B.; Alt, E. U.; Izadpanah, R., Molecular characterization of exosome-like vesicles from breast cancer cells. *BMC Cancer* **2014,** *14*, 44.

10. Griffiths, S. G.; Cormier, M. T.; Clayton, A.; Doucette, A. A., Differential Proteome Analysis of Extracellular Vesicles from Breast Cancer Cell Lines by Chaperone Affinity Enrichment. *Proteomes* **2017,** *5* (4), 16.

11. An, M.; Wu, J.; Zhu, J.; Lubman, D. M., Comparison of an optimized ultracentrifugation method versus size-exclusion chromatography for isolation of exosomes from human serum. *J. Proteome Res.* **2018,** *17*, 3599-3605.

12. Randunu, K. M.; Dimartino, S.; Marcus, R. K., Dynamic evaluation of polypropylene capillary-channeled fibers as a stationary phase in high-performance liquid chromatography. *J. Sep. Sci.* **2012,** *35* (23), 3270-80.

13. He, M.; Zeng, Y., Microfluidic Exosome Analysis toward Liquid Biopsy for Cancer. *J Lab Autom.* **2016,** *21* (4), 599-608.

14. Ko, J.; Hemphill, M. A.; Gabrieli, D.; Wu, L.; Yelleswarapu, V.; Lawrence, G.; Pennycooke, W.; Singh, A.; Meaney, D. F.; Issadore, D., Smartphone-enabled optofluidic exosome diagnostic for concussion recovery. *Sci. Rep.* **2016,** *6*, 31215.

15. He, M.; Crow, J.; Roth, M.; Zeng, Y.; Godwin, A. K., Integrated immunoisolation and protein analysis of circulating exosomes using microfluidic technology. *Lab Chip* **2014,** *14* (19), 3773-80.

16. Contreras-Naranjo, J. C.; Wu, H. J.; Ugaz, V. M., Microfluidics for exosome isolation and analysis: enabling liquid biopsy for personalized medicine. *Lab Chip* **2017,** *17* (21), 3558-3577.

17. He, F.; Liu, H.; Guo, X.; Yin, B. C.; Ye, B. C., Direct Exosome Quantification via Bivalent-Cholesterol-Labeled DNA Anchor for Signal Amplification. *Anal. Chem.* **2017,** *89* (23), 12968-12975.

18. van der Pol, E.; Coumans, F. A.; Grootemaat, A. E.; Gardiner, C.; Sargent, I. L.; Harrison, P.; Sturk, A.; van Leeuwen, T. G.; Nieuwland, R., Particle size distribution of exosomes and microvesicles determined by transmission electron microscopy, flow cytometry, nanoparticle tracking analysis, and resistive pulse sensing. *J. Thromb. Haemost.* **2014,** *12* (7), 1182-92.

19. Sumida, S., Transfusion and transplantation of cryopreserved cells and tissues. *Cell Tissue Bank* **2006,** *7* (4), 265-305.

20. Lehrich, B. M.; Liang, Y. X.; Khosravi, P.; Federoff, H. J.; Fiandaca, M. S., Fetal Bovine Serum-Derived Extracellular Vesicles Persist within Vesicle-Depleted Culture Media. *Int. J. Mol. Sci.* **2018,** *19* (11), 11.

21. Vagenende, V.; Yap, M. G. S.; Trout, B. L., Mechanisms of Protein Stabilization and Prevention of Protein Aggregation by Glycerol. *Biochemistry* **2009,** *48* (46), 11084-11096.

22. Vagenende, V.; Han, A. X.; Pek, H. B.; Loo, B. L. W., Quantifying the Molecular Origins of Opposite Solvent Effects on Protein-Protein Interactions. *PLoS Comput. Biol.* **2013,** *9* (5), 9.

23. Kjaer, S.; Stausbol-Gron, B.; Wind, T.; Ravn, P.; Jensen, K. P.; Kahns, L.; Clark, B. F. C., Glycerol diversifies phage repertoire selections and lowers non-specific phage absorption. *FEBS Lett.* **1998,** *431* (3), 448-452.

24. Jackson, K. K.; Powell, R. R.; Bruce, T. F.; Marcus, R. K., Solid-phase extraction of exosomes from diverse matrices via a polyester capillary-channeled polymer (C-CP) fiber stationary phase in a spin-down tip format. *Anal. Bioanal. Chem.* **2020,** *412* (19), 4713-4724.

25. Jackson, K. K.; Powell, R. R.; Bruce, T. F.; Marcus, R. K., Rapid isolation of extracellular vesicles from diverse biofluid matrices via capillary-channeled polymer fiber solid-phase extraction micropipette tips. *Analyst* **2021,** *146* (13), 4314-4325.

26. Donaldson, J. G., Immunofluorescence Staining. *Curr. Protoc. Cell Biol.* **2015,** *69* (1), 4 3 1-4 3 7.

27. Huang, S.; Ji, X.; Jackson, K. K.; Lubman, D. M.; Ard, M. B.; Bruce, T. F.; Marcus, R. K., Rapid separation of blood plasma exosomes from low-density lipoproteins via a hydrophobic interaction chromatography method on a polyester capillary-channeled polymer fiber phase. *Anal. Chim. Acta* **2021,** *1167*, 338578.

28. Huang, S.; Wang, L.; Bruce, T. F.; Marcus, R. K., Evaluation of exosome loading characteristics in their purification via a glycerol-assisted hydrophobic interaction chromatography method on a polyester, capillary-channeled polymer fiber phase. *Biotechnol. Prog.* **2020,** *36* (5), e2998.

29. Zurawski Jr., V. R.; Orjaseter, H.; Andersen, A.; Jellum, E., Elevated serum CA 125 levels prior to diagnosis of ovarian neoplasia: Relevance for early detection of ovarian cancer. *Int. J. Cancer* **1988,** *42* (5), 677-680.

30. Einhorn, N.; Sjovall, K.; Knapp, R. C.; Hall, P.; Scully, R. E.; Bast, R. C., Jr.; Zurawski, V. R., Jr., Prospective evaluation of serum CA 125 levels for early detection of ovarian cancer. *Obstet. Gynecol.* **1992,** *80* (1), 14-8.

31. Kimura, Y.; Fujii, T.; Hamamoto, K.; Miyagawa, N.; Kataoka, M.; Iio, A., Serum CA125 level is a good prognostic indicator in lung cancer. *Br. J. Cancer* **1990,** *62* (4), 676-8.

32. Fang, C.; Cao, Y.; Liu, X.; Zeng, X.-T.; Li, Y., Serum CA125 is a predictive marker for breast cancer outcomes and correlates with molecular subtypes. *Oncotarget* **2017,** *8* (38), 63963-63970.

33. Zimmerman, B.; Kelly, B.; McMillan, B. J.; Seegar, T. C. M.; Dror, R. O.; Kruse, A. C.; Blacklow, S. C., Crystal Structure of a Full-Length Human Tetraspanin Reveals a Cholesterol-Binding Pocket. *Cell* **2016,** *167* (4), 1041-1051 e11.

34. Simon, I.; Katsaros, D.; Rigault de la Longrais, I.; Massobrio, M.; Scorilas, A.; Kim, N. W.; Sarno, M. J.; Wolfert, R. L.; Diamandis, E. P., B7-H4 is over-expressed in early-stage ovarian cancer and is independent of CA125 expression. *Gynecol. Oncol.* **2007,** *106* (2), 334-341.

35. Hoshino, D.; Kirkbride, K. C.; Costello, K.; Clark, E. S.; Sinha, S.; Grega-Larson, N.; Tyska, M. J.; Weaver, A. M., Exosome secretion is enhanced by invadopodia and drives invasive behavior. *Cell. Rep.* **2013,** *5* (5), 1159-68.

36. Shao, C.; Yang, F.; Miao, S.; Liu, W.; Wang, C.; Shu, Y.; Shen, H., Role of hypoxia-induced exosomes in tumor biology. *Mol. Cancer* **2018,** *17* (1), 120.

37. Cappi, G.; Dupouy, D. G.; Comino, M. A.; Ciftlik, A. T., Ultra-fast and automated immunohistofluorescent multistaining using a microfluidic tissue processor. *Sci. Rep.* **2019,** *9* (1), 4489.

CHAPTER SIX

A RAPID CAPILLARY-CHANNELED POLYMER (C-CP) FIBER SPIN-DOWN TIP APPROACH FOR THE ISOLATION OF PLANT-DERIVED EXTRACELLULAR VESICLES (PDEVS) FROM 20 COMMON FRUIT AND VEGETABLE SOURCES

6.1 Introduction

It is now becoming clear that in many organisms, intercellular communication processes are facilitated by nanometer-scale extracellular vesicles (EVs), which contain host cell-specific proteins, lipids, and genetic content. [1, 2] Though the EV creation and transport mechanisms are not well understood, EVs are generically classified as apoptotic bodies, microvesicles, or exosomes, based on their creation pathway and size [3]. Apoptotic bodies are large, 500 – 4,000 nm vesicles formed through the spontaneous bulging of the plasma membrane during cellular apoptosis [4]. Microvesicles (MVs) are 50 – 2,000 nm EVs formed by the outward membrane budding and fission of the origin cell's plasma membrane [5, 6]. Exosomes are 30 to ~200 nm EVs, created through the multivesicular body (MVB)-mediated endosomal pathway [7, 8]. Due to the overlapping MV and exosome size ranges, the similarities in content, and the inability to determine EV origin, the collection of EVs in the exosome size range is often generically referred to as EVs or small EVs (sEVs). Still, because sEVs characteristically contain the biomolecular contents of the secreting cell and may be collected non-invasively through biofluids, this class of EVs has been widely proposed in clinical diagnostic applications [9, 10] and for large-scale therapeutic vector production approaches [11, 12].

To date, much of EV research has been performed using EVs sourced from human patient biofluid samples or from cell culture media, with hopes of assessing the critical roles these vesicles play in disease prevention and progression [13-15]. Additionally, the therapeutic application of EVs introduces unique advantages, including the ability to strategically deliver drug and gene therapies to local tissues of neighboring cells or distant organs throughout the circulatory system [10, 11, 16]. Since exosomes are cell secretion products, obtaining concentrated collections of EVs depends upon the ability to harvest them from large quantities of cell or biofluid sources without significant alterations to EV structure and/or function. However, with many of the large-scale cell culture conditions, transformations are often performed within the cell line, which alters the cellular phenotype, and thereby, the composition and function of the EVs obtained from these cell stocks [11]. The primary limitations of using mammalian-sourced EVs for therapeutics are 1) insufficient methods for isolation and characterization preventing EVs from being fully understood, 2) biocompatibility concerns of the transformed EVs, and 3) time, capital, and labor-consuming methods for large-scale EV production [16].

As EV vector technologies continue to develop, researchers have begun to explore alternative, natural sources for EVs to use as novel therapeutic delivery vectors. With this, a growing body of literature has revealed that several natural EV sources produce nanovesicles that display many of the exosome-characteristic structural and functional features. [1, 2] To date, exosome-like vesicles have been discovered in all three domains of life, including species such as bacteria (outer-membrane vesicles, OMVs), [17, 18] fungi [19, 20], parasites [21], and plants [19, 22-25]. Still, though the nanovesicles from

all sources remain poorly understood, researchers have suggested the use of plant-derived extracellular vesicles (PDEVs) in therapeutic applications because of the prominent roles they play in the transport of bioactive molecules from plants to human cells [24, 26].

PDEVs have shown to be a promising candidate for use as therapeutic delivery vectors because of their non-immunogenic traits and potentially cost-effective production from natural renewable sources [27]. The first examples of PDEVs were identified in wheat-sourced mesophyll cells by Shaw et al. [28] and carrot sample stocks by Jensen et al. [29] in the 1960s, even before human-sourced "exosomes" were identified. During the initial PDEV assessment using electron microscopy, the EV-characteristic size and structural features were revealed, though not fully appreciated due in part to the recent emphasis on mammalian EV research [28]. Continued works have confirmed these initial findings and have shown that PDEVs, like human-sourced EVs, do indeed contain a cell-derived lipid bilayer membrane and miRNAs, mRNAs, proteins, lipids, and metabolites from the originating plant cell [30]. Further, works by Zhang et al. [31] have demonstrated that the PDEVs obtained from common edible plant sources are actively endocytosed by macrophages and intestinal stem cells and are able to activate signaling pathways in murine (mice) cells.

Though little is known about the biogenesis, uptake, release, composition, function, and stability of PDEVs relative to their mammalian counterparts [24], it is known that PDEVs contain specific surface marker proteins that are incorporated through the biogenesis process such as Penetration1 (PEN1) or Syntaxin121 (SYP121) [32-36]. Though there are some differences in function, the PEN1 protein seems to serve a similar

role to that of tetraspanin proteins (i.e., CD9, CD81, CD63) in human-sourced EVs for vesicle identification purposes. The PEN1 protein generically functions as a positioning anchor for the KAT1 K+ channel protein on the plasma membrane and is involved in biological processes such as endo- and exo-cytosis, intracellular protein transport, and vesicle docking and fusion [33]. Likewise, the PEN1 protein has been previously found in high concentrations when PDEVs are present and have allowed for the identification of PDEVs based on PEN1 protein detection via immunoassays. Alongside PEN1 protein assessment, the assessment of other biomolecular targets, like lipids and microRNAs, have allowed for correlations to be made between PDEV composition and function [37]. But further, PDEVs can be modified to provide a means of targeted drug transport to specific areas where homeostasis regulation is required [37, 38]. Regardless of the many promising applications of PDEVs (and EVs of all origins), the exact mechanisms of these interactions are largely unknown and require additional investigation. A recent review by Rutter and Innes very succinctly lays out the state of the art and challenges in PDEV research [26]. Additionally, much work is needed to standardize the processing and characterization of PDEVs before their full implementational impacts can be realized [24, 39].

One of the most limiting factors to the understanding of PDEV fundamentals is the lack of methods for the isolation of these nanometer-scale vesicles. Several studies have demonstrated that PDEVs may be isolated from various parts of plants, including plant juices, [40-42] roots, [43, 44] seeds, [45, 46] and dried plant materials [47]. Most commonly, fluids from these sample types are obtained through a

blending/homogenization process and then applied to standard EV isolation protocols (i.e., ultracentrifugation, UC). Though multiple techniques are available for the isolation of EVs from mammalian sources, the majority of published works have reported the use of the ultracentrifugation (UC) method for PDEV sample processing. [27, 30] But as seen with human EVs, the UC method is likely to produce PDEV recoveries that are compromised by concomitant matrix species and low yields [48-50]. Overall, the performance of the available isolation methods does not yield the concentration and purity of EVs needed for fundamental research, much less therapeutic applications. [26, 27, 51] In a recent review by Innes and colleagues, it was recommended that PDEV researchers pay close attention to the progression of the EV field, so that the "pitfalls" and challenges commonly experienced during EV research can potentially be evaded. [26] For instance, the standardization of relevant isolation and characterization protocols for EVs and PDEVs is largely lacking. Because EVs are not able to be well isolated/characterized, they are not able to be well-classified, causing there to be a lack of field-wide agreement on standard protocols, fundamental structure-function correlations, and EV nomenclature [39]. These disagreements have been limiting in the mammalian EV field as a whole, but particularly in the development of exosome/EV standardized reference materials. With all of these concerns being relevant to PDEV research as well, it is essential for researchers in the PDEV realm to consider these as the field continues to progress. Though all of these shortcomings limit the pursuit of novel PDEV therapeutic approaches, the lack of isolation methods to efficiently provide representative populations of PDEVs is potentially most limiting to the progression of research [26].

Hence, the introduction of an isolation method to provide highly pure, concentrated, and functionally-preserved collections of PDEVs is necessary for the fundamental characterization of PDEVs to be performed and the therapeutic vector potential to be explored.

As the potential pitfalls in mammalian exosome isolation are well known, there are two primary sources of error/contamination in PDEV isolation. The first, is a high possibility that the populations included in extracts are co-inclusive of vesicles both of extracellular origin and endosomal vesicles which were released due to the destruction of plant cellular membranes by homogenization. As an alternative to this destructive sample preparation method, Innes et al. [23, 25, 26, 35, 52, 53] have developed a protocol for non-destructive PDEV harvest through the collection of apoplastic wash from *Arabidopsis thaliana* plants, where these plant biofluids are employed in UC protocols to obtain PDEVs of true extracellular origin. The second source of non-targeted vesicles is the due to possible carryover of EVs originating from plant material having bacteria of various sorts on their surface. Works by Gourabathini et al. have revealed the presence of bacterial pathogens in high concentrations in produce stocks obtained from local grocery stores [54]. These pathogens expel vesicles that settle on vegetable leaves and aid in the proliferation and survival of these bacterial species on these surfaces [17, 18, 55]. While these EVs would certainly have different surface and cargo makeup from the PDEVs, their presence would certainly bear on the results of fundamental studies as well as further use of extracted EV populations in vector applications. Eventually, all proposed methods of PDEV recovery and use must address these potential challenges.

Ongoing work by Marcus and colleagues has produced a novel EV isolation method based on hydrophobic interaction chromatography (HIC) via a polyester (PET) capillary-channeled polymer (C-CP) fiber stationary phase [56-60]. The C-CP fiber phase consists of melt-extruded fibers with an 8-legged peripheral shape, creating single-micron sized channels when collinearly aligned and packed into a column format. The relative hydrophobicity of the PET C-CP phase and gentle HIC solvent system allows for effective, vesicle-preserving EV isolations to be performed, where a high-to-low salt solvent transition drives the capture and subsequent release of EVs based on the vesicle's intrinsic hydrophobicity. The straightforward and cost-effective HIC C-CP method was first performed using a traditional HPLC workflow, where the simultaneous isolation and quantification of EVs was allowed using on-line absorbance (scattering) detection [56-58, 60]. More recently, the method has been adapted to a clinically practical solid-phase extraction (SPE) spin-down tip format, where the batch processing of EVs is only limited by the capacity of the table-top centrifuge [59, 61, 62]. The C-CP spin-down tip method has demonstrated the ability to produce highly concentrated (up to 1 x 10^{12} particles mL^{-1}), high-purity (>90% removal of protein/lipoprotein contaminants), and bioactive EV recoveries from a plethora of biofluids in less than 15 minutes [59, 62-64]. Here, the capabilities of the fiber spin-down tip method for the isolation of PDEVs from various plant sample stocks is explored. The recovered PDEVs are evaluated using absorbance (scattering), multi-angle light scattering (MALS) detection, and transmission electron microscopy (TEM). The purity of the PDEVs was assessed using a Bradford assay based on the removal of unwanted free/matrix proteins. The identity of the PDEVs is confirmed

using antibodies to the PEN1 protein via an indirect enzyme-linked immunosorbent assay (ELISA), allowing differentiation from bacteria-originating EVs. The methodology presented here addresses the limitations in isolation hindering the fundamental research and downstream application of PDEVs, which will enable future studies of therapeutic relevance to be performed.

6.2 Materials and Methods

6.2.1 Chemicals and reagents - Deionized water (DI-H_2O, 18.2 MΩ cm) was obtained from a Milli-Q water purification system (Millipore Sigma, Merck, Darmstadt, Germany). Biotechnology-grade glycerol and ammonium sulfate were purchased from VWR (Sokon, OH, USA). Phosphate buffered saline (PBS, pH = 7.4), bovine serum albumin (BSA), and Pierce™ Coomassie Plus (Bradford) Assay Reagent were purchased from ThermoFisher Scientific (Waltham, MA, USA).

6.2.2 *Instrumentation* - A NanoVue Plus UV-Vis spectrophotometer (GE Healthcare, Chicago, IL, USA) was used during the PDEV absorbance quantification (203 nm). The DAWN multi-angle light scattering (MALS) detector (Wyatt Technology, Goleta, CA, USA) was used for size determination efforts. A Synergy H1 Hybrid Multi-Mode Plate Reader (BioTek, Winooski, VT, USA) was used to measure the UV-Vis absorbance (595 nm) of samples in the 96 cell-well format, where the colorimetric Pierce™ Coomassie Plus (Bradford) Assay Reagent was used for Bradford assay detection. The Hitachi HT7830 transmission electron microscope (Chiyoda City, Tokyo, Japan) was used for TEM imaging for EV visualization and structural characterizations.

6.2.3 Extracellular Vesicle Sources - Exosome standards employed during the quantification work were sourced from a commercial lyophilized exosome standard stock from HEK293 cell culture media by HansaBioMed (Tallinn, Estonia). To clarify, the "exosome standards" employed here are not standardized EV reference materials, and with this, no purity or classification metrics were supplied by the manufacturer. However, the product does serve as an EV source of known concentration (2.7×10^{12} particles mL^{-1}). Concerns with the size (including EVs of < 30 nm and > 200 nm diameter) and purity (the absence of contaminant matrix species like lipoproteins and other protein contaminants) of the exosomes included in these materials have previously been expressed, and this potential avenue for systematic error is acknowledged here.

The raw fruits and vegetables used in this study were obtained from the produce section of the local Walmart (Central, SC, USA). The produce stocks included in this study were loosely categorized by type: leafy greens (represented in green font in data sets), vegetables (represented in red), and fruit (represented in blue). Shown in Table 6.1 are the plant samples in each category, along with the scientific name of each plant. If PDEVs from the presented sample stock have been previously identified in the literature, the size of PDEVs obtained from each, and the employed isolation method used to obtain such, are also presented in the Table.

Common Name	Species Name	Size (nm)	Isolation Method	References
Baby Spinach	*Spinacia oleracea*	-	-	-
Lettuce	*Lactuca sativa*	-	-	-
Green Onions	*Allium fistulosum*	-	-	-
Cilantro	*Coriandrum sativum*	-	-	-
Carrots	*Daucus carota subsp. sativus*	150 nm (Average)	Size-Exclusion Chromatography	[65]
Roma Tomato	*Solanum lycopersicum 'Roma'*	-	-	-
Beefsteak Tomato	*Solanum lycopersicum 'Beefsteak'*	100 – 1000 nm	Ultracentrifugation, Density Gradient Centrifugation, and Filtration	[42, 66, 67]
Cucumber	*Cucumis sativus*	-	-	-
Sweet Onion	*Allium cepa 'White onion'*	113 – 153 nm	Ultracentrifugation	[68]
Red Onion	*Allium cepa 'Red onion'*	113– 153 nm	Ultracentrifugation	[68]
Ginger	*Zingiber officinale*	50-800 nm (Average 189 nm)	Ultracentrifugation	[42, 69, 70]
Blueberries	*Vaccinium sect. Cyanococcus*	100 – 800 nm	Ultracentrifugation, Differential Centrifugation	[42, 71]
Cherries	*Prunus avium*	-	-	-

Red Apple	*Malus domestica 'Red Delicious'*	-	-	-
Green Apple	*Malus domestica 'Granny Smith'*	-	-	-
Strawberries	*Fragaria × ananassa*	30 – 191 nm	Ultracentrifugation	[72]
Lime	*Citrus × aurantiifolia*	-	-	-
Lemon Juice	*Citrus limon L.*	50 – 100 nm	Differential Centrifugation, Filtration, Ultracentrifugation	[66]
Orange	*Citrus sinensis*	100 – 800 nm	Differential Centrifugation	[42]
Aloe Vera Juice	*Aloe vera barbadensis*	50 – 200 nm	Ultracentrifugation, Ultrafiltration, Tangential Flow Fractionation	[73]

Table 6.2: Scientific name, reported size, and isolation method used for the extraction of plant-derived EVs. Sample categories: leafy greens (represented in green), vegetables (represented in red), and fruit (represented in blue).

The raw plant samples were first rinsed with DI water, then chopped into manageable portions, placed into a weighing boat, and weighed using a standard analytical scale. For the solid plant samples, 10 mL of Milli-Q water was added, then the sample was placed in a Magic Bullet™ (Homeland Housewares, Los Angeles, CA) blender and blended until a homogeneous liquid was obtained. For the difficult-to-blend samples (ginger, cilantro, carrots, and strawberry), a mortar and pestle were used for

further sample homogenization. The resulting fluid from each sample was aspirated using a sterile, 3 mL single-use syringe (with a 21 G x 1 1/2 in. needle attached; BD, Franklin Lakes, NJ), then filtered using a 0.22 µm PES syringe filter. Finally, 100 µL of the filtered fluid from each sample was processed through the C-CP tip isolation workflow. A visual representation of the sample preparation process is presented in Fig. 6.1.

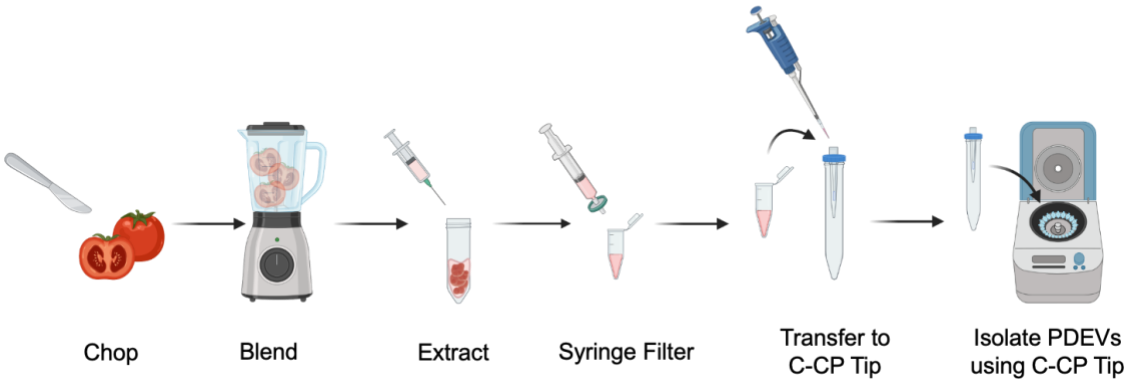

Figure 6.1: Diagrammatic representation of the sample processing workflow for the isolation of plant-derived extracellular vesicles (PDEVs) using the capillary-channeled polymer (C-CP) fiber solid-phase extraction tip and a tabletop centrifuge.

For the already-liquid samples included here (aloe vera juice and lemon juice), the samples were filtered using a 0.22 µm PES syringe filter before C-CP tip processing.

6.2.4 C-CP Fiber Spin Down Tip Assembly and Sample Processing - The C-CP fiber SPE spin-down tips were assembled following the previously reported protocols, and the same HIC isolation workflow was performed [59, 62]. To summarize, 1 cm C-CP fiber-packed tips (with an additional 0.5 cm of void space for attachment) were cut from a 30 cm long, 0.8 mm inner diameter fluorinated ethylene–propylene (FEP) C-CP packed

columns consisting of 456 individual PET C-CP fibers to create an interstitial fraction of ~0.6, and bed volume of ~3 μL. The 1.5-cm C-CP fiber-packed tips were press-fit to the narrow end of a 200 μL low retention micropipette tip and held in place using a small amount of liquid adhesive around the periphery of the 200 μL tip.

The PDEV isolations were performed as previously described [59, 62]. After sample processing, 100 μL of the resultant filtered plant supernatant was mixed with 100 μL of ammonium sulfate (2M final concentration) and deposited inside the sample reservoir of the C-CP tip. The C-CP tip was secured into a 15 mL conical tube using a tip-modified conical adapter cap, then placed inside the table-top centrifuge tube and spun at 300 *x g* (*rcf*) for 1 minute. The tip-bound EVs were then washed with 200 μL of PBS (300 *x g*, 1 min), and the matrix proteins eluted using 200 μL of 25% glycerol with 1M ammonium sulfate in PBS (300 *x g*, 1 min). Finally, the PDEVs were eluted from the C-CP tip surface using 50 μL of 50% glycerol in PBS (300 *x g*, 1 min) into an Eppendorf tube conical insert.

6.2.5 Absorbance/Scattering Detection – As previous reports have demonstrated, absorbance (technically, scattering) measurements are a valid means of EV quantification based on the generation of standard response (calibration) curves using commercial exosome standard stocks or via the method of standard addition [59, 62]. The two methods have been compared in detail in previous works for the quantification of EVs in human biofluids [62]. In this case, the method of standard addition was applied because of the potential for matrix effects across the diverse plant specimens, which could cause the absorbance quantification of EVs to be skewed. Across the previous work with

biofluids, the method was able to overcome the intense sample matrix effects, and the absorbance quantification of the EVs using the standard addition method was also able to determine EV concentrations with high precision (<5% RSD) [62]. As done previously, serial additions of the commercially-obtained exosome standard stock were used to create a standard addition response curve. In these experiments, the absorbance of each sample was measured at 203 nm (n = 5) using the NanoVue spectrophotometer. The resulting linear regression was used to determine the concentration of the recovered PDEVs.

Several recent works have employed multiangle light scattering (MALS) detection for human EV size determinations [74-76]. Here, the diameters (actually the root-mean-square (RMS) radii) of the PDEVs of the recovered particles were determined using the DAWN multi-angle light scattering (MALS) detector (Wyatt Technology, Goleta, CA, USA), controlled using the ASTRA software. After the C-CP tip isolation process, the recovered EVs were passed through to the MALS detector cell using a Dionex (Thermo Fisher Scientific, Sunnyvale, CA, USA) Ultimate 3000 HPLC system (LPG-3400SD quaternary pump with MWD-3000 UV-Vis absorbance detector), which was controlled by the Chromeleon 7 software. The experimentally-determined RMS radii were multiplied by 2 to represent the approximate diameter/size of the PDEVs. For the entirety of MALS analyses, the refractive index was set to that of 50% glycerol in PBS, 1.4096 (experimentally determined using a Reichert AR7 Series Automatic Refractometer at 22ºC). Three replicate measurements were collected for each sample in 60-second increments.

6.2.6 Transmission Electron Microscopy (TEM) – The biophysical characteristics of the collected PDEVs, including size and shape, were evaluated using a Hitachi HR7830 TEM. The TEM sample preparation was performed as previously reported [59, 62-64]. Briefly, 7 µL of each EV sample was applied to a copper/formvar grid and incubated at room temperature for 20 min. before the excess sample liquid was removed. Next, the EVs were fixed on the grids using 2% paraformaldehyde (RT, 5 min). Afterward, the excess paraformaldehyde was removed from the grids, and they were washed with 50 µL droplets of water for 5 min. The grid was then negatively stained using 50 µL of a filtered 1% uranyl acetate solution (RT, 1 min). After staining, the excess uranyl acetate solution was removed using a paper towel, and the prepared grid was again washed with water before being allowed to dry in a desiccator for 30 minutes. The size of the vesicles visualized in the TEM micrographs was determined using ImageJ.

6.2.7 Bradford Assay – As stated previously, the removal of matrix proteins is perhaps the most significant challenge in isolation of EVs, whether for fundamental studies or in vector applications. The Bradford assay is the classic means of determining free protein content in diverse media and was used here to assess the presence of free proteins in the plant sample stocks and the removal of those 'contaminants' from the test solution following isolation of the PDEVs using the C-CP tips. For this, 250 µL of Bradford reagent was added to 25 µL of each sample stock or the PDEV recovery in a 96 well plate before incubation at room temperature for 20 minutes and absorbance detection of the Bradford reagent at 595 nm using the Synergy H1 Plate Reader. A standard curve

using serial dilutions of a BSA solution was used to determine the total protein concentration of the samples. All samples and standards were applied to the well plate in triplicate.

6.2.8 *Enzyme-Linked Immunosorbent Assay (ELISA)* – Analogous to the identification of mammalian EVs based on the presence of the tetraspanin proteins (e.g., CD81), the PEN1 protein serves as a surface marker for PDEVs. A polyclonal antibody to the PEN1 protein (custom-prepared by CUSABIO, Houston, TX) was employed in an indirect ELISA assay to confirm both the presence and bioactivity of PDEVs after isolation using the C-CP tip method. Prior, the tip-isolated PDEVs were applied to a 100 kDa filter unit, and the latent glycerol was removed, as glycerol is known to interfere with antibody binding [77, 78]. The ELISA protocol was performed as previously described [61, 62], with samples applied in triplicate. The PEN1 purified protein, obtained from the manufacturer, was used as the positive control, and the neat EV elution buffer – 50% glycerol in PBS was used as the negative control. The Synergy H1 microplate reader was used to detect the chemiluminescent response of the HRP-catalyzed oxidation of the detection substrate.

6.3 Results and Discussion

6.3.1 Verification of C-CP Tip Isolated PDEV Structure and Size by Transmission Electron Microscopy (TEM) - As a complement to other EV characterization methods, TEM is used to confirm the presence of EVs based on the presentation of the

characteristic spherical or cup-shaped structure. TEM is used to assess the size, shape, and vesicular integrity of the PDEVs collected using the C-CP fiber tip method. Representative micrographs of a) HEK293 EVs from a commercial standard stock, and b) PDEVs from green onion, c) blueberry, d) ginger, e) strawberry, f) red onion, g) baby spinach, and h) beefsteak tomato samples are shown in Fig. 6.2.

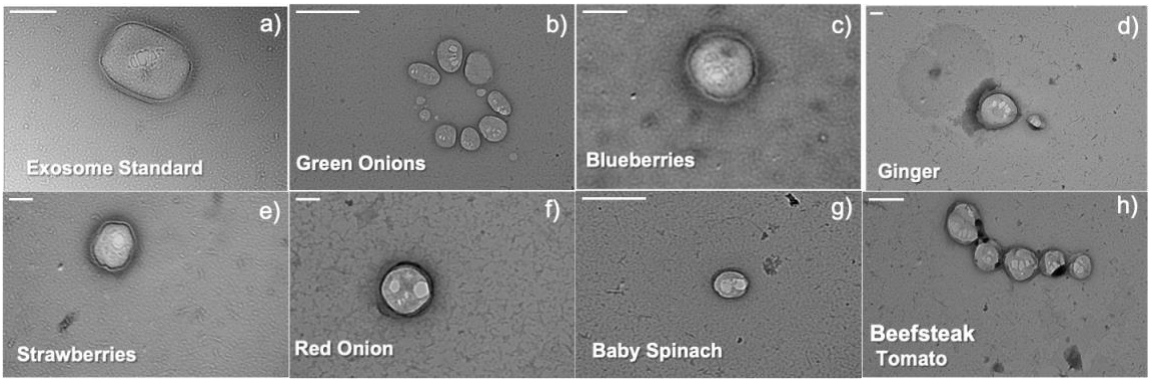

Figure 6.2: Transmission electron micrographs of commercial EVs from a) HEK293 exosome standards, and plant-derived extracellular vesicles (PDEVs) from b) green onion, c) blueberry, d) ginger, e) strawberry, f) red onion, g) baby spinach, and h) beefsteak tomato samples following isolation using the C-CP fiber spin-down tip method. The TEM images were taken using the Hitachi HT7830. Scalebar = 100 nm.

The TEM micrographs confirm the presence of vesicles in the sEV size range (< 200 nm) from both the exosome standard stock and the PDEVs isolated from the bulk plant supernatant, all exhibiting the characteristic spherical, membranous shape. Intact exosome-like vesicles are visualized, showing the preservation of the membrane integrity after isolation via the C-CP tip method. Of note, there is little evidence of contaminants (debris), despite the complexity of the original sample matrices. Individual vesicles are present in the majority of the samples, but some small vesicle aggregates are observed in

the micrographs from the green onion, ginger, and beefsteak tomato samples. Still, the TEM micrographs confirm the presence of 50-200 nm particles with apparent phospholipid bilayer membranes isolated from the plant extracellular fluids using the C-CP fiber spin-down tip.

6.3.2 Size Determination of C-CP Tip-Isolated EVs using MALS - In addition to TEM sizing of the vesicles, Nanosight nanoparticle tracking analysis (NTA) is commonly used for size determinations of EVs [79, 80]. However, many reports reveal concerns with the accuracy of EV size determinations via NTA due to variability/irreproducibility in size determinations and number densities, and because the method is not able to differentiate between EVs and large protein aggregates of EV-like size [81, 82]. In order to address these limitations during the PDEV size determinations, the MALS detection method has been previously suggested [74, 83, 84].

The average sizes of the PDEVs recovered from each plant sample type as determined by MALS are shown in Fig. 6.3.

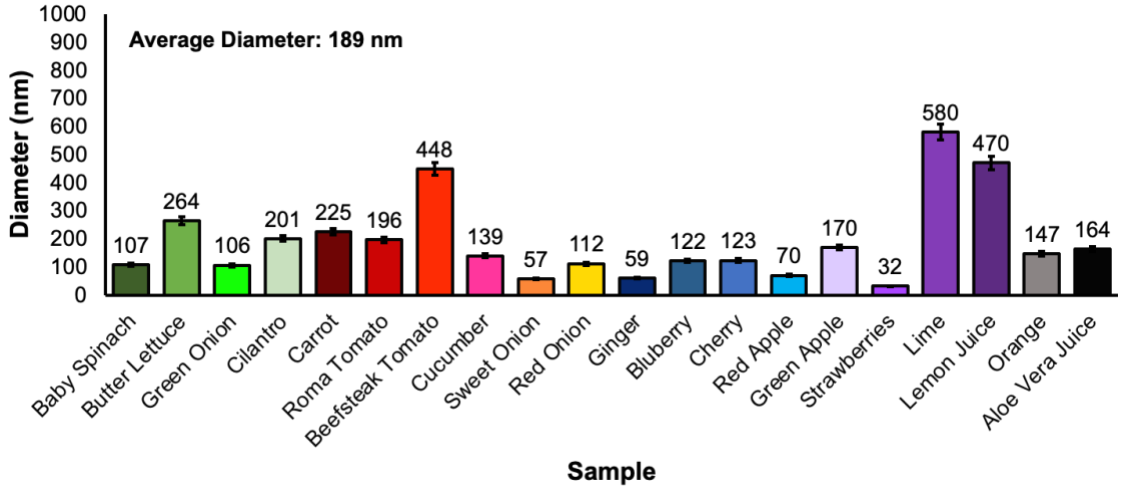

Figure 6.3: Size determinations of the C-CP tip isolated PDEVs using the Wyatt Dawn MALS instrument. Presented are the average sizes of the PDEVs resulting from 3 consecutive 60-second runs.

The C-CP tip-isolated PDEVs yield average diameters of 32 – 580 nm across the plant sample stocks, with an average diameter of 189 nm across all sample types. These PDEV size determinations align well with the previously-reported diameters as presented in Table 1 for those plant samples subjected to other EV isolation workflows, and with the TEM micrographs shown in Fig. 6.2, where the exosome/EV-like size and structure of the recovered vesicles are shown. The MALS analysis average diameters of the C-CP tip-eluted PDEVs are also in line with EVs recovered from human biofluids using the C-CP tip isolation method [59, 62]. Despite the vast differences in the PDEV sources, the relative precision of the MALS determinations of average PDEV diameters is remarkable versus NTA analysis, with less than 5% RSD across the triplicate size determinations of the PDEVs recovered from each plant source.

6.3.3 Quantification of Recovered PDEVs via UV-Vis Absorbance - The quantification of EVs from human biofluid and cell culture sources by optical absorbance at 203 nm has been previously demonstrated [59, 62, 64], using response curves generated from exosome stock solutions or via the standard addition method. To clarify, the "absorbance" response observed at the 203 nm wavelength is not accredited to electronic transitions of individual analyte molecules. More accurately, the absorbance detection is due to the Mie scattering by the EV nanobodies, which is proportional to the concentration of EVs in solution. Conveniently, the absorbance spectra obtained for the PDEVs from all sample types follow the EV-characteristic scattering/absorbance

responses, where an exponential decrease in absorbance response is observed (200 – 700 nm, λ_{max} = 203 nm).

The EV standard addition quantification method is applied here for the quantification of PDEVs recovered from the plant sample extracts after isolation using the C-CP tip method, as shown in Fig. 6.4.

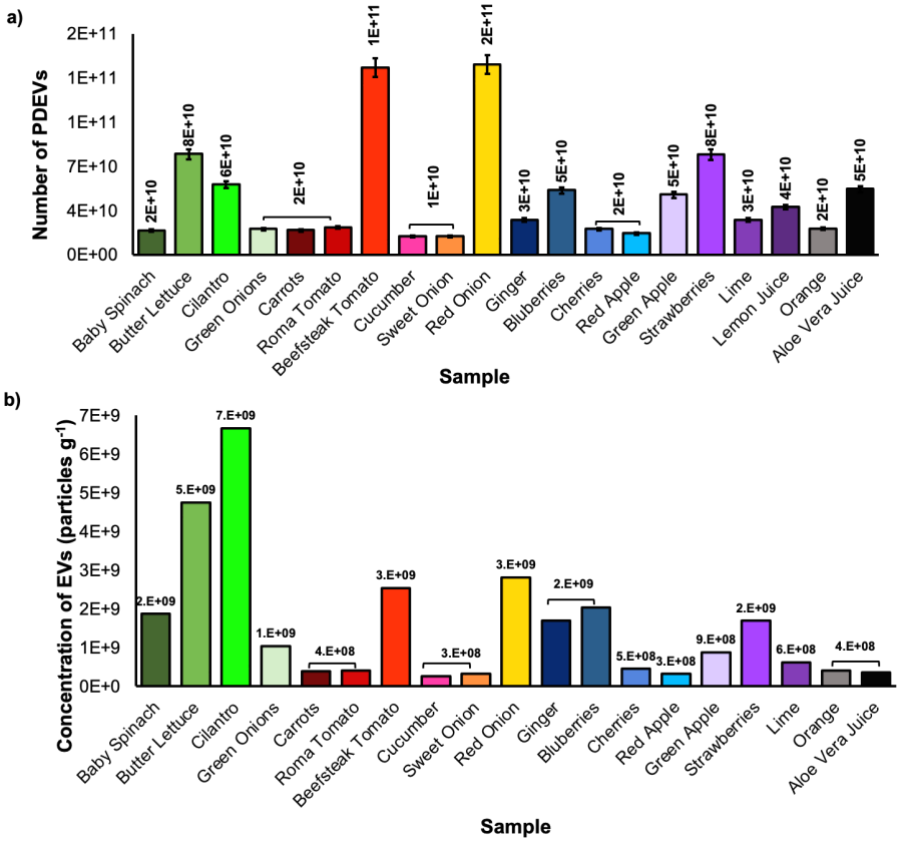

Figure 6.4: a) Numbers of recovered PDEVs using the C-CP spin-down tip isolation method, determined using the method of standard addition, and b) recovered PDEV concentrations with respect to the mass of starting material.

Using this quantitative approach, number densities of 1 x 10^{10} to 2 x 10^{11} PDEVs were obtained via processing of only 100 µL of plant sample extracts (Fig. 6.4a). The largest

numbers of PDEVs were obtained from the beefsteak tomato and red onion samples. However, as shown in Fig. 6.4b, the PDEVs from the butter lettuce and cilantro samples were recovered in higher concentrations with respect to starting material mass, accounting for ~3.6 x 10^9 EVs per gram of starting material. Alternatively, those PDEVs obtained from the fruit sample category were approximately 4 times lower with respect to starting mass, with 8.4 x 10^8 EVs per gram of starting material obtained on average. At this point, there is no body of literature suggesting which sorts of species should produce more or less EVs. There are also aspects of growth conditions, stress, etc. which surely will contribute to variation within species. Despite the growing body of PDEV literature, none of the identified previous works have attempted to provide a means of efficient vesicle quantification, as again the methodologies are sorely lacking. At this point, there is no way to verify the accuracy of this quantification effort, but the absorbance quantification-determined values agree with the MALS particle count by plus/minus 10%, based on the flow rate and dilution factor of the PDEVs upon injection into the instrument. Additionally, in the realm of mammalian EV determinations, the C-CP tip isolation coupled with absorbance detection has proven to be a reliable approach [59, 64].

6.3.4 Purity Assessment of PDEV isolates via Bradford Assay - Bradford assays are commonly employed for total protein content determinations in diverse biospecimens and were used here to determine the concentration of protein in the native plant sample extracts, then to quantify the removal of the contaminant protein species by the C-CP tip isolation/purification method. To be clear, there is the expectation that some detectible proteins would be present in the PDEV isolate solutions, as proteins decorating the

vesicle shells will register positively via the Bradford assay. Presented in Fig. 6.5 are the Bradford assay-determined total protein concentrations for each plant sample extract and their respective PDEV isolate solutions.

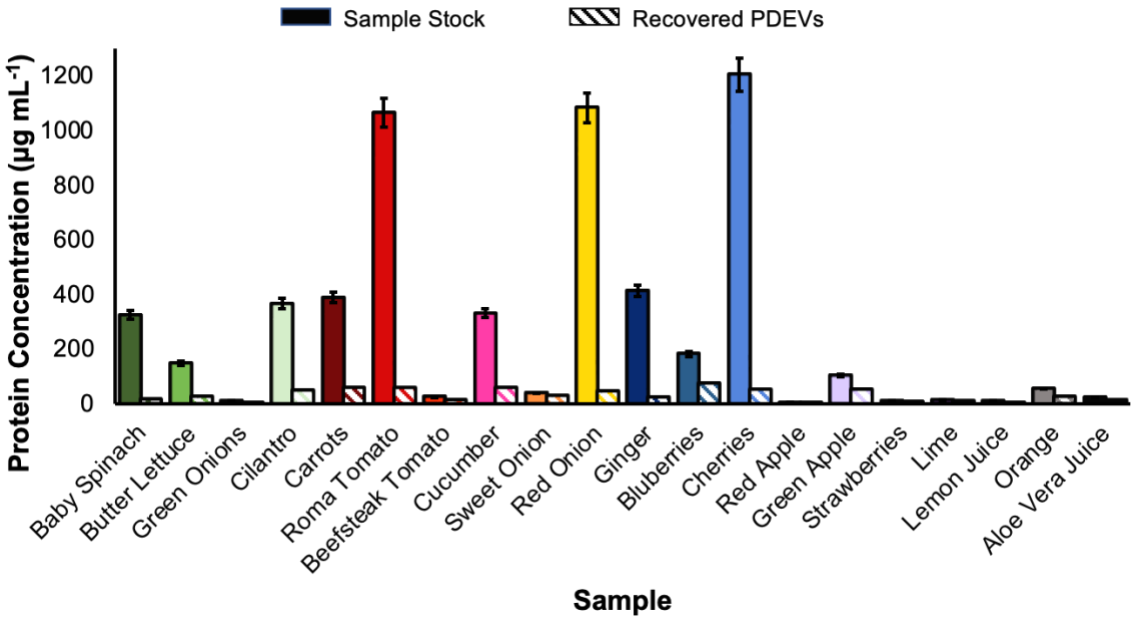

Figure 6.5: Total protein content (as determined by Bradford assays) of raw samples and the resulting PDEV isolates using the C-CP spin-down tip isolation method. All samples were analyzed in triplicate, corrected for the average response of triplicate blanks.

The Roma tomato, red onion, and cherry sample stocks contained the highest starting protein concentrations (> 1000 µg mL^{-1}), which intuitively makes sense due to the original masses of these samples ranging from 45-60 g of starting material, which is in the upper quartile of mass for the samples employed in this study (average: 35 g, range: 11 to 60 g). Regardless of the significant differences in original protein content, after processing the plant stocks using the C-CP tip method, the total protein concentrations for each PDEV extract were reduced by 48-95%. All of the recovered PDEV collections

resulted in total protein concentrations of less than 100 μg mL^{-1}, which is sufficient given the high concentration of PDEVs recovered in the assessed fraction, and with precise (< 6% RSD) determinations of the total protein concentration of the PDEV stocks. The purification of the PDEVs from matrix contaminants based on the decrease in total protein content is also comparable to that obtained from the EVs purified from human biofluids [62]. Again, Bradford assays have not been widely employed for the plant or PDEV stocks, so a point of comparison study comparing the total protein concentration of plant and PDEV stocks is undoubtedly warranted. It is hypothesized that the high purity and high yields using the C-CP tip will translate to broad use of the materials for PDEV isolations in comparison to UC sample processing.

A critical EV purity metric is the concentration of EVs versus the total protein content with respect to volume in the isolate solutions [85, 86]. In this regard, an EV-to-protein purity ratio of 3 x 10^{10} particles μg^{-1} of protein is the metric used to qualify a population of EVs as "pure" [85, 87]. In comparing to the absorbance-determined concentrations of the recovered PDEVs to the total protein values from this Bradford assay, all of the PDEV recoveries here are considered to be pure, as shown in Fig. 6.6.

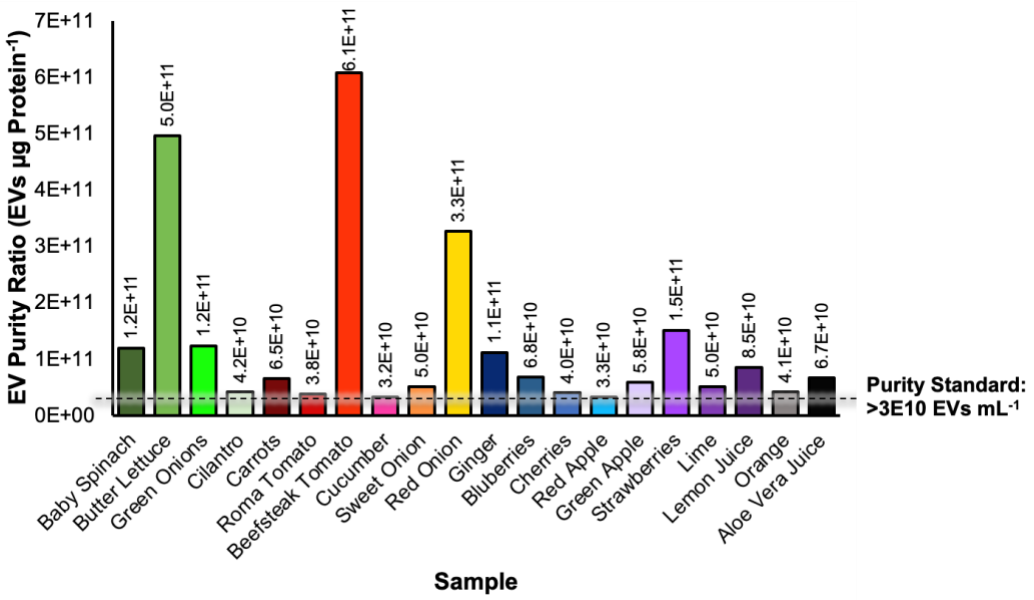

Figure 6.6: Determined PDEV purities based on the EV recoveries presented in Fig. 4, and the residual protein content presented in Fig. 6.5.

On average, the PDEVs recovered from the leafy green (1.95 x 10^{11} PDEVs μg^{-1}) sample category were of the highest purity, followed by those from the vegetable (1.87 x 10^{11} PDEVs μg^{-1}) and fruit (7.05 x 10^{10} PDEVs μg^{-1}) categories respectively. Importantly, the purity of the PDEVs obtained here are quite comparable to those obtained for human urine samples using an identical C-CP tip isolation protocol [62]. Furthermore, as a point of reference, the EVs obtained using this isolation method have 10 times higher purity than EVs processed using competitive UC and polymeric precipitation EV isolation methods [62]. Future works to directly compare the isolation performance of the C-CP tip to other traditionally-used EV isolation techniques are necessary for the case of PDEVs. Still, the data presented here suggest that the previously

demonstrated benefits of high purity and yield through the processing of EV-containing biofluids using C-CP tip methods will translate to PDEVs.

6.3.5 PEN1 Assessment via an Indirect Enzyme-Linked Immunosorbent Assay (ELISA) - Just as tetraspanin proteins have been used to verify the identity and bioactivity of mammalian EVs [39, 88, 89], immunoassays to the PEN1 protein have been employed to confirm the presence and activity of PDEVs [25, 26, 35, 90]. While no universally-expressed PDEV marker exists, the PEN1 protein has been identified at significant concentrations in PDEV isolates. As such, PEN1 has been employed as a PDEV marker protein during immunoassays and is also applied for this purpose. It should be reiterated here that positive response to PEN1 does not allow for differentiation between those EVs that existed in the intra- or extracellular regions of the original plant samples, but there will be no response for those EVs which are bacterial in nature.

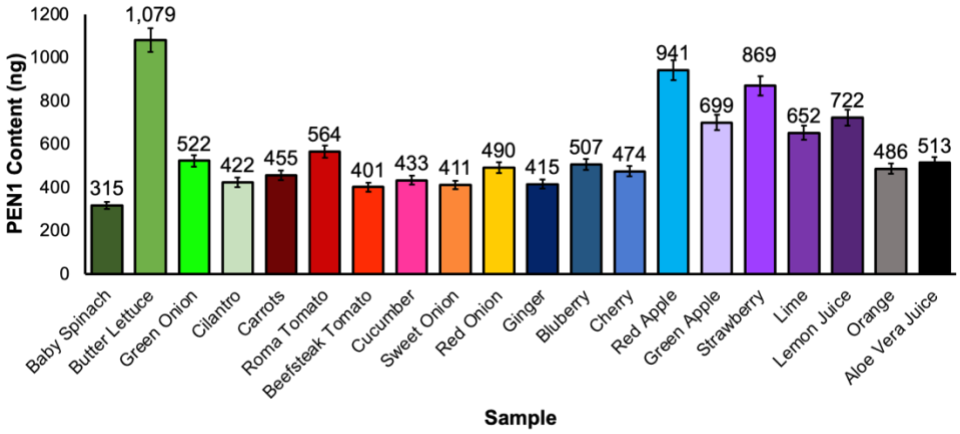

Figure 6.7: Indirect ELISA confirmation of the presence of the PEN1 marker protein for PDEVs recovered from plant samples using the C-CP spin-down tip method. Samples were analyzed in triplicate, corrected for the average response of triplicate blanks.

As shown in Fig. 6.7, each of the PDEV isolates yields a positive response in the PEN1 ELISA. Serial dilutions of the PEN1 purified protein were used to create a

standard curve of linear response ($R^2 = 0.995$) for ELISA quantification purposes, and the concentration of PEN1 in each sample's PDEV recovery was determined. With this, the presence of the PEN1 protein in the eluates is semi-quantitatively assessed. As shown, 315 – 1,079 ng of PEN1 were detected in the PDEV eluates, with the highest response for the PEN1 seen in the red apple recovery. It must be emphasized, that the preponderance of expression of PEN1 in each of these plant species has not been thoroughly explored. Indeed, just as in the case of different mammalian cells from the same species, which display highly variable levels of the respective tetraspanins, it would not be expected that PEN1 would be expressed to the same extents in these species.

6.4 Conclusions

While the evolution of methodologies for the isolation of EVs from mammalian sources is very much in a mode of expansion, methodologies applicable to plant-derived EVs are very much in their infancy. The C-CP fiber spin down tip method has been demonstrated as an efficient, practical method for the isolation of PDEVs from 20 plant sample sources, including those from vegetable, fruit, and leafy green sample categories. It is important to note that the present authors have not yet identified works describing the isolation of exosome-like vesicles in baby spinach, butter lettuce, green onion, cilantro, Roma tomato, cucumber, cherry, apple (green and red), and lime samples. Because of this, the presented work is potentially the first application of PDEV isolations from these plant types. The C-CP spin-down tip method yields representative collections of PDEVs, with significant benefits relative to standard methods based on centrifugation

or size exclusion isolation. The HIC-based C-CP fiber spin down tip method is demonstrated to provide the sample integrity, yield, and purity required to allow for critical PDEV characterization studies to be performed. High purity recoveries are achieved in less than 15 min processing times, using sample extract volumes of only 100 mL. The materials costs for each isolation are <$1 and are affected on simple benchtop centrifuges.

While much promise is demonstrated here, challenges remain in terms of implemented methods of extraction which ensure that the isolated vesicles are truly extracellular in nature [26]. The use of mechanical homogenization certainly has the potential to disrupt the cellular structure of plant materials and so means of assuring proper sampling are required as discussed by Innes and co-workers [35, 53]. Additionally, methods of sample preparation which alleviate potential contamination from bacterially-generated EVs must be part of the overall processing protocol.

This innovative approach to PDEV isolations will enable more comprehensive assessments of both fundamental and therapeutic relevance to be performed with higher efficiency and using a practical workflow. It is anticipated that future developments of the isolation method presented during this work can be scaled-up towards volume and concentration levels of relevance towards the production of PDEV therapeutic vectors.

Credit author statement

Kaylan K. Jackson: Methodology, Data Curation, Visualization, Writing – Original Draft Preparation; **Carolina Mata**: Methodology; R**. Kenneth Marcus:** Conceptualization, Supervision, Writing – Reviewing and Editing

Declaration of competing interest

The authors declare that they have no known competing financial interests or personal relationships that could have appeared to influence the work reported in this paper.

6.5 Acknowledgements

Financial support from the National Science Foundation under grant no. CHE-2107882 is gratefully acknowledged.

6.6 References

[1] S. Gill, R. Catchpole, P. Forterre, Extracellular membrane vesicles in the three domains of life and beyond, FEMS Microbiol. Rev. 43(3) (2018) 273-303.

[2] E. Woith, G. Fuhrmann, M.F. Melzig, Extracellular Vesicles—Connecting Kingdoms, *Int. J. Mol. Sci.* 20(22) (2019) 5695.

[3] J.C. Akers, D. Gonda, R. Kim, B.S. Carter, C.C. Chen, Biogenesis of extracellular vesicles (EV): exosomes, microvesicles, retrovirus-like vesicles, and apoptotic bodies, *J. Neurooncol.* 113(1) (2013) 1-11.

[4] M. Battistelli, E. Falcieri, Apoptotic Bodies: Particular Extracellular Vesicles Involved in Intercellular Communication, *Biology (Basel)* 9(1) (2020) 21.

[5] E. Cocucci, G. Racchetti, J. Meldolesi, Shedding microvesicles: artefacts no more, *Trends Cell Biol*. 19(2) (2009) 43-51.

[6] V. Muralidharan-Chari, J.W. Clancy, A. Sedgwick, C. D'Souza-Schorey, Microvesicles: mediators of extracellular communication during cancer progression, *J. Cell Sci.* 123(Pt 10) (2010) 1603-11.

[7] R. Kalluri, V.S. LeBleu, The biology, function, and biomedical applications of exosomes, *Science* 367(6478) (2020) eaau6977.

[8] D.M. Pegtel, S.J. Gould, Exosomes, *Annu. Rev. Biochem.* 88(1) (2019) 487-514.

[9] J. Lin, J. Li, B. Huang, J. Liu, X. Chen, X.M. Chen, Y.M. Xu, L.F. Huang, X.Z. Wang, Exosomes: novel biomarkers for clinical diagnosis, *Sci. World J.* 2015 (2015) 657086.

[10] Y. Zhang, Y. Liu, H. Liu, W.H. Tang, Exosomes: biogenesis, biologic function and clinical potential, *Cell Biosci.* 9(1) (2019) 19.

[11] I.L. Colao, R. Corteling, D. Bracewell, I. Wall, Manufacturing Exosomes: A Promising Therapeutic Platform, *Trends Mol. Med.* 24(3) (2018) 242-256.

[12] S. Kourembanas, Exosomes: vehicles of intercellular signaling, biomarkers, and vectors of cell therapy, *Annu. Rev. Physiol.* 77(1) (2015) 13-27.

[13] E.I. Buzas, B. Gyorgy, G. Nagy, A. Falus, S. Gay, Emerging role of extracellular vesicles in inflammatory diseases, *Nat. Rev. Rheumatol.* 10(6) (2014) 356-64.

[14] C.M. Boulanger, X. Loyer, P.E. Rautou, N. Amabile, Extracellular vesicles in coronary artery disease, *Nat. Rev. Cardiol.* 14(5) (2017) 259-272.

[15] A.G. Thompson, E. Gray, S.M. Heman-Ackah, I. Mager, K. Talbot, S.E. Andaloussi, M.J. Wood, M.R. Turner, Extracellular vesicles in neurodegenerative disease - pathogenesis to biomarkers, *Nat. Rev. Neurol.* 12(6) (2016) 346-57.

[16] T. Yamashita, Y. Takahashi, Y. Takakura, Possibility of Exosome-Based Therapeutics and Challenges in Production of Exosomes Eligible for Therapeutic Application, *Biol. Pharm. Bull.* 41(6) (2018) 835-842.

[17] A.T. Jan, Outer Membrane Vesicles (OMVs) of Gram-negative Bacteria: A Perspective Update, *Front. Microbiol.* 8 (2017) 1053.

[18] A. Kulp, M.J. Kuehn, Biological functions and biogenesis of secreted bacterial outer membrane vesicles, *Annu. Rev. Microbiol.* 64(1) (2010) 163-84.

[19] M. Samuel, M. Bleackley, M. Anderson, S. Mathivanan, Extracellular vesicles including exosomes in cross kingdom regulation: a viewpoint from plant-fungal interactions, *Front. Plant. Sci.* 6 (2015) 766.

[20] J.S. Schorey, Y. Cheng, P.P. Singh, V.L. Smith, Exosomes and other extracellular vesicles in host-pathogen interactions, *EMBO Rep.* 16(1) (2015) 24-43.

[21] G. Coakley, R.M. Maizels, A.H. Buck, Exosomes and Other Extracellular Vesicles: The New Communicators in Parasite Infections, *Trends Parasitol.* 31(10) (2015) 477-489.

[22] Q. An, A.J. van Bel, R. Huckelhoven, Do plant cells secrete exosomes derived from multivesicular bodies?, *Plant Signal Behav.* 2(1) (2007) 4-7.

[23] P. Baldrich, B.D. Rutter, H.Z. Karimi, R. Podicheti, B.C. Meyers, R.W. Innes, Plant Extracellular Vesicles Contain Diverse Small RNA Species and Are Enriched in 10- to 17-Nucleotide "Tiny" RNAs, *Plant Cell* 31(2) (2019) 315-324.

[24] M. Pinedo, L. de la Canal, C. de Marcos Lousa, A call for Rigor and standardization in plant extracellular vesicle research, *J. Extracell. Vesicles* 10(6) (2021) e12048.

[25] B.D. Rutter, R.W. Innes, Extracellular vesicles as key mediators of plant-microbe interactions, *Curr. Opin. Plant Biol.* 44 (2018) 16-22.

[26] B.D. Rutter, R.W. Innes, Growing pains: addressing the pitfalls of plant extracellular vesicle research, *New Phytol.* 228(5) (2020) 1505-1510.

[27] N. Kameli, A. Dragojlovic-Kerkache, P. Savelkoul, F.R. Stassen, Plant-Derived Extracellular Vesicles: Current Findings, Challenges, and Future Applications, *Membranes (Basel)* 11(6) (2021) 411.

[28] M.S. Manocha, M. Shaw, Occurrence of Lomasomes in Mesophyll Cells of 'Khapli' Wheat, *Nature* 203(4952) (1964) 1402-1403.

[29] W. Halperin, W.A. Jensen, Ultrastructural changes during growth and embryogenesis in carrot cell cultures, *J. Ultrastruct. Res.* 18(3) (1967) 428-43.

[30] T. Karamanidou, A. Tsouknidas, Plant-Derived Extracellular Vesicles as Therapeutic Nanocarriers, *Int. J. Mol. Sci.* 23(1) (2022) 191.

[31] J. Mu, X. Zhuang, Q. Wang, H. Jiang, Z.B. Deng, B. Wang, L. Zhang, S. Kakar, Y. Jun, D. Miller, H.G. Zhang, Interspecies communication between plant and mouse gut host cells through edible plant derived exosome-like nanoparticles, *Mol. Nutr. Food Res.* 58(7) (2014) 1561-73.

[32] Q. An, R. Huckelhoven, K.H. Kogel, A.J. van Bel, Multivesicular bodies participate in a cell wall-associated defence response in barley leaves attacked by the pathogenic powdery mildew fungus, *Cell Microbiol.* 8(6) (2006) 1009-19.

[33] O.N. Johansson, E. Fantozzi, P. Fahlberg, A.K. Nilsson, N. Buhot, M. Tor, M.X. Andersson, Role of the penetration-resistance genes PEN1, PEN2 and PEN3 in

the hypersensitive response and race-specific resistance in Arabidopsis thaliana, *Plant J.* 79(3) (2014) 466-76.

[34] G. Liu, G. Kang, S. Wang, Y. Huang, Q. Cai, Extracellular Vesicles: Emerging Players in Plant Defense Against Pathogens, *Front. Plant Sci.* 12 (2021) 757925.

[35] B.D. Rutter, R.W. Innes, Extracellular Vesicles Isolated from the Leaf Apoplast Carry Stress-Response Proteins, Plant Physiol. 173(1) (2017) 728-741.

[36] J. Zhang, Y. Qiu, K. Xu, Characterization of GFP-AtPEN1 as a marker protein for extracellular vesicles isolated from Nicotiana benthamiana leaves, *Plant Signal Behav.* 15(9) (2020) 1791519.

[37] S. Rome, Biological properties of plant-derived extracellular vesicles, *Food Funct.* 10(2) (2019) 529-538.

[38] J. Kim, S. Li, S. Zhang, J. Wang, Plant-derived exosome-like nanoparticles and their therapeutic activities, *Asian J. Pharm. Sci.* 17(1) (2022) 53-69.

[39] C. Thery, K.W. Witwer, E. Aikawa, et. al, Minimal information for studies of extracellular vesicles 2018 (MISEV2018): a position statement of the International Society for Extracellular Vesicles and update of the MISEV2014 guidelines, *J. Extracell. Vesicles* 7(1) (2018) 1535750.

[40] S. Raimondo, F. Naselli, S. Fontana, F. Monteleone, A. Lo Dico, L. Saieva, G. Zito, A. Flugy, M. Manno, M.A. Di Bella, G. De Leo, R. Alessandro, Citrus limon - derived nanovesicles inhibit cancer cell proliferation and suppress CML xenograft growth by inducing TRAIL-mediated cell death, *Oncotarget*; Vol 6, No 23 (2015).

[41] G. Pocsfalvi, L. Turiák, A. Ambrosone, P. del Gaudio, G. Puska, I. Fiume, T. Silvestre, K. Vékey, Protein biocargo of citrus fruit-derived vesicles reveals heterogeneous transport and extracellular vesicle populations, *J. Plant Physiol.* 229 (2018) 111-121.

[42] J. Xiao, S. Feng, X. Wang, K. Long, Y. Luo, Y. Wang, J. Ma, Q. Tang, L. Jin, X. Li, M. Li, Identification of exosome-like nanoparticle-derived microRNAs from 11 edible fruits and vegetables, *PeerJ* 6 (2018) e5186.

[43] X. Zhuang, Z.-B. Deng, J. Mu, L. Zhang, J. Yan, D. Miller, W. Feng, C.J. McClain, H.-G. Zhang, Ginger-derived nanoparticles protect against alcohol-induced liver damage, *J. Extracell. Vesicles* 4(1) (2015) 28713.

[44] Y. Teng, Y. Ren, M. Sayed, X. Hu, C. Lei, A. Kumar, E. Hutchins, J. Mu, Z. Deng, C. Luo, K. Sundaram, M.K. Sriwastva, L. Zhang, M. Hsieh, R. Reiman, B. Haribabu, J. Yan, V.R. Jala, D.M. Miller, K. Van Keuren-Jensen, M.L. Merchant, C.J. McClain, J.W. Park, N.K. Egilmez, H.G. Zhang, Plant-Derived Exosomal MicroRNAs Shape the Gut Microbiota, *Cell Host Microbe* 24(5) (2018) 637-652.e8.

[45] M. Potestà, A. Minutolo, A. Gismondi, L. Canuti, M. Kenzo, V. Roglia, F. Macchi, S. Grelli, A. Canini, V. Colizzi, C. Montesano, Cytotoxic and apoptotic effects of different extracts of Moringa oleifera Lam on lymphoid and monocytoid cells, *Exp. Ther. Med.* 18(1) (2019) 5-17.

[46] M. Potestà, V. Roglia, M. Fanelli, E. Pietrobono, A. Gismondi, S. Vumbaca, R.G. Nguedia Tsangueu, A. Canini, V. Colizzi, S. Grelli, A. Minutolo, C. Montesano,

Effect of microvesicles from Moringa oleifera containing miRNA on proliferation and apoptosis in tumor cell lines, *Cell Death Discov.* 6(1) (2020) 43.

[47] E. Woith, M.F. Melzig, Extracellular Vesicles from Fresh and Dried Plants—Simultaneous Purification and Visualization Using Gel Electrophoresis, *Int. J. Mol. Sci.* 20(2) (2019) 357.

[48] P. Li, M. Kaslan, S.H. Lee, J. Yao, Z. Gao, Progress in Exosome Isolation Techniques, *Theranostics* 7(3) (2017) 789-804.

[49] G.K. Patel, M.A. Khan, H. Zubair, S.K. Srivastava, M. Khushman, S. Singh, A.P. Singh, Comparative analysis of exosome isolation methods using culture supernatant for optimum yield, purity and downstream applications, *Sci. Rep.* 9(1) (2019) 5335.

[50] N. Ludwig, T.L. Whiteside, T.E. Reichert, Challenges in Exosome Isolation and Analysis in Health and Disease, *Int. J. Mol. Sci.* 20(19) (2019) 4684.

[51] Y. Cui, J. Gao, Y. He, L. Jiang, Plant extracellular vesicles, *Protoplasma* 257(1) (2020) 3-12.

[52] H. Zand Karimi, P. Baldrich, B.D. Rutter, L. Borniego, K.K. Zajt, B.C. Meyers, R.W. Innes, Arabidopsis apoplastic fluid contains sRNA- and circular RNA–protein complexes that are located outside extracellular vesicles, *Plant Cell* 34(5) (2022) 1863-1881.

[53] B.D. Rutter, K.L. Rutter, R.W. Innes, Isolation and Quantification of Plant Extracellular Vesicles, *Bio. Protoc.* 7(17) (2017) e2533-e2533.

[54] P. Gourabathini, M.T. Brandl, K.S. Redding, J.H. Gunderson, S.G. Berk, Interactions between food-borne pathogens and protozoa isolated from lettuce and spinach, *Appl. Environ. Microbiol.* 74(8) (2008) 2518-25.

[55] R. Acevedo, S. Fernandez, C. Zayas, A. Acosta, M.E. Sarmiento, V.A. Ferro, E. Rosenqvist, C. Campa, D. Cardoso, L. Garcia, J.L. Perez, Bacterial outer membrane vesicles and vaccine applications, *Front. Immunol.* 5 (2014) 121.

[56] T.F. Bruce, T.J. Slonecki, L. Wang, S. Huang, R.R. Powell, R.K. Marcus, Exosome isolation and purification via hydrophobic interaction chromatography using a polyester, capillary-channeled polymer fiber phase, *Electrophoresis* 40(4) (2019) 571-581.

[57] S. Huang, L. Wang, T.F. Bruce, R.K. Marcus, Isolation and quantification of human urinary exosomes by hydrophobic interaction chromatography on a polyester capillary-channeled polymer fiber stationary phase, *Anal. Bioanal. Chem.* 411(25) (2019) 6591-6601.

[58] S. Huang, L. Wang, T.F. Bruce, R.K. Marcus, Evaluation of exosome loading characteristics in their purification via a glycerol-assisted hydrophobic interaction chromatography method on a polyester, capillary-channeled polymer fiber phase, *Biotechnol. Prog.* 36(5) (2020) e2998.

[59] K.K. Jackson, R.R. Powell, T.F. Bruce, R.K. Marcus, Solid-phase extraction of exosomes from diverse matrices via a polyester capillary-channeled polymer (C-CP) fiber stationary phase in a spin-down tip format, *Anal. Bioanal. Chem.* 412(19) (2020) 4713-4724.

[60] L. Wang, T.F. Bruce, S. Huang, R.K. Marcus, Isolation and quantitation of exosomes isolated from human plasma via hydrophobic interaction chromatography using a polyester, capillary-channeled polymer fiber phase, *Anal. Chim. Acta.* 1082 (2019) 186-193.

[61] S. Huang, X. Ji, K.K. Jackson, D.M. Lubman, M.B. Ard, T.F. Bruce, R.K. Marcus, Rapid separation of blood plasma exosomes from low-density lipoproteins via a hydrophobic interaction chromatography method on a polyester capillary-channeled polymer fiber phase, *Anal. Chim. Acta.* 1167 (2021) 338578.

[62] K.K. Jackson, R.R. Powell, T.F. Bruce, R.K. Marcus, Rapid isolation of extracellular vesicles from diverse biofluid matrices via capillary-channeled polymer fiber solid-phase extraction micropipette tips, *Analyst* 146(13) (2021) 4314-4325.

[63] K.K. Jackson, R.R. Powell, T.F. Bruce, R.K. Marcus, Facile, generic capture and on-fiber differentiation of exosomes via confocal immunofluorescence microscopy using a capillary-channeled polymer fiber solid-phase extraction tip, *Sens. Diagn.* in press. (2022).

[64] K.K. Jackson, R.R. Powell, R.K. Marcus, T.F. Bruce, Comparison of the capillary-channeled polymer (C-CP) fiber spin-down tip approach to traditional methods for the isolation of extracellular vesicles from human urine, *Anal. Bioanal. Chem.* 414(13) (2022) 3813-3825.

[65] D.K. Kim, W.J. Rhee, Antioxidative Effects of Carrot-Derived Nanovesicles in Cardiomyoblast and Neuroblastoma Cells, Pharmaceutics 13(8) (2021) 1203.

[66] P. Akuma, O.D. Okagu, C.C. Udenigwe, Naturally Occurring Exosome Vesicles as Potential Delivery Vehicle for Bioactive Compounds, *Front. Sustain. Food Syst.* 3 (2019).

[67] P. Perez-Bermudez, J. Blesa, J.M. Soriano, A. Marcilla, Extracellular vesicles in food: Experimental evidence of their secretion in grape fruits, *Eur. J. Pharm. Sci.* 98 (2017) 40-50.

[68] B. Liu, X. Li, H. Yu, X. Shi, Y. Zhou, S. Alvarez, M.J. Naldrett, S.D. Kachman, S.H. Ro, X. Sun, S. Chung, L. Jing, J. Yu, Therapeutic potential of garlic chive-derived vesicle-like nanoparticles in NLRP3 inflammasome-mediated inflammatory diseases, *Theranostics* 11(19) (2021) 9311-9330.

[69] M. Zhang, X. Wang, M.K. Han, J.F. Collins, D. Merlin, Oral administration of ginger-derived nanolipids loaded with siRNA as a novel approach for efficient siRNA drug delivery to treat ulcerative colitis, *Nanomedicine (Lond)* 12(16) (2017) 1927-1943.

[70] F. Man, C. Meng, Y. Liu, Y. Wang, Y. Zhou, J. Ma, R. Lu, The Study of Ginger-Derived Extracellular Vesicles as a Natural Nanoscale Drug Carrier and Their Intestinal Absorption in Rats, *AAPS PharmSciTech.* 22(6) (2021) 206.

[71] M. De Robertis, A. Sarra, V. D'Oria, F. Mura, F. Bordi, P. Postorino, D. Fratantonio, Blueberry-Derived Exosome-Like Nanoparticles Counter the Response to TNF-α-Induced Change on Gene Expression in EA.hy926 Cells, *Biomolecules* 10(5) (2020) 742.

[72] F. Perut, L. Roncuzzi, S. Avnet, A. Massa, N. Zini, S. Sabbadini, F. Giampieri, B. Mezzetti, N. Baldini, Strawberry-Derived Exosome-Like Nanoparticles Prevent Oxidative Stress in Human Mesenchymal Stromal Cells, *Biomolecules* 11(1) (2021) 87.

[73] M.K. Kim, Y.C. Choi, S.H. Cho, J.S. Choi, Y.W. Cho, The Antioxidant Effect of Small Extracellular Vesicles Derived from Aloe vera Peels for Wound Healing, *Tissue Eng. Regen. Med.* 18(4) (2021) 561-571.

[74] P. Pužar Dominkuš, M. Stenovec, S. Sitar, E. Lasič, R. Zorec, A. Plemenitaš, E. Žagar, M. Kreft, M. Lenassi, PKH26 labeling of extracellular vesicles: Characterization and cellular internalization of contaminating PKH26 nanoparticles, *Biochim. Biophys. Acta. Biomembr.* 1860(6) (2018) 1350-1361.

[75] H. Zhang, D. Lyden, Asymmetric-flow field-flow fractionation technology for exomere and small extracellular vesicle separation and characterization, *Nat. Protoc.* 14(4) (2019) 1027-1053.

[76] S. Sharma, M. LeClaire, J. Wohlschlegel, J. Gimzewski, Impact of isolation methods on the biophysical heterogeneity of single extracellular vesicles, *Sci. Rep.* 10(1) (2020) 13327.

[77] V. Vagenende, A.X. Han, M. Mueller, B.L. Trout, Protein-associated cation clusters in aqueous arginine solutions and their effects on protein stability and size, *ACS Chem. Biol.* 8(2) (2013) 416-22.

[78] V. Vagenende, M.G. Yap, B.L. Trout, Mechanisms of protein stabilization and prevention of protein aggregation by glycerol, *Biochemistry* 48(46) (2009) 11084-96.

[79] C.Y. Soo, Y. Song, Y. Zheng, E.C. Campbell, A.C. Riches, F. Gunn-Moore, S.J. Powis, Nanoparticle tracking analysis monitors microvesicle and exosome secretion from immune cells, *Immunology* 136(2) (2012) 192-197.

[80] J.M. Noble, L.M. Roberts, N. Vidavsky, A.E. Chiou, C. Fischbach, M.J. Paszek, L.A. Estroff, L.F. Kourkoutis, Direct comparison of optical and electron microscopy methods for structural characterization of extracellular vesicles, *J. Struct. Biol.* 210(1) (2020) 107474.

[81] E. Van der Pol, F. Coumans, A. Grootemaat, C. Gardiner, I.L. Sargent, P. Harrison, A. Sturk, T. Van Leeuwen, R. Nieuwland, Particle size distribution of exosomes and microvesicles determined by transmission electron microscopy, flow cytometry, nanoparticle tracking analysis, and resistive pulse sensing, *J. Thromb. Haemostasis* 12(7) (2014) 1182-1192.

[82] C. Gardiner, Y.J. Ferreira, R.A. Dragovic, C.W.G. Redman, I.L. Sargent, Extracellular vesicle sizing and enumeration by nanoparticle tracking analysis, *J. Extracell. Vesicles* 2(1) (2013) 19671.

[83] M. Holcar, J. Ferdin, S. Sitar, M. Tušek-Žnidarič, V. Dolžan, A. Plemenitaš, E. Žagar, M. Lenassi, Enrichment of plasma extracellular vesicles for reliable quantification of their size and concentration for biomarker discovery, *Sci. Rep.* 10(1) (2020) 1-13.

[84] E. Oeyen, K. Van Mol, G. Baggerman, H. Willems, K. Boonen, C. Rolfo, P. Pauwels, A. Jacobs, K. Schildermans, W.C. Cho, Ultrafiltration and size exclusion chromatography combined with asymmetrical-flow field-flow fractionation for the isolation and characterisation of extracellular vesicles from urine, *J. Extracell. Vesicles* 7(1) (2018) 1490143.

[85] J. Webber, A. Clayton, How pure are your vesicles?, *J. Extracell. Vesicles* 2(1) (2013) 19861.

[86] M.Y. Konoshenko, E.A. Lekchnov, A.V. Vlassov, P.P. Laktionov, Isolation of extracellular vesicles: general methodologies and latest trends, *BioMed Res. Int.* 2018 (2018).

[87] R.J. Lobb, M. Becker, S.W. Wen, C.S. Wong, A.P. Wiegmans, A. Leimgruber, A. Moller, Optimized exosome isolation protocol for cell culture supernatant and human plasma, *J. Extracell. Vesicles* 4(1) (2015) 27031.

[88] B.J. Tauro, D.W. Greening, R.A. Mathias, H. Ji, S. Mathivanan, A.M. Scott, R.J. Simpson, Comparison of ultracentrifugation, density gradient separation, and immunoaffinity capture methods for isolating human colon cancer cell line LIM1863-derived exosomes, *Methods* 56(2) (2012) 293-304.

[89] J. Kowal, G. Arras, M. Colombo, M. Jouve, J.P. Morath, B. Primdal-Bengtson, F. Dingli, D. Loew, M. Tkach, C. Théry, Proteomic comparison defines novel markers to characterize heterogeneous populations of extracellular vesicle subtypes, *Proc. Nat. Acad. Sci. U. S. A.* 113(8) (2016) E968-E977.

[90] H.A. Dad, T.W. Gu, A.Q. Zhu, L.Q. Huang, L.H. Peng, Plant Exosome-like Nanovesicles: Emerging Therapeutics and Drug Delivery Nanoplatforms, *Mol. Ther.* 29(1) (2021) 13-31.

CHAPTER SEVEN

RAPID ISOLATION AND QUANTIFICATION OF EXTRACELLULAR VESICLES FROM SUSPENSION-ADAPTED HUMAN EMBRYONIC KIDNEY CELLS USING CAPILLARY-CHANNELED POLYMER FIBER SPIN-DOWN TIPS

7.1 Introduction

As primary vehicles of intercellular communication, nanometer-scale extracellular vesicles (EVs) allow for bioactive cargos to be transferred between cells in close and far proximity, even crossing barriers of bodily systems [1]. EVs are secreted by all living cells and are composed of a phospholipid bilayer membrane, and contain lipid, protein, and genetic (DNA, mRNA, miRNA) cargos from the cell of origin [1-4]. Overall, EV populations are heterogeneous in size (30-4000 nm), composition, and function, reflecting the original microenvironment from which they were secreted and their mode of creation [5]. Depending on the state of the origin cell, secreted EVs can contribute to either the maintenance of normal/healthy physiology or the progression of disease [6-9]. The abundance of EVs in excreted biofluids (i.e., urine, saliva, blood) has made them ideal targets for liquid biopsies and other bioassays, while the collection of EVs from cell culture milieu (CCM) has proven beneficial for therapeutic vector production [10,11].

Limiting EV applications are the lack of understanding of EV fundamentals, the inability to well characterize EV subtypes, and potentially most limiting: the absence of scalable methods to isolate pure, populated collections of EVs and quantify them efficiently [12-14]. EVs are generically classified into three main subtypes based on the

biogenesis process used to create them and their size. The three main sub-classes of EVs are 1) microvesicles (MVs) which are shed from the cell membrane of living cells, ranging from 50 – 1000 nm in size [1,15]; 2) apoptotic bodies of 50 – 4000 nm diameter, which are stochastically released from dying cells [16,17]; and 3) exosomes, smaller EVs (sEVs) of roughly 30 – 200 nm diameter, uniquely created through the multivesicular body (MVB)-mediated endosomal pathway and released via exocytosis [10-12]. Of the EV subtypes, exosomes are considered the "main mediators" of cellular communication to affect functional changes in the recipient cell [18]. However, the effective isolation of exosomes from other EV types is particularly challenging, so the assignment of exosome-specific activities to functional responses has been impeded [19]. Moreover, the overlapping of the exosome and MV size ranges and similarities in composition and morphology have led to collections of vesicles in the sEV size range (50-200 nm) to be generically referred to as EVs [12,20].

Because EVs are cell secretion products, the production of concentrated pools of EVs depends upon the ability to provide large quantities of cells in a way that does not cause alterations in the cellular phenotype (thereby, EV cargos) [13,21,22]. Of the many cell types, human embryonic kidney (HEK293) cells are prime candidates for the scalable production of EVs because of the previous success with this host cell line in the production of recombinant proteins, monoclonal antibodies (mAbs), and adeno-associated virus (AAV) vectors for biotherapeutics [23-27]. Previous works have demonstrated that after the harvest of the EVs from HEK293 cells, they can be bioengineered to contain specific gene, drug, or protein contents for therapeutic

applications ranging from opioid addiction [28] to cancer [29]. In all, HEK293-derived EVs hold the potential to provide a means of delivering powerful drug and gene therapies in a way that is practical in terms of cost and scalability.

A downfall of the use of traditional HEK293 cell lines for EV production is that standard protocols require the cells to be grown in cell culture media that is supplemented with fetal bovine serum (FBS) [24]. FBS is widely used as a universal growth supplement for *in vitro* cell culture, which is composed of many of the factors required for cell attachment, growth, and proliferation [30]. There are over 1000 components found in the bovine-sourced biofluid, including proteins, lipids, hormones, enzymes, carbohydrates, and EVs [30,31]. This causes an inevitable challenge: an additional EV source, especially since to date, the definitive determination of EV origin has been a challenge [32-35]. Many FBS manufacturers have introduced "exosome-depleted" FBS, which is often produced using an ultracentrifugation (UC) process. But with the incredibly low percentage recovery of the EVs obtained using the UC method, the "exosome-free" FBS stock remains significantly contaminated with high concentrations of EVs [32-37]. These vesicles thereby contaminate the cell culture media stock with non-human EVs to be detected downstream in future characterization approaches. Alternatively, several HEK293 cell lines have been conditioned for growth in suspension serum-free cell culture environments to eliminate this external EV source, such as the HEK293T/17 SF cell line from ATCC [30,31]. However, the downstream alterations of the EVs obtained from these modified HEK293 sources have not been thoroughly explored because of the lack of efficient isolation methods to provide representative populations of EVs.

To be clear, while the challenges of production-scale isolation/purification of EVs are immense, the inability to perform high-throughput, high-purity separations on clinical/research scales of single milliliters has prevented better fundamental research. (The same can be said for potential clinical diagnostic applications of EVs.) There is much to be learned to affect the better production of targeted EV populations, and so there are gains to be made in terms of fundamental biochemistry if better analytical strategies could be implemented. Along the same lines, suitable analytical-scale methods would take a position as part of the process monitoring toolbox for EV production. Taken a step further, demonstration of strategies for high fidelity isolation/purification from production CCM could yield platforms suitable for implementation on the preparative scale.

Marcus and colleagues have developed a hydrophobicity-based EV isolation method employing capillary-channeled polymer (C-CP) fiber stationary phases to address the shortcomings of the currently available EV isolation methods [37-45]. These C-CP fiber phases have been employed in highly efficient EV isolations via high-performance liquid chromatography (HPLC) [38-40,43,44] and solid-phase extraction (SPE) tip [37,41,42,45] formats, concentrating on what would be called analytical-scale processing. In both cases, the isolation of EVs is driven by an organic modifier-assisted hydrophobic interaction chromatography (HIC) solvent system, where EVs have been obtained from several complex biofluids, including urine, saliva, blood serum, cervical mucus, and CCM from *Dictyostelium discoideum* cell culture [38,41]. In all cases, high concentrations of EVs (up to 7×10^{12} EVs mL^{-1}) have been obtained from microliter-

scale initial sample volumes, with over 95% removal of contaminating proteins and lipoproteins as confirmed by mass spectrometric proteomics analysis [37,40]. Thus the method allows collections of EVs fit for fundamental research and clinical assays, as well as potential use for production system monitoring.

In previous C-CP-based HIC isolations of EVs, ACN and glycerol solvent additives were utilized to aid the elution of the vesicles from the fiber surface [38,44]. The ACN solvent additive was proven most compatible for EVs subsequently analyzed by mass spectrometric, RNA sequencing, and immune characterization approaches [40]. Nevertheless, high concentrations of ACN are not ideal for the long-term stability of EVs—as externally-exposed proteins may begin to degrade over time, and ACN is toxic to living cells, so EVs eluted using this solvent could not be used in cell-feeding assays. Despite these shortcomings, most of the latent ACN can be removed using a simple off-gassing process under a low vacuum. Alternatively, a glycerol solvent modifier was introduced for use in the case when the long-term structural preservation of the EVs was the end goal [44,45]. Though the glycerol solvent does provide cryopreservative properties, the high viscosity of the solvent can prevent the accurate assessment of the vesicles during proteomic analysis, immunoassays, and flow cytometry assays [46,47]. Though some latent glycerol can be removed via a post-processing ultrafiltration step, there can still be some interference with downstream analyses due to remnant glycerol content blocking access to surface proteins, etc. Overall, though the ACN and glycerol HIC solvent additives were able to provide high concentrations of pure EVs, both solvent types can limit the characterization and utilization of recovered EVs [45]. To affect EV

separations without the required post-isolation solvent removal steps, where a portion of the recovered EVs may be lost due to transfer, the identification of alternative elution solvents is of interest. As an alternative to the formerly used solvent additives, a Tween-20 EV elution solvent was considered, since Tween-20-based solvents are common to many standard immunoassays and EV analysis (i.e., Spectradyne) protocols [48,49]. Studies have also suggested that the exosome EV-subtype is resistant to detergent activity, and the morphology of the exosomes is unaffected by low concentrations of detergents (including Tween-20) [49,50]. Since the HIC C-CP tip isolation process is driven by a high-to-low salt solvent transition, an aqueous Tween-20 solution could be utilized as an organic modifier in the isolation workflow for the final elution of EVs.

In this report, a C-CP-based HIC isolation of EVs from suspension-adapted human embryonic kidney cells (HEK293T/17 SF) grown in a serum-free environment is performed. Aliquots of CCM from varying time points in cell growth were collected and processed using the HIC C-CP spin-down tip method with the Tween-20-based EV elution buffer to provide high concentrations of purified EVs. A comprehensive suite of characterization methods has been employed to follow the recovery characteristics of EVs in the course of the HEK293 cell culture cycle. Transmission electron microscopy (TEM) was used to verify the size, shape, and structural integrity of the EVs recovered using the C-CP tip method. A simple, flow-through multi-angle-light scattering (MALS) detection apparatus was used to determine the size of the recovered EVs. The method of standard addition using absorbance (scattering) detection was used for the efficient quantification of EVs. A Bradford assay was used to monitor the concentration of protein

eluted at each step in the isolation process and assess the purity of the vesicles based on the removal of host cell proteins. An indirect enzyme-linked immunosorbent assay (ELISA) using antibodies to the CD9 and CD81 exosomal surface marker proteins was used to confirm the presence and bioactivity of the collected EVs. In summary, the C-CP tip isolation method employing the Tween-20 solvent additive was able to rapidly provide high concentrations of high-purity EVs while being compatible with every characterization method utilized. While the intent of this report is not to make specific implications to cell culture biochemistry, it is believed that the approach demonstrated here has immediate relevance in research and analytical laboratories, with opportunities for production-level scale-up projected.

7.2 Materials and Methods

7.2.1 Chemicals, solvents, and antibodies – Deionized water (DI-H_2O, 18.2 MΩ-cm) was obtained from a Milli-Q water purification system (Millipore Sigma, Merck, Darmstadt, Germany). Ammonium sulfate and Tween-20 were purchased from VWR (Sokon, OH, USA). Phosphate-buffered saline (PBS, pH = 7.4) and bovine serum albumin (BSA) were purchased from ThermoFisher Scientific (Waltham, MA, USA). Paraformaldehyde and formvar/carbon 200 mesh copper grids were obtained from Electron Microscopy Science (Hatfield, PA). Polyclonal rabbit anti-CD9 and CD81 primary antibodies and a goat anti-rabbit HRP-conjugated secondary antibody were obtained from System Biosciences (SBI, Palo Alto, California). The Pierce™ Coomassie

Plus (Bradford) Assay Reagent was purchased from ThermoFisher Scientific (Waltham, MA, USA).

7.2.2 Commercial Exosomes – Lyophilized exosomes of 3.6 x 10^{11} particles mL^{-1} concentration from the cell culture media of human embryonic kidney (HEK293) cells were obtained from Hansa BioMed (Tallinn, Estonia). Per the manufacturer's instructions, the 100 µg of lyophilized exosomes were reconstituted in 100 µL of Milli-Q water before being applied to future characterization and quantification approaches. Though the commercial exosome material provides a point of reference for the quantification of EVs, this exosome stock is not a certified reference material; i.e., no quantitative/qualitative values to reflect the purity and exclusivity of the exosome stock are supplied. The shortcoming of implementing this material as an exosome "standard" stock is acknowledged here.

7.2.3 HEK293T/17 SF Cell Culture – A human embryonic kidney (HEK293T/17 SF) cell line, adapted for serum-free suspension cell culture conditions, was obtained from American Type Culture Collection (ATCC, Manassas, VA, USA). The HEK293T/17 SF cell line was cultured in BalanCD HEK293 cell culture media (Irvine Scientific, Santa Ana, CA, USA), supplemented with 8 mM L-glutamine and 10 µm mL^{-1} of insulin-transferrin-selenium (ITS, Corning, Corning, NY, USA) on a 37°C shaking incubator (160 rpm) with 5% CO_2. A Vi-CELL XR Cell Viability Analyzer (Beckman Coulter, Brea, CA, USA) was used to determine the concentration and viability of the cell line, employing the trypan blue dye exclusion method [51]. It must be noted that the

conditions employed here are considered to be typical, and not intended to represent the state of the art in HEK culture technology.

7.2.4 C-CP SPE Tip Assembly – C-CP fiber micropipette tips were prepared through the previously described process [37,41,42,45]. Briefly, colleagues from the Clemson University School of Materials Science used a melt-extrusion process to create the C-CP fibers from bulk polyester (polyethylene terephthalate, PET), where they were formed to have an 8-pronged shape of ~24 x 38 mm cross-section. To create the C-CP tips, eight rotations of the PET fiber bundles (57 fibers per bundle, 456 polymer fibers total) were collinearly aligned, pre-shrunk with boiling water, washed with ACN, water, then ACN to remove any lingering static coatings, and pulled through a 30 cm-long segment of fluorinated ethylene propylene (FEP) tubing of 0.8 mm inner diameter. The fibers co-linearly packed inside of the column were cut to create 1 cm fiber-packed tips, with an additional 0.5 cm of empty tubing allowing the columns to be attached to a 200 µL low-retention micropipette tip (SureOne™ Micropoint Pipette Tips, Universal Fit, Non-Filtered, Fisherbrand™, Pittsburgh, Pennsylvania), which was held in place with a small amount of liquid adhesive. The C-CP modified micropipette tip was then placed inside a 1 mL micropipette for structural support and secured inside a 15-mL conical tube using a customized adapter cap to hold the C-CP tip.

7.2.5 EV Isolations using the HIC Elution Protocol – An HIC solvent system was used with the C-CP tips to isolate the EVs from the HEK293T/17 SF EVs cell culture media. For this, 200 µL of the cell culture supernatant was filtered using a 0.22 µm PES filter, then mixed with an equal part of ammonium sulfate (2M final concentration), with

the 400 mL mixture applied to the C-CP tip. The entire tip apparatus was placed in the turret of a tabletop centrifuge (Symphony 4417, VWR) and spun down at 300 *x g* (rcf) for one minute. The higher hydrophobicity species (i.e., proteins and EVs) are captured on the fiber tip surface during the initial spin-down step, while the small ionic/hydrophilic sample components (i.e., salts, sugars, amino acids) pass unretained. To remove the free host-cell protein and lipoprotein contaminants, 200 µL of the protein elution buffer containing 25% ACN with 1M ammonium sulfate was loaded into the C-CP tip reservoir and spun down at 300 *x g* for one minute. This protein elution step was repeated to ensure that all contaminant protein/lipoprotein species had been removed. Finally, to release the now-purified EVs from the fiber tip surface, 100 µL of an EV elution buffer consisting of 1% Tween 20 in PBS was applied to the C-CP tip and centrifuged at 300 *x g* for one minute.

7.2.6 Transmission Electron Microscopy (TEM) – TEM imaging, performed using a Hitachi HR7830, was used to provide the physical identification of cup-shaped EVs after processing the cell culture media collections via the C-CP tips. In preparation for TEM imaging, 7 µL of each HEK-EV recovery was placed on an EM-grade copper/formvar grid and incubated at room temperature for 20 min. The excess sample liquid was then removed using a paper towel, and the EVs on the grids were immediately fixed using 2% paraformaldehyde (RT, 5 min). After fixation, the excess paraformaldehyde was removed from the grids using a paper towel before gently washing them with water for 5 min. Next, the EVs immobilized on the grids were stained using a filtered 1% uranyl acetate solution (RT, 1 min), the excess staining solution was

removed, and the prepared grids were again washed with water. Finally, the prepared TEM grids were allowed to dry in a cell culture dish for 30 minutes in a desiccator at room temperature before imaging. The size of the vesicles visualized in the TEM micrographs was determined using ImageJ.

7.2.7 Absorbance Quantification using the Method of Standard Addition - This laboratory has previously reported the use of standalone UV–Vis spectrometers to determine EV concentrations following spin-down tip processing, employing standard response curves and the method of standard addition [37,41,45]. In this work, the EVs from HEK293T/17 cell culture media were quantified via standard additions as it shows greater precision for complex matrices. Here, recovered EVs are spiked once, twice, and three times with the commercial exosome standards (3.6×10^{11} particles mL^{-1}) derived from HEK293 cells, using the absorbance at 203 nm using a NanoVue Plus UV–Vis spectrophotometer (GE Healthcare, Chicago, IL, USA). Though this exosome standard stock is not a standardized reference material, a general approximation of EV quantification can be obtained.

7.2.8 Size Determinations using Multi-Angle Light Scattering (MALS) Detection – A DAWN multi-angle light scattering (MALS) detector (Wyatt Technology, Goleta, CA), controlled using the ASTRA software, was used for the size determination of the recovered HEK-EVs. After isolating the EVs from the bulk cell culture media, 20 µL of each eluate was injected and transferred to the MALS detector at 0.5 mL min^{-1} using a Dionex Ultimate 3000 HPLC system (LPG-3400SD quaternary pump and MWD-3000 UV-Vis absorbance detector, Thermo Fisher Scientific, Sunnyvale, CA, USA) controlled

by the Chromeleon 7 software. The MALS-determined RMS radii were then multiplied by 2 to represent the approximate diameter/size of the vesicles. Throughout MALS analysis, the refractive index was set to that of 1% Tween in PBS at 22ºC, 1.3363, which was determined experimentally using a Reichert AR7 Series Automatic Refractometer. Three replicate measurements were collected for each sample in 60-second increments.

7.2.9 Isolate Purity Verification by Bradford Assay – A critical EV purity metric has become the number of EVs with respect to the total protein content in the isolates [12,52]. A standard Bradford assay was used to determine the total protein concentration of each CCM sampling and the protein content of the respective C-CP tip elution fractions (protein and EV). Here, it is important to emphasize that even in the case of pure EVs, there will be some positive response towards the Bradford assay due to the proteins incorporated in the vesicle walls. For total protein determinations, 25 µL of each sample was combined with 250 µL of Bradford reagent in a 96 cell well plate and incubated on a shaker at room temperature for 20 minutes before the detection of absorbance response at 595 nm using the Synergy H1 Hybrid Plate Reader (BioTek, Winooski, VT). The sample absorbance responses were compared to a BSA standard curve of linear response to determine the total protein concentration. All samples and standards were applied to the 96 cell well plate in triplicate, and triplicate absorbance measurements were performed.

7.2.10 EV Identity Confirmation using an Enzyme-Linked Immunosorbent Assay (ELISA) – To verify the presence of bioactive EVs (based on tetraspanin protein expression) after the C-CP tip isolation process, an indirect ELISA employing antibodies

to the CD9 and CD81 tetraspanin proteins was used. For this, 50 µL of each C-CP tip eluate was applied to the ELISA 96 cell well plate with equal volumes of ELISA coating buffer (0.05 M carbonate-bicarbonate in PBS) and allowed to incubate overnight at 4ºC. Each sample was applied in triplicate, along with triplicate applications of an exosome standard positive control and negative controls of PBS and the respective protein and EV elution buffers. Following this sample incubation, each well was washed with 200 µL of sterile PBS (6 buffer changes, 30 min total) before a 5% BSA blocking solution was applied and allowed to incubate on a shaker at room temperature for 30 minutes. 200 µL of the anti-CD9 and anti-CD81 antibody solutions of 1 µg mL^{-1} concentration was added to each sample well and allowed to incubate overnight on a shaker at 4ºC. Following incubation, the washing and blocking steps were repeated as done previously. 200 µL of the goat anti-rabbit HRP-conjugated secondary antibody (1 µg mL^{-1}) was applied to each sample well and allowed to incubate at room temperature for 2 hours. Here again, the cell well plate was washed using 200 µL of PBS per well (6 buffer changes, 30 min. total) before applying 50 µL of the 1-Step™ Ultra TMB-ELISA Substrate Solution. The colorimetric ELISA reagent was allowed to incubate for 30 min. at room temperature before the absorbance response was measured at 562 nm using the Synergy H1 Hybrid Plate Reader.

7.3 Results and Discussion

7.3.1 Cell Concentration and Viability as a Function of Culture Time – Previous reports have shown that changes in the concentration of EVs can be used to assess the

health of a cell line [53], with the upregulated release of EVs being attributed to environments or situations contributing to cell stress, and a decrease in release of EVs as being a response to nutrient depletion. Because of these sorts of relationships, scientists have suggested that a simple EV quantification/characterization method could provide insight into the productivity of a cell line, which could be particularly useful in large-scale bioreactor applications for therapeutics [13,54]. Herein lies the potential use of a rapid EV characterization tool as in a process monitoring mode. Intuitively, essential factors to assess are the viable cell concentration and the concentration of cell secretion products. The purpose of this study is to potentially characterize the state of an HEK293 cell culture based on EV release at various time points in the cell culture process using the C-CP spin-down tip method.

Shown in Fig. 7.1 are the growth characteristics of the HEK293T/17 SF cells as a function of culture time.

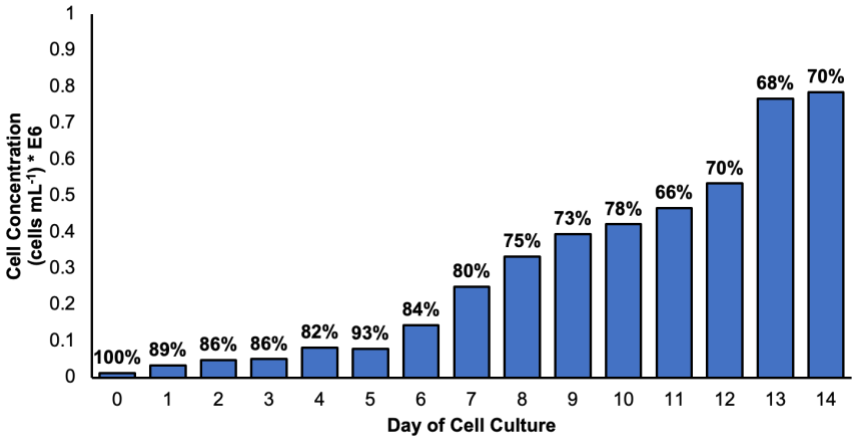

Figure 7.1: Concentration of HEK293 cells in native CCM supernatant with the percentage viability on each day of cell culture as determined using the Vi-Cell XR instrument via trypan blue cell exclusion assay.

An exponential growth phase, which is characteristic of healthy HEK293 cell growth [55-58], is observed ($R^2 = 0.9236$), with 66 – 100% of the cells collected at each time point determined as viable based on the trypan blue dye exclusion method. Typically, a collection of cells with a percentage viability of greater than 80% is considered to be a "healthy" culture [59,60]. In this case, the cells on days 0 – 7 of cell culture fall within the healthy cell viability range but decreases below 80% viability on days 8 – 14 of culture. To assess the EV release throughout the 14-day time window, collections of CCM from each time point were processed using the C-CP tip isolation method to provide concentrated, representative EV populations for further characterization.

7.3.2 Structural Verification using Transmission Electron Microscopy (TEM) – Though many EV characterization approaches are available, TEM remains the "gold standard" technique to visually confirm EV characteristics such as size and the cup/spherical EV shape [19]. TEM was used as a benchmarking approach to verify that the EVs were present in the original cell culture milieu sample, and that their physical characteristics were retained during the subsequent isolation of EVs from CCM using the C-CP tip method with the 1% Tween EV elution buffer. Representative TEM micrographs for the HEK293 cell culture milieu starting material (Fig. 7.2a) and the eluate from each C-CP tip isolation step (Fig. 7.2 b-d) are presented in Fig. 7.2 (scalebar = 200 nm).

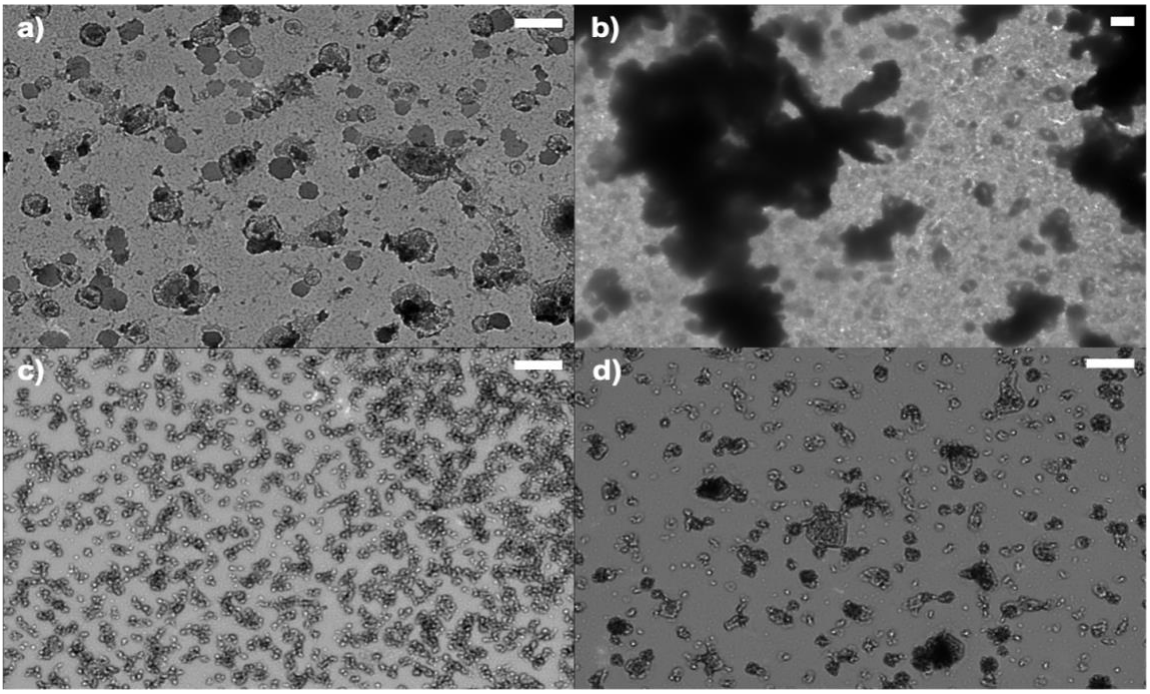

Figure 7.2: Transmission electron micrographs of eluates from each step in the HIC C-CP tip EV process. Representative micrographs from the a) native HEK293 CCM supernatant, b and c) exposure to first and second protein elution buffers and d) the EV elution buffer. The TEM images were taken using the Hitachi HR7830, scalebar = 200 nm.

Indeed, in Fig. 7.2a, EVs of 110 nm average diameter are observed in the cell culture milieu stock, with the characteristic spherical and dimpled shapes. Some EV aggregates and potential proteinaceous contaminants are also observed in the field of view, with some vesicles being > 200 nm or < 50 nm in diameter.

After applying the CCM sample to the C-CP tip and proceeding with the first protein elution step, matrix-originating components such as cell debris and protein contaminant aggregations were eluted from the C-CP tip, as shown in Fig. 7.2b. Also present are many globules of salt due to the presence of the 1M ammonium sulfate in the protein elution buffer. Interestingly, in Fig. 7.2c, the second protein elution step results in

a much cleaner image in terms of spurious debris, along with the release of a concentrated collection of small, vesicle-like species likely having hydrophobic properties similar to proteins. The population of vesicles eluted during the second protein elution step likely consists of lipoproteins, given their presence in cell culture conditions and lesser hydrophobicity in comparison to EVs, with the average diameter of the vesicles being 27 nm. Still, based on TEM analysis alone, no comments can be made on the exclusivity of this elution fraction, given that small EVs, exomeres, or exosomes in the 20-40 nm size range would likely have similar hydrophobicity characteristics because of the similarities in size and content. But, based on previous mass spectrometric proteomic studies [40,41], this elution fraction is inferred to be mainly enriched in lipoproteins. The TEM micrograph of the targeted EV elution fraction is presented in Fig. 7.2d, where vesicles of 30 – 298 nm (144 nm average diameter) are observed. Many of the vesicles visualized in Fig. 7.2d contain the characteristic cup or dimpled shape, with few matrix contaminants shown and the absence of large protein aggregates and the 20 – 40 nm fraction of the vesicles. The presented TEM micrographs verify the ability to obtain structurally-preserved EVs of the correct size from the HEK293 cell culture milieu using the C-CP spin down tip method with the 1% Tween elution buffer.

7.3.3 Quantification of Recovered EVs as a Function of Culture Time and EV Yield per Cell – The C-CP tip method allows for the isolation of highly concentrated EV samples in a quantitative and reproducible manner, using minute (100 mL) sample volumes [37,41,42,45]. These qualities are ideal in the case of small population (analytical) sampling of large-scale cell culture conditions to monitor the health of the

cell line based on EV production. The cell milieu collections from each time point were processed by the C-CP tip EV isolation method, and the eluted EVs were quantified using the method of standard addition with absorbance detection at 203 nm.

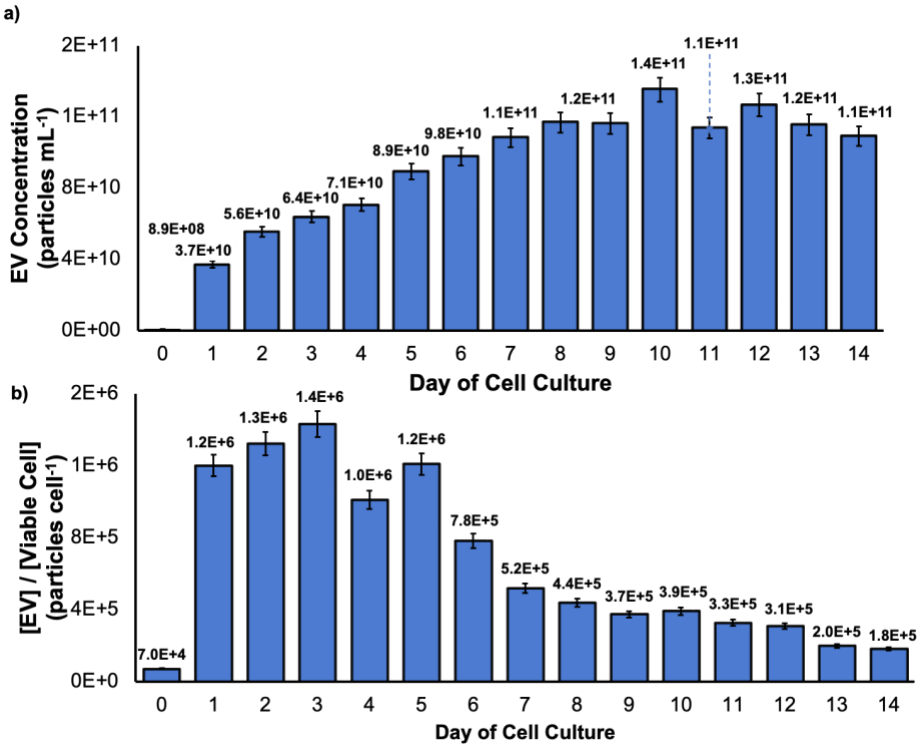

Figure 7.3: a) Concentration of EVs collected from each CCM aliquot using the C-CP tip isolation method and b) concentration of EVs released per viable cell. Quantification performed using the method of standard addition via absorbance detection at 203 nm.

As shown in Fig. 7.3a, the EVs isolated from the initial seeding aliquot of the cells into the new media and suspension culture flask yielded an EV concentration of 8.9 x 10^8 particles mL^{-1}. In only 24 hours, a ~40-fold increase in EV concentration was realized (3.7 x 10^{10} particles mL^{-1}). Further, with each day of cell culture, there was an increase in EV secretion until day 7, where the secreted EV concentration plateaus (1.1-1.4 x 10^{11} EVs mL^{-1}). This is representative of healthy cellular growth and proliferation on days 0 –

7 of cell culture, where likely beyond the day 7 time-point, the cells become overpopulated, and the cell multiplication begins to decrease as the cell culture nutrients are depleted, and cell waste by-products, such as lactate, begin to inhibit cell growth [56,61,62]. This is further confirmed by the total number and percentage of viable cells shown in Fig. 7.1, where beyond day 7 of culture, the viability of the cells decreases below 80%, remaining on the level of ~70%, and the total number reaches its maximum. Important across this set of EV number determinations and the subsequent methods of characterization is the very high level of measurement precision, wherein triplicate determinations fall below 10% RSD; and impressive value in comparison to more traditional EV isolation methods [45].

It is well known that there is a practical difference between the *viability* of cells in a given culture and their *productivity* towards an end product [13,21,63]. This concept would certainly be of relevance in the production of EVs as vectors, but also may allow for EV production to provide insights into cellular processes. In Fig. 7.3b, the concentration of recovered EVs is presented with respect to the viable cell concentration on each day of the cell culture process. After isolation of EVs from the initially-seeded cells, 7 x 10^4 EVs per viable HEK293 cell were collected, which is reasonable as the viable cells were just released into the new media-containing suspension flasks, and a minuscule amount of time was allowed to pass – lowering the probability for the occurrence of cellular communication processes (therefore EV release). Still, the initially collected EVs were likely released into the cell culture flask in response to the cell seeding process, a physical stressor for the seeded cells [53,64-66]. After the first 24

hours of incubation, a 17-fold increase in the concentration of EVs secreted per cell is observed (1.2 x 10^6 EVs per cell). This high level of EV secretion per cell is observed on days 1-5, with a dramatic 50% decrease in EV productivity observed on day 6, followed by a steady decrease up to 14 days of culture. The drop in EV productivity corresponds with the lower cell viability (Fig. 7.1), though it has been suggested that as culture media components become depleted with time, they continuously become nutrient-deprived and begin to prioritize cargo preservation, causing the EV output to decrease [61,62]. Though none of the identified works have monitored EV release during the production of therapeutic vectors/products, it would be interesting to assess potential relationships between the productivity of mAb- or viral vector-producing cell lines and EV release characteristics [67-70].

7.3.4 CD9 and CD81 Expression of HEK293T/17 EVs – Despite the absence of a discrete EV biomarker to verify the bioactivity and quantity of EVs, antibodies to the CD9 and CD81 tetraspanin proteins are commonly employed during immunoassays to verify the identity of exosomes and other EVs based on the presence of the proteins on the vesicular surfaces [1,71-73]. It is important to note that some individual tetraspanin proteins (including CD9 and CD81) are also expressed in the plasma membranes and endosomal/lysosomal compartments of cells, therefore these (free) proteins could be present to some extent in CCM samples [71]. Regardless of the various origins of the proteins, antibodies to CD9 and CD81 have been used in numerous immunoassays to verify the presence of EVs [74,75]. An indirect ELISA approach was used here to identify the C-CP tip-recovered EVs based on the tetraspanin proteins in the collections

of CCM from each time point. Because of the heterogeneity of EV protein expression, even for EVs of the same origin and exposed to identical conditions, one cannot assume that the tetraspanin protein expression is directly correlated with the absolute concentration of EVs [18,26]. That said, the absolute identification of tetraspanin proteins on the surface of the EVs is a confirmation of their identity and is suggestive of their retention of surface protein activity.

The responses to the ELISA assays for CD9 and CD81 over the course of the culture program are presented in Fig. 7.4.

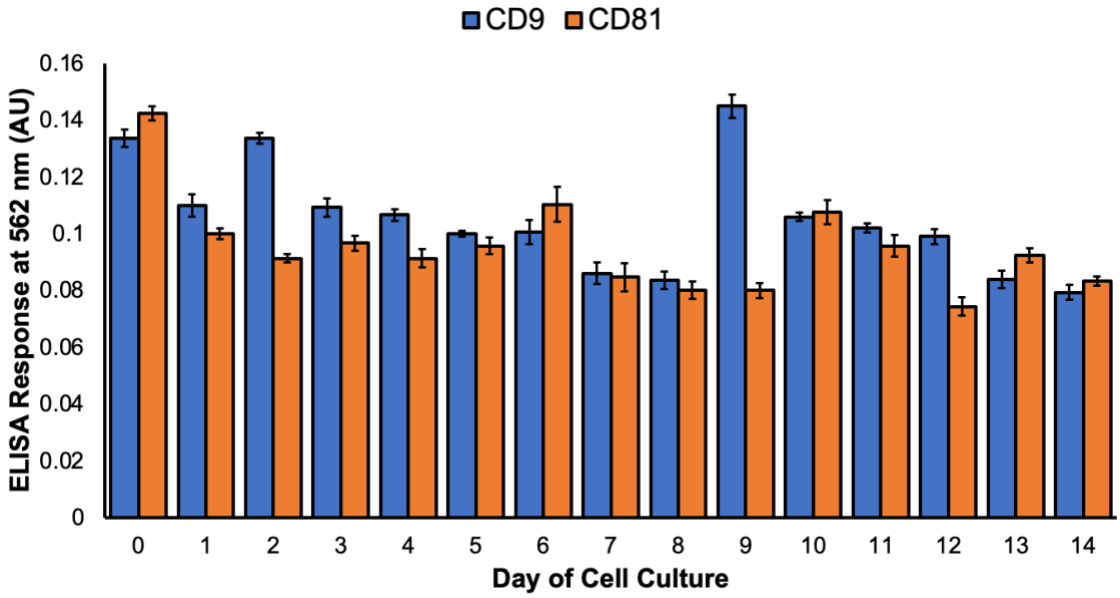

Figure 7.4: CD9 and CD81 tetraspanin protein responses of C-CP tip isolated EV recoveries from each time point, determined using an indirect ELISA. All samples were applied in triplicate with the average of the triplicate measurements minus the average response of the blank is presented.

As can be seen, the expression of the two tetraspanins remains relatively constant across the incubation period, with the absolute responses for the two proteins being fairly equivalent. This is a fortuitous situation and cannot be interpreted as meaning that the

vesicular surface concentrations for the two species is actually the same. Across the entire suite of analyses, it is clear that the triplicate isolation procedures (as well as the assay steps) are indeed very reproducible; a consistent feature of the C-CP tip isolation methodology. It is interesting that there are specific sampling days where the production of CD9 is enhanced, but it is beyond the scope of this effort to interpret the underlying reasons. As a final note, it is interesting that the ELISA responses remain consistent even though the raw number of EVs changes in the course of the culture cycle. This might suggest some sort of bias in the assay, but these samplings were all run in parallel with suitable controls/blanks. It may be that the production of tetraspanins themselves may be an indication of the health of the cell line. The ability to rapidly, and repeatably obtain this information will provide researchers with the opportunities to investigate these relationships.

7.3.5 Size of Recovered EVs via MALS – Most commonly in EV research, nanoparticle tracking analysis (NTA) methods are used for EV size determinations [76,77]. Previous use of the NTA instrument for evaluating EV size in this laboratory and others has raised concerns about the accuracy and precision of determinations due to significant inconsistencies in standard analyses [19,37,45,78,79]. The NTA methodology is susceptible to many different forms of interference, with the results having a tendency to be very operator dependent. To potentially circumvent the limitations of the NTA approach, researchers have previously employed MALS instruments for EV size determinations [14,80,81]. MALS size determination was used here to confirm that the EVs collected from the CCM samples had sizes that were within expected ranges. More

importantly, the use of MALS in combination with the C-CP tip isolation method was hoped to yield far higher levels of precision than previously obtained using NTA. Finally, as a flow-through detection method, it is anticipated that the approach can be integrated into C-CP fiber column-based separations that are performed on standard HPLC instruments [38,40,44,82]. The average diameters of the EVs isolated from the cellular milieu samples are shown in Fig. 7.5.

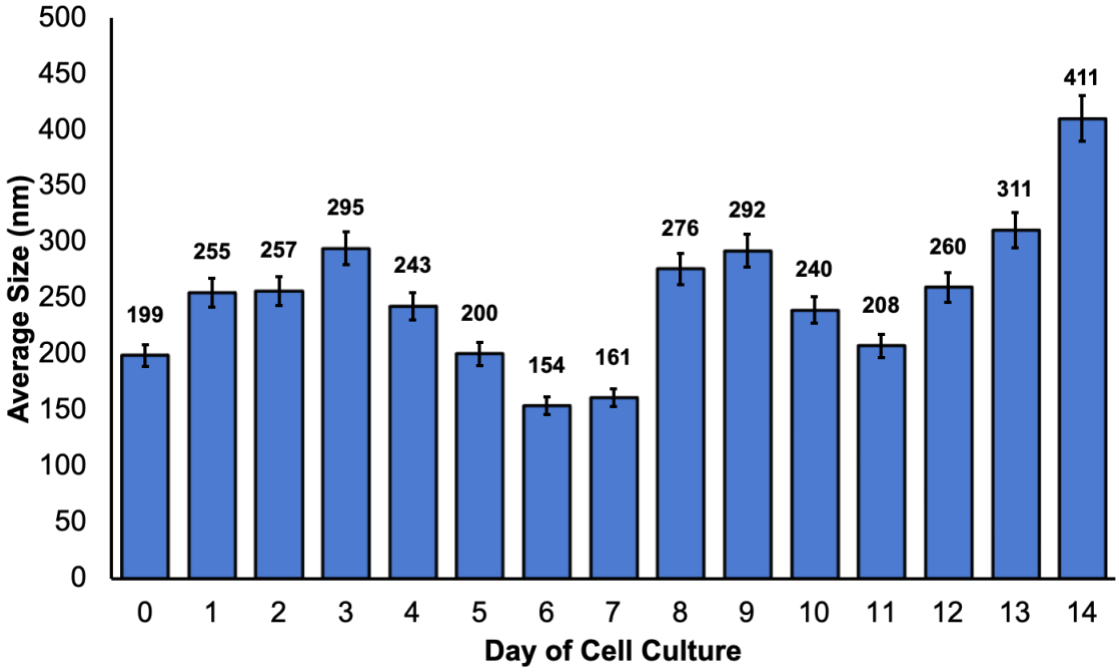

Figure 7.5: Size determination of the EVs recovered using the C-CP tip isolation method on each day of cell culture, performed using the Wyatt Dawn MALS instrument. Presented is the average size of the EVs resulting from 3 consecutive 60-second runs.

The eluted EVs presented average diameters of 145 – 411 nm across the CCM sample collections across the incubation period, with an average diameter of 249 nm overall. In comparison to previously-obtained populations of EVs collected using the C-CP tip, the average diameter of the vesicles is 50 – 100 nm larger than those obtained

from human biofluids using the acetonitrile or glycerol solvent systems and NTA determinations [41,45]. The significant difference in EV size could potentially be due to the use of the Tween-20 EV elution buffer or could be a basic characteristic of the suspension-adapted HEK293 source. Nonetheless, the relative precision of the EV size determinations using the MALS instrument is excellent, with less than 7% RSD across triplicate measurements of EV size. Given the high level of precision, the clear systemic variations in EV sizes may be of biological significance. The assessment of the various C-CP tip elution solvents in parallel isolations of EVs from identical sources is undoubtedly warranted for future experimentation, as is a direct comparison of determination methods, including NTA, MALS, and dynamic light scattering (DLS).

7.3.6 Protein Concentration of Cell Culture Milieu and Purity Assessment of Recovered EVs – Bradford assays are commonly utilized to determine the total amino acid/protein content of diverse biological samples [52]. Here, the Bradford assay was used to investigate the purity of the EVs recovered from the HEK293 cell culture collections based on the removal of host cell proteins. To clarify, the response to the Bradford assay reflects the total proteinaceous material present in a sample. Therefore, even in the case of "pure" EVs, a positive yet lower Bradford response results due to the interaction between the Bradford reagent and the externally exposed EV-associated proteins and amino acid residues. Figure 7.6 shows the Bradford assay-determined protein concentrations for the raw CCM supernatants and the eluates of the subsequent C-CP tip processing steps; i.e., the "protein" and "exosome" fractions.

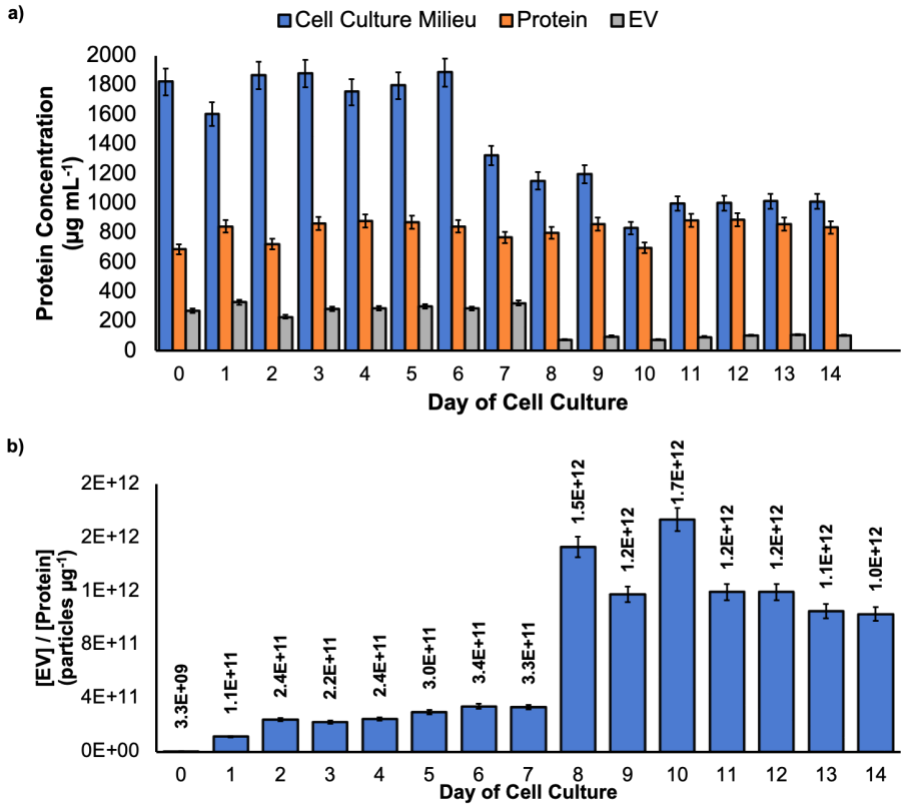

Figure 7.6: a) Concentration of protein in HEK293 sample stocks and EV eluates from the C-CP tip at each step in the isolation, determined using a Bradford assay. b) EV purity ratio comparing number of EVs to the mass of protein. All samples applied in triplicate and the average of the triplicate measurements minus the average response of the blank is presented. Purity standard = 3 x 10^{10} EVs μg^{-1}.

As shown in Fig. 7.6a, the CCM supernatant collections from days 0 – 6 of cell culture contained a consistent level of ~1800 µg mL^{-1} of protein. Then, on days 7 – 14 of culture, the protein concentration drops to the level of ~1000 µg mL^{-1}. Efforts by Martinez-Monge and co-workers have suggested that with increasing cell culture time, comes inhibited HEK293 cell growth due to the presence of harmful cell waste by-products, which causes a decrease in protein expression efficiency [56]. Indeed, this change in total protein content appears to correspond to the point where the percentage of

cell viability drops significantly (Fig. 1). This drop in "protein" content in the supernatant is not seen at all in the values derived in the first fiber tip wash step. Herein, the complementary aspects of the determinations may provide significant insights. Many previous efforts using the C-CP fiber phases have shown that small polar/ionic molecules are not retained on the fibers, as such the first-wash eluates should not contain proteins; but amino acids. The impact here is that the drop in "total protein" content in the supernatant observed after day 6 may be more reflective of decreased amino acid content in the CCM, not proteins per se. Processing the CCM samples using the complete C-CP tip protocol reduces the apparent protein concentrations of each sampling by 76 – 95% for the "EV" fractions. In each case, a high level of precision is seen following the Bradford assay, with the variability of each triplicate determination being <5 %RSD. It is noteworthy that the time response of the protein concentrations in the final eluate parallels those of the supernatant samples, reflecting a very consistent level of overall purification efficiency.

Ultimately, the goal of any EV extraction protocol, be the end application fundamental research, clinical diagnostics, or vector production, is the isolation of the vesicles to the exclusion of the diversity of CCM constituents; most specifically proteins. The most common metric used to assess the purity of EV isolates is the fraction relationship between the number of EVs per mass of protein in the isolate, with >3 x 10^{10} EVs per μg of protein considered to be "high purity" [52]. As recently demonstrated for the case of human urine-derived EVs, this is one of the metrics where the C-CP fiber tip method excels in comparison to other methods [45]. The relationship between EV and the

protein concentration (i.e., purity) is depicted across the culture cycle in Fig. 7.6b. Highly pure EV collections were obtained on days 1-14 of cell culture, while those EVs collected on day 0 are considered "impure" simply because of the low concentration of EVs obtained at the initial cell seeding. In every other case, the determined values exceed the purity target of 3×10^{10} EV mg^{-1} protein (designated by dashed line) by a full order of magnitude. Indeed, in the case of the low-viability cell conditions (beyond day 7), the values exceed the target by almost 2 orders of magnitude. In those latter data, the variability observed (<10 %RSD) is due to the low protein values via the Bradford assay. Overall these findings are in accordance with previous demonstrations of EV isolations using the C-CP tip, where the purity of the tip-recovered vesicles well exceeds the purity of vesicles processed using competitive UC or polymeric precipitation methods for EV isolation [41,45], on shorter time scales, low sample volumes, and lower capital costs.

7.4 Conclusions

There is a pressing need for methods to rapidly isolate, purify, and characterize extracellular vesicles (EVs) across very different size scales and matrices. The needs touch areas of fundamental biochemical research, clinical diagnostics, and vector production. In all, the C-CP tip isolation method employing the Tween solvent is able to produce highly concentrated, pure, structurally-preserved collections of EVs in a manner that is relevant in the scales of time, cost, and practicality, for fundamental research and clinical applications, with downstream applications of cell culture-sourced EVs holding promise using the fiber column format. The C-CP tip isolation method was applied here

to the isolation of HEK293-derived EVs, suggested as a vector for the delivery of biotherapeutics. The C-CP tip method provides rapid isolation, which provides high-purity materials for subsequent characterization via a multitude of analytical methods. Initial characterization included the evolution of the purity of the materials via TEM imaging. The absorbance-based quantification approach allows the tracking of EV release during the course of the cell culture process, where rapid processing of small aliquots (100 mL) of CCM would be advantageous for process monitoring. The C-CP tip isolation method provided bioactive EVs of up to 1.4×10^{11} EVs mL^{-1} concentration, as verified via ELISA determinations. Ultimately, the purity of the derived EVs exceeded the target metrics in all relevant cases, by greater than one order of magnitude, with up to 95% removal of contaminant host cell proteins at various time points in cell culture.

As presented, the method demonstrated here should allow researchers across diverse fields to gain greater fundamental information as to the roles of EVs in cell culture processes or as means of process monitoring. We make no biochemical inferences here, only demonstrating capabilities to obtain information. Future iterations of this technique will enable the collection of repeatable, active EV collections from cell culture and bioreactor sources on the relevant scales of time, cost, and functionality, perhaps providing a purification platform for the future production of EVs on the therapeutic scale. Further research efforts will concentrate on comparison of the use of the various elution solvents using the C-CP fiber tip method, perhaps identifying protocols that are tailored for the end use of the EVs. Collaboration with bioengineers will look to bring the

methods into the realm of bioprocess monitoring. Finally, a scale-up of the C-CP fiber column platform to allow high-volume processing will be pursued.

Credit author statement

Kaylan K. Jackson: Methodology, Data Curation, Visualization, Writing – Original Draft Preparation; R**. Kenneth Marcus:** Conceptualization, Supervision, Writing – Reviewing and Editing

Declaration of competing interest

The authors declare that they have no known competing financial interests or personal relationships that could have appeared to influence the work reported in this paper.

7.5 Acknowledgments

Financial support from the National Science Foundation under grant no. CHE-2107882 is gratefully acknowledged. The assistance of Tom Caldwell and Stephanie Klaubert of the research group of Professor Sarah Harcum (Department of Bioengineering, Clemson University) is also gratefully acknowledged.

7.6 References:

[1] Raposo, G., Stoorvogel, W., *J. Cell Biol.* 2013, *200,* 373-383.

[2] Robbins, P. D., Morelli, A. E., *Nat. Rev. Immunol.* 2014, *14,* 195-208.

[3] Shao, H., Im, H., Castro, C. M., Breakefield, X., Weissleder, R., Lee, H., *Chem. Rev.* 2018, *118,* 1917-1950.

[4] Tkach, M., Théry, C., *Cell* 2016, *164,* 1226-1232.

[5] Ferguson, S. W., Nguyen, J., *J. Controlled Release* 2016, *228,* 179-190.

[6] Anderson, M. R., Kashanchi, F., Jacobson, S., *Neurotherapeutics* 2016, *13,* 535-546.

[7] Malm, T., Loppi, S., Kanninen, K. M., *Neurochem. Int.* 2016, *97,* 193-199.

[8] Jing, H., He, X., Zheng, J., *Transl. Res.* 2018, *196,* 1-16.

[9] Moghadasi, S., Elveny, M., Rahman, H. S., Suksatan, W., Jalil, A. T., Abdelbasset, W. K., Yumashev, A. V., Shariatzadeh, S., Motavalli, R., Behzad, F., Marofi, F., Hassanzadeh, A., Pathak, Y., Jarahian, M., *J. Transl. Med.* 2021, *19,* 302.

[10] Peterson, M. F., Otoc, N., Sethi, J. K., Gupta, A., Antes, T. J., *Methods* 2015, *87,* 31-45.

[11] Zhou, B., Xu, K., Zheng, X., Chen, T., Wang, J., Song, Y., Shao, Y., Zheng, S., *Signal Transduction and Targeted Ther.* 2020, *5,* 1-14.

[12] Witwer, K. W., Soekmadji, C., Hill, A. F., Wauben, M. H., Buzas, E. I., Di Vizio, D., Falcon-Perez, J. M., Gardiner, C., Hochberg, F., Kurochkin, I. V., Lotvall, J., Mathivanan, S., Nieuwland, R., Sahoo, S., Tahara, H., Torrecilhas, A. C., Weaver, A. M., Yin, H., Zheng, L., Gho, Y. S., Quesenberry, P., Thery, C., *J. Extracell. Vesicles* 2017, *6,* 1396823.

[13] Colao, I. L., Corteling, R., Bracewell, D., Wall, I., *Trends Mol. Med.* 2018, *24,* 242-256.

[14] Koritzinsky, E. H., Street, J. M., Star, R. A., Yuen, P. S., *J. Cell Physiol.* 2017, *232,* 1587-1590.

[15] Cocucci, E., Racchetti, G., Meldolesi, J., *Trends Cell Biol.* 2009, *19,* 43-51.

[16] Akers, J. C., Gonda, D., Kim, R., Carter, B. S., Chen, C. C., *J. Neurooncol.* 2013, *113,* 1-11.

[17] Battistelli, M., Falcieri, E., *Biology (Basel)* 2020, *9,* 21.

[18] Pegtel, D. M., Gould, S. J., *Annu. Rev. Biochem.* 2019, *88,* 487-514.

[19] Thery, C., Witwer, K. W., Aikawa, E., Alcaraz, et. al, *J. Extracell. Vesicles* 2018, *7,* 1535750.

[20] van Niel, G., D'Angelo, G., Raposo, G., *Nat. Rev. Mol. Cell Biol.* 2018, *19,* 213-228.

[21] Whitford, W., Guterstam, P., *Future Med. Chem.* 2019, *11,* 1225-1236.

[22] Jo, W., Kim, J., Yoon, J., Jeong, D., Cho, S., Jeong, H., Yoon, Y. J., Kim, S. C., Gho, Y. S., Park, J., *Nanoscale* 2014, *6,* 12056-12064.

[23] Kim, J., Song, Y., Park, C. H., Choi, C., *EVCNA* 2021, *2,* 3-17.

[24] Liste-Calleja, L., Lecina, M., Cairo, J. J., *J. Biosci. Bioeng.* 2014, *117,* 471-477.

[25] Thomas, P., Smart, T. G., *J. Pharmacol. Toxicol. Methods* 2005, *51,* 187-200.

[26] Stepanenko, A. A., Dmitrenko, V. V., *Gene* 2015, *569,* 182-190.

[27] Spidel, J. L., Vaessen, B., Chan, Y. Y., Grasso, L., Kline, J. B., *J. Immunol. Methods* 2016, *439,* 50-58.

[28] Liu, Y., Li, D., Liu, Z., Zhou, Y., Chu, D., Li, X., Jiang, X., Hou, D., Chen, X., Chen, Y., Yang, Z., Jin, L., Jiang, W., Tian, C., Zhou, G., Zen, K., Zhang, J., Zhang, Y., Li, J., Zhang, C. Y., *Sci. Rep.* 2015, *5,* 17543.

[29] Faruqu, F. N., Xu, L., Al-Jamal, K. T., *J. Vis. Exp.* 2018, e58814.

[30] Gstraunthaler, G., Lindl, T., van der Valk, J., *Cytotechnology* 2013, *65,* 791-793.

[31] Van der Valk, J., Brunner, D., De Smet, K., Svenningsen, Å. F., Honegger, P., Knudsen, L. E., Lindl, T., Noraberg, J., Price, A., Scarino, M., *Toxicol. In Vitro* 2010, *24,* 1053-1063.

[32] Beninson, L. A., Fleshner, M., *Immunol. Lett.* 2015, *163,* 187-192.

[33] Zhou, Q., Xie, F., Zhou, B., Li, C., Kang, Y., Wu, B., Li, L., Dai, R., *Differentiation* 2020, *115,* 11-21.

[34] Shelke, G. V., Lasser, C., Gho, Y. S., Lotvall, J., *J. Extracell. Vesicles* 2014, *3,* 24783.

[35] Sawada, A., Yamamoto, T., Sato, T., *Int. J. Mol. Sci.* 2022, *23,* 2036.

[36] Lehrich, B. M., Liang, Y., Khosravi, P., Federoff, H. J., Fiandaca, M. S., *Int. J. Mol. Sci.* 2018, *19,* 3538.

[37] Jackson, K. K., Powell, R. R., Bruce, T. F., Marcus, R. K., *Anal. Bioanal. Chem.* 2020, *412,* 4713-4724.

[38] Bruce, T. F., Slonecki, T. J., Wang, L., Huang, S., Powell, R. R., Marcus, R. K., *Electrophoresis* 2019, *40,* 571-581.

[39] Wang, L., Bruce, T. F., Huang, S., Marcus, R. K., *Anal. Chim. Acta* 2019, *1082,* 186-193.

[40] Huang, S., Ji, X., Jackson, K. K., Lubman, D. M., Ard, M. B., Bruce, T. F., Marcus, R. K., *Anal. Chim. Acta* 2021, *1167,* 338578.

[41] Jackson, K. K., Powell, R. R., Bruce, T. F., Marcus, R. K., *Analyst* 2021, *146,* 4314-4325.

[42] Jackson, K. K., Powell, R. R., Bruce, T. F., Marcus, R. K., *Sens. Diag.* 2022, *1,* 525-533.

[43] Lal, A., Pike, J. F. W., Polley, E. L., Huang, S., Sanni, M., Hailat, T., Zimmerman, S., Clay-Gilmour, A., Bruce, T. F., Marcus, K. R., Roudebush, W. E., Chosed, R. J., *Andrologia* 2022, *54,* e14325.

[44] Huang, S., Wang, L., Bruce, T. F., Marcus, R. K., *Biotechnol. Prog.* 2020, *36,* e2998.

[45] Jackson, K. K., Powell, R. R., Marcus, R. K., Bruce, T. F., *Anal. Bioanal. Chem.* 2022, *414,* 3813-3825.

[46] Vagenende, V., Yap, M. G., Trout, B. L., *Biochemistry* 2009, *48,* 11084-11096.

[47] Vagenende, V., Trout, B. L., *Biophys. J.* 2012, *103,* 1354-1362.

[48] Han, C., Kang, H., Yi, J., Kang, M., Lee, H., Kwon, Y., Jung, J., Lee, J., Park, J., *J. Extracell. Vesicles* 2021, *10,* e12047.

[49] Osteikoetxea, X., Sodar, B., Nemeth, A., Szabo-Taylor, K., Paloczi, K., Vukman, K. V., Tamasi, V., Balogh, A., Kittel, A., Pallinger, E., Buzas, E. I., *Org. Biomol. Chem.* 2015, *13,* 9775-9782.

[50] Kumeda, N., Ogawa, Y., Akimoto, Y., Kawakami, H., Tsujimoto, M., Yanoshita, R., *Biol. Pharm. Bull.* 2017, *40,* 1183-1191.

[51] Perry, S. W., Epstein, L. G., Gelbard, H. A., *Biotechniques* 1997, *22,* 1102-1106.

[52] Webber, J., Clayton, A., *J. Extracell. Vesicles* 2013, *2,* 19861.

[53] King, H. W., Michael, M. Z., Gleadle, J. M., *BMC Cancer* 2012, *12,* 421.

[54] Zhang, B., Yeo, R. W., Tan, K. H., Lim, S. K., *Int. J. Mol. Sci.* 2016, *17,* 174.

[55] Liste-Calleja, L., Lecina, M., Lopez-Repullo, J., Albiol, J., Sola, C., Cairo, J. J., *Appl. Microbiol. Biotechnol.* 2015, *99,* 9951-9960.

[56] Martinez-Monge, I., Albiol, J., Lecina, M., Liste-Calleja, L., Miret, J., Sola, C., Cairo, J. J., *Biotechnol. Bioeng.* 2019, *116,* 388-404.

[57] Vallee, C., Durocher, Y., Henry, O., *J. Biotechnol.* 2014, *169,* 63-70.

[58] Dietmair, S., Hodson, M. P., Quek, L. E., Timmins, N. E., Gray, P., Nielsen, L. K., *PLoS One* 2012, *7,* e43394.

[59] Standardization, I. O. f., in, ISO Geneva, 2009.

[60] Lopez-Garcia, J., Lehocky, M., Humpolicek, P., Saha, P., *J Funct Biomater* 2014, *5,* 43-57.

[61] Baixauli, F., Lopez-Otin, C., Mittelbrunn, M., *Front. Immunol.* 2014, *5,* 403.

[62] Xu, J., Camfield, R., Gorski, S. M., *J. Cell Sci.* 2018, *131*.

[63] Kamen, A., Henry, O., *J. Gene Med.* 2004, *6 Suppl 1,* S184-192.

[64] Beninson, L. A., Fleshner, M., *Semin. Immunol.* 2014, *26,* 394-401.

[65] Kanemoto, S., Nitani, R., Murakami, T., Kaneko, M., Asada, R., Matsuhisa, K., Saito, A., Imaizumi, K., *Biochem. Biophys. Res. Commun.* 2016, *480,* 166-172.

[66] Villarroya-Beltri, C., Baixauli, F., Gutierrez-Vazquez, C., Sanchez-Madrid, F., Mittelbrunn, M., *Semin. Cancer Biol.* 2014, *28,* 3-13.

[67] Padawer, I., Ling, W. L., Bai, Y., *Biotechnol. Prog.* 2013, *29,* 829-832.

[68] Minh, A. D., Kamen, A. A., *Vaccines* 2021, *9,* 823.

[69] Duan, L., Xu, L., Xu, X., Qin, Z., Zhou, X., Xiao, Y., Liang, Y., Xia, J., *Nanoscale* 2021, *13,* 1387-1397.

[70] Schiller, L. T., Lemus-Diaz, N., Rinaldi Ferreira, R., Boker, K. O., Gruber, J., *Mol. Ther. Methods Clin. Dev.* 2018, *9,* 278-287.

[71] Stipp, C. S., Kolesnikova, T. V., Hemler, M. E., *Trends Biochem. Sci.* 2003, *28,* 106-112.

[72] Termini, C. M., Gillette, J. M., *Front. Cell Dev. Biol.* 2017, *5,* 34.

[73] Thery, C., Zitvogel, L., Amigorena, S., *Nat. Rev. Immunol.* 2002, *2,* 569-579.

[74] Rana, S., Yue, S., Stadel, D., Zoller, M., *Int. J. Biochem. Cell Biol.* 2012, *44,* 1574-1584.

[75] Perez-Hernandez, D., Gutierrez-Vazquez, C., Jorge, I., Lopez-Martin, S., Ursa, A., Sanchez-Madrid, F., Vazquez, J., Yanez-Mo, M., *J. Biol. Chem.* 2013, *288,* 11649-11661.

[76] Soo, C. Y., Song, Y., Zheng, Y., Campbell, E. C., Riches, A. C., Gunn-Moore, F., Powis, S. J., *Immunology* 2012, *136,* 192-197.

[77] Oosthuyzen, W., Sime, N. E., Ivy, J. R., Turtle, E. J., Street, J. M., Pound, J., Bath, L. E., Webb, D. J., Gregory, C. D., Bailey, M. A., Dear, J. W., *J. Physiol.* 2013, *591,* 5833-5842.

[78] Vestad, B., Llorente, A., Neurauter, A., Phuyal, S., Kierulf, B., Kierulf, P., Skotland, T., Sandvig, K., Haug, K. B. F., Ovstebo, R., *J. Extracell. Vesicles* 2017, *6,* 1344087.

[79] van der Pol, E., Coumans, F. A., Grootemaat, A. E., Gardiner, C., Sargent, I. L., Harrison, P., Sturk, A., van Leeuwen, T. G., Nieuwland, R., *J. Thromb. Haemost.* 2014, *12,* 1182-1192.

[80] Petersen, K. E., Manangon, E., Hood, J. L., Wickline, S. A., Fernandez, D. P., Johnson, W. P., Gale, B. K., *Anal. Bioanal. Chem.* 2014, *406,* 7855-7866.

[81] Chia, B. S., Low, Y. P., Wang, Q., Li, P., Gao, Z., *TrAC Trends Anal. Chem.* 2017, *86,* 93-106.

[82] Huang, S., Wang, L., Bruce, T. F., Marcus, R. K., *Anal. Bioanal. Chem.* 2019, *411,* 6591-6601.

CHAPTER EIGHT

SUMMARY AND FUTURE WORK

The works presented in this dissertation describe the development and evaluation of a polyester capillary-channeled polymer (C-CP) fiber solid-phase extraction spin-down tip for the isolation of extracellular vesicles (EVs) from highly diverse biological sources, which is driven by a hydrophobic interaction chromatography (HIC) solvent system. The C-CP fiber spin-down tip has repeatedly demonstrated the ability to provide highly concentrated, pure, bioactive EVs able to be employed in the physiochemical, microscopic, and biochemical techniques necessary to allow EV fundamentals to be thoroughly understood, and impactful EV biomedical approaches developed. Compared to the traditionally used isolation methods, the innovative C-CP spin-down tip approach introduces significant benefits in time, cost, practicality, and EV purity, yield, and integrity. Though many questions remain, the introduction of the C-CP tip method for the isolation of EVs has addressed many of the isolation-specific technological barriers limiting the expansion of EV research, and with the use of this novel approach, the development of potentially impactful EV-based diagnostics and therapeutics will be permitted.

With the foundational methods of EV isolation and assessment established in the works included here, the pursuit of future developments of the C-CP-based methods would surely be of interest. In the future, C-CP fiber platforms could be tailored to the processing of EVs for therapeutic product manufacturing on the relevant volume and concentration scales fit for biomanufacturing, even with the potential to be paired with

automated liquid handler systems on hands-free and labor-free workflows. Further, the versatile chemistries available by the use of C-CP fiber phases allow for the ability to customize each application to the required downstream intent of the recovered vesicles by choice of the polymer used to create the fiber phases, solvent additives, and/or fiber derivatization protocols allowing for alternative capture chemistries (i.e. biotin-streptavidin, affinity-based isolations, etc.) to be applied. Since much of the scope of this work has focused on the development and evaluation of the C-CP tip isolation method, there is much room for the exploration of the extent to which the HIC C-CP method can be utilized for the separation of relevant biovesicle analytes, i.e. the separation of EV subtypes, liposomes, synthetic nanoparticles, viruses/virus-like particles, and EVs of origins not included here. Moreover, the downstream methods to which the C-CP tip-recovered EVs can be applied have yet to be assessed. The comprehensive assessment of the biomolecular cargos of the recovered EVs using proteomic, RNA sequencing, cell barcoding mass spectrometric, and next-generation sequencing approaches are of much interest before the clinical and therapeutic applications of EVs can be pursued.

APPENDICES

Appendix A:

Supplementary Information for Chapter Two - *"Solid-phase extraction of exosomes from diverse matrices via a polyester capillary-channeled polymer (C-CP) fiber stationary phase in a spin-down tip format"*

Appendix B:

Supplementary Information for Chapter Four - *"Facile, Generic Capture and On-Fiber Differentiation of Exosomes via Confocal Immunofluorescence Microscopy using a Capillary-Channeled Polymer Fiber Solid-Phase Extraction Tip"*

APPENDIX A

SUPPLEMENTARY INFORMATION FOR *"SOLID-PHASE EXTRACTION OF EXOSOMES FROM DIVERSE MATRICES VIA A POLYESTER CAPILLARY-CHANNELED POLYMER (C-CP) FIBER STATIONARY PHASE IN A SPIN-DOWN TIP FORMAT"*

A-1 Electron Microscopy

Scanning electron microscopy (SEM) was performed using a Hitachi S-4800 to confirm the capture of intact exosomes on the C-CP fiber surface. The fiber-bound vesicles were fixed with 1% osmium tetroxide for 1 hour, then washed in microcentrifuge tubes on a shaker (3 times, 5 minutes each). The samples were then dehydrated in an ethanol-distilled water gradient from 0% to 100% ethanol, followed by 3 washes of 100% ethanol for 3 minutes each. The sample was then washed in a 50–50 hexamethyldisilazane (HMDS)-ethanol solution for 3 minutes and allowed to dry in a fume hood in 100% HMDS overnight. The dehydrated samples were sputter-coated with platinum at 70 mTorr argon for 2 minutes.

Transmission electron microscopy (TEM) was performed using a Hitachi HT7830 (Chiyoda, Tokyo, Japan) to confirm the release of intact exosomes from the C-CP fiber surface. In preparation, eluted exosomes were fixed with 1 mL of 2% paraformaldehyde (PFA) for 5 min. An aliquot of 7 μL of the fixed exosome suspension was placed on a thin formvar/carbon film-coated 200 mesh copper EM grid and incubated for 1 minute. The grids were then stained using 20 drops of filtered 1% uranyl acetate. The excess

uranyl acetate solution was removed, and the sample grids were allowed to dry for 10 minutes before imaging at 100 kV.

A-2 C-CP Fiber Tip Assembly and Centrifuge Adapter

An eight-rotation loop of the PET fibers (corresponding to a total of 450 fibers, ~241 μm each in circumference) were pulled collinearly through approximately 30 cm lengths of 0.8 mm inner diameter fluorinated ethylene polypropylene (FEP) polymer tubing (Cole Parmer, Vernon Hills, IL, USA), yielding an interstitial fraction of ~0.6. The fibers were pulled out of the column to create a 3 mm open space at the opposite end for attachment to a 200 μL micropipette tip (Molecular BioProducts, San Diego, CA, USA). The capillary was cut to create a 1 cm length of fiber-packed tubing. This procedure was repeated for the entire length of the capillary, yielding 10-15 PET C-CP fiber tips. The C-CP fiber tips were prepared for application by washing with five successive, 100 μL aliquots of 40% ACN in DI water at 300 x g for 1 minute each, to ensure the entire aliquot had spun down through the tip.

For centrifugation processing, a means of holding the tips within the centrifuge tube had to be created. A utility knife was used to remove the center portion of the cap of a 15 mL centrifuge tube (Nalge Nunc International, Rochester, NY, USA), with the bottom portion of a 1.5 mL microcentrifuge tube (Fisher Scientific, Pittsburgh, PA, USA), placed into the center of the cap, to act as the micropipette tip receptacle. The C-CP fiber tips could then be inserted in the microcentrifuge tube and placed in the rotor of

a table-top centrifuge. A VWR® Symphony™ 4417/R table-top centrifuge (Radnor, PA, USA) was used for spin-down processing.

A-3 Confocal Microscopy

After the induction of exosome adsorption to the fiber surface under the high salt condition (1:1000 exosome standards in 2M NH3SO4), the captured vesicles were rinsed with DI water (50 µL each, 300 x g, 1 minute, three times), and the elution of contaminant-free proteins was induced by rinsing the fiber surface with 25% glycerol in PBS (50 µL each, 300 x g, 1 minute, three times) to leave cleanly isolated exosomes on the fiber surface. To prevent non-specific binding of subsequently used antibodies, the free fiber surface was blocked using a blocking solution of 1% bovine serum albumin (2 hours at room temperature on a rotator). For the immuno-identification of the captured EVs, the fibers were exposed (spin-down) then incubated with a rabbit primary antibody to the CD81 protein on the exosome surface (1:1000, overnight incubation at 4° C on a rotator). Following primary antibody incubation, the fibers were washed using 6 cycles of spin-down (50 µL), then incubation with washing buffer (PBS) for 5 minutes each. To prevent non-specific binding of the secondary antibody, the fiber surface was again blocked using a blocking solution of 1% bovine serum albumin (2 hours at room temperature on a rotator). The fibers were exposed to the secondary antibody solution containing an Alexa Fluor 647 goat anti-rabbit secondary antibody by spin-down, then incubated (1:1000, 1 hour at room temperature) with the solution to obtain a visualized fluorescence response. After incubation with the secondary antibody, the fibers were

washed with PBS to remove unbound secondary antibody in preparation for imaging using the Leica SP8 Confocal Microscope.

A-4 ELISA

The mouse CD81 capture antibody was diluted 1:250 in coating buffer (0.2 M sodium carbonate/carbonate, pH=9.4), and 50 µL of the coating antibody solution was added to each well and incubated overnight at 4°C, then at 37°C for 2 hours on a shaking platform. The solution was removed, and the plate was washed using 200 µL of wash buffer (PBS) per well for 3 x 5 minutes each on a shaking platform. To prevent non-specific binding, the wells were incubated with 200 µL of blocking buffer (1% BSA) at room temperature for 1 hour. The samples were then applied to the 96-well plate in 50 µL aliquots and incubated overnight at 4°C, then at 37°C for 2 hours on a shaking platform. The solution was removed, and the plate was washed using 200 µL of wash buffer (PBS) per well for 3 x 5 minutes each. A rabbit CD81 primary antibody of 1:1000 concentration was added to each well and incubated at 4°C, then at 37°C for 2 hours on a shaking platform. The solution was removed, and the plate was washed using 200 µL of wash buffer (PBS) per well for 3 x 5 minutes each. Then, the wells were incubated with 200 µL of blocking buffer (1% BSA) at room temperature for 1 hour. Next, the wells were incubated with 50 µL of a goat anti-rabbit horseradish peroxidase (HRP) enzyme conjugate of 1:1000 concentration for 1 hour at room temperature. The solution was removed, and the plate was washed using 200 µL of wash buffer (PBS) per well for 6 x 5 minutes each. Finally, the well was incubated with the 1-Step Ultra TMB Substrate for 30

minutes at room temperature, and the resulting UV-Vis absorbance at 450 nm was measured using the Synergy H1 Hybrid Multi-Mode Reader (BioTek). The ELISA was run in triplicate (n=3) with each obtained absorbance value an average of 9 measurements. The results were quantified based on the comparison of the absorbance values to a standard curve of linear response (y = 3E-10x + 0.2093) using commercial exosome standards.

A-5 Dot Blot

In preparation for the experiment, a piece of polyvinylidene fluoride (PVDF) membrane was cut into three 1 cm by 4 cm strips. Next, the micropipette-attachment side of a 10 μL micropipette tip was used to create 3 small indentations on the PVDF strips to prevent sample run-off from the region of interest. The indentations on the PVDF strip were then labeled for the samples applied as followed: + (positive control, (sample), and – (negative control). The membranes were then wet in methanol for 15 seconds, then equilibrated in PBS buffer for 5 minutes. Next, a transfer stack assembly was set up to promote sample adsorption while keeping the membrane hydrated. Dry paper towels were placed on the lab bench surface, followed by a dry piece Whatman® 3MM filter paper, then a piece of Whatman® 3MM paper wet with PBS buffer, and finally, the pre-wet PVDF membrane. A 1 μL dot of 1:1000 secondary antibody, sample, and PBS were placed on their labeled regions on the membranes and allowed to wick into the membrane. The blots were then placed in a 1% BSA blocking solution and incubated for 1 hour at room temperature on a shaking platform. Next, each dot blot was placed in a

conical tube containing rabbit primary antibody solutions of 1:1000 concentration to CD9, CD81, and CD63 proteins, and incubated overnight at 4°C on a rotator. Next, the dot blots were washed with PBS for 30 minutes total with 5 buffer changes. The dot blots were then incubated with a goat anti-rabbit silver nanoparticle conjugate for 30 minutes at room temperature on a shaking platform. Finally, the resulting dot blot signal was enhanced using the silver enhancement kit for membranes (Cytodiagnostics), by incubating the dot blots in 2 mL of equal parts solution A and solution B for 45 minutes. The dot blots were finally washed for 5 minutes in PBS to stop the enhancement reaction.

A-6 Nanoparticle Tracking Analysis (NTA)

Averaged Nanosight NTA distribution profiles for eluted exosomes from the spiked aqueous and spiked exosome-depleted FBS samples. Tabulated statistics are presented below each.

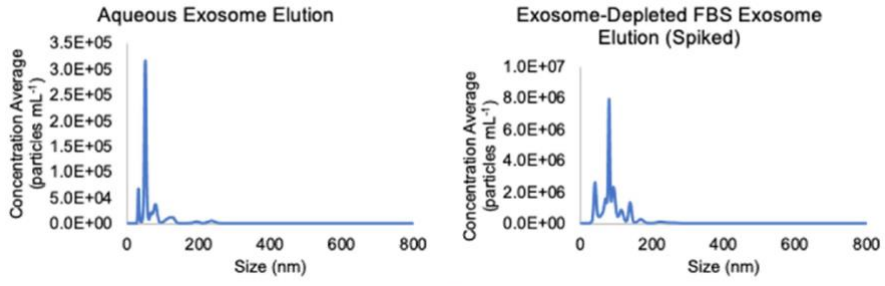

Aqueous Exosome Recovery Statistics:

Mean	95.9
Mode	77.7
RSD	5.1%
D10	71.2
D50	82.2
D90	130.1

FBS Exosome Recovery Statistics:

Mean	95.9
Mode	74.3
RSD	7.2%
D10	51.2
D50	74.3
D90	155.4

APPENDIX B

SUPPLEMENTARY INFORMATION FOR CHAPTER FOUR - *"FACILE, GENERIC CAPTURE AND ON-FIBER DIFFERENTIATION OF EXOSOMES VIA CONFOCAL IMMUNOFLUORESCENCE MICROSCOPY USING A CAPILLARY-CHANNELED POLYMER FIBER SOLID-PHASE EXTRACTION TIP"*

B-1 Standard (overnight) immunolabeling procedure

Following the HIC C-CP tip capture of EVs, the immobilized exosomes were exposed to a 5% BSA blocking solution in PBS to decrease non-specific binding of the primary and secondary antibodies. For this, 200 µL aliquots of 5% BSA were spun down 5 times at 300 x g for 60 s each. Then, the C-CP tips were submerged and incubated in 1 mL of blocking solution for 15 min on a shaker. After the blocking step, three 200 µl aliquots of PBS were spun down the tip (300 x g for 60 s each), then washed in 1 mL of PBS on a shaker for 15 min (employing 3 buffer changes where the PBS was replaced). Antibodies to the CD81 (mouse) and CA125 (rabbit) biomarker proteins were diluted 1:1000 in PBS, then 200 µL of the solution was applied to the C-CP tip, where it was allowed to wick down for 5 minutes, before centrifugation at 150 x g for 3 min. After the initial spin down, the C-CP tip was submerged and incubated in 1 mL of the primary antibody solution overnight at 4°C. Next, the washing and blocking steps were repeated as previously described. The AlexaFluor 488 (anti-rabbit) and Alexa Fluor 647 (antimouse) secondary antibodies were then diluted 1:1000 in PBS, and 200 µL of the secondary antibody solution was applied to the tip reservoir and allowed to wick for 5

minutes. Then the C-CP tip was centrifuged at 500 x g for 3 min before incubation in 1 mL of the secondary antibody for 1 hour at room temperature. Prior to confocal imaging, a final PBS wash was performed 5 times to remove the non-specifically bound secondary antibody.

B-2 Negative control experiments

In order to demonstrate the essential concepts of generic exosome capture, with the ability to affect selective immunofluorescence imaging, it is essential to demonstrate that non-specific interactions between the target proteins (and subsequently the labeled antibodies) and the fiber surfaces are not occurring. Shown below are immunofluorescence images of blank fibers treated with the antibody labels (Fig. B-1a), exposed to purified CD81 and then the antibody labels (Fig. B-1b), and the purified CD81 incubated with the antibody and applied to the fibers previously exposed to exosomes (Fig. B-1c). Essential experimental details are provided with each. In each case, the desired response was realized, with virtually no indication of non-specific binding occurring at the fiber surfaces.

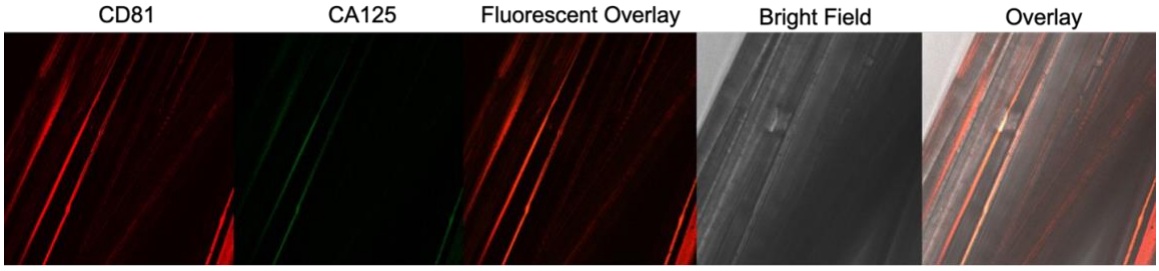

Fig. B-1a. Antibody interaction with blank PET Fiber: Blank PET fiber was washed with PBS, then the cleanup and labeling protocol was performed: 1-hour primary antibody incubation, 30 min. secondary antibody incubation, wash and block cycles between each

incubation. Very minimal non-specific binding of the primary and/or secondary antibodies was observed.

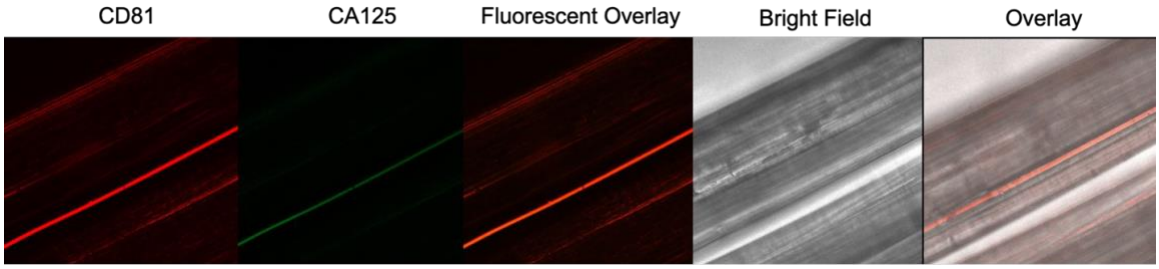

Fig. B-1b. CD81 exposure to blank fiber: Purified CD81 protein was applied during the load step in 2M ammonium sulfate, then the protein cleanup and labeling steps were performed. Very minimal non-specific binding of the primary and/or secondary antibodies was observed.

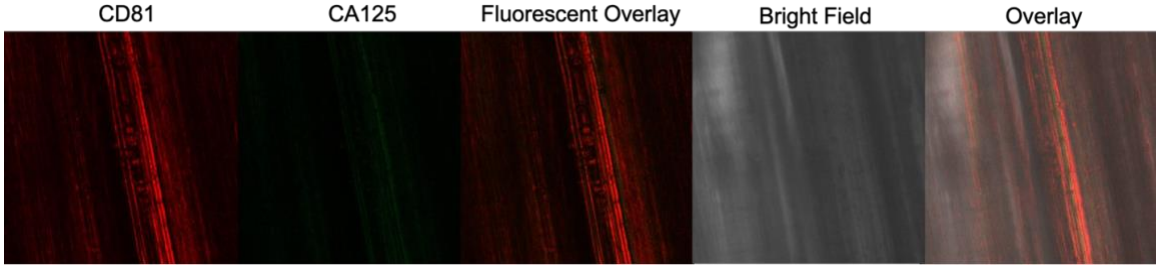

Fig. B-1c. CD81/antibody conjugate applied to fiber surface in presence exosomes: Exosome Standards (1:100 dilution, ~3 x 10^{10}) were loaded onto the fiber surface, and the protein cleanup step was performed, CD81 protein was incubated with the CD81 antibody (1 hour) before applying to tip, and labeling protocol was continued. Evidence is seen for excess antibody binding to captured exosomes, but very minimal nonspecific binding of the antigen/antibody complex is observed.

Electron microscopy

In preparation, exosomes from exosome standards were isolated using the previously described C-CP tip method, then fixed by incubation with 1% osmium tetroxide for 1 hour and washed in microcentrifuge tubes on a shaker (3 times, 5 minutes each). After fixation, the samples were dehydrated using an ethanol-distilled water gradient from 0% to 100% ethanol, followed by three washes of 100% ethanol for 3 minutes each. Following dehydration, the sample was washed in a 50–50 hexamethyldisilazane (HMDS)-ethanol solution for 3 minutes and allowed to dry in a fume hood in 100% HMDS overnight. The dehydrated samples were sputter-coated with imaging, the prepared EV-coated C-CP fibers were placed directly on carbon tape and into the instrument. During the STEM imaging of the tip eluates, the liquid eluates were dropcasted onto a small piece of EM-grade silica wafer for 60 seconds, and the sample liquid was removed using a small piece of paper towel before imaging.

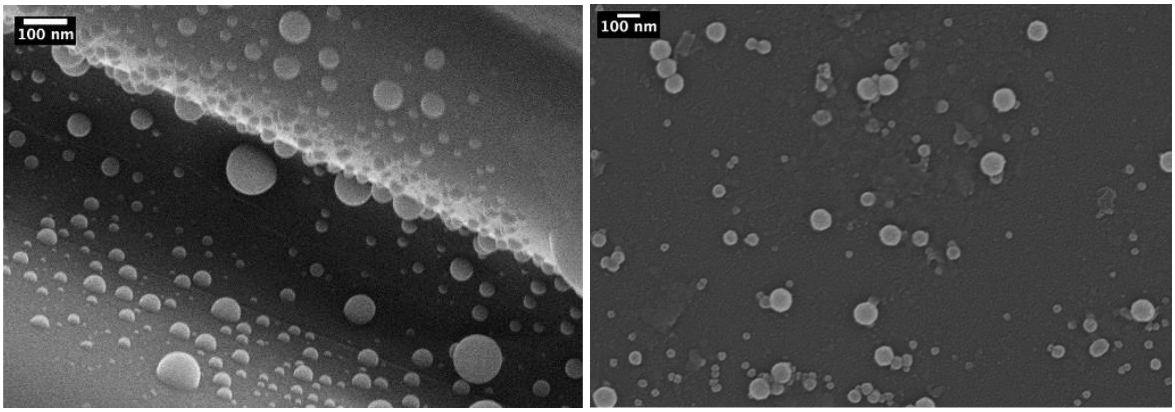

a) b)

Figure B-2: a) SEM micrograph of exosome standards (using the Hitachi S4800) captured on the C-CP fiber surface due to the HIC mode capture of the vesicles. b) STEM

micrograph of exosome standards eluted from the C-CP fiber tip immobilized on a silica wafer. (taken using Hitatchi SU9000)

B-3 Nanoparticle Tracking Analysis

The NanoSight NS300 nanoparticle tracking analysis (NTA) system (Malvern Panalytical, Malvern, Worcestershire, United Kingdom) was used to determine the size distribution and concentration of EVs isolated from 100 μL of HEK293 cell culture media using the C-CP tip. The NTA determinations were performed as previously reported. Briefly, the NTA system was equipped with a 532 nm laser, and five replicate measurements were performed in 60-second intervals. Throughout experimentation, the focal plane was manually adjusted for the best optical field of view. The syringe pump was set to a constant flow rate of 50 μL per minute, the camera level was set to 14, and the detection threshold was set to 3. Before NTA measurement, the EV recoveries were diluted 1:1000 to be compatible with the working concentration range of the NanoSight instrument (10^7–10^9 particles per mL). The EV concentration value presented in Fig. B-3 compensates for this dilution factor.

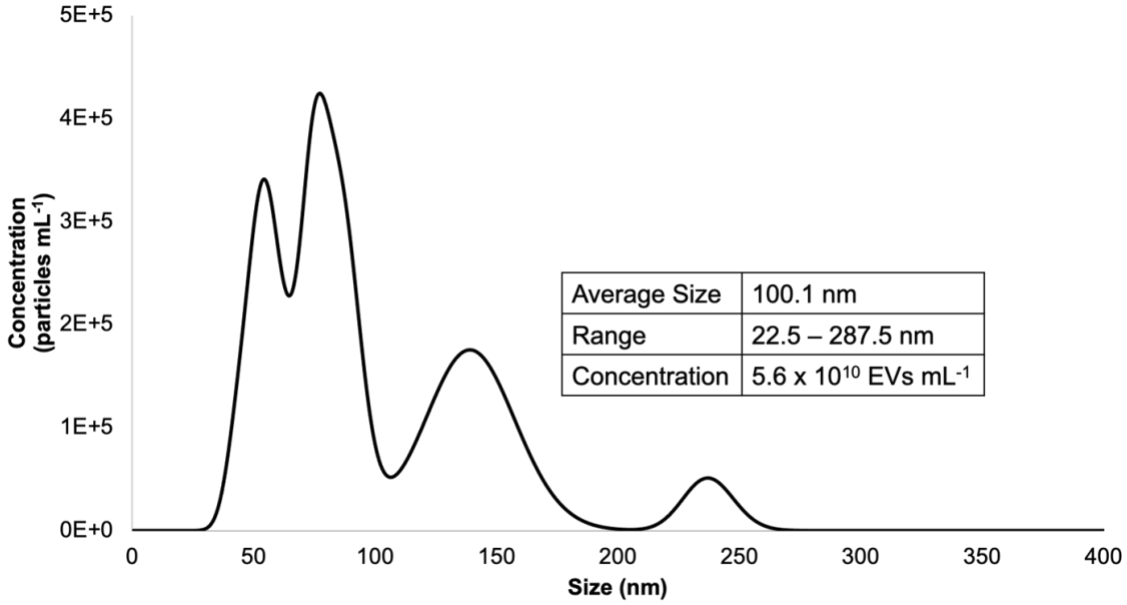

Figure B-3: Size distribution and concentration of EVs isolated using the C-CP tip from HEK293 cell culture milieu, as determined using the NanoSight NS300 NTA instrument. The average of five 60-seconds runs is presented. A 1:1000 dilution of each EV aliquot was made prior to NTA, and the determined EV concentration accounts for this dilution factor.